UNIVERSITY OF OKLAHOMA

GRADUATE COLLEGE

DEVELOPMENT OF ECOLOGICAL ENGINEERING SOLUTIONS TO MINE WATER BIOGEOCHEMISTRY AND HYDROLOGY CHALLENGES

A DISSERTATION

SUBMITTED TO THE GRADUATE FACULTY

in partial fulfillment of the requirements for the

Degree of

DOCTOR OF PHILOSOPHY

By

NICHOLAS L. SHEPHERD

Norman, Oklahoma

2022

DEVELOPMENT OF ECOLOGICAL ENGINEERING SOLUTIONS TO MINE WATER BIOGEOCHEMISTRY AND HYDROLOGY CHALLENGES

A DISSERTATION APPROVED FOR THE
SCHOOL OF CIVIL ENGINEERING AND ENVIRONMENTAL SCIENCE

BY THE COMMITTEE CONSISTING OF

Dr. Robert W. Nairn, Chair

Dr. Russell C. Dutnell

Dr. Kato T. Dee

Dr. Randall L. Kolar

Dr. Robert C. Knox

Acknowledgments

I would like to thank everyone in CREW who has helped with my research in both the field and laboratory, including M'Kenzie Dorman, Carlton Folz, Justine McCann, Brandon Holzbauer-Schweitzer, Zepei Tang, Juan Arango, Peter Wolbach, David Wilcox, Olivia Overton, and Ali Meek. This dissertation would not have been possible without their assistance and support. A special thanks to my committee members: Dr. Robert Knox, Dr. Russell Dutnell, Dr. Randall Kolar, and Dr. Kato Dee. I was incredibly fortunate to have worked with Dr. Bill Matthews and Dr. Edie Marsh-Matthews on the fish recolonization study of the unnamed tributary. Their support and guidance were essential to the success of my biological work that was a continuation of their hard work since 2005. They are both incredible role models and great friends.

A special thanks to my friend, professor, and advisor, Dr. Robert Nairn. Without his guidance and encouragement, I would not have gone to graduate school. I do not think I will ever work under someone whom I respect and enjoy as much as him.

I want to acknowledge the many landowners throughout my study area because my research would not have been possible without their cooperation and land access. These landowners include the Corbus, Keheley, Martin, Mayer, Pritchard, and Robinson families, along with Kevin Reeding of Neo Rare metals, Richard Adams of Williams Diversified Materials, and Scott Engelbrecht and the Jurgensmeyer family of J&M Farms, Inc, and the City of Commerce.

I would like to thank those who provided financial support for this project, including Oklahoma Department of Environmental Quality (ODEQ), Grand River Dam Authority (GRDA), U.S. Environmental Protection Agency, U.S. Geological Survey and U.S. Army Corps of Engineers, and the Quapaw Nation. I am also grateful for Ed Keheley who spent multiple days discussing historical mining in the Picher mining field and provided me with hundreds of gigabytes of historical records that created a foundational understanding of the underground workings.

Lastly, I want to thank my family and friends who have continued to support and encourage me throughout college and enabled me to get this degree.

Table of Contents

List of Tables

List of Figures

Abstract

Abandoned underground mines can cause a variety of environmental problems, including mine drainage (MD) that negatively impacts thousands of kilometers of streams worldwide. Underground mines accumulate water after pumping operations cease that can discharge to the surface as MD via hydraulically connected mine features such as mine shafts, drill holes, and mining fractures. Aquatic ecosystems receiving MD show signs of impairment such as decreased dissolved oxygen and increased metals concentrations, acidity, and turbidity which can result in habitat alterations and decreases in biological diversity. However, passive treatment can effectively remediate MD.

The study site is the abandoned Picher mining field, located in northeast Oklahoma and southeast Kansas in the central United States, which is part of the Tri-State Lead-Zinc Mining District, Tar Creek Superfund Site (TCSS) and Cherokee County Superfund Site. In the Picher field, mining operations occurred from the early 1900s through the 1970s, producing over 1.5 million metric tons (m-tons) of Pb and 8.0 million m-tons of Zn. The Picher field covers approximately 145 km^2, with an estimated underground void volume of at least 9,870 hectare-meters (80,000 ac-ft). After mining ceased and the last pumps were stopped, the mine voids refilled. The first identified MD discharges occurred in 1979 and contained elevated concentrations of Cd, Fe, Pb, and Zn. Today, there are multiple sources of MD throughout the TCSS, two of which continue to be successfully remediated following the implementation of passive treatment systems (PTSs). However, the largest sources of MD, located near the abandoned town of Douthat, OK, remain untreated.

The first objective of this research was to evaluate the effects of implementing PTS on the fish communities of the receiving stream, an unnamed tributary (UT) to Tar Creek that was historically impacted by two sources of MD (Chapter Two). Fish collections were periodically conducted over sixteen years: before the implementation of PTS (2005-2007), after the implementation of the first PTS (Mayer Ranch PTS (MRPTS), 2009-2016), and after the implementation of the second PTS (Southeast Commerce (SECPTS),2017-2021). It was hypothesized that the species richness and diversity of the fish communities would significantly increase following the implementation of PTS. The fish communities in the UT were negatively impacted by the elevated metals concentrations before the implementation of PTS. Both PTSs were shown to significantly decrease Cd, Fe, Pb, and Zn total metals concentrations of the MD discharges ($p < 0.05$). Fish communities downstream of Mayer Ranch showed a significant increase in species richness and diversity following the implementation of MRPTS ($p < 0.05$). The mean species richness and Shannon diversity at one site increased from 2.22 to 5.83 and 0.26 to 1.04, respectively.

Similarly, after the implementation of SECPTS, the site immediately downstream of the system effluent showed an increase in mean species richness and Shannon diversity of 1.83 to 6.83 and 0.20 to 1.21, respectively. Overall, the findings of this study showed the implementation of PTS to remediate MD can result in a significant increase in the fish species richness and diversity in the receiving stream.

The next study focused on the evaluation of the biological communities in Tar Creek. Rapid bioassessment protocols (RBPs) for fish, benthic macroinvertebrates, and habitat were conducted at six sites along an 11-km reach of Tar Creek to determine if the contamination from the abandoned mining operations in the Picher field were negatively impacting the biological communities and to examine the longitudinal extent of these impacts downstream (Chapter Three). It was hypothesized that biological indices for fish and benthic macroinvertebrate communities in a MD impacted stream would improve with distance from the mining-impacted area and that the sites furthest from the mining-impacted area would have statistically similar metric scores when compared to reference conditions from the same ecoregion. The two most upstream locations (TC1 and TC2) were within the mining-impacted area. TC1 was impacted by waste material from the mining operations which generate elevated aqueous metals concentrations and highly erodible streambeds. TC2, located immediately downstream, received additional contamination from approximately 3,000 liters per minute (lpm) of untreated MD from the Douthat discharges that entered the stream between TC1 and TC2, resulting in increased aqueous iron concentrations that formed iron hydroxide precipitates coating the stream channel bottom. The benthic macroinvertebrate and fish communities at TC1 and TC2 were substantially impaired with significantly lower taxa richness, Shannon diversity, and total RBP metric scores compared to regional reference conditions ($p < 0.05$). However, the RBP metric scores increased with increasing distance from the mining impacts, and the RBP metric scores at the most downstream site (11 km from the mining impacts) were not significantly different than the regional reference conditions. The study concluded that contamination from abandoned mining operations caused substantial impairments on biological communities in the receiving stream, but high-quality communities downstream are a potential source for upstream recolonization if the contamination were to be remediated.

The remainder of this dissertation focused on untreated MD discharges at Douthat, including mapping the underground mine workings to better understand mine pool hydrology and connectivity (Chapter Four), characterizing the water quality and quantity of untreated discharges (chapter Five), proposing conceptual PTS designs to remediate untreated MD (Chapter Six), and characterizing the mine pool to identify possible mine pool recharge sources (Chapter Seven). The nominal head elevations of the mine pool intersect ground elevations at Douthat, resulting in multiple artesian MD discharges from

open boreholes, collapse features, and mine shafts. Five discharges were regularly sampled for water quality from 2018 to 2021, and weirs were installed at three locations with pressure sensors that logged measurements every fifteen minutes to collect continuous flow measurements (Chapter Five). Flow data were plotted against corresponding mine pool elevations to develop trendlines to estimate MD flow rates at any mine pool elevation. It was hypothesized that MD water quality and quantity at Douthat was treatable via PTS. Water quality data showed that the Douthat discharges were treatable via PTS because metals concentrations were less than values for discharges at Southeast Commerce and Mayer Ranch that have been successfully remediated by MRPTS and SECPTS since 2008 and 2017, respectively. The flow weighted average total metals concentrations of the five discharges at Douthat were 0.022 mg/L Cd, 22.6 mg/L Fe, 0.045 mg/L Pb, and 5.76 mg/L Zn. The calculated flow rates that corresponded with the median and maximum mine pool elevations measured from 2009 to 2021 at a USGS monitoring station were 4,046 lpm and 154,000 lpm, respectively. The maximum flow rates were short duration, often less than 37 hours, that corresponded with substantial increases in mine pool elevations that correlated with elevated streamflow-associated flooding events. Multiple open mine shafts near streams were field located and were verified to take-on substantial amounts of water from the stream during elevated streamflow events and were referred to as known inflow locations. The mapped underground mined voids showed these known inflow locations were connected via open void space to the Douthat discharge locations (Chapters Four and Five). The study concluded that the water quantity of the Douthat discharges was treatable via PTS, despite the elevated flow rates, because other treatment wetlands with design flowrates exceeding the maximum flow rate calculated at the Douthat discharges have been designed, constructed, and continue to successfully operate.

The findings from Chapter five were used to design two conceptual PTSs capable of remediating MD at Douthat. PTS-1 was designed based on the median flow rate, assuming elevated flow events would be eliminated following the closure of known inflow locations. PTS-2 was designed to remove 90% of the metals contamination from the discharges based on the current flow rates, which included the elevated flow events. An 11-year simulation based on mine pool elevations and streamflow measurements from USGS stations was then performed to compare the metals loading to Tar Creek from MD and downstream metals concentrations for three scenarios: 1) untreated MD, 2) implementation of PTS-1, and 3) implementation of PTS-2. It was hypothesized that without the implementation of a passive treatment system to treat net-alkaline MD discharges, Tar Creek water quality would not meet state-designated beneficial use classifications more than 50% of the time, even if all other sources of metals contamination upstream of the discharges (e.g., waste piles) were addressed

(Chapter Six). The simulation showed that the annual average metals loading from untreated MD to Tar Creek was approximately 46 kg Cd, 65,900 kg Fe, 137 kg Pb, and 15,454 kg Zn, resulting in downstream Zn concentrations not meeting hardness adjusted acute Zn criteria 82% of the time and downstream Cd concentrations not meeting the hardness adjusted chronic Cd criteria 90% of the time. However, the implementation of either conceptual PTS significantly decreased metals loading of Cd, Fe, Pb, and Zn to the receiving stream. The simulation showed PTS-1 treated 66% of the MD volume, and the downstream concentrations met the state-designated beneficial use criteria for fish and wildlife propagation for all metals 95% of the time. PTS-2, which treated 90% of the MD volume during the simulation period, met the state-designated beneficial use criteria for all metals 99.997% of the time. The study concluded that even if all other sources of contamination to Tar Creek were remediated, the stream would not meet the state-designated beneficial use criteria for fish and wildlife propagation a majority of the time. However, the conceptual PTS designs showed that PTS can be implemented to remediate the Douthat MD discharges, and the downstream water quality would substantially improve.

The final study of this dissertation characterized water chemistry of the mine pool to determine if stable isotope ratios of ^{2}H and ^{18}O in water and selected water quality parameters could be used to identify individual mine pool recharge sources (Chapter Seven). The three potential recharges sources included: 1) precipitation, 2) the unconfined aquifer where the mining occurred, and 3) a confined aquifer located below the unconfined aquifer and the underground mine workings. It was hypothesized that aqueous isotope ratios ^{2}H and ^{18}O measured in each potential recharge source would be significantly different, and the differences in the isotopic signatures of each potential recharge source could be used to identify distinct sources of water contributing to the mine pool. The study found that there was no significant difference in deuterium between the three sources ($p > 0.05$), and only the confined aquifer had significantly different ^{18}O values ($p < 0.05$). However, conservative ions that were present in elevated concentrations in the groundwater compared to rainfall, such as sodium and chloride, may be an effective tool to differentiate between mine pool recharge sources. The unconfined aquifer had mean chloride and sodium concentrations of 23.7 mg/L and 45.4 mg/L, respectively, while rainfall measured <0.15 mg/L for both ions. Comparatively, mean chloride and sodium concentrations measured in the mine pool were 11.4 mg/L and 30.3 mg/L, respectively. These findings suggest that the unconfined aquifer and rainfall are substantial recharges sources. Mass balances of mean concentrations of Na and Cl indicate rainfall accounts for 30% to 50% of mine pool recharge. Therefore, the study concluded that limiting surface water interactions with the mine pool could substantially decrease mine pool recharge and flow rates at Douthat.

CHAPTER 1

Introduction

1.0 Introduction

Mine drainage (MD) is generated from biogeochemical processes that occur when sulfide minerals in host rock are exposed to air and water (e.g., Nordstrom and Alpers 1999; Gagliano 2004). MD can be net acidic or alkaline and can originate from waste rock piles, open pits, and mine voids. MD often contains elevated concentrations of sulfate, acidity, and metals such as Fe, Zn, Cd, As, and Pb (Gagliano 2004; Nairn et al. 2009). MD is a global concern, negatively impacting thousands of miles of streams and other aquatic ecosystems (Watzlaf et al. 2004). When MD enters a stream, it leads to considerable human health risks, decreases in ecological richness, and ecotoxicity due to the precipitation and bioaccumulation of metals (Taylor et al. 2005; Nairn et al. 2009; Williams and Turner 2015).

Numerous processes can be utilized to treat MD and selecting the most applicable treatment option or processes is based on a variety of factors including, but not limited to, initial water quality, water quantity, treatment goals, available land, surrounding land use and accessible funds. In the case of abandoned mining operations, passive treatment is often preferred because of the operational simplicity of the systems compared to traditional treatment options, resulting in lesser operation and maintenance costs (Watzlaf et al. 2004). Additionally, passive treatment does not rely on the regular addition of chemicals or require grid energy, and it may have the added benefit of creating wildlife habitat (Younger et al. 2002; Watzlaf et al. 2004; Nairn et al. 2009).

This dissertation focused on multiple aspects of MD, including 1) the biological impacts of MD on receiving streams, 2) evaluation of the water quality and quantity of untreated MD discharges, 3) a conceptual treatment system for MD in a hydrologically and topographically challenging watershed, 4) determination if an MD impacted stream would meet state-designated beneficial use classifications if a conceptual design was implemented, and 5) investigation of the use of aqueous light isotope ratios of ^{2}H and ^{18}O and other water quality parameters to identify distinct recharge sources of groundwaters and surface waters contributing to mine pool recharge. The overall working hypotheses of this dissertation were that 1) passive treatment can be implemented in a hydrologically and topographically challenging watershed to remediate elevated and highly variable flow rates of MD, 2) if the MD was remediated passively, the water quality of the receiving stream would be capable of meeting state-designated

beneficial use criteria, and 3) biological communities would recolonize the stream. The following chapters of this dissertation present six studies to evaluate these hypotheses.

Chapters Two and Three focus on the effects of untreated MD and MD remediated via passive treatment on the aquatic communities of the receiving streams. Chapter Two evaluated fish communities of an unnamed tributary (UT) over a 16-year period before and after the implementation of two passive treatment systems (PTSs) to determine if remediated MD resulted in significant increases in species richness and diversity of the fish communities without any improvements to instream habitat. Chapter Three evaluated the current status of the biological communities in a second-order stream that is impacted by the untreated MD that is the focus of this dissertation. Rapid bioassessment protocols for fish, benthic macroinvertebrates, and habitat assessments were used at six locations along 11 km of the second-order stream to determine if the most upstream sites, located in the mining contaminated area, were negatively impacted when compared to regional references. The objective of this study was to evaluate downstream communities to determine the extent of negative impacts from the abandoned mining operations. If sites furthest from contamination were capable of supporting biological communities that were equivalent to the regional reference conditions, then the downstream communities could serve as a source pool for recolonization, namely for fishes, if the mining contamination was remediated.

Chapter Four is a site-specific study focused on reviewing and compiling historical information to better understand the hydraulic connections and complexities of the abandoned underground mine voids and the resulting mine pool. Hundreds of historical mine maps, drill logs, publications, and reports were reviewed to create 2-dimensional and 3-dimensional renderings of the underground mine voids in AutoCAD, and to locate, compile, and update the status of mine shafts and collapse features throughout the abandoned mining region. All of the historical information was used to evaluate which portions of the underground voids were hydraulically connected and to field locate open mine shafts that could potentially contribute to the MD at the study site.

Chapter Five includes the evaluation of the water quality and quantity of the untreated MD at the study site to determine if passive treatment was a viable option for remediation. Routine water quality samples were collected and analyzed from the known MD discharges and weirs were installed throughout the study site with pressure sensors to collect continuous flow measurements. Trendline equations were generated using the calculated flow rates from the weirs versus the corresponding water elevations of the mine pool measured at a USGS groundwater monitoring station. These trendlines were used to approximate the MD flow rates in Chapter Six.

Chapter Six used the findings from Chapter Five to propose two conceptual PTSs to remediate the MD at the study site. The conceptual PTSs used a phased approach, with Phase 1 for both systems consisting of an initial oxidation pond and a total land area of approximately 51 acres. The Phase 2 system footprints varied, with PTS-1, the smaller of the two, sized to fit into an existing wetland because the landowner did not currently utilize it. PTS-1 Phase 2 covered approximately 37 acres of land, with a design flow rate of 1,200 gpm. PTS-2 Phase did not consider existing land use and was sized to remediate 90% of the annual MD by volume, resulting in a design flow rate of 2,150 gpm, and a land coverage of approximately 66 acres. Metals removal efficiencies of the two PTSs were simulated over an 11 year period using historical mine pool elevations recorded at the USGS monitoring station to determine the changes in metal loading to the receiving stream compared to the untreated MD.In-stream water quality of the receiving stream was simulated over the same period to determine if the stream would meet state-designated water quality guidelines assuming the only source of contamination was MD under three scenarios: 1) untreated MD, 2) implementation of conceptual PTS-1, and 3) implementation of conceptual PTS-2.

The final study presented in Chapter Seven evaluated potential mine pool recharge sources using stable isotope ratios of ^{2}H and ^{18}O, and other water chemistry parameters from precipitation, an unconfined aquifer, and a confined aquifer. The objective of this study was to determine if the water chemistry of these recharge sources could be compared to water chemistry in the mine pool to identify the primary mine pool recharge source. Secondly, samples collected from the mine pool throughout the abandoned mining region were evaluated on a spatial and temporal basis to determine how the mine pool has evolved over the past forty years since the end of the mining operations, and where the most contaminated regions of the mine pool were located.

CHAPTER 2

Re-establishment of Fish Communities Following Implementation of Ecologically Engineered Passive Treatment Systems to Remediate Mine Drainage

This chapter was formatted for submission to *Freshwater Biology*

Abstract

1. Mine drainage (MD) contaminates thousands of kilometers of streams worldwide by altering water chemical composition, decreasing dissolved oxygen, pH, and/or alkalinity, and increasing metal concentrations, turbidity, and sedimentation, all of which negatively impact aquatic communities. Passive treatment is one option proven effective to remediate MD before it enters receiving streams. Passive treatment relies on natural processes, including biogeochemical, microbiological, and physical mechanisms, to remove metals and acidity from MD.
2. This study investigated the recolonization of fishes in a first-order stream following the implementation of two passive treatment systems addressing MD sources that historically flowed into and contaminated the stream. The study was conducted in an unnamed tributary (UT) to Tar Creek, located in Ottawa County, Oklahoma, USA, within the Tar Creek Superfund Site and the Tri-State Lead-Zinc Mining District. Periodic fish collections consisted of 10 seine hauls per event per site at four locations along the UT. Analyses of three time periods were used to evaluate the effects of passive treatment on fish communities: 1) 2005-2007, before the implementation of passive treatment, 2) 2009-2016, after the implementation of the first passive treatment system (PTS), known as the Mayer Ranch PTS (MRPTS), and 3) 2017-2021, after the implementation of the second PTS, known as the Southeast Commerce PTS (SECPTS). Two sites (UT1 and UT2) were located downstream of MRPTS, with the remaining two sites (UT3 and UT4) located upstream of MRPTS but downstream of SECPTS. The PTSs address source water quality, and no in-stream remediation or restoration efforts were conducted in the UT.
3. The implementation of MRPTS showed a significant decrease in total aqueous cadmium, iron, lead, and zinc concentrations at both sites below MRPTS, correlated with significant increases in fish species richness and diversity. UT1, located approximately

700 m downstream of MRPTS effluent, showed an increase in average species richness (2.22 to 5.83) and Shannon diversity (0.26 to 1.04) Following the implementation of the first PTS. The implementation of SECPTS correlated with increases in fish species richness and diversity at UT3 and UT4 when comparing time periods 2 and 3, showing an increase in species richness from 3.00 to 6.82 at UT3 and from 1.83 to 6.83 at UT4, and Shannon diversity increased from 0.36 to 1.26 at UT3 and 0.20 to 1.21 at UT4.

4. Overall, this study showed that utilizing passive treatment to remediate MD can decrease metals concentrations in receiving streams, thus allowing fish communities to recolonize the stream.
5. The findings of this study can inform a broader audience about the potential recovery of a fish community in a first order stream if the MD is successfully treated and provides evidence that passive treatment technology is a viable option to remediate MD.

Key Words: Tar Creek, Water Quality, Stream Recovery, Fish Recolonization

2.1 Introduction

Contamination of surface streams by mine drainage (MD) is a massive problem on a worldwide scale (Dudka & Adriano, 1997; Byrne et al., 2011; Pokhrel & Dubey, 2013). Especially troublesome are the effects of abandoned underground mines, as cessation of pumping operations can lead to the release of accumulated mine waters to the surface via mining fractures or openings (Banks et al., 1997). Lentic and lotic ecosystems receiving untreated MD often show characteristic water quality changes, including decreased dissolved oxygen, pH, and/or alkalinity, with increased metal concentrations, turbidity, and sedimentation (Gray, 1997; Hogsden & Harding, 2012; Williams & Turner, 2015). These water quality changes negatively impact the biota of receiving aquatic ecosystems through the elimination of species or alteration of their habitats (Taylor et al., 2005; Hogsden & Harding, 2012).

This study was conducted within the abandoned Picher mining field in Oklahoma and Kansas (USA), covering approximately 145 km^2 (Shepherd et al., 2022). The Picher field and surrounding area, known as the Tri-State Mining District (TSMD), was one of the largest lead (Pb) and zinc (Zn) producers in the United States. The Picher field was extensively mined for Pb (principally galena) and Zn (principally sphalerite) ores beginning in 1904 and continuing through the early 1970s. Underground mining operations left approximately 3,560 acres of land undermined and a minimum underground mined void volume of 9,870 hectare-meters (Shepherd et al., 2022).

As mining decreased, the pumps used to dewater the underground mine workings were deactivated, and the large underground mined void began to fill with water. The first artesian flowing metal-laden mine discharge was documented in 1979, with elevated concentrations of cadmium (Cd), iron (Fe), Pb, and Zn (Oklahoma Water Resources Board, 1983). The metals contamination resulting from the mining activities led to the Oklahoma portion of the Picher field being proposed for the Comprehensive Environmental Response, Compensation, and Liability Act National Priorities List in 1981, with a final listing in 1983. The Tar Creek Superfund Site (TCSS) is named after the creek that is most impacted by the contamination (United States Environmental Protection Agency (USEPA), 1994; Oklahoma Department of Environmental Quality, 2006; Nairn et al., 2009). The TCSS encompasses an approximate area of 105 km^2 and includes six small towns.

Within the TCSS, multiple artesian flowing MD discharges contaminate Tar Creek and its tributaries. Additionally, the creek flows through and alongside multiple tailings piles (i.e., the waste material from the underground mining operations). The USEPA ruled that “the impacts to Tar Creek are due to irreversible man-made damages resulting from past mining operations at the site” (USEPA, 1994).

Based on extensive experience addressing coal mine waters by the University of Oklahoma Center for Restoration of Ecosystems and Watersheds (CREW), a passive treatment system was proposed in the early 2000s to treat the TCSS MD discharges.

Passive treatment utilizes a combination of biogeochemical, microbiological, physical processes, and naturally available energy sources to remediate MD (Hedin et al., 1994; Younger et al., 2002). Passive treatment systems (PTS) are often utilized to remediate abandoned MD due to the low long-term costs, limited operation and maintenance requirements, and independence from grid energy.

2.1.1 Study Site

This study focused on a 1.7 km reach of an unnamed, first order tributary to Tar Creek. The unnamed tributary (UT) has been historically contaminated with metal-laden MD since at least 1979. There are two primary sources of MD entering the UT: discharges at Mayer Ranch and Southeast Commerce (Figures 2.1 and 2.2). The MD discharges under artesian pressure through abandoned mining features at both sites. Several land and water reclamation projects in the UT watershed occurred throughout this study that influenced the water quality of the UT.

At the beginning of this study in 2005, the Mayer Ranch and Southeast Commerce MD discharges flowed into separate volunteer cattail (*Typha*) marshes, which provided partial natural treatment before water entered the UT. Despite this partial treatment, the UT was heavily orange stained downstream of Mayer Ranch, with oxidized Fe flocculant covering much of the water's surface and adhering to all wetted surfaces and substrates (Figure 2.3A and 2.3B). In mid-2006, a land reclamation project at Southeast Commerce filled two large mine collapse features. Part of the reclamation project was the installation of a collection drain that captured the MD subsurface and directed it into a 225-meter-long, 122-cm in diameter stormwater pipe located near the headwaters of the UT. The collection drain eliminated the partial treatment of MD at Southeast Commerce that was previously provided by the volunteer cattail marsh.

In 2008, the Mayer Ranch MD discharges, which enter the UT, near the middle of the study reach, were captured and treated using passive treatment technology, consisting of 10 process units covering approximately 2 ha. After years of successfully treating the discharges at Mayer Ranch, a second, 1-ha PTS was constructed in 2017 at Southeast Commerce to treat the last contributing source of artesian-flowing MD to the UT.

This study investigated the effects of these two ecologically engineered PTSs on the fishes in the UT. The design initially focused on a "before and after" assessment of the UT fish community relative to the construction of the Mayer Ranch passive treatment system (MRPTS). Subsequently, a "before and

after" assessment of the effect of the Southeast Commerce passive treatment system (SECPTS) was incorporated into the study with an additional site located immediately downstream of the 122-cm stormwater pipe that receives the effluent from SECPTS. It was hypothesized that in-stream water quality improvement following the implementation of passive treatment would result in increased fish community diversity and species richness despite no anthropogenic restoration efforts to address instream habitat.

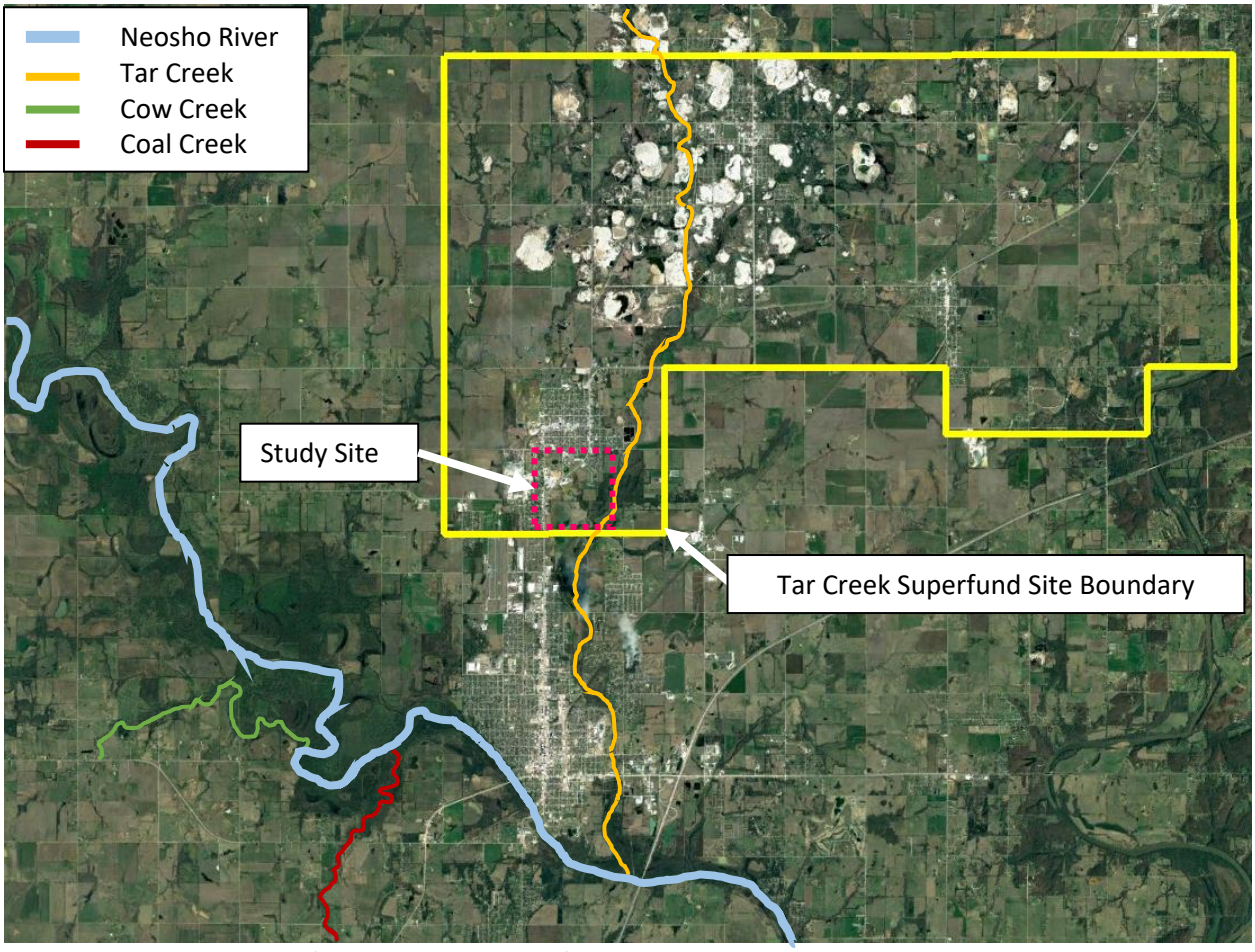

Figure 2.1: Aerial image of the Tar Creek Superfund Site and the surrounding area in Ottawa County, OK, USA showing study stream (Tar Creek) and reference streams (Cow and Coal Creeks) (*Source:* "Tar Creek Superfund Site". 36.971661° N, 94.816936° W. Google Earth. Sept. 7, 2021. Dec. 20, 2021.)

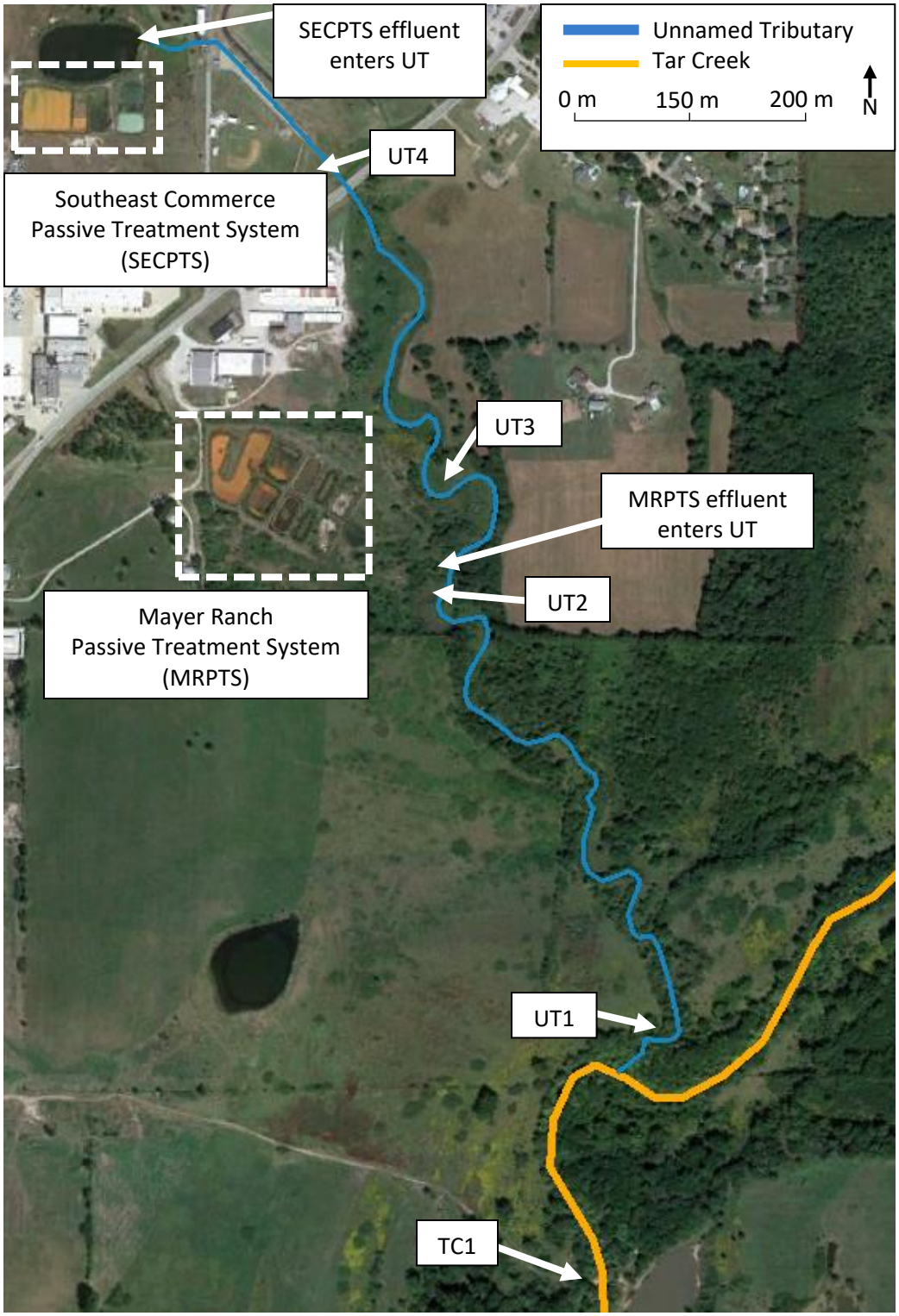

Figure 2.2: Aerial image of an Unnamed Tributary (UT) to Tar Creek (TC) showing the existing passive treatment systems, Mayer Ranch and Southeast Commerce, and sampling locations along the UT (MapQuest, 2021) (*Source:* "Unnamed Tributary to Tar Creek". 36.923922° N, 94.872845° W. Google Earth. Sept. 7, 2021. Dec. 20, 2021.)

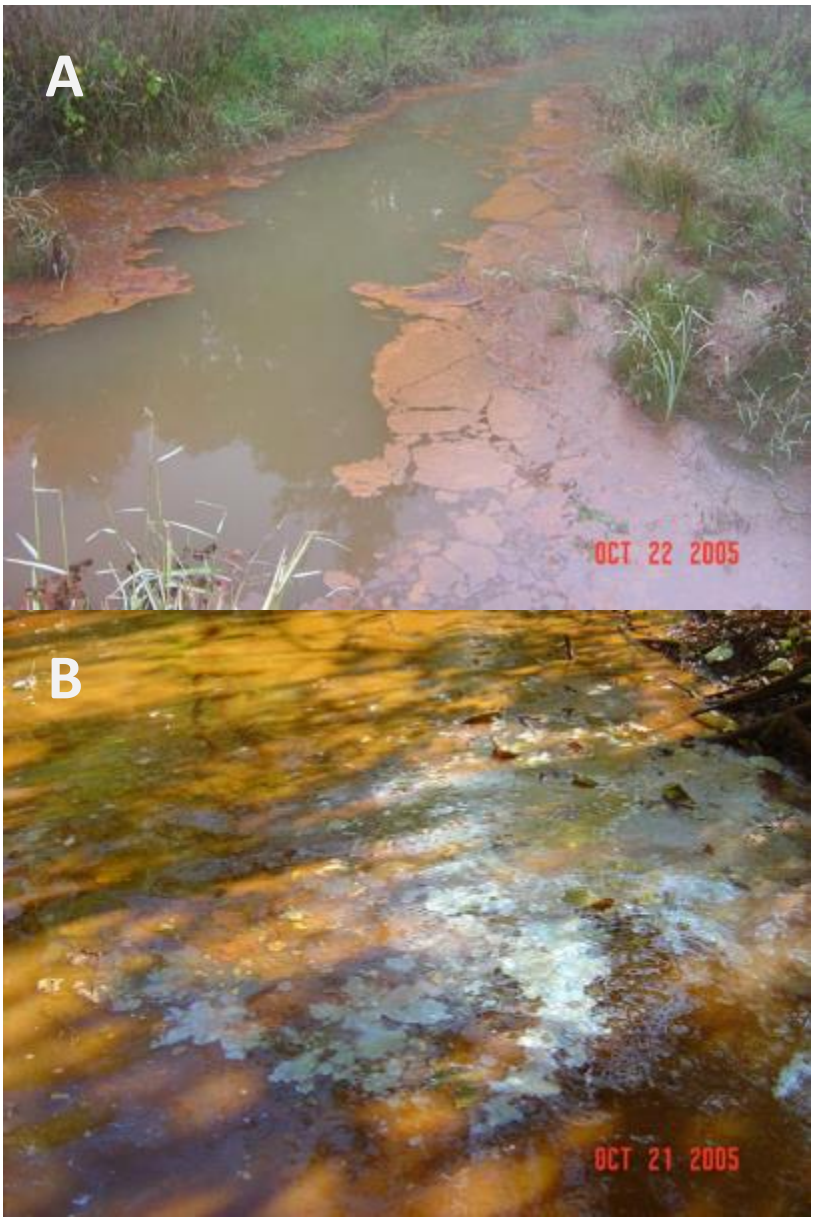

Figure 2.3: (October 2005). A: Oxidized iron flocculant in the Unnamed Tributary to Tar Creek, near the planned Mayer Ranch passive treatment system (MRPTS) outfall. B: Biofilm on water downstream from the planned MRPTS outfall from iron oxidizing bacteria (Photos by W. Matthews)

2.2 Methods

2.2.1 Fish Field Study Design and Sampling Locations

This study consisted of seven sampling sites, four sites on the UT, one site on Tar Creek, and two reference sites (Figures 2.1 and 2.2). All sites are on low-gradient streams in the Central Irregular Plains ecoregion, within the sparsely populated Neosho River watershed in Ottawa County, OK. The UT sites and Tar Creek proper are all within the TCSS, contaminated by abandoned Picher field mining. The reference sites, Coal and Cow Creeks, are outside the known mining-affected area and drain separately into the Neosho River (Figure 2.1).

This study was divided into three time periods: before MD treatment 2005-2007 (Period 1); after MRPTS completion but before SECPTS construction, 2009-2016 (Period 2); and after construction of SECPTS, 2017-2021 (Period 3). During Period 1, before implementation of passive treatment, three permanent sites were established on the UT relative to the effluent from the planned MRPTS to determine the status of the existing fish community in the UT. These sites were UT1, located approximately 700 m downstream of the planned MRPTS effluent near the confluence of the UT and Tar Creek; UT2, immediately downstream from the planned MRPTS effluent on the UT; and UT3, centered about 175 m upstream from the effluent of MRPTS on the UT (Figure 2.2). Therefore, during Period 2, after the construction of MRPTS, untreated MD from Southeast Commerce MD discharge was diluted at UT1 and UT2 with treated MD from the outfall of MRPTS, while UT3 continued to receive only untreated MD from the Southeast Commerce MD discharge.

A fourth site was added in December of 2014 at the headwaters of the UT, following confirmation that a second PTS, SECPTS, to better evaluate the effects of SECPTS rather than only relying on data from UT3. UT4 was located approximately 300 m downstream of SECPTS effluent, where the UT emerges from a 225-meter-long, 122-cm diameter, stormwater pipe. This site was sampled with the other sites on all subsequent collection dates during the second and third time periods.

Any improvement in fish communities in the UT resulting from the treatment of the MD would depend on a source pool of species for colonization. Accordingly, a permanent sampling site on the Tar Creek was established to monitor the availability of species that could enter the UT. The site, TC1, was located about 400 m downstream from the confluence of the UT, at the closest accessible point on Tar Creek near the UT (Figure 2.2).

The reference sites, Cow and Coal Creeks, provided controls to detect unknown region-wide changes that could affect fish communities. These sites were physically and ecologically comparable to

the UT sites, typically well-watered, and were monitored throughout the study.

The UT sites ranged seasonally from 2 to 7 m wide, with maximum depths ranging from 0.6 to 1.50 m. Cow and Coal Creeks were typically 4 to 7 m wide and 0.6 to 1.0 m deep, with one pool 10 m wide in the lower part of the Coal Creek reach. The Tar Creek site was a larger stream with two pools ranging 12 to 20 m wide, but with most of the sampled reach measuring about half that width; maximum depth ranged from 1.0 to 1.75 m in the large pools, but most of the reach was less than 0.6 m deep. Lengths of the reaches sampled varied with water level (e.g., if parts of a reach were dry), but typical reach lengths were: UT1, 105 m; UT2, 70 m; UT3, 130 m; UT4, 35 m (one single pool at the outfall pipe and a short, shallow segment downstream to the highway culvert); Tar Creek, 160 m; Cow Creek, 130 m; Coal Creek, 170 m (with lower parts of the Coal Creek reach sampled when upper parts on bedrock were dry or too shallow to seine).

2.2.2 Water Quality and Quantity Sampling

Water quality and quantity sampling events were regularly conducted by the University of Oklahoma Center for Restoration of Ecosystems and Watersheds (CREW) on Tar Creek and the UT at UT1, UT2, and UT3 since 2005, and UT4 since 2009. The UT4 water quality data from 2009 to 2016 was collected at the outflow of the subsurface collection drain, while the water quality data collected after the construction of SECPTS was collected at the UT4 site. In addition, CREW has conducted regular water quality sampling to monitor the performance of both MRTPS and SECPTS since the construction of the respective systems. Field water quality parameters (pH, dissolved oxygen, temperature, and conductivity) were measured with a YSI 6-series multiparameter datasonde; alkalinity and turbidity were measured in the field using Hach test kits. Sulfate and total metals samples for Cd, Fe, Pb, and Zn were collected and preserved in the field using nitric acid, then analyzed in the CREW laboratory following USEPA standard methods (USEPA, 2014). Streamflow measurements were collected at each site using a SonTek FlowTracker Handheld ADV. The flow rates of MRPTS were measured using a 20 L bucket and stopwatch, while at SECPTS, flow rates were calculated using a sharp-crested V-notch weir and a Solinst Level Logger pressure sensor that logged values every 15 minutes.

2.2.3 Fish Sampling

Fish sampling was standardized by taking 10 seine hauls per site in a downstream direction (or using the seine as a kicknet in riffles; Matthews and Marsh-Matthews, 2017), spaced haphazardly throughout the reach to include as many kinds of microhabitat as possible (e.g., open water, undercut banks, around structures or woody debris, and within vegetation). Seine hauls that were not completed

because of snags or other impediments were not included in the total count. Seines were of 3.17 mm (1/8 inch) “Ace” mesh, 1.22 m (4 ft.) deep, and 2.44 m (8 ft.) long for most samples, but a 4.57 m (15 ft.) long seine was used at portions of sites where stream width was > 2.44 m to adequately sample open water.

Sampling typically occurred when streams were at base flow. However, the base flow of these streams fluctuated seasonally, with greater flow in the spring and lesser flow during the summer. A few samples were excluded from analyses if seining was inadequate because of high water or flooding, impassible aquatic vegetation, or similar impediments, as recorded in field notes.

In a pilot study at all sites in 2004 and early 2005, fishes were Anesthetized using MS-222 and then preserved in 10% formalin for laboratory identification and vouchering in the Sam Noble Oklahoma Museum of Natural History at the University of Oklahoma. In most sampling events thereafter, fishes were identified, counted, and released, with a minimal number of individuals retained for laboratory analyses of reproductive traits (Franssen, 2009). Individuals not able to be identified species and voucher specimens of all species encountered during the study were also retained for laboratory and archival storage in the museum or reference collections in the CREW laboratory. Sampling events occurred monthly from April to October before MRPTS construction (Period 1; 2005-2007); omitted in 2008 because of disturbance from the construction of MRPTS; occurred sporadically 2009-2012 (due to funding availability); in December 2014, then regularly in once per season in spring, summer, and autumn from 2015 to 2019, with two additional sampling events in the summers of 2020 and 2021. Sampling was conducted under scientific collecting permits from the Oklahoma Department of Wildlife Conservation, and approvals by the Institutional Animal Care and Use Committee (IACUC) of the University of Oklahoma. Samples from the Tar Creek study in 2004 and 2005 were summarized by Franssen et al. (2006), which also provides a species distribution list for these and other nearby small streams in the Neosho River watershed in Ottawa County.

2.2.4 Statistical Analyses

2.2.4.1 Aqueous Metals

The metal removal efficiencies of the two PTSs were evaluated by calculating the flow-weighted average total metals concentrations of the three MD inflows for each system for Cd, Fe, Pb, and Zn. The flow weighted inflow total metals concentrations and the outflow total metals concentrations were evaluated for normality using a Kolmogorov–Smirnov test. The inflow and outflow metals concentrations were then compared using a one-tailed, paired T-test. The effect of passive treatment on

the metals concentrations in the UT was analyzed using a single factor analysis of variance (ANOVA), comparing the concentrations of each metal from the three time periods.

An initial Principal Component Analysis (PCA) of concentrations of Cd, Fe, Pb, and Zn across time at UT1 showed that Zn and Cd loaded primarily on a first axis in the same direction, but orthogonal to a second axis on which Fe and Pb were highly loaded in the same direction. A simple product-moment correlation also indicated that those metals within those pairs were highly correlated. Therefore, only one metal from each highly correlated pair was selected for comparison to fish community data: Fe and Zn.

2.2.4.2 Fishes

Fish sample data were divided into the same three time periods used in previous analyses. UT2 was abandoned after 2015 because beaver dams converted the stream in that reach to a wetland, where the aquatic vegetation and water depth made seining ineffective. Therefore, it was not included in period 3. Site UT4 was not included in Period 1, because it was not established until December 2014. Otherwise, UT1 and UT3 study sites, Coal and Cow Creeks reference sites, and Tar Creek were sampled during all three periods.

A database of species abundances by date was compiled for each site and checked against original field and laboratory counts. For fishes that were not able to be identified to species in the field, the following conventions were adopted. Buffalofish juveniles were recorded as "*Ictiobus* species." Small, young-of-year sunfish and gar were counted as "*Lepomis* YOY" and "*Lepisosteus* YOY," respectively. Topminnows in northeastern Oklahoma are mostly blackstripe topminnows (*Fundulus notatus*), but some key to blackspotted topminnows (*Fundulus olivaceus*), and where they co-occur, impossible to determine to which species a juvenile or a female belongs with confidence (Matthews and Marsh-Matthews, 2015). All *Fundulus* were recorded by convention as "*Fundulus notatus*."

The databases for each site were imported into PC-Ord Version 7, which was used to calculate species richness and the Shannon diversity index. these metrics were used because they are universally recognized and commonly reported metrics. For sites on the UT, notched box and whisker plots (MedCalc Version 20) were used to compare fish species richness and diversity to aqueous total Fe and Zn concentrations at the same locations. Notched box plots depict the median, the 1st and 3rd quartiles, the range for a sample, and a "notch" above and below the median which, if non-overlapping for any pair of samples, indicates that the samples statistically differ at a 95% confidence interval. See Ellison (2001) for an explanation of this method and Marsh-Matthews and Matthews (2010) for further explanation and examples.

In a pilot study for multivariate analyses at the scale of the whole fish community (i.e., including all sampling sites and events from the study), results of Detrended Correspondence Analysis (DCA), Reciprocal Averaging (RA), and Nonmetric Scaling (NMS) were compared with several different distance metrics for several of the UT sites. While results were similar, NMS using the Sorensen (Bray-Curtis) dissimilarity measure gave the best separation of samples within a site. Therefore, this approach was taken for the NMS analyses reported here.

NMS produces slightly different results for any given run starting with the same distance matrix, as it iteratively seeks a solution to place points in space (on new axes) in a pattern that best represents the relationships among all samples in the underlying distance matrix (McCune and Grace, 2002). Following McCune and Grace (2002), four NMS trial runs for each site were conducted, with data separated into the time periods described above, and with selected options of "no Autopilot," Sorensen (Bray-Curtis) distance measure, 250 iterations with real data, and stepping down from a 3-dimensional solution. The axis coordinates resulting from the NMS analyses were used to draw convex hulls enclosing each of the time periods for the study. The final stress (a measure of goodness of representation of the biplot), the plot of stress versus iterations (as a measure of the stability of the solution), and the similarity of patterns among the temporal groups in the NMS axis graphs comparing the four runs were examined. In every case but two, the NMS runs found acceptable 2-dimensional solutions, stress was acceptable (0.15 or lower), and at least three of four biplots showed similar relationships among groups. Once the NMS generated consistent and reliable results (e.g., no local minima, McCune and Grace, 2002), a final NMS run with the same options was completed to report in this publication. The final graphs for each site were inspected for patterns among the time periods. These periods were statistically tested for differences by the Multi-response Permutation Procedures (MRPP) of PC-Ord using the Sorensen (Bray-Curtis) distance measure. The MRPP is a non-parametric procedure testing the hypothesis of "no difference" among pre-defined groups (McCune and Grace, 2002).

2.3 Results

2.3.1 Water Quality

The combined discharge flow rates of MRPTS and SECPTS comprise approximately 80% of the base flow in the UT (Tables 2.1 and 2.2). Both PTSs significantly decreased the metals concentrations of Cd, Fe, Pb, and Zn comparing the flow weighted inflows and outflow of the systems ($p < 0.05$). The

average effluent total metals concentrations of Cd and Pb were decreased to below the detection limits, while Fe and Zn total metals concentrations were decreased by 99% and 93%, respectively (Table 2.1). In addition, both systems markedly increased pH from approximately 6 to a circumneutral pH (Table 2.1). Alkalinity and sulfate decreased in concentrations of approximately 50% and 5%, respectively. These constituents contribute to the chemical and biological reactions in PTSs that are necessary to retain the metals from the MD. The removal efficiencies of passive treatment are reflected in the total metals concentrations in the UT as well, where UT1, UT2, and UT3 showed a significant difference of all four metals concentrations when comparing the three time periods ($p < 0.05$) (Table 2.2).

Table 2.1: Total aqueous metals concentrations and selected physical parameters of the Mayer Ranch (MRPTS) and Southeast Commerce (SECPTS) passive treatment systems using flow weighted averages ± the standard deviations for the inflows of each treatment system

Site Name	Flow (lpm)		Sample Size (n)	pH	Specific Conductivity (mS/cm)	Alkalinity (mg/L $CaCO_3$ eq.)	Sulfate (mg/L)	Cd† (mg/L)	Fe (mg/L)	Pb† (mg/L)	Zn (mg/L)
MRPTS	415±48	In	181	6.00±0.21	3.38±0.44	385±54.6	2,215±386	0.016.1±0.012	159±38.8	0.110±0.130	7.30±1.88
		Out	57	7.05±0.19	3.13±0.28	191±45.4	2,079±494	<0.0006 (7)	0.45±0.41	<0.0195 (14)	0.53±0.83
SECPTS	465±35	In	127	5.97±0.23	3.24±0.31	328±32.3	2,106±396	0.019±0.009	141±20.5	0.268±0.124	6.69±1.14
		Out	54	6.78±0.33	2.83±0.43	139±43.2	1,825±228	<0.0006 (14)	1.42±1.22	0.021±0.009	0.58±0.99

†Values in parentheses indicate the number of samples with concentrations above the detection limit of 0.00064 mg/L for Cd and 0.0195 mg/L for Pb

Table 2.2: Mean values of total aqueous metals concentrations and selected physical parameters ± the standard deviations at three locations on the unnamed tributary (UT) to Tar Creek separated by three time periods: 1) 2005-2007 before implementation of passive treatment 2) 2009-2016 after the implementation of the Mayer Ranch passive treatment system 3) 2017-2021 after the implementation of the Southeast Commerce passive treatment system

Site Name	Date Range	Sample Size (n)	Flow (lpm)	pH	Alkalinity (mg/L $CaCO_3$ eq.)	Specific Conductivity (mS/cm)	Tot. Cd† (mg/L)	Tot. Fe (mg/L)	Tot. Pb† (mg/L)	Tot. Zn (mg/L)
UT1	2005-2007	36	2,094±4,648	6.31±0.28	160±65.4	2.61±0.74	0.017±0.029 (34)	44.3±38.3	0.025±.0.014 (28)	8.23±5.07
	2009-2016	36	2,058±4,996	6.83±0.26	146±108	2.45±0.73	0.003±0.003 (25)	2.64±5.06	<0.0195 (3)	2.71±1.49
	2017-2021	19	1,915±3,253	7.29±0.15	128±22.8	2.11±0.53	<0.0006 (8)	0.71±0.47	<0.0195 (2)	0.70±0.86
UT2	2005-2007	35	1,430±1,077	6.14±0.17	266±95.3	2.96±0.66	0.023±0.029 (35)	111±66.2	0.038±.0.019 (30)	9.72±4.92
	2009-2016	37	1,191±914	6.61±0.29	165±52.2	2.62±0.72	0.005±0.004 (32)	17.1±15.3	<0.0195 (11)	3.50±1.99
	2017-2021	19	N/A‡	7.05±0.50	146±35.5	2.02±0.53	<0.0006 (7)	1.45±2.12	<0.0195 (3)	0.89±1.06
UT3	2005-2007	35	660±852	6.73±0.37	118±44.6	1.92±0.82	0.026±0.046 (28)	9.94±20.51	0.020±0.015 (26)	8.26±6.62
	2009-2016	39	1,118±1,829	6.38±0.24	177±51.9	2.38±0.74	0.012±0.001 (37)	42.3±29.1	0.030±0.018 (27)	6.08±2.51
	2017-2021	19	1,064±838	7.17±0.29	134±28.1	1.97±0.53	0.009±0.008 (9)	2.20±4.08	<0.0195 (4)	0.90±1.09
UT4	2009-2016	50	343±53.1	6.02±0.13	296±39.3	3.05±0.30	0.026±0.011	130±15.0	0.066±0.011	8.31±1.30
	2019-2021	21	371±192	6.92±0.32	131±38.2	2.44±0.56	0.001±0.001 (9)	1.00±0.48	<0.0195 (9)	0.67±0.80

†Values in parentheses indicate the number of samples with concentrations above the detection limit of 0.00064 mg/L for Cd and 0.0195 mg/L for Pb

‡Flow data were not collected during this period due to the recolonization of the North American beaver (*Castor canadensis*) at the UT2 site

2.3.2 Fish Community Analyses

Results for fish, and total aqueous metals concentrations as applicable, are treated here site by site, as each provides unique insights into the effects of the two PTSs (MRPTS and SECPTS) on the fish communities in the UT, relative to a source pool of species in Tar Creek and the reference sites. The first alternative hypothesis to be examined was that there could have been unknown phenomena causing changes in fish communities throughout the Neosho River drainage area. This hypothesis was tested by examining variations in richness and diversity in the Cow and Coal Creek reference fish communities, outside the contaminated area, for any long-term trends (Figures 2.4A and 2.4B).

2.3.2.1 Reference Sites

Cow Creek and Coal Creek showed a wide range in species richness and Shannon diversity from 2005 to 2019, with no clear trends (Figures 2.4A and 2.4B). There was no evidence of any long-term change in species richness or Shannon diversity, although in some cases, climate conditions affected the fish communities at the reference sites. For example, no fishes were collected in October 2012 at Cow Creek, despite vigorous seining throughout the recently rewatered reach, due to a severe drought that left the entire reach dry for the previous summer (landowner, personal communication). Similarly, a drought in 2007 resulted in July and August collections at Coal Creek yielding only large numbers of the highly tolerant (Matthews and Marsh-Matthews, 2011) western mosquitofish (*Gambusia affinis*), and in September, four additional species were found but western mosquitofish comprised 98% of the total fishes collected (Figure 2.5).

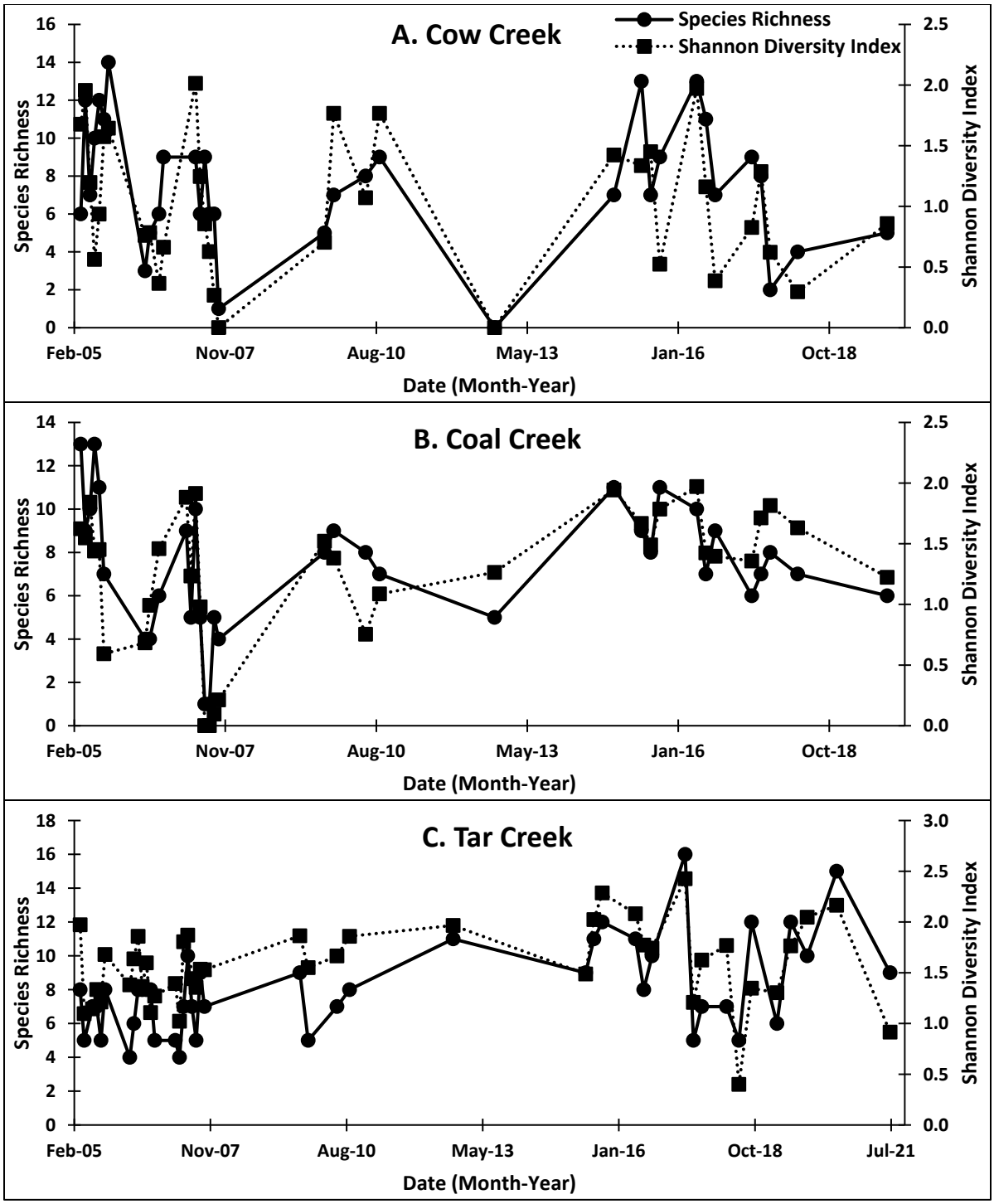

Figure 2.4: Total fish species and Shannon diversity index for each fish collection conducted in A. Cow Creek B. Coal Creek C. Tar Creek, located in Ottawa County, Oklahoma

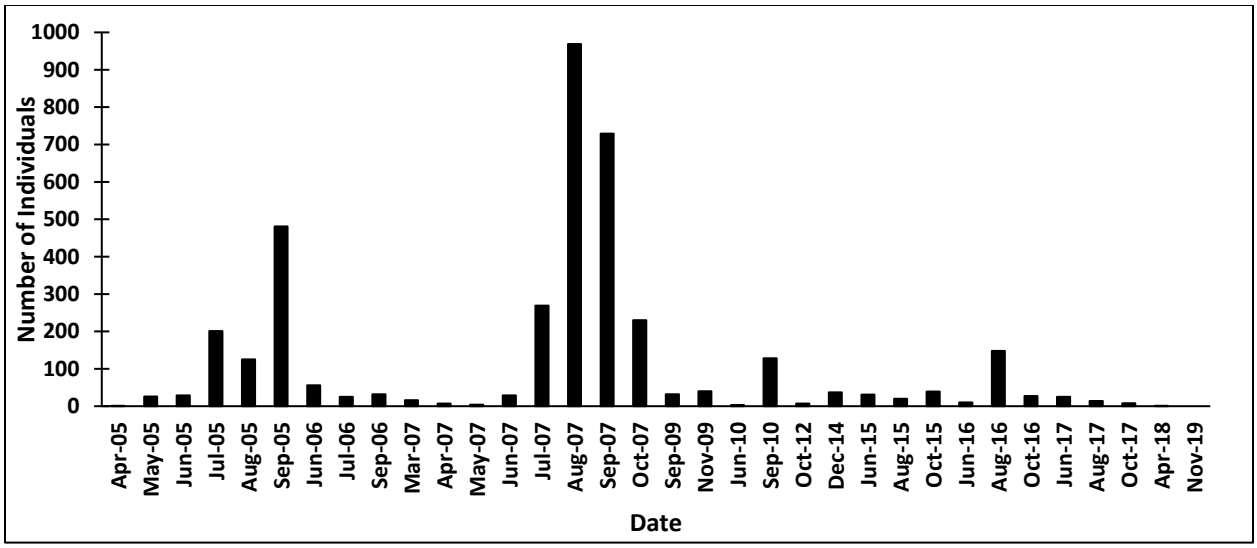

Figure 2.5: Number of western mosquitofish (*Gambusia affinis*) collected in Coal Creek in Ottawa County, Oklahoma from 2005 to 2019

A 2-dimensional NMS solution was the best fit for the Cow Creek fish community, with final stress = 0.1212 and final instability of zero. Convex hulls representing the three study periods overlapped strongly in the NMS space (Figure 2.6A). The MRPP showed no significant difference among the three time periods (p = 0.315). There was one noteworthy outlier in April 2018 when an unusually large number (n = 133) of red shiners (*Cyprinella lutrensis*) was collected, with few other fishes. Red shiners were present in most samples at this site, but not in such numbers at any other time. However, it is a common shoaling minnow in Oklahoma streams. It was hypothesized that the large number of individuals was due to chance capture of a shoal and not indicative of any pervasive change in the local community.

The Coal Creek community showed considerable overlap among the convex hulls for the three time periods (Figure 2.6B) in a recommended 2-dimensional solution. The final stress was 0.1586, with final instability of zero. Despite overlaps among time periods, the MRPP showed that the periods significantly differed (p = 0.006), with an effect size of A = 0.042. This overall difference among the three time periods was primarily driven by collections in September 2005 and four months from July to October 2007, all at the extreme left in ordination space on the biplot (Figure 2.6B). In those samples, there was an unusually high number of western mosquitofish (from 269 to 969 individuals) relative to all other samples at this site, and very different from the last three years of study, Post-PTS (Figure 2.6B) when few to zero mosquitofish were taken (Figure 2.5). Western mosquitofish populations can be very "flashy," varying greatly from year to year (Matthews and Marsh-Matthews, 2011). Therefore, finding large numbers in the late summer of any given year is neither surprising nor indicative of any trenchant

community change. Overall, both reference sites were highly variable but without any clear long-term trend. Therefore, the alternative hypothesis of “region-wide” pervasive changes in the fishes or fish communities was rejected.

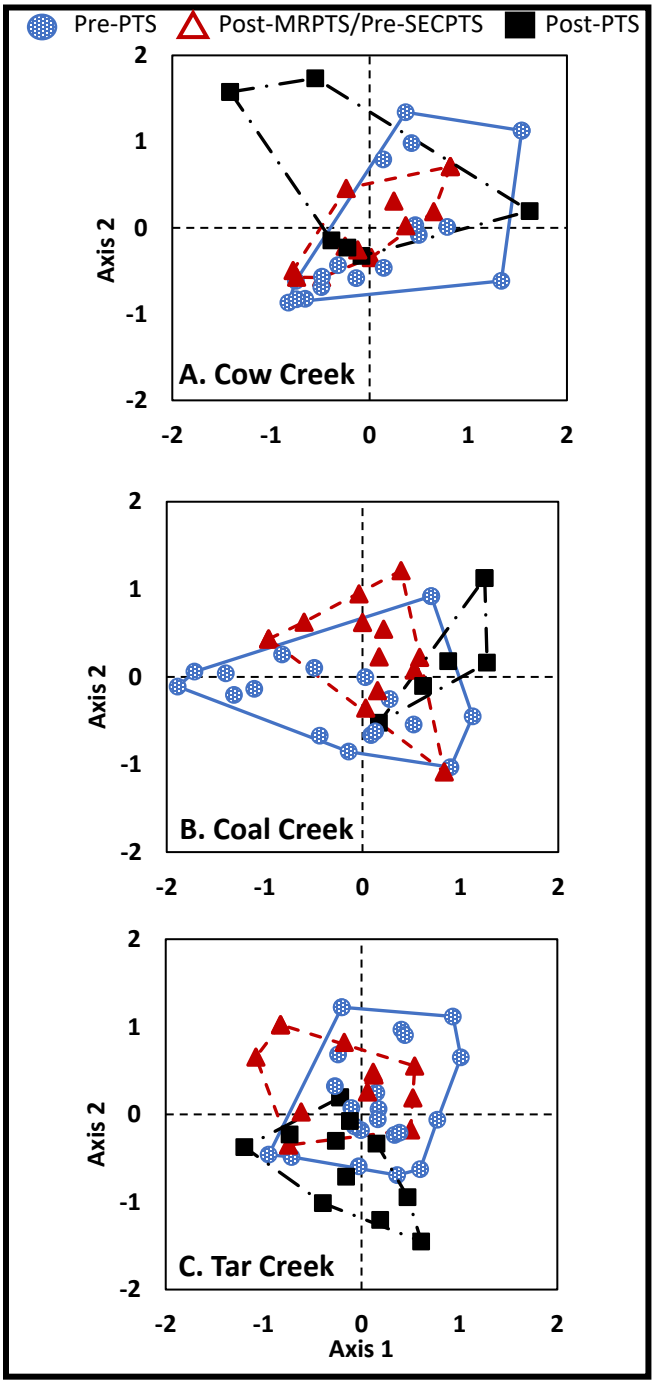

Figure 2.6: Nonmetric multidimensional scaling biplots with convex hulls representing the fish collections from three study periods before and after the implementation of two passive treatment systems (Mayer Ranch passive treatment system [MRPTS] and Southeast Commerce passive treatment system [SECPTS]) for A. Cow Creek, B. Coal Creek, and C. Tar Creek, located in northeastern Oklahoma

2.3.2.2 Tar Creek (source pool for UT recolonization)

Tar Creek, below the confluence of the UT, had a substantial pool of species available as potential colonists for the UT. From 2005 to 2021, there was an average of 8.05 species per sample, ranging from 4 to 16 species per collection (Figure 2.4C), with a total of 31 species overall. There was a weak trend for an increase in numbers of species over time, but the numbers of species from 2009 to 2021 were highly variable. The most abundant species in the Tar Creek fish community were six species of minnows (Leuciscidae), topminnows of the genus *Fundulus* (Fundulidae), western mosquitofish (Poeciliidae), six species of sunfish (genus *Lepomis*), and largemouth bass (*Micropterus salmoides*) (Centrarchidae), with the occasional presence of suckers (Catostomidae) and catfish (Ictaluridae).

The Tar Creek fish community NMS showed a 3-dimensional solution to be best, with final stress of 0.1572 and a final instability of zero. A biplot of Axis 1 x 3 showed a pattern very similar to the biplot of Axis 1 x 2 (Figure 2.6C). The Axis 1 x 2 biplot showed overlap in samples from the first two periods, but a substantial shift toward the lower right of ordination space in Figure 2.6C for the third period, after SECPTS began operation. The MRPP comparing the three time periods was significant ($p < 0.0001$). However, the study was not designed to specifically detect PTS-related changes in Tar Creek, but rather to determine which species were available to potentially colonize the UT if water quality conditions improved.

2.3.2.3 UT 1

At UT1, the most downstream UT site, total Fe and Zn concentrations significantly decreased from the first to the third period ($p < 0.05$), by 98.5% and 91.5%, respectively (Figures 2.7A and 2.7B, and Table 2.2). Fish species richness and Shannon diversity both significantly increased after MRPTS began operation in 2008. After the implementation of SECPTS, the total aqueous metals concentrations at UT1 continued to decrease, and the site showed a slight but non-significant trend for further improvement in the fish community (Figures 2.7C and 2.7D).

For the UT1 fish community, a 2-dimensional NMS solution was best, with final stress of 0.1071 and final instability of zero. The NMS biplot for UT1 (Figure 2.8A) showed the first period (before MRPTS) non-overlapping with the two later periods (after MRPTS and SECPTS began operation). The MRPP indicated an overall significant difference among groups ($p < 0.0001$).

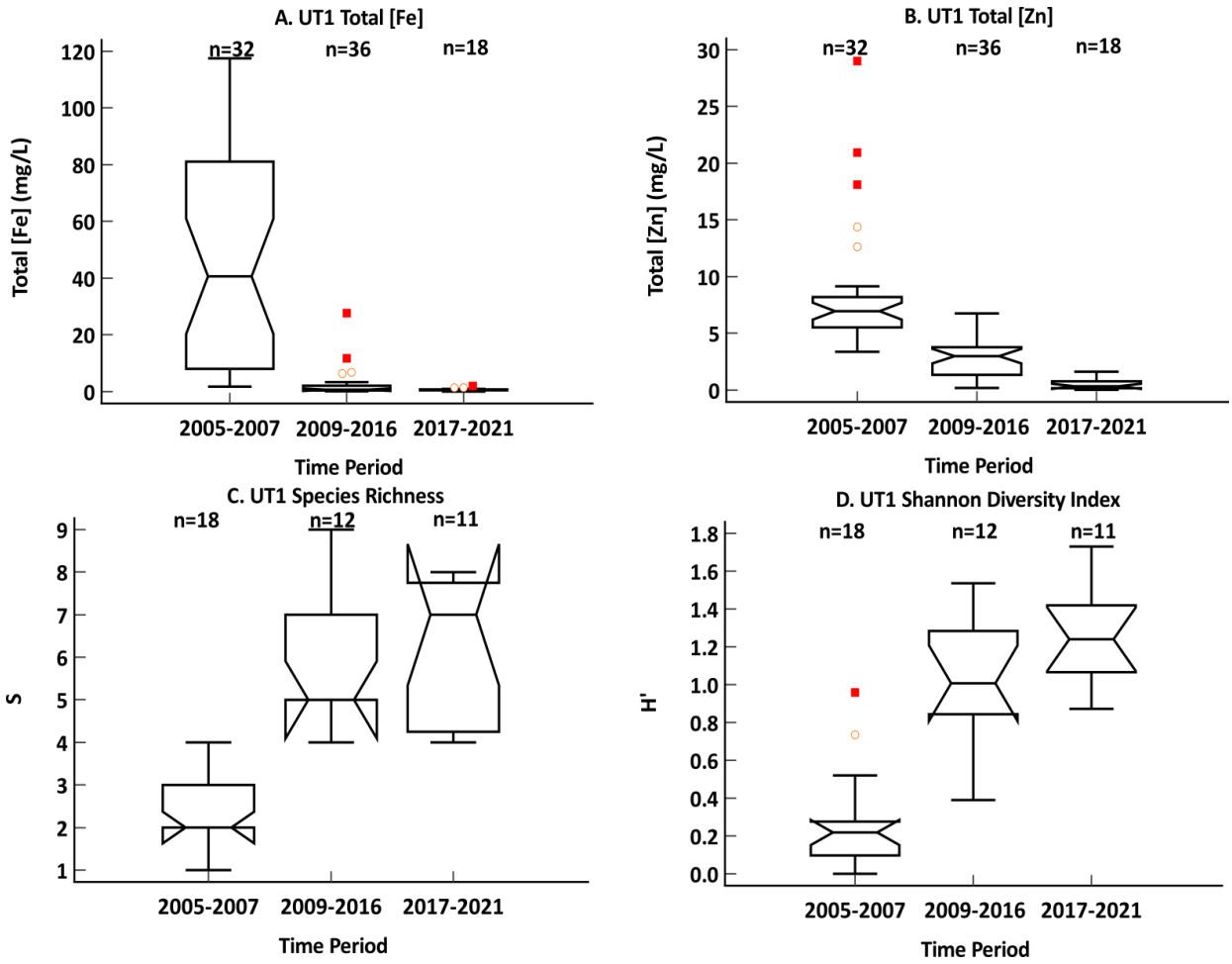

Figure 2.7: Notched box and whisker plots comparing total aqueous metals concentrations of Fe (A) and Zn (B) to the species richness (C) and Shannon diversity (D) at site UT1 on an Unnamed Tributary to Tar Creek, during three time periods, before and after the implementation of two passive treatment systems in Ottawa County, Oklahoma, where n indicates the sample size

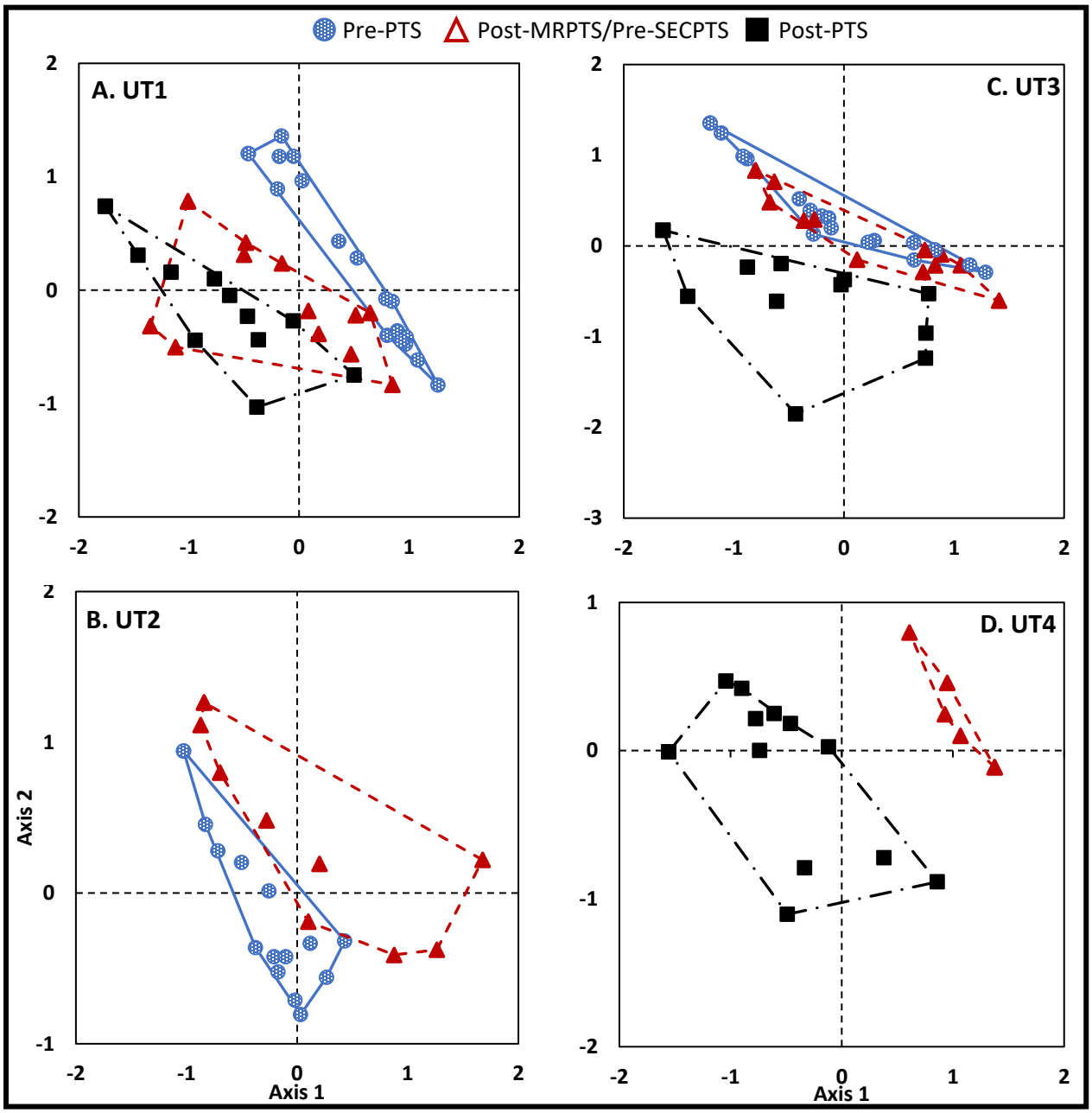

Figure 2.8: Nonmetric multidimensional scaling biplots with convex hulls representing fish collections on an Unnamed Tributary (UT) to Tar Creek at four locations along the UT, comparing three time periods, before and after the implementation of two passive treatment systems (Mayer Ranch passive treatment system [MRPTS] and Southeast Commerce passive treatment system [SECPTS])

2.3.2.4 UT2

At UT2, immediately downstream from MRPTS discharge, a significant decrease in Fe and Zn from Period 1 to Period 2 ($p < 0.05$) was seen similar to UT1, decreasing 85% and 64%, respectively (Figures 2.9A and 2.9B). Concomitantly, there was a significant increase in fish species richness and diversity at UT2. Before MRPTS began operation, the fish community in the UT2 reach was heavily dominated by western mosquitofish, often with only one or no other species present. After MRPTS began operation, the median richness was at five species, and Shannon diversity increased significantly ($p < 0.05$) (Figures 2.9C and 2.9D). Fishes were not collected during Period 3 at UT2 because of beaver activity that established a wetland full of pondweed (*Potamogeton*), making it impossible to effectively seine after 2015. However, the total aqueous metals concentrations during Period 3 continued to show a decreasing trend, following the implementation of SECPTS (Figures 2.9A and 2.9B).

A 2-dimensional NMS solution was the best option to describe the fish community at UT2, with final stress of 0.0575 and final instability of zero. The NMS groups showed a sharp difference before and after the implementation of MRPTS (Figure 2.8B) with little overlap, and the MRPP indicated the two groups of fish samples were significantly different ($p = 0.012$).

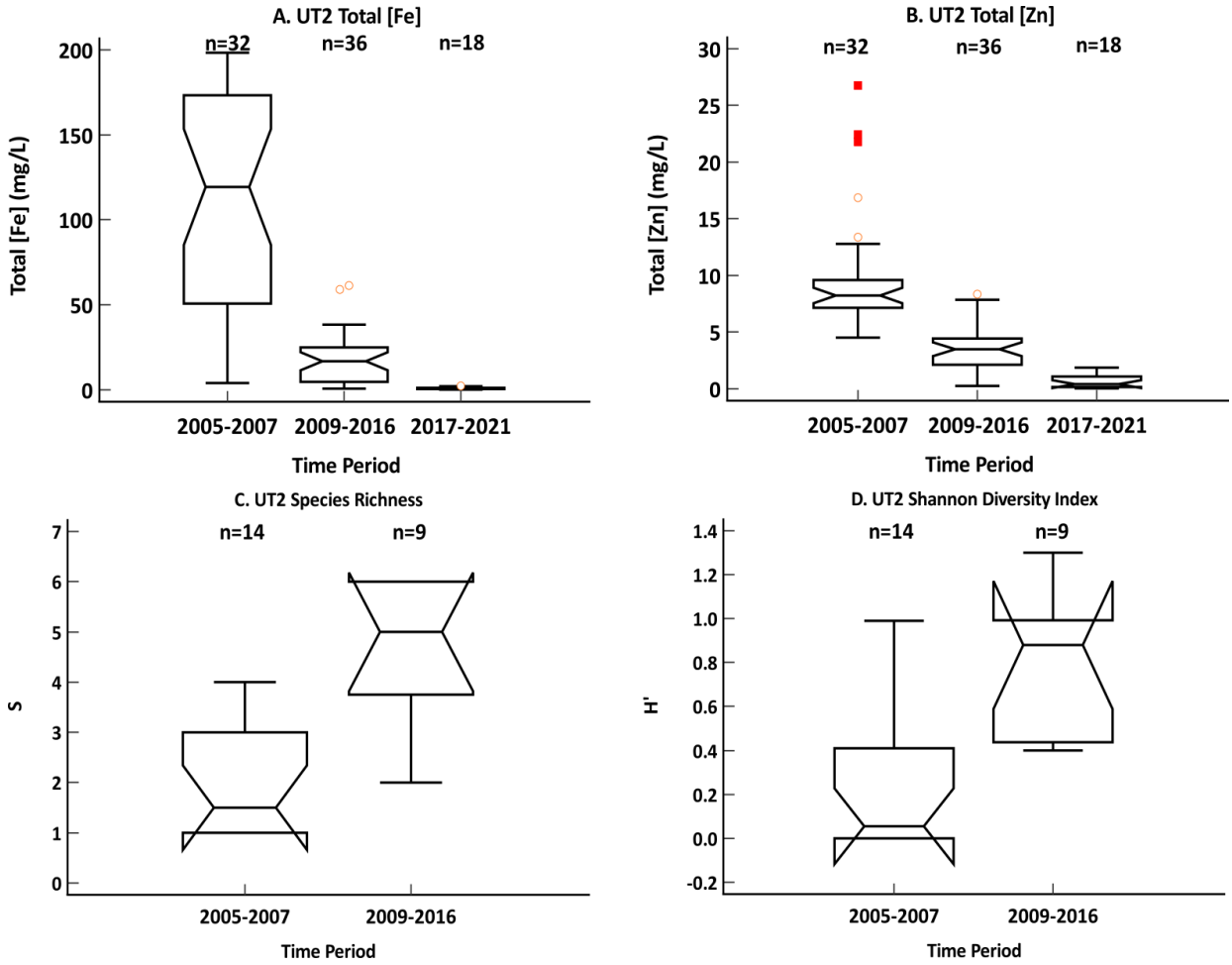

Figure 2.9: Notched box and whisker plots comparing total aqueous metals concentrations of Fe (A) and Zn (B) to the species richness (C) and Shannon diversity (D) at site UT2 on an Unnamed Tributary to Tar Creek, during three time periods, before and after the implementation of two passive treatment systems in Ottawa County, Oklahoma, where n indicates the sample size

2.3.2.5 UT3

The UT3 reach had the most complicated history for total aqueous metals concentrations and fish community data, because of the land reclamation at the Southeast Commerce site that occurred from 2006 to 2007. The partial natural treatment of MD provided by volunteer cattail marsh during Period 1 resulted in lesser Fe concentrations (Figure 2.10A). However, the upstream land reclamation at Southeast Commerce removed metal-laden sediments and the volunteer cattail marsh, which resulted in elevated Zn concentrations when the sediments were disturbed during the reclamation in the first period, and elevated Fe concentrations in the second period resulted from the loss of the natural treatment that was previously provided by the volunteer cattail marsh (Figures 2.10A and 2.10B). Between the first and second periods, fish species richness and Shannon diversity at UT3 increased slightly from 2.11 to 3.00 and 0.17 to 0.36, respectively, despite the presence of trace metals. In all sampling from 2005 through 2016, the local community in UT3 was dominated by western mosquitofish, often in very large numbers (>200 individuals), and often either the only species present or with one to three other species in low numbers.

After SECPTS began operation in February 2017, there was a marked, significant decrease in both Fe and Zn in the UT3 reach ($p < 0.05$) (Figures 2.10A and 2.10B). Similarly, fish species richness and diversity increased significantly ($p < 0.05$) (Figures 2.10C and 2.10D). During the third period, the species richness ranged from 5 to 12 species, with an average of 6.82. Compared to the previous periods, the Shannon diversity index approximately tripled to 1.26 (Figures 2.10C and 2.10D).

For the UT3 NMS analyses, a 2-dimensional solution was best, with final stress 0.621 and final instability of zero. The NMS biplot (Figure 2.8C) showed a strong overlap of the fish communities in the first two periods, but a complete divergence of the community in the third period, after SECPTS began operation. An MRPP with three groups showed a significant difference ($p = 0.0065$).

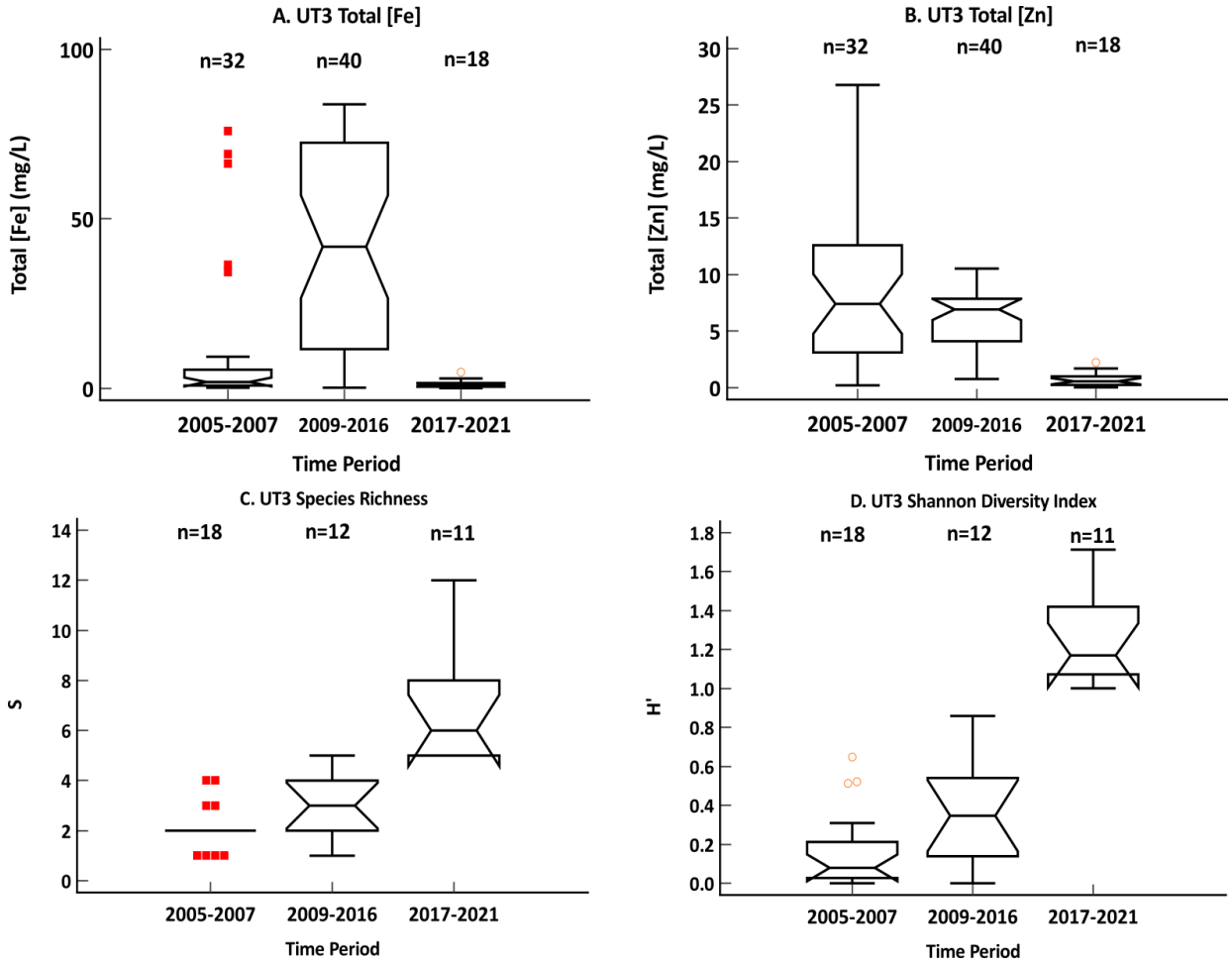

Figure 2.10: Notched box and whisker plots total aqueous metals concentrations of Fe (A) and Zn (B) to the species richness (C) and Shannon diversity (D) at site UT3 on an Unnamed Tributary to Tar Creek, during three time periods, before and after the implementation of two passive treatment systems in Ottawa County, Oklahoma, where n indicates the sample size

2.3.2.6 UT4

The total aqueous metals concentrations of Pb and Zn at UT4 collected during Period 3 were significantly less ($p < 0.05$) than the metals concentrations collected at the outflow of the subsurface collection pipe from Period 2 (Table 2.2 and Figures 2.11A and 2.11B). Before SECPTS operation, the fish species richness ranged from zero to three species (mean = 1.83), heavily dominated by western mosquitofish. During the third period, after SECPTS began operation in February 2017, the outflow from the stormwater pipe and the head pool at UT4 changed dramatically, returning to more natural water color, with a sharp decrease in orange color and flocculants (Figure 2.12). In 2017 and 2018, the species richness ranged from 3 to 12 per sample (mean = 6.83), with the last sample collected in July 2021 showing the greatest species richness (Figure 2.11C). Shannon diversity also showed a marked increase after SECPTS began operation (Figure 2.11D). During the third period, western mosquitofish remained present but in highly variable numbers, and they were no longer the dominant species. One year after the construction of SECPTS, there was a large increase in bluegill (*Lepomis macrochirus*), increasing from an average of 0.44 individuals captured per sample event before SECPTS to 111 individuals after the implementation of SECPTS. Additionally, multiple centrarchids colonized UT4 that were previously not present, including warmouth (*Lepomis gulosus*), longear sunfish (*Lepomis megalotis*), redear sunfish (*Lepomis microlophus*), and black crappie (*Pomoxis nigromaculatus*). Notably, largemouth bass, an important game fish, showed a substantial increase as well.

For UT4, the NMS analysis found a 2-dimensional solution with final stress of 0.0727 and instability of zero. The biplot (Figure 2.8D) showed complete separation of the fish community before (2014-2016) and after (2017-2021) the implementation of SECPTS. An MRPP of differences between the two periods was significant ($p < 0.0001$).

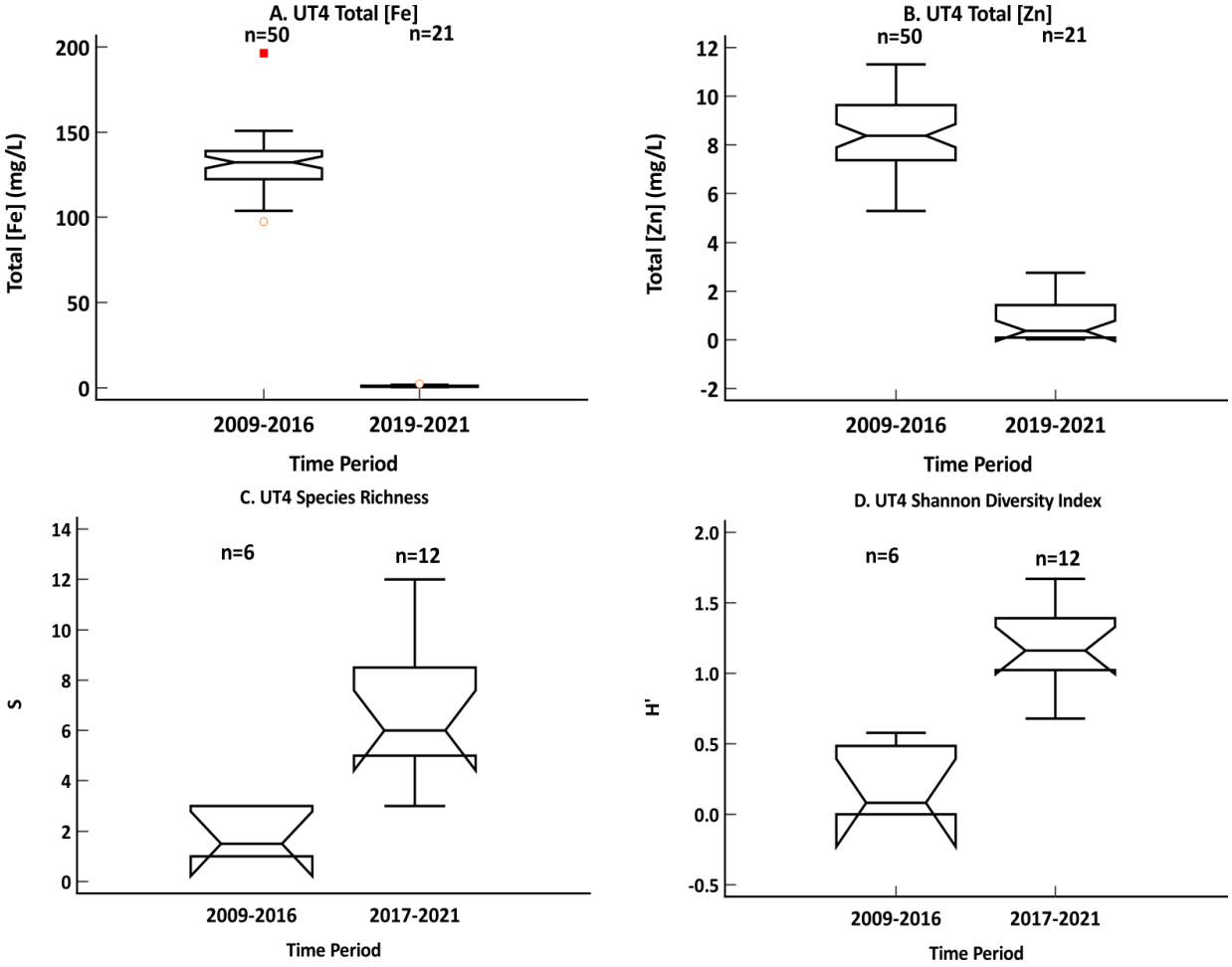

Figure 2.11: Notched box and whisker plots total aqueous metals concentrations of Fe (A) and Zn (B) to the species richness (C) and Shannon diversity (D) at site UT4 on an Unnamed Tributary to Tar Creek, during three time periods, before and after the implementation of two passive treatment systems in Ottawa County, Oklahoma, where n indicates the sample size

Figure 2.12: Images of an Unnamed Tributary (UT) to Tar Creek at site UT4, A. before the implementation of the Southeast Commerce passive treatment system (SECPTS) in October 2016 and B. after the implementation of SECPTS in May 2017

2.4 Discussion

Both MRPTS and SECPTS effectively treated the artesian-flowing MD that historically contaminated the UT. Both PTSs significantly decreased total Cd, Fe, Pb, and Zn aqueous metals concentrations, with Cd and Pb often below the practical quantitation limits after treatments began. Consequently, the total aqueous metals concentrations at the UT sites showed a significant decrease after the implementation of passive treatment, with Fe and Zn mean decreases ranging from 89% to 99%.

All indications show that the decrease in total aqueous metals concentrations in the UT, namely Cd, Fe, Pb, and Zn, following the implementation of two PTSs located within the TCSS directly resulted in the re-establishment of local fish communities. It is important to note that throughout this study, no anthropogenic stream restoration occurred on the UT, thus the improvements in the fish community are most likely attributed to water quality improvements and not any physical, instream habitat improvements or modifications. At all four UT sites, the decrease in total aqueous metals concentrations was followed by increases in fish species richness and Shannon diversity, and all multivariate NMS plots showed clear and significant (MRPP) changes in the local fish community. The potential alternative hypothesis of some unknown but pervasive change in fish communities throughout the region (by lack of directional changes in the Cow and Coal Creek reference sites) was rejected. Additionally, the Tar Creek site located downstream of the UT confluence showed a continued presence of fish species that were potential colonists for the UT.

The results indicate that passive treatment, which can be engineered to target specific

constituents, have great potential to improve water quality in surface waters contaminated by metal-laden MD, which was supported by the findings of Skousen and Ziemkiewicz (2005) that have reviewed the effectiveness of 116 PTSs and other studies (Hedin et al., 1994; Cravotta, 2007). The results from the UT make clear that once stress from metals and/or their impact on physical habitat (e.g., thick flocculants from the accumulation of metal hydroxide precipitates that impair nest-building fishes) or fish physiology (clogging of gills) have been removed, fishes can and will return to a system. The accumulation of metal hydroxides is a very common stressor cited for the impairment of streams impacted by untreated MD (Letterman & Mitsch, 1978; Scullion & Edwards, 1980; Hogsden & Harding, 2012; Williams & Turner, 2015).

Sampling immediately following the implementation of SECPTS at UT4, the most upstream site, indicated a marked change in fish community structure, from the presence of only a few western mosquitofish to an increasingly complex local fish community. The immediate increase in species and diversity at UT4 following the implementation of passive treatment is an important demonstration that fishes can and will return rapidly into reaches that have been heavily contaminated by MD for decades through the simple improvement of the water quality. As shown in Figure 2.12, UT4 was the smallest site, at approximately 35 m in length, with little to no shade and minimal habitat, yet despite the poor habitat, UT4 showed the most drastic change in the fish community out of all four sites.

Other studies have shown similar recovery following the implementation other MD treatment options for acid MD, such as Underwood et al. (2014) investigated changes in fish communities in a large watershed (Racoon Creek Watershed) in southeast Ohio, where over six million dollars had been spent to treat MD. The study found the stream was comprised primarily of tolerant species (93%) in the 1980s, but the downstream sampling locations had shifted to 43% tolerant, 30% moderately tolerant, and 17% sensitive species by 2010 (Underwood et al. 2014).

While both PTSs have been effectively treating the MD that has historically contaminated the UT for the past four years, the fish community appears to show signs of continuing improvement, based on the increasing trend of species richness and diversity at all the UT sites. Accordingly, all four UT sites will continue to be monitored to further assess trends in the fish community. It will be interesting to determine as more time passes if the entire UT can be restored to a full natural fish community relative to other similarly sized streams in Oklahoma and the region (e.g., Matthews and Gelwick, 1990; Franssen et al., 2006). The findings of this can be used to inform efforts attempting to implement passive treatment to remediate MD around the world and becoming a driving force to promote new efforts to remediate MD.

2.5 References

Banks, D., Younger, P.L., Arnesen, R., Iversen E.R., & Banks, S.B. (1997). Mine-water chemistry: the good, the bad and the ugly. *Environmental Geology,* 32, 157–174.
DOI: 10.1007/s002540050204

Byrne, P.A., Wood, P.J., & Reid, I. (2011). The impairment of river systems by metal mine contamination: A review including remediation options. *Critical Reviews in Environmental Science and Technology*, 42(19), 2017–2077.
ISSN 1064-3389
DOI: 10.1080/10643389.2011.574103

Cravotta III, C.A. (2007). Passive aerobic treatment of net-alkaline, iron-laden drainage from a flooded underground anthracite mine, Pennsylvania, USA. *The Journal of Mine Water and the Environment*, 26, 128–149.
DOI: 10.1007/s10230-007-0002-8

Dudka, S., & Adriano, D.C. (1997). Environmental impacts of metal ore mining and processing: A review. *Journal of Environmental Quality*, 26, 590–602.
DOI: 10.2134/jeq1997.00472425002600030003x

Ellison, A.M. (2001). Exploratory data analysis and graphic display. Pages 37-62. In: Design and Analysis of Ecological Experiments (2nd ed). (Eds: S.M. Scheiner & J. Gurevitch). Oxford University Press, New York.

Franssen, C.M., Brooks, M.A., Parham R.W., Sutherland K.G., & Matthews, W.J. (2006). Small-bodied fishes of Tar Creek and other small streams in Ottawa County, Oklahoma. *Proceedings of the Oklahoma Academy of Science*, 86, 9–16.

Franssen, C.M. (2009). The effects of heavy metal mine drainage on population size structure, reproduction, and condition of western mosquitofish, *Gambusia affinis*. *Archives of Environmental Contamination Toxicology,* 57, 145–156.
ISSN: 0090-4341

Gray, N.F. (1997). Environmental impact and remediation of acid mine drainage: A management problem. *Environmental Geology*, 30, 62–71.
DOI: 10.1007/s002540050133

Hedin R.S., Nairn R.W., & Kleinmann R.L.P. (1994). Passive treatment of coal mine drainage. Bureau of Mines, Department of the Interior.

Hogsden, K.L., & Harding, J.S. (2012). Consequences of acid mine drainage for the structure and function of benthic stream communities: A review. *Freshwater Science*, 31, 108–120.
DOI: 10.1899/11-091.1

Letterman, R.D., & Mitsch, W.J. (1978). Impact of mine drainage on a mountain stream in Pennsylvania. *Environmental Pollution*, 17, 53–73.
DOI: https://doi.org/10.1016/0013-9327(78)90055-1

Marsh-Matthews, E., & Matthews, W.J. (2010). Proximate and residual effects of exposure to simulated drought on prairie stream fishes. *Proceedings from the American Fisheries Society Symposium*, 73, 461–486.

Matthews, W.J., & Gelwick, F.P. (1990). Fishes of Crutcho Creek and the North Canadian River in Central Oklahoma: Effects of urbanization. *The Southwestern Naturalist*, 35 (4), 403–410.
DOI: 10.2307/3672037

Matthews, W.J., & Marsh-Matthews, E. (2011). An invasive fish species within its native range: community effects and population dynamics of *Gambusia affinis* in the central United States. *Freshwater Biology*, 56, 2609–2619.
DOI: 10.1111/j.1365-2427.2011.02691.x

Matthews, W.J., & Marsh-Matthews, E. (2015). Comparison of historical and recent fish distribution patterns in Oklahoma and western Arkansas. *American Society of Ichthyologists and Herpetologists*, 1, 170–180.
DOI: 10.1643/CE-14-005

Matthews, W.J., & Marsh-Matthews, E. (2017). Stream Fish Community Dynamics; A Critical Synthesis. Johns Hopkins University Press, Baltimore.
DOI: 10.1080/03632415.2017.1381530

McCune, B.P., & Grace, J.B. (2002). Analysis of Ecological Communities. MjM Software Design, Gleneden Beach, OR.

Nairn, R.W., Beisel, T., Thomas, R.C., LaBar, J.A., Strevett, K.A., Fuller, D., … Knox, R.C. (2009). Challenges in design and construction of a large multi-cell passive treatment system for ferruginous lead-zinc mine waters. *Proceedings, 2009 National Meeting of the American Society of Mining and Reclamation*. Billings, MT, Revitalizing the Environment: Proven Solutions and Innovative Approaches, May 30 – June 5, 2009.
DOI: 10.21000/JASMR09010871

Oklahoma Department of Environmental Quality. (2006). Oklahoma Plan for Tar Creek. Department of Environmental Quality, Oklahoma City, OK.

Oklahoma Water Resources Board (OWRB) (1983). Tar Creek Field Investigation. *OWRB*, Water Quality Division, Oklahoma City.

Pokhrel L.R., & Dubey, B. (2013). Global scenarios of metal mining, environmental repercussions, public policies, and sustainability: A review. *Critical Reviews in Environmental Science and Technology*, 43(21), 2352–2388.
DOI: 10.1080/10643389.2012.672086

Scullion, J., & Edwards, R.W. (1980). The effects of coal industry pollutants on the macroinvertebrate fauna of a small river in the South Wales Coalfield. *Freshwater Biology*, 10, 141–162. DOI: 10.1111/j.1365-2427.1980.tb01189.x

Shepherd, N.L., Keheley, E., Dutnell, R.C., Folz, C.A., Holzbauer-Schweitzer, B., & Nairn, R.W. (2022). Picher Field Underground Mine Workings of the Abandoned Tri-State Lead-Zinc Mining District in the United States. *Journal of Maps*.

Skousen, J., & Ziemkiewicz, P.F. (2005). Performance of 116 passive treatment systems for acid mine drainage. In: *Proceedings of the 22nd American Society of Mining and Reclamation*, Breckenridge, CO, pp 1100–1133.
DOI: 10.21000/JASMR05011100

Taylor, J., Pape. S., & Murphy. N. (2005). A summary of passive and active treatment technologies for acid and metalliferous drainage (AMD). In: Fifth Australian Workshop on Acid Drainage, Fremantle, Western Australia.

Underwood, B.E., Kruse, N.A., & Bowman, J.R. (2014). Long-term Chemical and Biological Improvement in an Acid Mine Drainage-Impacted Watershed. *Environmental Monitoring and Assessment*. 186,7539–7553. DOI: 10.1007/s10661-014-3946-8

United States Environmental Protection Agency Region 6. (1994). Five-Year Review: Tar Creek Superfund Site Ottawa County, Oklahoma. United States Environmental Protection Agency Region 6.

United States Environmental Protection Agency. (2014). Test Methods for Evaluating Solid Waste (SW-846), Update V, Revision 8, United States Environmental Protection Agency.

Williams, K.M., & Turner, A.M. (2015). Acid mine drainage and stream recovery: effects of restoration on water quality, macroinvertebrates, and fish. *Knowledge and Management of Aquatic Ecosystems*, 416(18), 1–12.
DOI: 10.1051/kmae/2015014

Younger P.L., Banwart S.A., & Hedin R.S. (2002). Mine Water: Hydrology, Pollution, Remediation. Kluwer Academic Publishers.

CHAPTER 3

Utilizing Rapid Bioassessment Protocols to Evaluate the Impacts of Abandoned Mine Drainage Discharges on the Receiving Stream

This chapter was formatted for submission to *Science of the Total Environment*

Abstract

Thousands of kilometers of waterways and associated aquatic communities around the world are negatively impacted by mine drainage (MD). MD alters the water chemistry of a receiving water body with increased metals concentrations that often result in decreased dissolved oxygen, pH, increased turbidity, and sedimentation. This study investigated the effects of contamination from abandoned mining operations on benthic macroinvertebrate and fish communities in a second-order stream using rapid bioassessment protocols (RBPs). The study sampled six sites along Tar Creek, in Ottawa County, Oklahoma, USA, which are negatively impacted by contamination from abandoned lead and zinc mining operations. Water quality samples were collected in conjunction with RBPs at each site during the summer months in 2018, 2020, and 2021. Two sites located in the mining-impacted area had the most impaired benthic macroinvertebrate and fish communities, with significantly lower taxa richness, Shannon diversity, and total RBP metric scores compared to regional reference conditions ($p < 0.05$). The impairments at the most upstream site (TC1) were attributed to waste material from the mining operations, which generate elevated aqueous metals concentrations and highly erodible streambeds. Additionally, TC2, immediately downstream of TC1 received 3,000 lpm of untreated MD that increased aqueous iron and lead concentrations and formed iron hydroxide precipitates which coated the bottom of the streambed. However, the fish and benthic macroinvertebrate communities showed increasing RBP metric scores with distance from the mining-impacted area. The communities at the most downstream site, 11 km from the mining contamination, were not significantly different than the regional reference conditions ($p > 0.05$). This study has shown that despite chronic contamination from abandoned mining operations, the stream still has an appropriate biological community downstream that can serve as a source pool for repopulation upstream if the contamination is remediated.

Key Words: Tri-State Mining District, Tar Creek, Fish, Benthic macroinvertebrates, Habitat Assessment

3.1 Introduction

Lotic ecosystems are some of the most vulnerable ecosystems on earth (Palmer and Hondula, 2014). This vulnerability is indisputable in mining regions, where hundreds of headwater streams are impacted in the Appalachians alone (Palmer and Hondula, 2014). Lentic and lotic ecosystems impacted by mine drainage (MD) often have characteristic water quality changes, including decreases in oxygen, decreases in pH and alkalinity, increases in dissolved metals and metal precipitates, and an increase in turbidity and sedimentation (Gray, 1997; Hogsden and Harding, 2012; Williams and Turner, 2015). The accumulation of metal hydroxide precipitates on the substrate is one of the most common negative impacts on instream habitat from MD (Letterman and Mitsch, 1978; Scullion and Edwards, 1980; Hogsden and Harding, 2012; Williams and Turner, 2015). The influence of MD negatively impacts the biota and habitat of the receiving aquatic ecosystems through the elimination of species, leading to a simplified food chain and, causing ecological instability (Gray, 1997; Taylor et al., 2005; Hogsden and Harding, 2012). One method of characterizing the severity of impairment to a water body is the use of rapid bioassessment protocols (Barbour et al., 1999).

Rapid bioassessment protocols (RBPs) are powerful tools to assess aquatic communities because RBPs utilize a wide variety of physical and biological parameters and simplify complex analyses into a single metric score. A combination of physical and biological parameters is necessary to determine the condition of the stream because each parameter represents a different time scale. Water quality data typically represent an instantaneous point in time. Benthic macroinvertebrates are indicators of short-term (weeks or months) and localized biological stream integrity. Many species of benthic macroinvertebrates live in aquatic environments during the larval stage, then undergo metamorphoses and live the remainder of their life on land (MacCausland and McTammany, 2006; Freund and Petty, 2007; Merritt et al., 2008). By comparison, fishes spend their entire lives in the water, tend to have longer life spans, and are more mobile than benthic macroinvertebrates, making fish better indicators for long-term (years) biological stream integrity (Freund and Petty, 2007). Since chemical water quality, benthic macroinvertebrates, and fishes each represent separate time intervals (instantaneous, months, and years, respectively) and spatial differences, combining the three can provide a more complete and accurate representation of the ecological condition of a water body. The habitat assessment portion of RBPs is a crucial component because habitat condition can be reflective of the biological communities, where poor quality habitat often corresponds to impaired biological communities.

The objective of this research was to conduct RBPs, including habitat assessments, benthic

macroinvertebrate collections, and fish collections, at multiple locations along a stream affected by contamination from an abandoned mining site to evaluate the longitudinal impacts of the contamination. It was hypothesized that the biological indices for fish and benthic macroinvertebrate communities in a MD impacted stream would improve with distance from the mining-impacted area and that the sites furthest from the mining-impacted area would have statistically similar metric scores when compared to reference conditions within the same ecoregion.

3.2. Materials and Methods

3.2.1 Site Background

The study site consists of six locations dispersed longitudinally along approximately 11 km of Tar Creek, located in Ottawa County, OK, USA (Figure 3.1). Tar Creek is a low-gradient (mean = 2.6 m/km), runoff-fed stream, arising in southern Kansas and flowing southward approximately 25 stream km through the small communities of Picher, Commerce, and Miami, Oklahoma, to its confluence with the Neosho River. Much of Tar Creek flows through rural pastureland with a wooded riparian zone in erodible soils. Additionally, the stream flows through abandoned lead (Pb) and zinc (Zn) mining operations, known as the Picher mining field (Shepherd et al., 2022). The abandoned Picher mining field is located on both sides of the Oklahoma and Kansas border in Ottawa and Cherokee Counties, respectively. The area was extensively mined for lead and zinc beginning in 1904 and continuing through the 1970s (Brockie et al., 1968; Luza, 1986; Oklahoma Department of Environmental Quality (ODEQ), 2006; Nairn et al., 2009). Approximately 1.5 million metric tons (m-tons) of Pb (principally galena) and 8 million m-tons of Zn (principally sphalerite) were produced from the Picher field during this time (Playton et al., 1980; Luza, 1986).

During active mining, large pumps dewatered the underground mines. The rate of pumping varied throughout the active mining period but reached values of at least 136,000 m^3 of water per day in 1947 (McCauley et al., 1983). As the mining decreased and the pumps were deactivated, the mine voids began to recharge. The first artesian flowing mine discharge was documented in 1979. The discharge contained elevated concentrations of metals, including cadmium (Cd), iron (Fe), Pb, and Zn (Oklahoma Water Resources Board, 1983). The contamination left behind from these mining activities resulted in the Picher field becoming two Superfund sites. The Oklahoma portion of the abandoned Picher mining field was proposed for the Comprehensive Environmental Response, Compensation, and Liability Act (CERCLA) National Priorities List (NPL) in 1981 and was listed in 1983 and is known as the Tar Creek

Superfund Site (TCSS). The Kansas portion of the Picher field joined the NPL shortly after, known as the Cherokee County Superfund Site (United States Environmental Protection Agency (USEPA), 1994; ODEQ, 2006; Nairn et al., 2009).

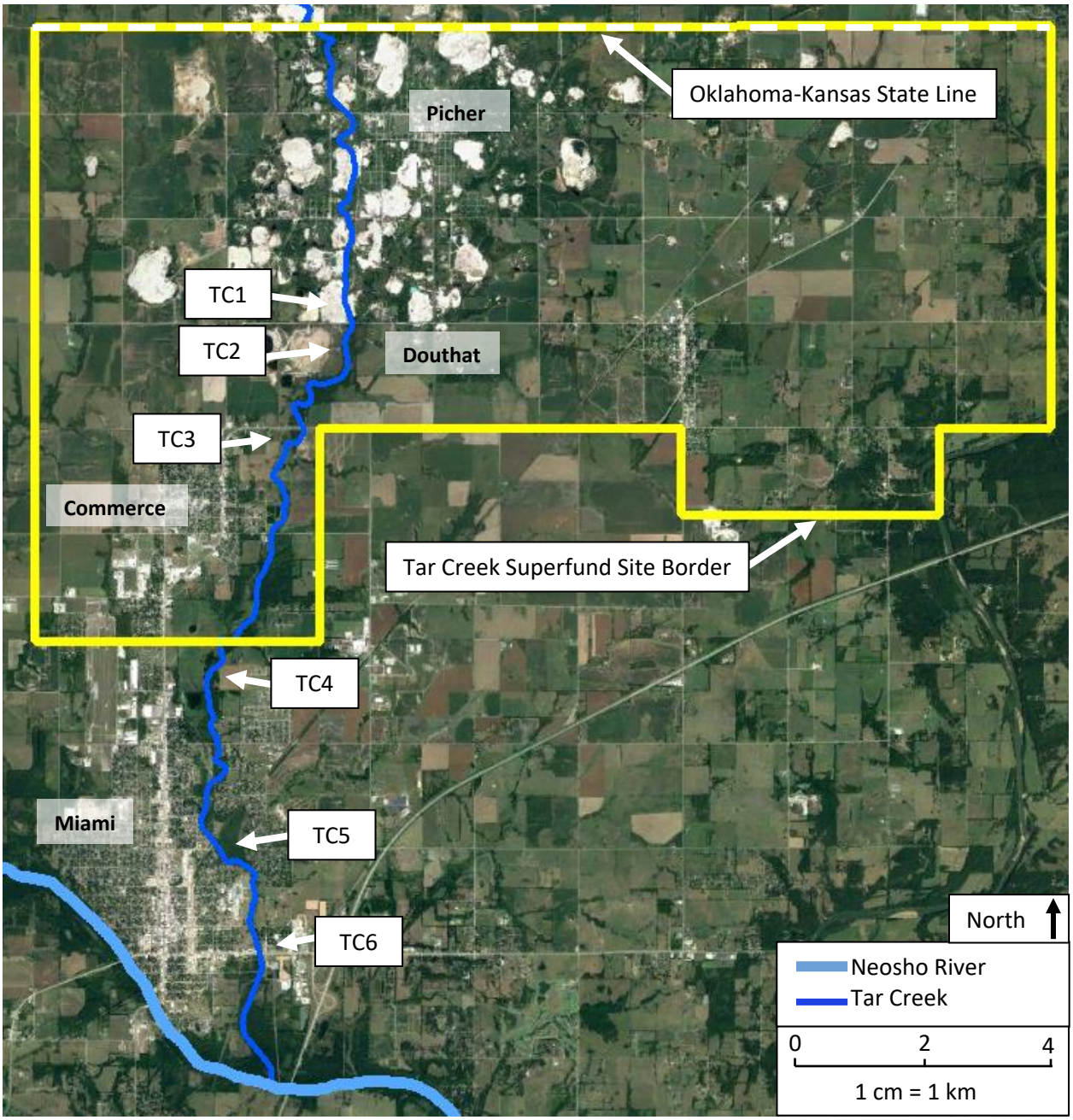

Figure 3.1: Sampling locations along Tar Creek where rapid bioassessment protocols were conducted in Ottawa County, OK, USA (*Source:* "Tar Creek Superfund Site". 36.971661° N, 94.816936° W. Google Earth. Sept. 7, 2021. Dec. 20, 2021.)

3.2.2 Sampling Locations

Each sampling location was comprised of a 400-meter length of stream. Three of the six sampling sites were located within the Tar Creek Superfund site. TC1 was the most upstream sampling site, where the primary source of contamination originates from the waste material of the underground mining operations, known as tailings. These tailings piles are the white areas shown within the Superfund site boundaries in Figure 3.1, some of which cover more than 35 ha, and reach heights up to 30 m. Runoff from the tailings results in elevated concentrations of Pb, Zn, and Cd in the water. Additionally, the stream beds at TC1 and TC2 were entirely composed of the highly erodible tailings material, limiting habitat for aquatic life (Figure 3.2A and B).

An old stream channel discharged metal-laden MD, with a median flow rate of approximately 3,000 lpm into Tar Creek at the road crossing between TC1 and TC2 (Figure 3.2A). An additional 1,000 lpm of MD enters Tar Creek approximately 100 m downstream of the first MD inflow. The MD has a median pH of 6.13 and median total metals concentrations of 0.022 mg/L Cd, 22.6 mg/L Fe, 0.045 mg/L Pb, and 5.75 mg/L Zn. Therefore, the sampled reach at TC1 began on the north side of the road crossing and extends upstream, above the inflow of MD. TC2 began on the south side of the road crossing and extends downstream, where the water was impacted by the MD.

TC3 was approximately 2.0 km downstream of TC2. The first 30 m of TC3 was comprised of a fractured shale bedrock streambed, with much of the remaining 370 m of streambed along the sampled reach composed of tailings material. The influence of the MD at TC3 remained highly visible as noted by the orange staining in Figure 3.2C. TC4 was 4.2 km downstream of TC3 and was the first site outside of the TCSS boundary. Historically, TC4 was contaminated by untreated MD that entered Tar Creek via an unnamed tributary approximately 400 m upstream of the site. However, since 2017, both sources of MD that contaminated this unnamed tributary have been captured and treated using passive treatment technologies, resulting in a significant decrease in total concentrations of Cd, Fe, Pb, and Zn in the unnamed tributary ($p < 0.05$). The water at TC4 was no longer orange from iron oxides since the implementation of the passive treatment systems at these nearby MD discharges (Figure 3.2D).

The final two sites, TC5 and TC6, were in the middle of the community of Miami, Oklahoma. TC5 and TC6 were approximately 3.2, and 4.8 km downstream of TC4, respectively, with TC6 being the most downstream site and approximately 11 km from the primary contamination at TC1 and TC2. TC5 and TC6 had minimal visual indicators of MD contamination, with only orange staining from iron oxide present on the riparian vegetation (Figures 3.2E and F).

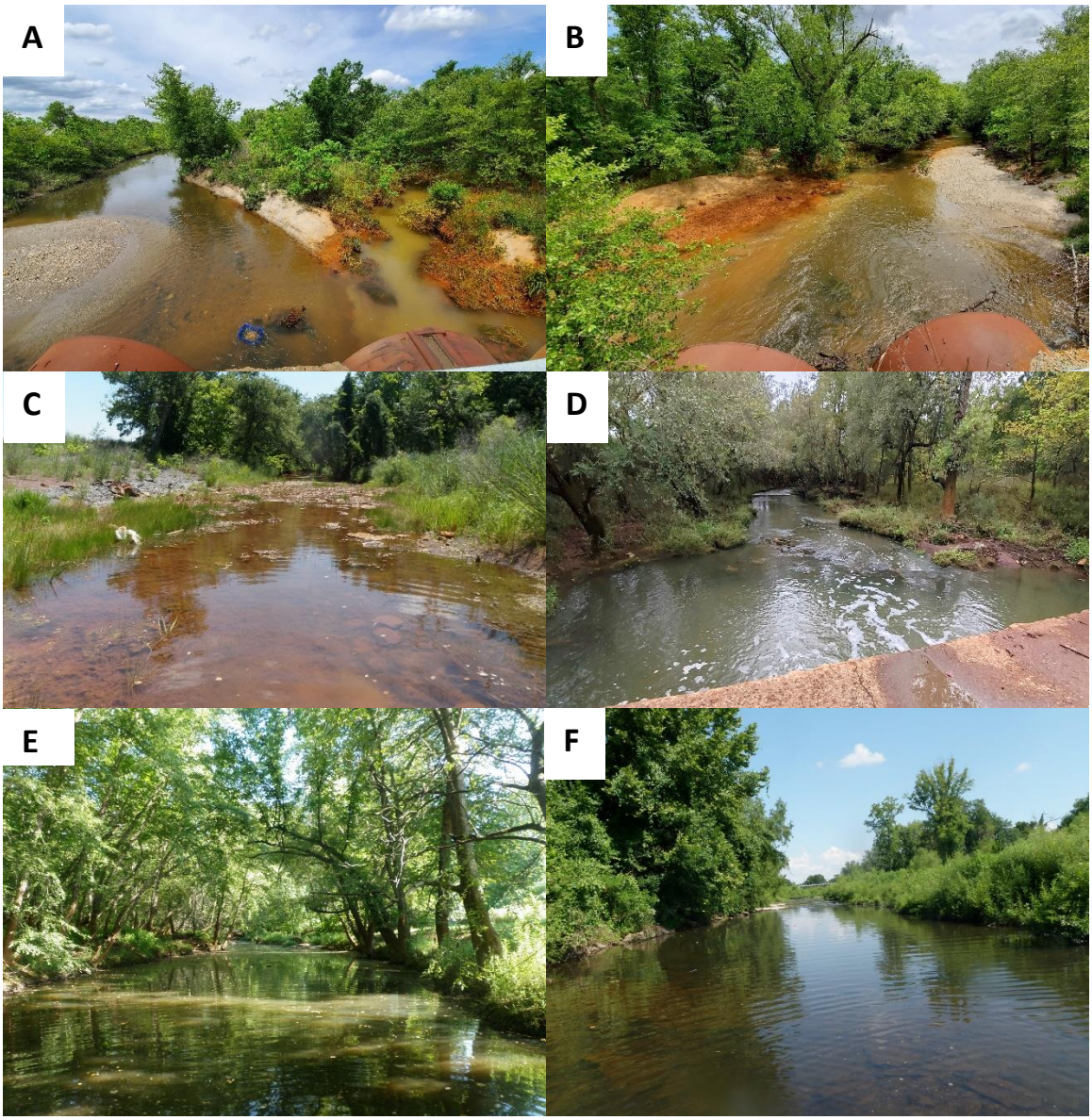

Figure 3.2: Site photos of each sampling location along Tar Creek taken during the 2018 collections. A) TC1 facing upstream B) TC2 facing downstream C) TC3 facing downstream D) TC4 facing downstream E) TC5 facing downstream F) TC6 facing upstream

3.2.3 Rapid Bioassessment

Rapid bioassessment sampling at each of the six sites followed the USEPA *Rapid Bioassessment Protocols for use in Streams and Wadable Rivers* for habitat assessments, fishes, and benthic macroinvertebrates (Barbour et al., 1999). Habitat assessments were conducted at each site in 2018, before the biological collections. Oklahoma-specific habitat assessment field forms created by the Oklahoma Conservation Commission (OCC) were used for this study (OCC, 2002). Each habitat assessment consisted of 20 m transects along a 400 m stream reach.

The biological collections were conducted each summer in 2018, 2020, and 2021 at all six sites. Benthic macroinvertebrate samples were collected at each location before the fish sampling using a one square meter kicknet with 0.5 mm mesh size. Three riffle areas, measuring one square meter each, were selected at each location, including as many kinds of microhabitats as possible (e.g., combinations of deep and shallow riffles, high and low stream velocities, and each available riffle media). The selected areas were then disturbed by kicking the material within the one square meter area and allowing the dislodged material to flow downstream into the kicknet. The material was then homogenized and preserved in a one-liter mason jar and filled with isopropyl alcohol until further laboratory analyses. In the laboratory, each sample was repeatedly halved and randomly selected via a coin flip until the sub-sample was visually estimated to contain 500 macroinvertebrates. The sub-sample was evenly dispersed in a sorting tray measuring 25 cm by 38 cm. A metal grid comprised of 28 5.5 cm x 5.5 cm numbered squares was placed into the tray. Squares were selected using a random number generator, and every macroinvertebrate from each selected square was counted until a minimum of 100 macroinvertebrates had been picked from the subsample. The macroinvertebrates were then identified to the Genus level.

Fish collections consisted of seining all water along a 400 m reach of the stream using three seine sizes, 1.22 m x 2.44 m (4 ft. x 8 ft.), 1.22 m x 4.57 m (4 ft. x 15 ft), and 1.83 m x 9.14 m (6 ft. x 30 ft.), all with 3.17 mm (1/8 inch) “Ace” mesh. Seine hauls were typically 10 to 20 m each. A seine haul was repeated each time a new species was captured for a given collection. Fishes were field identified and released when possible, tallying the number of released fishes. Individuals that could not be identified in the field and voucher specimens of each species from each collection were anesthetized using clove oil and then preserved in 10% formalin for laboratory identification. The preserved collections were retained in archival storage in the University of Oklahoma Center for Restoration of Ecosystems and Watersheds (CREW) laboratory. Fish sampling was led by an individual with an approved Oklahoma Department of Wildlife Conservation Scientific Collectors Permit and conducted per the Institutional Animal Care and Use Committee (IACUC) of the University of Oklahoma.

3.2.4 Water Quality

Water quality samples were collected in conjunction with the biological sampling. The on-site water quality parameters included collection and analyses for turbidity using a Hach 2100P Turbidimeter, and physical parameters including temperature, specific conductivity, dissolved oxygen (DO), and pH, collected using a 6-series YSI multiparameter datasonde. Additional samples for total and dissolved (< 0.45 μm) metals were collected and preserved for subsequent laboratory analyses that were conducted at CREW laboratories using a Varian Vista Pro ICP-OES, following USEPA SW-846 standard methods (USEPA, 2007a; USEPA, 2007b).

3.2.5 Statistical Analyses

Habitat assessment data from each site were analyzed following the parameters and scoring outlined for low gradient streams in the USEPA RBPs (Barbour et al., 1999). The scores associated with each parameter for each site were statistically compared to the regional reference conditions for the Central Irregular Plains ecoregion using a two-tailed, paired T-test with a 95% confidence interval. The metric scores associated with each parameter collected at each of the six Tar Creek sites were then analyzed for significant differences using a single factor ANOVA.

An Excel database of taxa abundance for each macroinvertebrate subsample was used to calculate the taxa richness, Shannon diversity, Modified Hilsenhoff Biotic Index (HBI), percent dominant two taxa, and Ephemeroptera (mayflies), Plecoptera (stoneflies), and Trichoptera (caddisflies) (EPT) taxa richness and abundance. HBI values from Plafkin et al. (1989) were used for each family. The metric scores for each of the raw results from these parameters were calculated based on the criteria specified in OCC (2002). The mean metric scores for each parameter at each site were then statistically compared to the regional reference conditions for summer benthic macroinvertebrate collections using a two-tailed, paired T-test with a 95% confidence interval. The benthic macroinvertebrate density was calculated using Equation 1.

$$\frac{\#\ individuals \times \frac{28\ squares}{\#\ squares\ picked} \times \frac{1}{\%\ subsample\ picked} \times \frac{1}{\%\ sample\ kept\ from\ kicknet}}{3\ m^2} = density \quad (1)$$

A database of species abundance for each fish sample was used to calculate the species richness, total individuals, Shannon diversity, and catch per unit effort (CPUE). The CPUE was calculated by dividing the amount of time spent seining at each site by the total number of individuals captured, resulting in units of individual fish captured per hour of seining. The CPUE normalizes the number of

individuals by accounting for the uneven amount of time spent seining at each site. The species richness and Shannon diversity for each site were statistically evaluated using a one-way ANOVA, with the residuals evaluated using the Shapiro-Wilk test for normal distribution.

Additional fish community metrics for each fish sample, including the number of sunfish species, sensitive benthic species, tolerant species, the proportion of tolerant individuals, insectivorous cyprinid individuals, and lithophilic spawners, were calculated to determine the index of biotic integrity (IBI) by following the OCC standard operating procedures (OCC, 2002; Plafkin at al., 1989). The mean metric scores for each parameter at each site were then statistically compared to the regional reference conditions using a two-tailed, paired T-test.

Lastly, the fish and benthic macroinvertebrate collections from the six sites were compared using a Principal Component Analysis (PCA) by importing the taxa abundance data into Pc-Ord, Version 7. The PCA setup used a correlation cross-product matrix and calculated scores for taxa using a distance-based biplot. The coordinate values from axes 1, 2, and 3 were plotted 2-dimensionally with convex hulls as 1 vs 2 and 1 vs 3 to evaluate if the plots showed any differences in the overlapping convex hulls. The plots showed different orientations of the data, but the overlapping convex hulls did not change, therefore the plot presented in this paper will represent axes 1 vs 2. The patterns were statistically tested for differences using the Multi-Response Permutation Procedures (MRPP) of Pc-Ord using the Sorensen (Bray-Curtis) dissimilarity measure.

3.3. Results and Discussion

3.3.1 Water Quality and Habitat Assessments Analyses

A comparison of the metric values of the parameters from each habitat assessment conducted on Tar Creek and the regional reference metric values showed no significant difference ($p > 0.05$). The sites with the lowest total scoring habitats occurred within the Superfund site (TC1, TC2, and TC3), which were also similar to the total score of the reference sites (Table 3.1). There was a weak overall trend showing an increase in habitat scores with increased distance from the mining contamination (Table 3.1). However, there was no significant difference between each of the six Tar Creek sites ($p > 0.05$ and $F < F\text{-critical}$). Although these results would appear to indicate the physical habitats at each of the six Tar Creek sites were similar, the RBP methodology does not have a parameter that incorporates some of the biologically harmful effects of abandoned mining sites and MD on the habitat, such as the precipitation of Fe that can coat underwater surfaces with iron oxides (Figure 3.3). Additionally, the

tailings material covers the stream bottom, banks, and riparian areas at TC1 and TC2. The tailings are highly mobile and contain harmful metals such as Pb, and Zn. The extensive surface coverage and depth of these tailings present a substantial challenge to identify bank erosion because as areas are eroded, additional tailings material settle in the eroded areas. This continuous process of mobilizing a seeming endless supply of tailings results in a highly unstable habitat, but these impacts are not represented in the habitat assessment scores at TC1 and TC2, rather the scores are representative of a gravel dominated stream with stable banks.

The greatest change in water quality occurred between TC1 and TC2, where the untreated MD enters the stream. TC2 showed a decrease in DO and pH, with an increase in specific conductivity, turbidity, and total aqueous Fe and Pb (Table 3.2). The changes in DO, pH, and turbidity are due to the oxidation and precipitation of Fe from the MD (Younger et al., 2002). From TC2 to TC6, there was a gradual improvement in water quality, with an increase in DO, and decreasing metals concentrations with increased distance from the mining contamination (Table 3.2).

Table 3.1: Metric values of habitat assessments conducted on Tar Creek in 2018 at six locations along the stream, compared to the Central Irregular Plains reference conditions

Parameter	TC1	TC2	TC3	TC4	TC5	TC6	Reference	Maximum Score
Instream Cover	18.5	10.7	16.7	16.4	16.3	14.6	5.32	20
Pool Bottom Substrate	12.0	7.00	7.50	9.50	9.50	11.5	6.92	10
Pool Variability	9.00	8.00	7.00	12.0	16.0	6.00	13.3	20
Canopy Cover Shading	7.18	15.0	11.9	11.4	14.9	4.15	13.5	20
Flow	10.4	9.36	10.1	9.34	19.1	17.1	7.67	20
Channel Alteration	4.00	9.00	9.50	8.50	8.50	10.5	12.2	20
Channel Sinuosity	0.06	0.26	0.88	0.63	0.15	0.03	3.63	20
Bank Stability	9.95	6.61	7.28	8.79	9.48	10.0	8.70	10
Bank Vegetation Stability	6.71	5.85	7.58	9.45	9.08	9.65	4.63	10
Streamside Cover	8.39	10.0	6.81	7.38	6.91	6.90	8.27	10
Total	86.2	81.7	85.2	93.5	110	90.4	84.1	160

Table 3.2: Mean values of selected water quality parameters ± the standard deviations of samples collected at six locations along Tar Creek in the summer of 2018, 2020, and 2021, with dissolved metals collected during summer of 2021

Site		TC1	TC2	TC3	TC4	TC5	TC6
Specific Conductivity (µS/cm)		1,337±272	2,042±232	1,674±179	1,768±54	1,766±195	1,473±259
DO Concentration (mg/L)		7.41±0.64	5.28±1.22	8.1±0.21	7.27±0.44	6.7±1.37	7.65±1.84
pH		7.35±0.14	6.29±0.16	7.39±0.08	7.39±0.07	7.73±0.05	7.86±0.21
Turbidity (NTU)		6.04±2.59	21±10.9	8.38±5.11	7.37±0.62	1.97±1.47	1.06±0.96
[1][Cd] (mg/L)	Total	0.021±0.004	0.028±0.017	0.016±0.011	0.004±0.001	0.002±0.001	<PQL
	Dissolved	0.015	0.022	0.014	0.004	0.001	0.001
[Fe] (mg/L)	Total	0.34±0.13	11.8±10.1	0.65±0.31	0.57±0.02	0.3±0.11	0.18±0.05
	Dissolved	0.038	6.33	0.028	0.028	0.039	0.028
[1] [Pb] (mg/L)	Total	<PQL	0.029±0.012	<PQL	<PQL	<PQL	<PQL
	Dissolved	<PQL	<PQL	<PQL	<PQL	<PQL	<PQL
[Zn] (mg/L)	Total	5.57±1.53	5.93±0.35	4.36±1.3	2.21±0.26	0.98±0.58	0.59±0.25
	Dissolved	3.66	5.4	4.59	2.37	1.5	0.86

[1]<PQL indicates values were below the detection limit of 0.00064 mg/L for Cd and 0.0195 mg/L for Pb

Figure 3.3: Iron flocculation accumulated on the bottom of stream sediment at Tar Creek Site #2, located downstream of Douthat Bridge, near Picher, Oklahoma, USA. (Photo taken in February 2010)

3.3.2 Fish Community Analyses

Fish collections conducted along Tar Creek showed an overall increasing trend in mean species richness, total individuals, Shannon diversity, and CPUE with increasing distance from the mining contamination (Figure 3.4a and b). The greatest outlier in this trend was TC5, where there was a substantial decrease in these parameters compared to TC4 and TC6. Although there is the possibility of an unknown influence impairing the fish community at this site when compared to TC4 and TC6, it is hypothesized that the difficulties of seining at this site were the cause. Approximately 150 m of the 400 m reach was composed of an eight-meter-wide channel that averaged one-meter deep, with nearly vertical banks. These conditions made it challenging to effectively land a seine haul without creating large gaps for fish to escape, possibly resulting in lower capture rates.

The fish community PCA biplot showed the sites located within the TCSS on the left side of the biplot, with TC2 separated from the overlapping convex hulls of TC1 and TC3, indicating a substantial difference between those sites (Figure 3.5). TC4 and TC6 covered the center and right side of the biplot, with clear separation from the three sites located within the TCSS (Figure 3.5). TC5 remained an outlier in the PCA as well, with a slight overlap of the TCSS sites but primarily filling the space between the other distinct groups (Figure 3.5). The MRPP supported the PCA, showing a significant difference between the six sites ($p = 0.044$).

The fish community metric scores continued to show the same trend as the other analyses, with the lowest metric scores occurring at the most upstream location and increasing scores with increased distance from the mining contamination (Table 3.3). A comparison of the metric scores for the fish communities at each Tar Creek site to the Central Irregular Plains reference conditions showed that the fish communities within the TCSS were significantly different than the reference conditions ($p < 0.05$). On the other hand, TC4 and TC6 fish communities were not significantly different than the reference conditions ($p > 0.05$), despite only achieving 81% and 87%, respectively, of the reference conditions total score (Table 3.3).

There was not a significant difference between the fish communities at TC1, upstream of the MD, and TC2, downstream of the MD. Although both sites contain elevated aqueous metals concentrations of Cd and Zn (Table 3.2), it was originally hypothesized that TC2 would have a more impaired fish community, with lower metric results, than TC1 because of the addition of elevated Fe and Pb from the MD that entered between TC1 and TC2, resulting in the Fe precipitates coating the stream and a decrease in DO (Table 3.2). However, provided that the fish communities at TC1 and TC2 were very similar, it is hypothesized that the MD contamination at TC2 not only had a direct influence on the

TC2 site, but the MD also created a barrier that prevented moderately tolerant and sensitive fish species from recolonizing portions of Tar Creek upstream of the MD. This hypothesis is supported by the findings from the fish recolonization of an unnamed tributary to Tar Creek, where recolonization was shown to be based on the treatment of MD, without any modifications or improvements to instream habitats (Chapter Two).

In addition to the low species richness at TC1 and TC2, there was also an abundance of highly tolerant western mosquitofish (*Gambusia affinis*), accounting for 36% of the individuals captured (Appendix 3A). By comparison, at TC6 western mosquitofish accounted for 22% of the individuals captured. A recent study published by Coffin et al. (2022) found western mosquitofish in Tar Creek had gene expression differences primarily in the gills that decreased the transfer of metal ions from the blood into cells compared to fishes from non-metal contaminated reference streams. The study concluded the mosquitofish cannot block metal uptake any better than the other tested fish species, but the mosquitofish in Tar Creek may be able to live in the metal-laden environment because of the differentially expressed genes (Coffin et al., 2022).

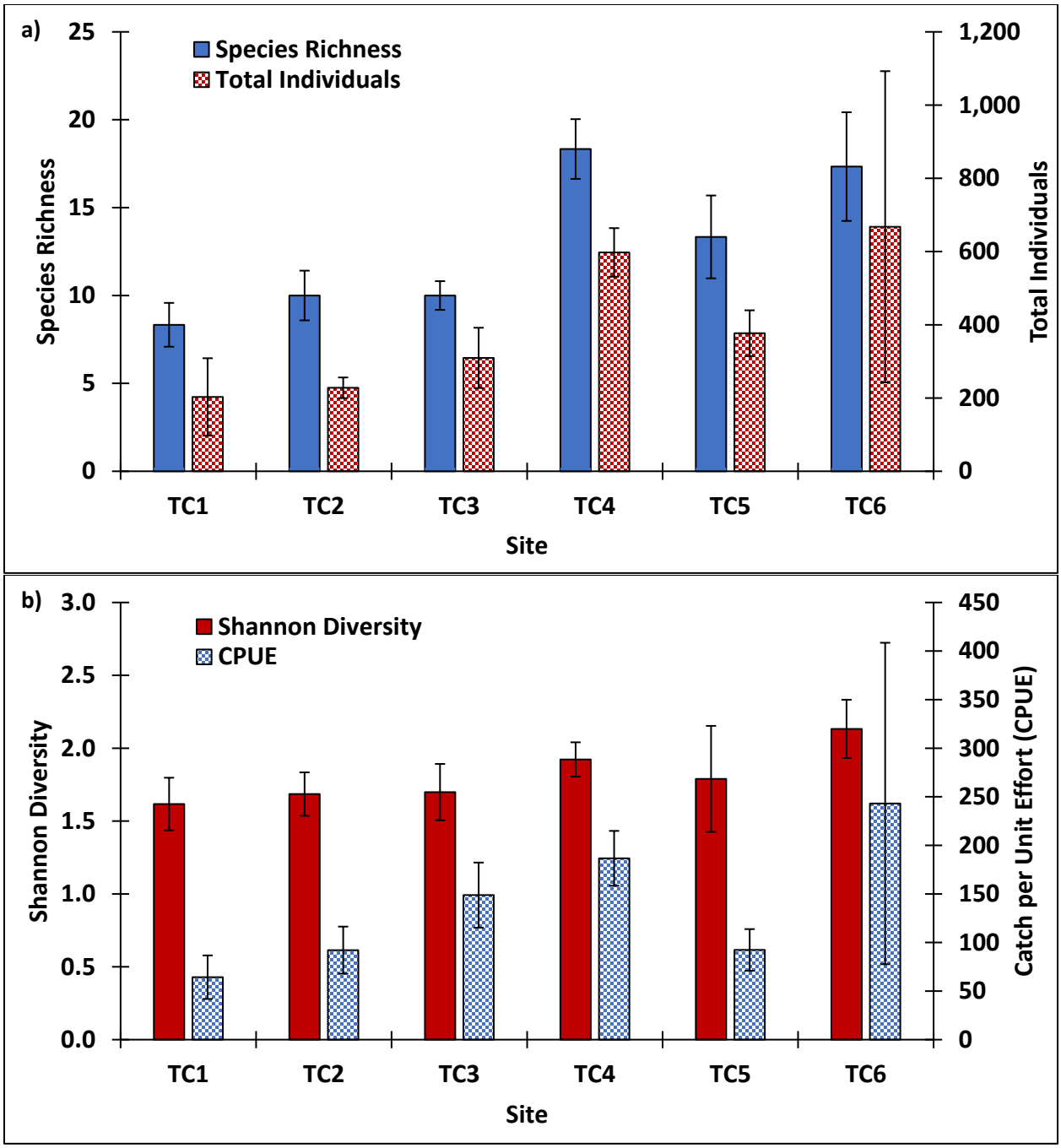

Figure 3.4: Fish community parameters from fish collections conducted in 2018, 2020, and 2021 at six locations along Tar Creek; a) mean species richness and total individuals captured b) mean Shannon diversity and catch per unit effort (CPUE), with standard deviations shown

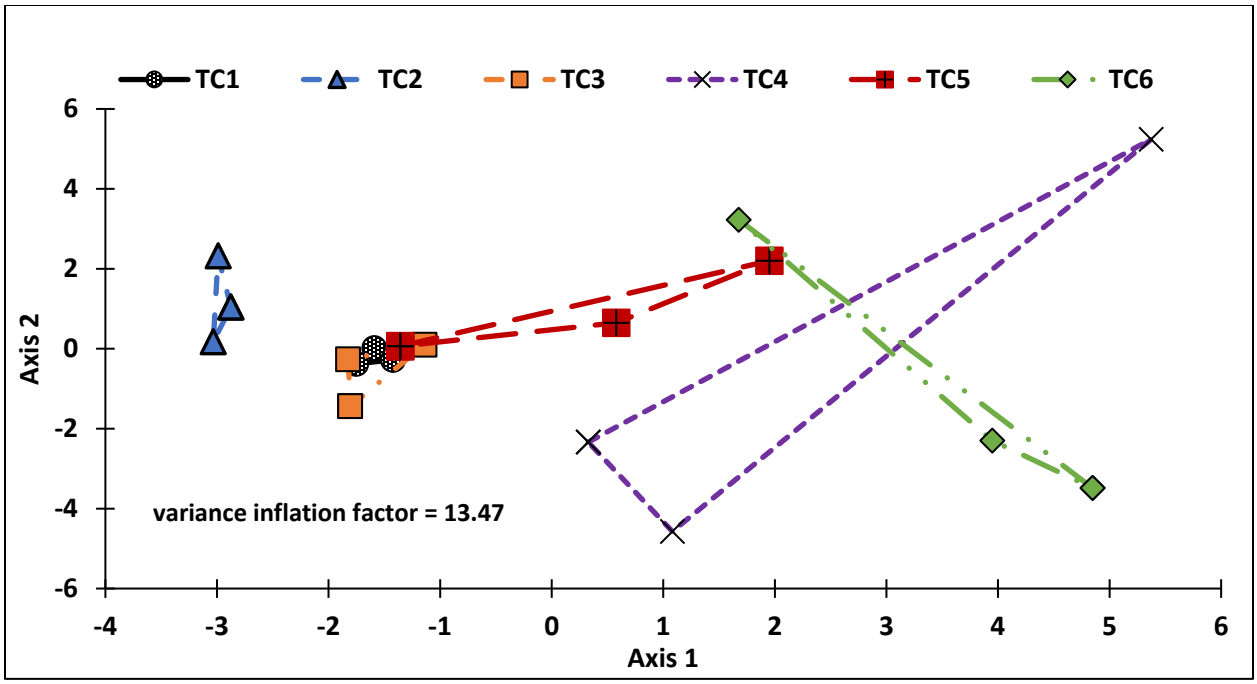

Figure 3.5: Principal Component Analysis biplot with convex hulls representing fish collections conducted at six locations along Tar Creek in 2018, 2020, and 2021

Table 3.3: Mean metric results of fish collections conducted at six locations along Tar Creek in 2018, 2020, and 2021, compared to regional Central Irregular Plains ecoregion reference conditions

Parameter	TC1	TC2	TC3	TC4	TC5	TC6	Reference
Richness	2.33	3.00	3.00	5.00	4.33	4.33	5
No. of sensitive benthic species	1.67	2.33	2.33	3.67	3.00	3.67	5
No. of Sunfish Species	3.67	4.33	4.33	5.00	5.00	5.00	5
No. of intolerant species	1.00	1.00	1.67	3.67	3.00	5.00	5
Proportion of tolerant individuals	1.00	1.00	1.00	1.00	1.00	1.00	1
Proportion insectivorous cyprinid individuals	1.00	1.00	1.00	1.00	1.00	1.00	1
Proportion of lithophilic spawners	1.67	1.00	2.33	1.00	1.00	1.67	3
Total Score	12.33	13.67	15.67	20.33	18.33	21.67	25
Comparison to Reference as Percentage	49%	55%	63%	81%	73%	87%	
p-value comparing each site to the reference	0.023	0.028	0.038	0.086	0.047	0.094	

3.3.3 Benthic Macroinvertebrate Community Analyses

The benthic macroinvertebrate communities showed substantial increases in taxa richness, Shannon diversity, and total metric scores with increasing distance from the mining contamination (Table 3.4 and Figure 3.6a). The benthic macroinvertebrate communities at TC1 and TC2 were very similar and comprised of primarily tolerant species, with only a single EPT taxon appearing once in six collections. TC1 and TC2 were also frequently dominated by two taxa, accounting for over 80% of the total community on average, with a maximum of 98% two taxa dominance at TC2 in 2021. The dominant taxa at TC1 and TC2 were members of the midge fly family (*Chironomidae*) (Appendix 3B).

Not only were sites TC1 and TC2 impaired based on taxa richness, but also in overall density, with an average density of approximately 300 individuals per square meter (Figure 3.6b). In contrast, TC4, TC5, and TC6 had mean densities more than five times that of TC1 and TC2, with the greatest mean density of 2,600 benthic macroinvertebrates per square meter at TC4 (Figure 3.6b). However, the large error bars in Figure 3.6b and the elevated mean density of benthic macroinvertebrates at TC4 were because of the 2021 collection that had a density of 5,800 benthic macroinvertebrates per square meter whereas the two previous collections averaged a density of just above 1,000.

The PCA biplot supported the findings of the metric results, with TC1 and TC2 grouped to the upper right of the plot. TC3, TC4, and TC5 comprise a second distinct group from TC1 and TC2, filling the center of the plot, leaving TC6 stretching across the lower portion of the biplot (Figure 3.9). The separation of the two Douthat sites (TC1 and TC2) and the next three downstream sites suggest a difference was likely. However, the MRPP showed no significant differences among the six sites ($p = 0.067$).

Although TC2 was expected to have a more impaired benthic macroinvertebrate community compared to TC1 due to the influence of metal hydroxide precipitates that has been identified as a primary source of impairment in previous studies (Letterman and Mitsch, 1978; Scullion and Edwards, 1980; Hogsden and Harding, 2012; Williams and Turner, 2015), the highly erodible mine tailings present at both TC1 and TC2 that substantially limit the availability of stable benthic macroinvertebrate habitat might have been an equally important factor impacting the communities at both sites, resulting in very poor metric scores (Figure 3.7 and Table 3.4).

The improvement in the benthic macroinvertebrate community at TC3 compared to TC1 and TC2 was likely due to the improvement in riffle habitat. Although most of TC3 has a streambed composed of the highly erodible tailing material, the benthic macroinvertebrate collections were conducted within the first 30 m of the site because of the presence of riffles. The first 30 m of

streambed was largely composed of bedrock and provided substantially better habitat compared to TC1 and TC2. Despite the substantial increasing trend in metric scores that occurred from TC1 to TC5, these five sites were still significantly different than the regional reference conditions ($p < 0.05$, Table 3.4). However, the most downstream location, TC6, was statistically similar to the regional reference conditions ($p > 0.05$), supporting the hypothesis of this study.

Table 3.4: Mean metric results of benthic macroinvertebrate collections conducted at six locations along Tar Creek in 2018, 2020, and 2021, compared to regional Central Irregular Plains ecoregion reference conditions

	TC1	TC2	TC3	TC4	TC5	TC6	Reference
Taxa Richness	1.33	1.33	2.67	3.33	4.00	5.33	6.00
EPT Taxa Richness	0.00	0.00	0.00	0.00	0.67	0.00	6.00
EPT Abundance	0.00	0.00	1.33	3.33	4.00	5.33	6.00
HBI Score	3.33	4.00	6.00	6.00	6.00	4.67	6.00
% Contribution Dominant Two Taxa	0.67	2.00	1.33	2.00	2.67	4.67	6.00
Shannon Diversity	0.00	0.67	0.67	0.00	0.67	2.00	2.00
Total Score	5.33	8.00	12.00	14.67	18.00	22.00	32.00
Comparison to Reference as Percentage	17%	25%	38%	46%	56%	69%	
p-value comparing each site to the reference	0.001	0.004	0.016	0.017	0.026	0.120	

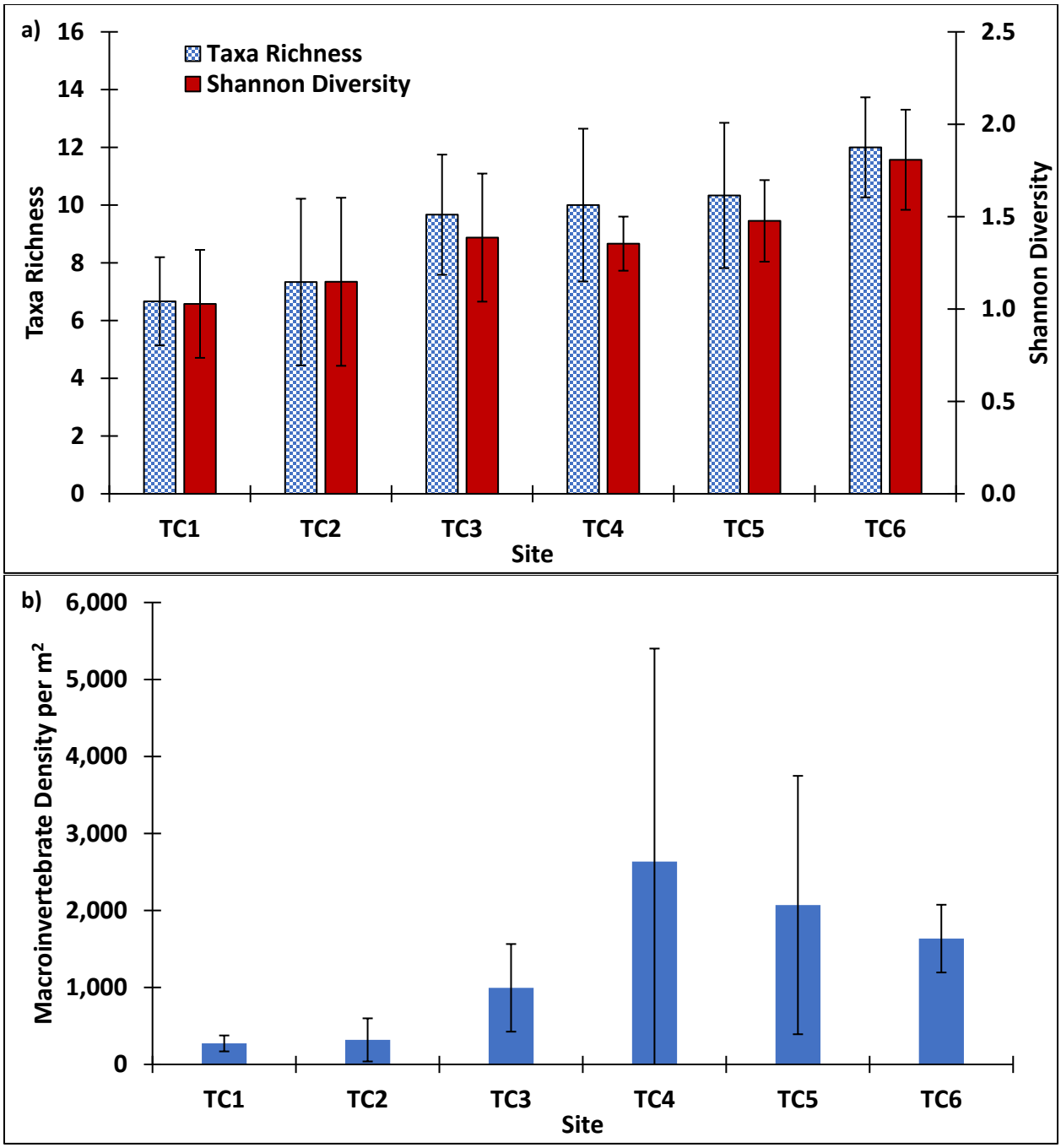

Figure 3.6: Benthic macroinvertebrate community parameters from collections conducted in 2018, 2020, and 2021 at six locations along Tar Creek; a) mean taxa richness and mean Shannon diversity b) mean benthic macroinvertebrate density, with standard deviations shown

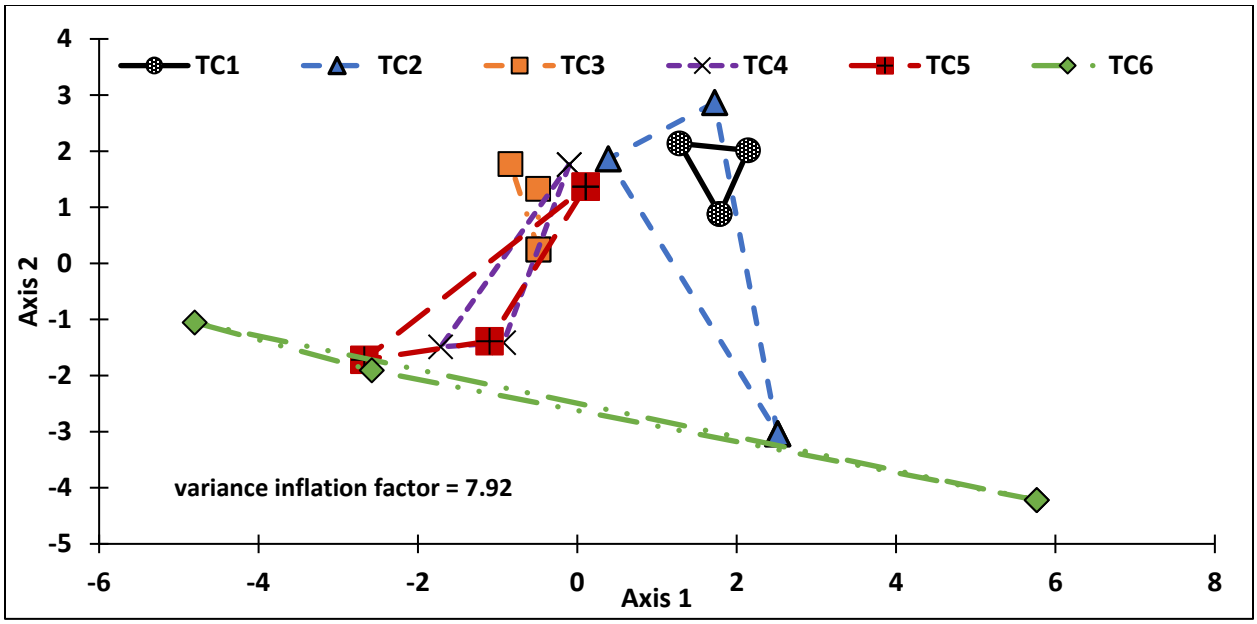

Figure 3.7: Principal component analysis biplot with convex hulls representing benthic macroinvertebrate collections conducted at six locations along Tar Creek in 2018, 2020, and 2021

3.4. Conclusions

Overall, the RBP results show increasing metric scores with increased distance from the mining-impacted area. Although there was not a significant difference between the Tar Creek habitat assessments and the regional reference conditions, the metric scores for the habitat assessments at all six sites were greater than the regional reference conditions, despite the obvious impacts from the abandoned mining operations at TC1 and TC2. The hypothesis that the biological indices for fish and benthic macroinvertebrate communities in a MD impacted stream would improve with distance from the mining-impacted area was accepted. The mean fish and benthic macroinvertebrate metric scores at TC6 increased by 76% and over 300%, respectively compared to TC1. The hypothesis that the sites furthest from the mining-impacted area would have statistically similar biological metric scores when compared to reference conditions within the same ecoregion was accepted. Both TC4 and TC6 fish communities and the benthic macroinvertebrate community at TC6 were statistically similar to the reference conditions ($p > 0.05$). However, neither the fish communities nor the benthic macroinvertebrate communities had a total metric score greater than the reference conditions. Ultimately, the findings of this study show that contamination from the abandoned mining operations had a negative impact on the biological communities, but downstream communities were not significantly different than regional reference conditions, and the downstream fish community is a source pool of diverse species that can repopulate upstream reaches if the contamination is remediated.

3.5 References

Barbour MT, Gerritsen J, Snyder BD, Stribling JB (1999) Rapid bioassessment protocols for use in streams and wadable rivers (Second Edition). *United States Environmental Protection Agency*. Washing, DC. EPA 841-B-99-002.

Brockie DC, Hare EH Jr, and Dingess PR (1968) The Geology and Ore Deposits of the Tri-State District of Missouri, Kansas, and Oklahoma. *American Institute of Minerals and Metallurgical Engineers*. 20:400-430.

Coffin JL, Kelley JL, Jeyasingh PD, and Tobler M (2022) Impacts of heavy metal pollution on the ionomes and transcriptomes of Western mosquitofish (*Gambusia affinis*). *Molecular Ecology*. 00:1-16. DOI: 10.1111/mec.16342

Freund JG, and Petty JT (2007) Response of Fish and Macroinvertebrate Bioassessment Indices to Water Chemistry in a Mined Appalachian Watershed. *Environmental Management*. 39:707–720. DOI: 10.1007/s00267-005-0116-3

Gray NF (1997) Environmental Impact and Remediation of Acid Mine Drainage: A Management Problem. *Environmental Geology*. 33:62–71.
DOI: 10.1007/s002540050133

Hogsden KL, and Harding JS (2012) Consequences of Acid Mine Drainage for the Structure and Function of Benthic Stream Communities: A Review. *Freshwater Science*. 31:108–120.
DOI: 10.1899/11-091.1

Letterman RD, and Mitsch WJ (1978) Impact of Mine Drainage on a Mountain Stream in Pennsylvania. *Environmental Pollution*. 17:53–73.
DOI: https://doi.org/10.1016/0013-9327(78)90055-1

Luza KV (1986) Stability problems associated with abandoned underground mines in the Picher field, northeastern Oklahoma. *Oklahoma Geological Survey*. Circular 88, ISSN 0078-4397.

MacCausland A, and McTammany ME (2007) The Impact of Episodic Coal Mine Drainage Pollution on Benthic Macroinvertebrates in Streams in the Anthracite Region of Pennsylvania. *Environmental Pollution*. 149:216–226. DOI: 10.1016/j.envpol.2006.12.030

McCauley JR, Brady LL, and Wilson FW (1983) Study of Stability Problems and Hazard Evaluation of the Kansas Portion of the Tri-State Mining Area. *Kansas Geological Survey*. Open File Report.

Merritt RW, Cummins KW, Berg MB (2008) An Introduction to the Aquatic Insects of North America – Fourth Edition. *Kendall Hunt Publishing*. Dubuque, IA.

Nairn RW, Beisel T, Thomas RC, LaBar JA, Strevett KA, Fuller D, Strosnider WH, Andrews WJ, Bays J, and Knox RC (2009) Challenges in Design and Construction of a Large Multi-Cell Passive Treatment System for Ferruginous Lead-Zinc Mine Waters. *Proceedings, 2009 National Meeting of the American Society of*

Mining and Reclamation. Billings, MT, Revitalizing the Environment: Proven Solutions and Innovative Approaches, May 30 – June 5, 2009. DOI: 10.21000/JASMR09010871

Oklahoma Conservation Commission: Water Quality Division (2002) Standard Operating Procedures for Water Quality Monitoring and Measurement Activities*. Oklahoma Conservation Commission*. Oklahoma City, Oklahoma.

Oklahoma Department of Environmental Quality (ODEQ) (2006) Oklahoma Plan for Tar Creek. *ODEQ*. Oklahoma City, Oklahoma.

Oklahoma Water Resources Board (OWRB) (1983) Tar Creek Field Investigation. *OWRB*. Oklahoma City, Oklahoma.

Palmer MA, and Hondula KL (2014) Restoration as Mitigation: Analysis of Stream Mitigation for Coal Mining Impacts in Southern Appalachia. *Environmental Science and Technology*. 28:10522-10560. DOI: 10.1021/es503052f

Plafkin JL, Barbour MT, Porter KD, Gross SK, and Hughes RM (1989) Rapid Bioassessment Protocol for Use in Streams and Rivers. EPA/ 444/4-89-001, *U.S. Environmental Protection Agency.*

Playton SJ, Davis RE, and McClaflin RG (1980) Chemical Quality of Water in Abandoned Zinc Mines in Northeastern Oklahoma and Southeastern Kansas: *Oklahoma Geological Survey*. Circular 82.

Scullion J, and Edwards RW (1980) The Effects of Coal Industry Pollutants on The Macroinvertebrate Fauna of a Small River in the South Wales Coalfield. *Freshwater Biology*. 10:141–162. DOI: 10.1111/j.1365-2427.1980.tb01189.x

Shepherd NL, Keheley E, Dutnell RC, Folz CA, Holzbauer-Schweitzer B, and Nairn RW (2022) Picher Field Underground Mine Workings of the Abandoned Tri-State Lead-Zinc Mining District in the United States*. Journal of Maps*.

Taylor J, Pape S, and Murphy N (2005) A Summary of Passive and Active Treatment Technologies for Acid and Metalliferous Drainage (AMD). *Proceedings, Fifth Australian Workshop on Acid Drainage*.

United States Environmental Protection Agency Region 6 (1994) Five Year Review: Tar Creek Superfund Site Ottawa County, Oklahoma. *USEPA Region 6*.

United States Environmental Protection Agency (2007a) Inductively Coupled Plasma-Atomic Emission Spectrometry: Method 6010C. *USEPA*.

United States Environmental Protection Agency (2007b) Microwave Assisted Acid Digestion of Aqueous Samples and Extracts: Method 3015A. *USEPA.*

Williams KM, and Turner AM (2015) Acid Mine Drainage and Stream Recovery: Effects of Restoration on Water Quality, Macroinvertebrates, and Fish. *Knowledge and Management of Aquatic Ecosystems*. 18. DOI: 10.1051/kmae/2015014

Younger PL, Banwart SA, and Hedin RS (2002) Mine Water: Hydrology, Pollution, Remediation. Kluwer Academic Publishers.

CHAPTER 4

Picher Field Underground Mine Workings of the Abandoned Tri-State Lead-Zinc Mining District in the United States

This chapter has been accepted for publication in the *Journal of Maps*.

Abstract

Mining began in the Picher field, in the Oklahoma and Kansas portion of the Tri-State Lead-Zinc Mining District in the United States, during the 1900s and ceased in the 1970s, producing an estimated 1.5 million metric tons (m-tons) of lead and 8 million m-tons of zinc. Over 400 historical maps of the underground mine workings were compiled into a single, easily editable map. This map was used to create 3D renderings for calculation of underground mine workings area and volume estimates. The workings have an estimated volume of 9,870 hectare-meters (80,000 ac-ft), covering an area of 1,440 hectares (3,560 acres). The map and subsequent calculations should be considered to be based on the minimum extent of the mining field due to the likelihood that many historical maps were likely lost or destroyed. The format of the map allows for continuous updates as new information becomes available.
Key Words: Tri-State Mining District, Tar Creek, Mining Map

4.1 Introduction

The abandoned Picher mining field, located on the Oklahoma - Kansas border in the central United States, covers approximately 145 km^2 of land area (Figure 4.1). The field was extensively mined for lead and zinc ores (primarily galena and sphalerite, respectively) from 1904 through the early 1970s (Brockie et al. 1968; Luza 1983; ODEQ 2006; Nairn et al. 2009; Manders and Aber 2014). Approximately 1.5 million metric tons (m-tons) of lead and 8 million m-tons of zinc were produced from the Picher field during this time (Playton et al. 1980; Luza 1983; DeHay et al. 2004). The Picher field and adjacent areas, known as the Tri-State Mining District (TSMD), was one of the largest producers of lead and zinc in the world. During peak production, Oklahoma was the leading producer of zinc in the U.S. nearly every year from 1918 to 1945 (Luza 1983). From 1921 to 1925, the TSMD accounted for 55% of total zinc production in the U.S. (Playton et al. 1980). From 1911 to 1964, the annual average percentage of metal recovery was 2.88% zinc and 0.76% lead, with lower recovery occurring during the later years of mining (McKnight and Fischer 1970). The lead and zinc ores also contained a variety of other elements in lower quantities. One element of interest was germanium. In the 1940s, one mining company, Eagle-Picher, perfected the recovery of high purity germanium from the zinc smelting process, becoming the sole producer of germanium from the 1940s through the early 1950s (O'Connor 1952; Knerr 1991).

Ore production began to decline in the mid-1950s due to ore body depletion, and by the late 1960s substantial mining efforts ceased (Playton et al. 1980; Luza 1983). The Picher field contained approximately 1,500 mine shafts and over 100,000 boreholes by the time mining ceased (McCauley et al. 1983; Luza 1983; United States Environmental Protection Agency (USEPA) 1994; Luza and Keheley 2006). Today, at least 200 mine shafts remain open.

After mining cessation, the Picher field workings were abandoned, leaving behind mine tailings that contaminate the land and waters, and extensive subsurface void spaces that are now full of contaminated mine water and prone to collapse (Childress 1953; Stroup and Stroud 1967; Westfield and Blessing 1967; Brockie et al. 1968; McCauley et al. 1983; Luza 1983; Oklahoma Water Resources Board (OWRB) 1983; DeHay et al. 2004; Oklahoma Department of Environmental Quality (ODEQ) 2006; United States Army Corps of Engineers (USACE) 2006; Nairn et al. 2009; CH2M 2010; USEPA 2020). Due to the contamination, two USEPA Superfund sites include the Picher field. The Oklahoma portion of the Picher field was proposed for the Comprehensive Environmental Response, Compensation, and Liability Act (Superfund) National Priorities List (NPL) in 1981 and was listed as the Tar Creek Superfund Site in 1983. The Kansas portion, the Cherokee County Superfund Site, joined the NPL shortly after (USEPA 1994;

ODEQ 2006; Nairn et al. 2009). Mining has not occurred in the Picher field for over 40 years. However, status as a Superfund site where hundreds of millions of U.S. dollars have been spent on remediation prevent the abandoned area from being forgotten.

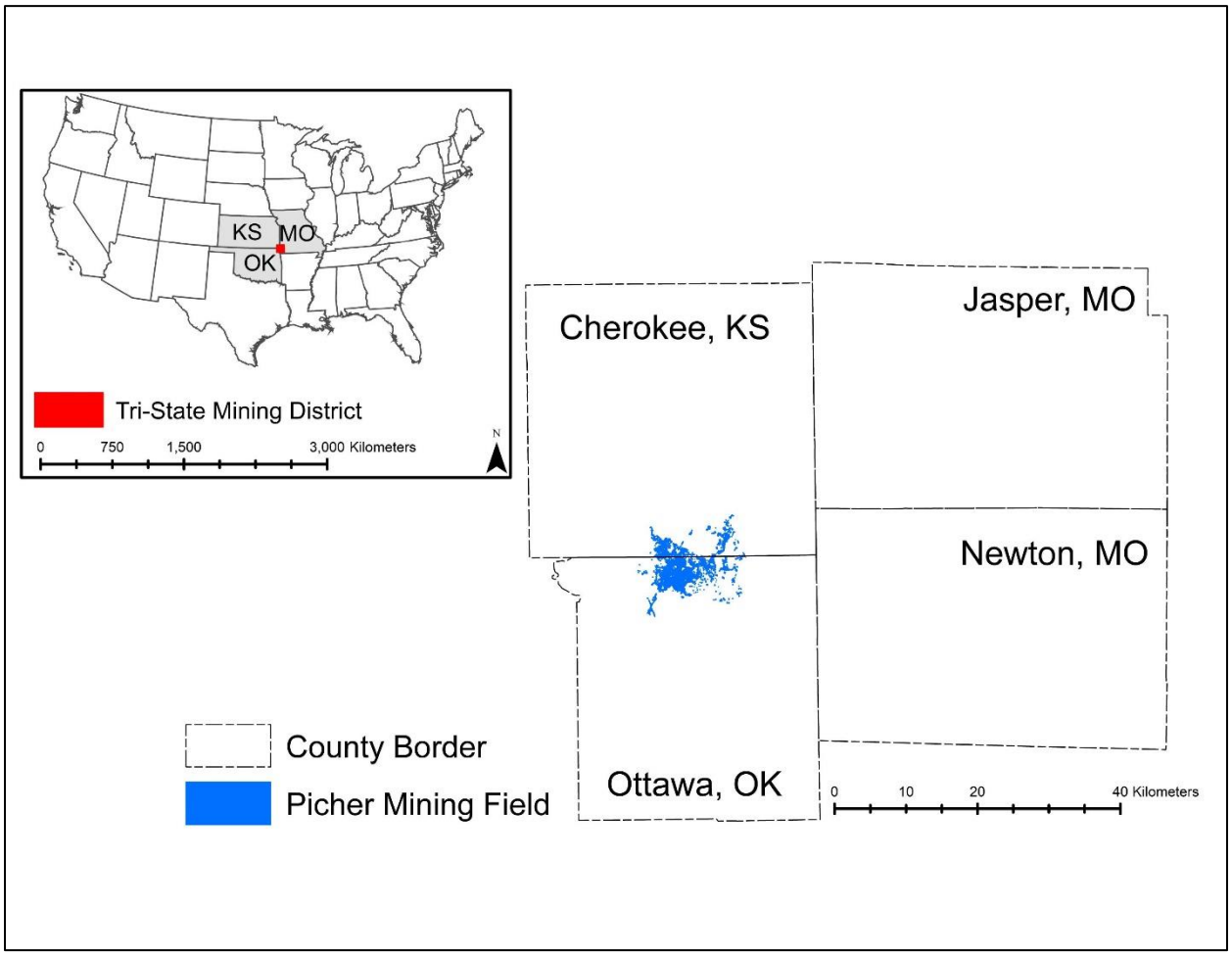

Figure 4.1: Location map of the Picher field underground mine workings and an inset map of the Tri-State Mining District, located in portions of Ottawa County Oklahoma, Cherokee County Kansas, Jasper County Missouri, and Newton County Missouri

Picher field geology was well documented over the lifespan of active mining (Snider 1912; Siebenthal 1925; Fowler and Lyden 1932; Fowler 1942; Reed et al. 1955; Brockie et al. 1968; McKnight and Fischer 1970; Luza 1983). Ore-bearing formations were in Mississippian aged units, primarily in the Meramec and Osage series, commonly referred to as the Boone formation (Luza 1983). The Boone formation is approximately 120 meters thick and was originally limestone (Fowler 1942; Luza 1983). However, erosion and deformation of the limestone resulted in the deposition of cotton rock, nodular chert, and fossiliferous dolomite, all of which contained ore-bearing inclusions (Figure 4.2). The distinct differences of the deposited material in the Boone formation allowed geologists to make minute

subclassifications of the formations and members. These subdivisions are based on an informal letter classification system and have been widely used since the 1930s in both the literature and to designate working layers on historical mining maps (Fowler and Lyden 1932; Fowler 1942; Brockie et al. 1968; McKnight and Fischer 1970; Luza 1983).

Mining in the Picher field consisted of random room and pillar mining where most of the ore bearing material was removed, leaving irregularly spaced pillars to support the mine ceiling (Westfield and Blessing 1967; Luza 1983). Originally, pillars typically ranged from 6 to 15 meters in diameter and were spaced 9 to 30 meters apart to prevent roof collapses (Luza 1983). These pillars contained approximately 12% to 20% of the remaining ore (Westfield and Blessing 1967). Therefore, as a mine was preparing for closure, pillar robbing to extract the remaining ore was conducted, resulting in unsupported roofs prone to rock falls and collapses (Weidman et al. 1932; Westfield and Blessing 1967; Luza 1983). Invention of the "extension jumbo" (Figure 4.3), a mobile platform capable of reaching 21 meters high, allowed for additional mining of the ceiling during closure operations, leaving behind mined voids with heights exceeding 36 meters (Westfield and Blessing 1967; Brockie et al. 1968; Luza 1983).

Most of the underground workings were surveyed and mapped by lease owners to track progress during production. However, many of the older mines do not have underground mining maps, and the maps that do exist of these older mines are likely sketches rather than surveyed maps (McCauley et al. 1983). The most comprehensive maps are known as the 40-acre (16 ha) maps (Oklahoma Office of the Secretary of Environment (OSE) 2000).

The 40-acre maps are named after the land area of a quarter-quarter section based on the Public Land Survey System (PLSS), still used today in the U.S. The PLSS is a method of describing and subdividing the land, laid out in typically square sections that measure 2.59 km^2 (640 acres). Each section can be divided into quarters, then subdivided by quarters again, resulting in sixteen equal squares that are 40 acres in size (16 ha), known as quarter-quarter sections. These PLSS grids were used by the lease owners and mining companies to define ownership boundaries because most of the leases were 40 acres in size and based on the quarter-quarter sections.

System	Series	Formation/Member		Informal Letter Classification	Thickness (m)	Description
Pennsylvanian	Des Moines	Cherokee Group			0-91.5	Cherokee group is the surface formation in the Picher Field
Upper Mississippian	Chester	Fayetteville Shale		Chester Beds	0-21.5	The Chester series is composed of limestone, sandstone, and shale. It overlies the Boone formation and can contain minor ore bodies
		Batesville Sandstone			0-21.5	
		Hindsville Limestone			0-26	
		Unconformity				
	Meramec	Quapaw Limestone			0-9.5	Medium to coarse grained crinoidal limestone
		Boone Formation	Moccasin Bend Member	B	0-6	Limestone and dolomite, some chert
				C	0-10	Limestone; chert commonly found in basal
				D	5.5-6.5	Limestone; cotton rock; chert., contains commercial ore bodies in some mines
				E	1.5-2.5	Limestone and chert, important ore bed in a few mines
				F	3.5-4.5	Limestone, chert, white cotton rock
				G	9-12	Limestone; chert, Resembles H bed; an important ore horizon
				H		Limestone, chert with alternating bands 5 to 12 cm thick; important ore horizon and often mined with G bed
			Baxter Springs Member	J	0-12	Limestone with some chert; very glauconitic
				K	0-12	Crinoidal limestone; with abundant nodules of chert. Important ore zone
				L	0-10.5	Limestone with massive chert or cotton rock
			Short Creek Oolite Member	M	0-3	Oolitic limestone, slightly glauconitic occurring with rounded chert nodules
			Disconformity			
Lower Mississippian	Osage		Joplin Member		0-30	Crinoidal limestone and nodular or bedded chert
			Grand Falls Chert Member	N	6-9	Limestone somewhat molted; chert occurs in bands and very large nodules; bands are up to 0.3 m thick, and nodules are 1.5 m to 4.5 m diameter. Generally barren in Picher field
				O	2.5-3	Some limestone and abundant chert occurring in bands and round nodules. Important sheet ground ore zone
				P	0-3	Chert in bands and large flat nodules, some limestone and mineralized locally
				Q	0-3	Chert dense; massive limestone; mineralized locally
			Reeds Spring Member	R	15-30.5	Limestone; abundant chert occurs as irregularly shaped nodules and thin beds, altering with limestone

Figure 4.2: Generalized section of geology in the Picher mining field portion of the Tri-state Lead-Zinc Mining District, located in Oklahoma and Kansas, United States (Modified from Fowler 1942; Reed at al. 1955; Brockie et al. 1968; McKnight and Fischer 1970; Luza 1986)

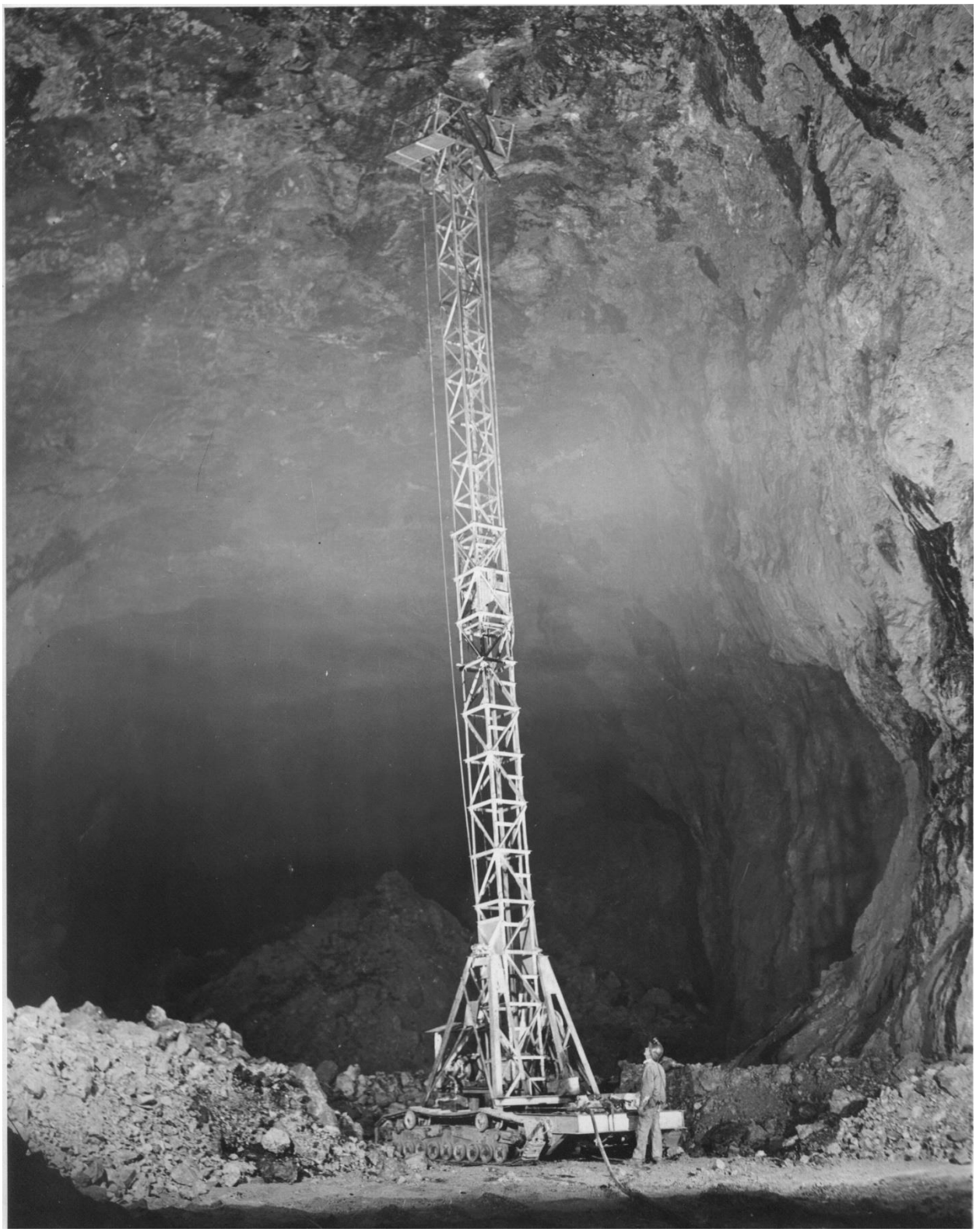

Figure 4.3: Roof trimming of underground workings in the Picher mining field using a 70-foot (21 m) extension jumbo. Source: Baxter Springs Heritage Center and Museum, Kansas, United States

The 40-acre mining maps still have some shortcomings. These maps were typically hand-drawn, rarely contained a legend of symbols or linework, and often had additional handwritten notes to explain expansions of the workings beyond what was originally drawn. Although many of these historical mining maps have likely been destroyed or lost, numerous groups and individuals have worked to scan and archive the surviving mining maps over the past few decades (USACE 2006; Keheley 2020; Missouri Southern State University 2020; Oklahoma Department of Mines (ODM) 2020). When combined, these archives contain thousands of mining maps in a variety of digital formats.

The objectives of this work were to 1) utilize historical mining map repositories to create a complete map of the Picher field underground workings in a digital format that is readily accessible and can be easily updated as new information becomes available; 2) determine the areal extent and void volume of the mine workings in the Picher field using AutoCAD Civil 3D and ArcMap; and 3) address and quantify uncertainties of historical mining maps that were not updated before mining operations were abandoned, thus producing a map that represents the minimum extent of the mine workings. The purpose of this research was to create digitized 2D and 3D renderings of abandoned underground mining voids to help develop a better understanding of environmental liabilities to support future remediation and research activities.

4.2 Materials and Methods

4.2.1 2-Dimensional Map Creation

Approximately four thousand historical mining maps of the Picher field, in a variety of file types, from numerous sources were reviewed (USACE 2006; Keheley 2020; Missouri Southern State University 2020; ODM 2020). Over 1,400 of these maps were collected and indexed for the creation of the Picher field mining map. This repository was searchable by publication year, mine lease name(s), map creator, and legal description.

A shapefile of the quarter-quarter sections from the PLSS of the area of interest was imported into AutoCAD and ArcMap and served as the primary method to georectify historical mining maps. The map repository was used to identify the newest and/or most detailed historical map of the underground workings for each quarter-quarter section that contained mine workings. The map was then imported into AutoCAD Civil 3D and aligned 2-dimensionally by aligning opposite corners of the quarter-quarter section drawn on the mining map with the corners of the corresponding quarter-quarter section. The line types present on each historical map were identified and associated with the correct geologic

bedding layers. Then all the workings were traced using splines with the corresponding AutoCAD layer.

The two-point alignment tool in AutoCAD Civil 3D was often not sufficient to properly align the quarter-quarter section borders of the historical mining maps with the corresponding PLSS borders due to slight deformations, such as wrinkles, which were present on the original paper maps. Therefore, linework from each quarter-quarter section was exported as a shapefile from AutoCAD Civil 3D and imported into ArcMap. Using spatial adjustment tools and the rubbersheeting method, mine workings were more accurately aligned in ArcMap. A minimum of fifty alignment points were placed along each border of the quarter-quarter section. Any mine shafts in the section with known coordinates were used as additional alignment points. After completing the alignment, the shapefiles were imported into AutoCAD Civil 3D, where the linework from each quarter-quarter section was combined into a single AutoCAD file. The combined file was used to create the 2D Picher field map and served as the base file to create a 3-dimensional (3D) rendering of the mined voids. In addition, a version of the 2D map was modified to calculate the areal extent of the mine workings as a single layer to make a direct comparison to previous estimates of the areal extent and average height of the mine workings.

4.2.2 3-Dimensional Rendering for Mined Volume and Area Calculations

The linework in the Picher field mining map was divided based on legal section boundaries and saved into separate AutoCAD files to decrease the computational power needed for 3D rendering. The historical mining maps used to create the 2D drawings that contained floor and ceiling elevations of the mined voids were prioritized over other maps in the repository to create the 3D rendering. However, if the map used in the 2D map did not contain elevation data, the map repository was searched to find the best replacement map for a given area that contained elevations. In total, over 400 historical mining maps were used to complete the Picher field mining map and subsequent 3D rendering (Appendix 4A and 4B).

The majority of the elevation data were inserted by typing values from the historical maps into separate point groups for the floor and ceiling of each bedding layer. However, 3D linework was available in select areas on the Oklahoma side of the Picher field that was used in a previous subsidence study conducted by the USACE (USACE 2006). The accuracy of these 3D lines was verified with the historical mining maps and adjustments were made if necessary.

Next, the elevation data from the point groups or 3D linework were used to create surfaces that represented the floor and ceilings of each bedding layer in each section. Boundaries were added to each surface to create an outer boundary for each bedding layer, then the pillars within the boundary were hidden. The 2D area of each of these surfaces was computed in AutoCAD and recorded in a spreadsheet.

The respective floor and ceiling surfaces for each bedding layer were then used to extract a 3D solid between the surfaces, allowing the volume for each piece to be computed by AutoCAD and creating a 3D representation of the underground workings. Figure 4.4 is an example of the 3D rendering. The land surface shown in Figure 4.4 was generated from 0.3-meter contours (1 foot) from a LiDAR flight flown in 2005 and provided by the Oklahoma Department of Environmental Quality. The solids from each bedding layer were merged into a single solid per bedding layer to compute the mean heights of void spaces. A flowchart briefly describing these methods is shown in Figure 4.5.

4.2.3 Evaluation of Potential Inaccuracies within Historical Mining maps: Domado Case Study

The historical mining maps selected to create the Picher field map and the 3D rendering were the best available maps. However, it is likely that in many instances, the selected historical mining map pre-dated the closure of a given lease, thus potentially not representing the full extent of the workings at the time of mine closure. The Domado lease was selected for this case study because there were numerous historical maps available spanning a period of 40 years. Four maps with dates ranging from 1927 to 1966 were used to quantify the expansion that occurred over the lifetime of the Domado lease, thus representing the inaccuracies that would result in the Picher field map and subsequent calculations on the Domado lease if the best available map for the lease pre-dated the 1966 map. The 2D and 3D methods previously described were used to calculate the area and volume of the M-bed in the Domado workings for each of the four maps to quantify the expansion that occurred on this lease between each date.

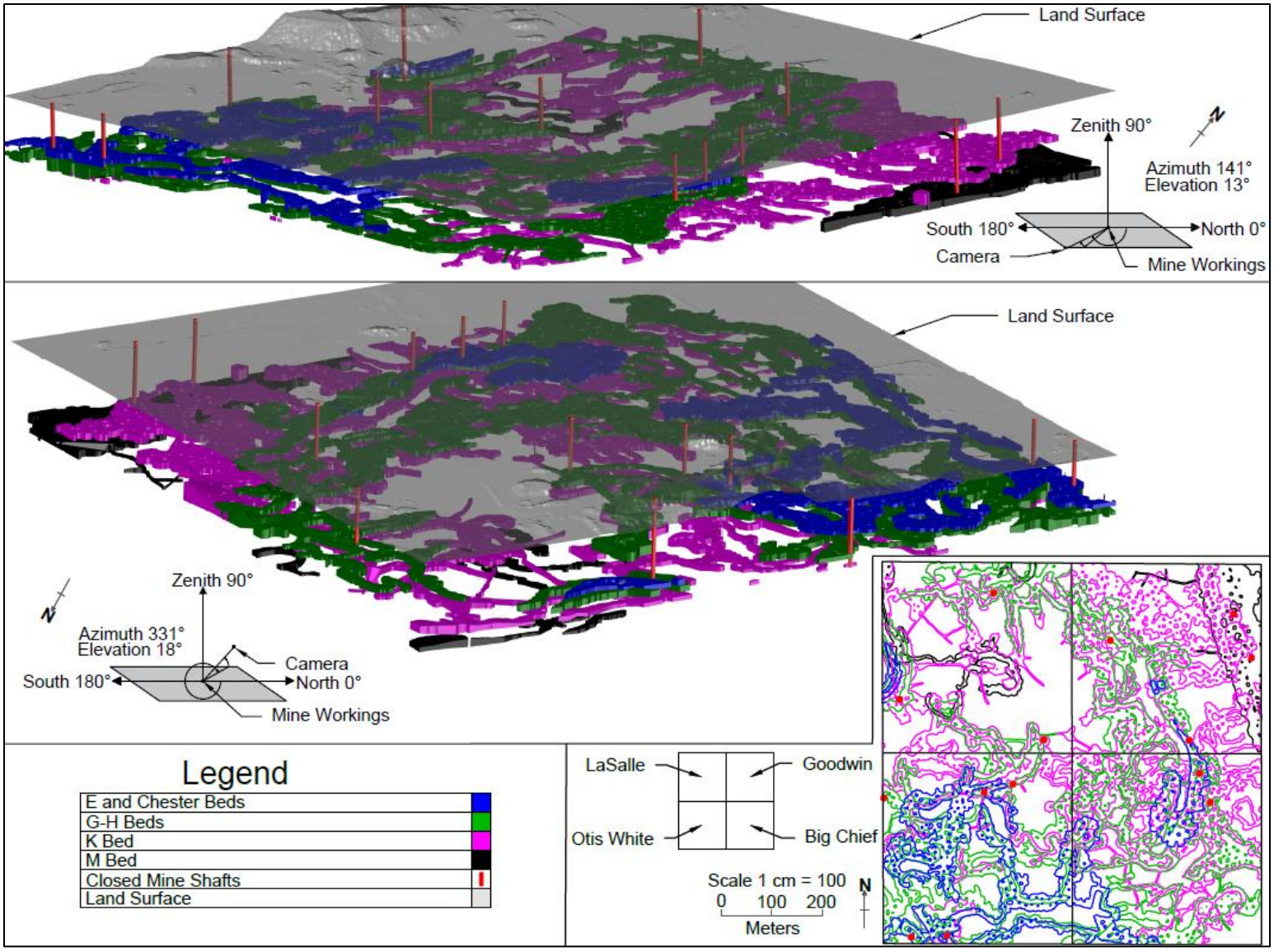

Figure 4.4: 3-Dimensional rendering of portions of the Lasalle, Goodwin, Otis White, and Big Chief mines, located on the eastern half of legal section 29N 23E 17, in the Oklahoma portion of the Tri-State Mining District

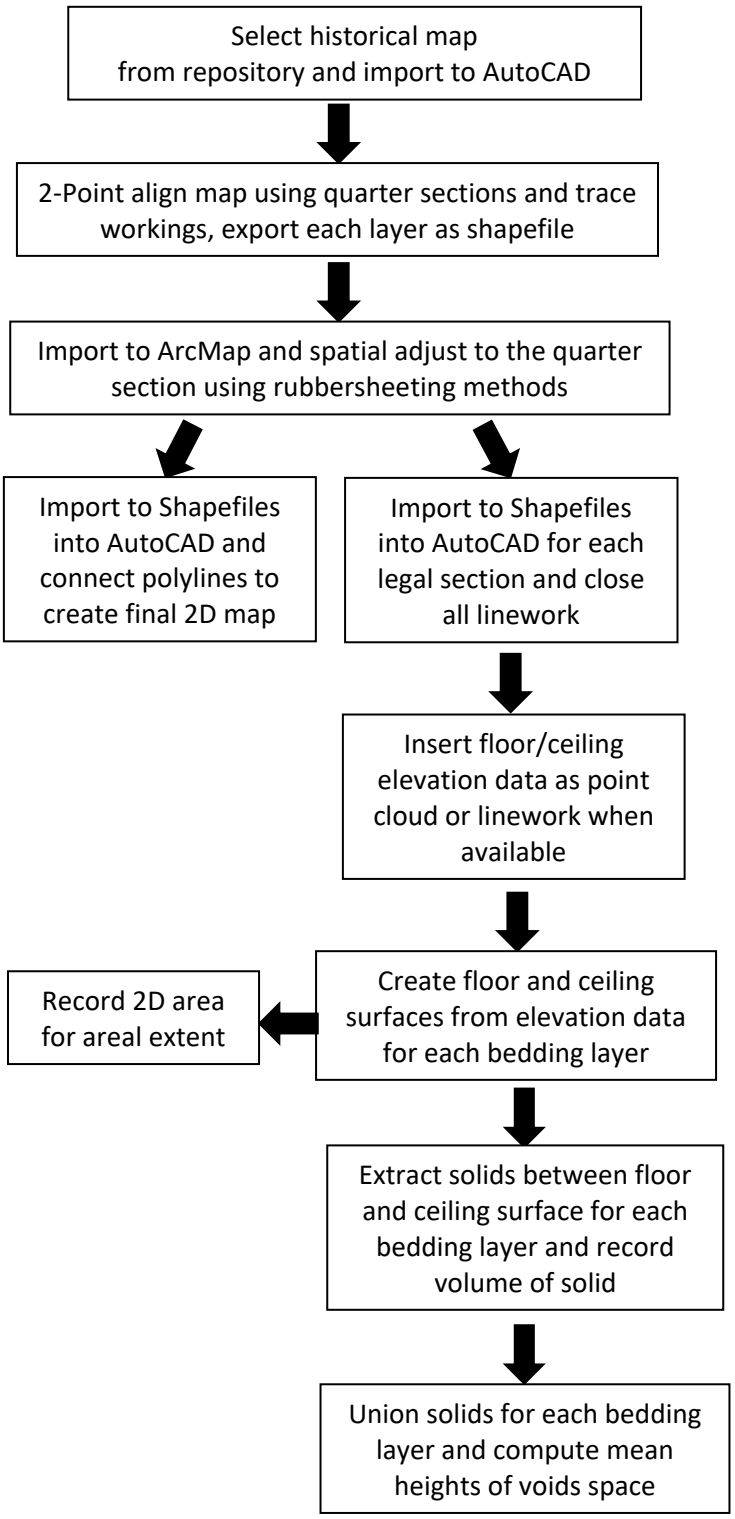

Figure 4.5: Flowchart describing the workflow to convert scanned historical mine maps into 2D and 3D AutoCAD renderings

4.3 Results and Discussion

4.3.1 2-Dimensional Map Creation

The final 2D Picher field mining map represents the first comprehensive mining map of the Picher field since mining ceased in the 1970s. The digitization of the historical mining maps used to create the 2D Picher field map was straightforward, with only a few challenges. First, the selection of the correct historical mining map for a given area was often a time consuming and tedious process. In many instances, multiple maps were similarly dated, but the details (e.g., handwritten notes describing pillar removal, roof trims, or mine expansion) on each varied. Thus, more than one map would be used to draw a given set of workings, with the most recent details from each used in the AutoCAD drawings to create the most-likely accurate representation of the mine.

Perhaps the greatest challenge was determining the correct bedding layer of a particular set of workings. Most of the historical mining maps did not contain a legend. If legends were present, they were often incomplete, with little to no consistency between line types or symbology between companies or decades. L. Stepp, a former surveyor in the Picher field, gave an example during a personal interview where a solid black line on the Netta East lease indicated the main workings as the M bed level, while the Netta White lease, located to the northwest, the solid black line was representative of the main workings in the G-H bed (Stepp 2004). Therefore, best approximations of the bedding layers in each area were established based on partial legends written on the maps, surrounding workings with known bedding layers, drill logs, and descriptions of mines from published articles. Despite these challenges, the final product of the Picher field map currently represents the best 2D depiction of the Picher mining field, incorporating information from hundreds of historical mining maps. In addition, providing the map as an easily accessible and editable file type promotes its use in novel and creative manners by technical and non-technical audiences.

4.3.2 3-Dimensional Rendering for Mined Volume and Area Calculations

The area, volume, and subsequent mean void heights were calculated for each of the bedding layers based on 1) the entire Picher field, 2) the Oklahoma portion, and 3) the Kansas portion (Tables 4.1 and 4.2). It is important to differentiate between the 2D area of each bedding layer and the areal extent of the mine workings. Many mines had multiple levels of workings that overlapped, resulting in the summed areas of the bedding layers exceeding the areal extent. In fact, comparing the areal extent (1,440 ha) to the summed area of the bedding layers (1,547 ha) suggests that approximately 7.5% of the mine workings had overlapping mined layers (Tables 4.1 and 4.3).

Table 4.1: Area in hectares of mined voids and pillars for each geologic bedding layer in the Picher field portion of the Tri-State Mining District, and the pillar to void ratio of all workings and the percentage of mined void area located on the Oklahoma side of the Picher field

Bedding Layer	Mined Voids (ha)			Pillars (ha)			Pillar:Void	Voids in Oklahoma
	All	Oklahoma	Kansas	All	Oklahoma	Kansas	(%)	(%)
E and Chester	44.1	30.8	13.3	6.51	4.91	1.60	15	70
G-H	151.5	90.0	61.5	56.1	45.5	10.6	37	59
K	242	170	72.0	78.5	60.8	17.7	32	70
M	909	718	191	386.4	322	64.4	43	79
Sheet Ground Workings	201.3	123	78.3	32.49	26.6	5.89	16	61
					Weighted Average:		36	74

Table 4.2: Volume (hectare-m) and mean height (m) of mined voids for each geologic bedding layer in the Picher mining field and the percentage of mined voids by volume located on the Oklahoma side of the Picher field

Bedding Layer	Mined Void Volume (ha-m)			Mean Height of Voids (m)			Voids in Oklahoma
	All	Oklahoma	Kansas	All	Oklahoma	Kansas	(%)
E and Chester	203.8	136	67.8	4.62	4.41	5.11	67
G-H	1,019	576	443	6.73	6.40	7.20	57
K	1,293	902	391	5.37	5.30	5.43	70
M	6,399	5,179	1,220	7.03	7.21	6.38	81
Sheet Ground Workings	956	319	637	4.75	2.59	8.14	33
Total/Weighted Average:	9,871	7,111	2,759	6.86	7.02	6.46	72

Table 4.3: Comparison of published estimates of the areal extent and volume of mined voids of the Picher field underground mine workings

	Areal Extent (ha)	Estimated Void Height (m)	Mined Volume (ha-m)
1953-Childress	1,445	8.84	12,770
1967-Stroup & Stroud	1,457	8.84	12,878
1982-Luza (Only Oklahoma)	1,028	7.62	7,833
1982-Luza[1]	1,316	7.62	10,025
1983-OWRB	1,236	7.62	9,418
2021-Shepherd et al.	1,440	6.86	9,870

[1]Kansas portion estimated to be 28% of total void volume

The majority of mining in the Picher field occurred in the Oklahoma portion, accounting for nearly 75% of the mined voids by volume and area (Tables 4.1 and 4.2). The most frequently mined bed in the Picher field was the M-bed, accounting for 65% of the mined volume. The M-bed was one of the most prevalent and thickest ore-bearing layers in the Picher field (Fowler 1942). On the opposite end, the least commonly mined bedding layers were the E and Chester beds (2% by volume), due to the small intermittent pockets of ore (Brockie et al. 1968). The E and Chester beds were often mined when an ore-bearing pocket was intersected while sinking a mine shaft to a deeper level or if the ore-bearing pocket was present in the ceiling of a previously mined bedding layer, frequently occurring in the GH-bed (Brockie et al. 1968). The intermittent pockets of ore in the E and Chester bed led to sporadic and small workings that were often too small to justify leaving pillars, resulting in the lowest pillar to void ratio (Table 4.1).

The historical mining maps created an additional challenge when constructing the 3D renderings. Most of the historical mining maps used in the 2D creation contained elevation data for the floor and ceilings of the mined voids. However, some of the older mining maps did not. These mined voids were often smaller mines, located on the outer portions of the Picher field. The mined voids that did not contain elevation data accounted for 1.8% of the overall 2D area. The mined void volume of the workings without elevation data was estimated by multiplying the areas of these workings by the average ceiling height of the corresponding bedding layer.

The creation of the 3D rendering represents the first time that the Picher mining field area and volume were calculated using a computer model. Over the years, there has been a wide range of reported values for the volume of the mined voids and areal extent of the Picher field (Childress 1953; Stroup and Stroud 1967; Luza 1983; OWRB 1983; USEPA 1994; ODEQ 2006). These values are often accompanied by oversimplified assumptions due to technological limitations at the time. In the past, the areal extent of the workings was often a best estimate, with the total volume calculation based on the areal extent and multiplied by a single value to represent the height of the workings across the entire Picher field. It is important to note that some of these estimates were made before mining ceased in the 1970s (Childress 1953; Stroup and Stroud 1967) but still exceeded the volume calculated in this paper by over 20% (Table 4.3). Surprisingly, some of the past estimates were very similar to the values calculated in this study. The volume reported by the Oklahoma Water Resources Board (OWRB) (1983) for the entire Picher field differed by 4.5%, with the percentage of the volume occurring in Oklahoma differing by 0.1% (Table 4.3). However, the mean void height calculated in this study was at least 75 cm below the estimated void heights used in past publications (Table 4.3). Two potential causes for the differences in

the void heights are 1) the previous publications may have had a cognitive bias towards extreme ceiling heights when determining the estimated void height, resulting in overestimates and 2) previous publications, especially those occurring during the active mining period, may have had a more thorough knowledge of the workings than what is shown on the surviving mining maps that were used in this study, resulting in an underestimated mean void height calculated in this study.

While the 3D rendering is not as easily accessible as the 2D Picher field map due to expensive software and large file sizes, it provides a wealth of knowledge that can be used to improve the work of researchers and reclamationists. The 3D rendering can identify shallow workings or large mine rooms that may exist below ongoing surface remediation. Additionally, it provides the best available visualization of the underground connectivity of the mined voids, which will improve the understanding of the flow paths of the contaminated water that has filled the mines and now discharges into nearby streams. As new CAD software is developed; future research may be able to convert the 3D objects into a more user-friendly form in order to make the information widely available and accessible by any user.

4.3.3 Domado Case Study

The need for this case study became apparent while reviewing thousands of mining maps in the repositories. The mining was reportedly active during the 1970s, yet the most recent historical reference map was last updated in 1970, and only 16% of the reference maps were updated in the 1960s (Appendix A). During the final days of mining, Eagle-Picher mining company was the only large company remaining and held the most up-to-date 40-acre maps, along with drill logs, survey notes, and other mining records (OSE 2000). In 1970, Eagle-Picher moved all records and maps to Reno, Nevada, USA. Since then, Eagle-Picher officials have stated that a flood had heavily damaged or destroyed the majority of the records, with little or no maps remaining (OSE 2000).

The Domado case study was incorporated to show how these mines evolved over their operational lifetimes and to quantify the extent of the workings that would be unrepresented if the most recent map was not found. The objectives of the Domado case study were to identify potential uncertainties and provide an example by quantifying the expansion of the mine workings at the Domado lease that occurred over a forty-year period.

The volume of voids could not be calculated for the 1927 map because sufficient elevation data were unavailable. However, the areal extent increased by 115% from 1927 to 1946, illustrating the magnitude of uncertainties that can occur when the best available historical map was last updated nearly two decades prior (Table 4.4, Figure 4.6). At least one instance with similar circumstances to the date range between these two Domado maps has been identified. The historical reference maps used

for the Old Mission and Petersburg leases, located in the southeast section of the Picher field, were published in 1907 and 1912, respectively. However, the Bureau of Mines annual ore production records show the Old Mission mine was still producing ore as late as 1935 (U.S. Department of the Interior: Bureau of Mines 1936).

A comparison of the later Domado maps highlights the importance of updated elevation data. From 1955 to 1966, the Domado lease does not show any 2D expansion of the outer workings, rather the 2D map showed only pillar removal was occurring (Figure 4.6). The pillar removal accounted for less than a 4% change in the area, while the volume of mined voids increased by nearly 11% (Table 4.4). Therefore, the elevation data show that in addition to pillar removal, roof trimming was occurring throughout the mine, which resulted in a mean void height increase of nearly 90 cm. The quantifiable and visual differences determined in this case study emphasize that the Picher field map and 3D rendering should be viewed as the minimum amount of mine workings present in the Picher mining field.

Table 4.4: Expansion of M-bed mine workings on the Domado Lease in the Picher field portion of the Tri-State Mining District over a period of four decades

Map Date	Area (ha)	Mean Void Height (m)	Volume (ha-m)
1927	3.629	N/A[1]	N/A[1]
1946	7.807	11.33	88.44
1955	9.163	13.88	127.2
1966	9.527	14.76	140.6

[1]The 1927 map did not contain surveyed floor or ceiling elevations, therefore mean ceiling height and volume could not be determined

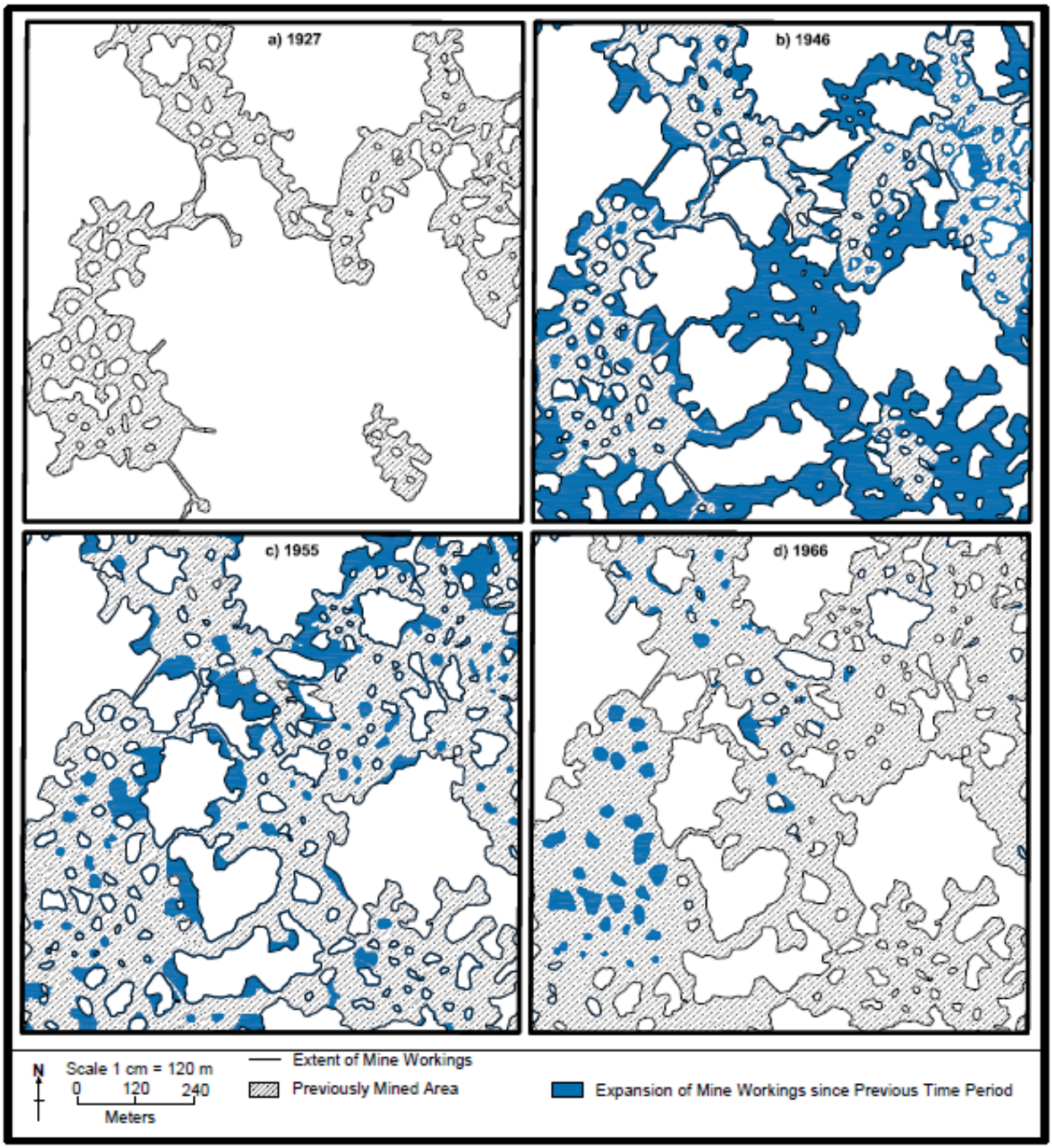

Figure 4.6: 2-dimensional comparison of historical mine maps of the Domado mine claim of the Picher mining field from 1927, 1946, 1955. and 1966. a) 1927 extent of workings b) expansion of mine workings occurring from 1927 to 1946 c) expansion of mine workings occurring from 1927 to 1955 d) expansion of mine workings occurring from 1927 to 1966

4.4 Conclusions

The Picher field maps represent the first attempt to compile hundreds of historical mining maps to depict the entire mining field in a modern format, and the first time a 3D computer rendering was used to calculate the mined volume. The areal extent of the Picher field is approximately 1,440 hectares, with a total mined volume of nearly 9,870 hectare-meters (Table 4.3). However, the Domado case study emphasizes that this is likely the minimum extent of the workings present in the Picher field. The availability of a modern format of the Picher field workings allows the map to be easily updated as additional maps are found, and it can be used in new and creative ways by researchers and reclamationists.

4.5 References

Brockie DC, Hare EH Jr., Dingess PR (1968) The Geology and Ore Deposits of the Tri-State District of Missouri, Kansas, and Oklahoma. American Institute of Minerals and Metallurgical Engineers. Ch 20 pp. 400-430.

Childress HL (1953) Statement of Harold L. Childress. Tri-State Zinc and Lead Ore Producers Association, Baxter Springs, Kansas, Presented Before the House Ways and Means Committee.

CH2MHill (2010) Hydrogeologic Characterization Study Report; Tar Creek Superfund Site, Operable Unit 4. United States Environmental Protection Agency Region 6.

DeHay KL, Andrews WJ, Sughru MP (2004) Hydrology and Groundwater Quality in the Mine Workings within the Picher Mining District, Northeastern Oklahoma, 2002-03. Report 2004-5043, U.S. Department of the Interior – U.S. Geological Survey.

Fowler GM, Lyden JP (1932) The Ore Deposits of the Tri-State District (Missouri-Kansas-Oklahoma). American Institute of Mining and Metallurgical Engineers. Technical Publication No. 446.

Fowler GM (1942) Ore Deposits in the Tri-State Zinc and Lead District. Princeton University Press. pp. 206-211

Keheley (2020) Ed Keheley Private Collection of Picher Mining Field Underground Mining Maps. See appendix A for list of referenced mining maps.

Knerr D (1991) Eagle-Picher Industries: Strategies for Survival in the Industrial Marketplace, 1840-1980. Ohio State University Press.

Luza KV (1983) A study of stability problems and hazard evaluation of the Oklahoma portion of the Tri-State Mining Area. U.S. Bureau of Mines Mining Research Contract Report J0100133.

Luza KV, Keheley E, (2006) Inventory of Mine Shafts and Collapse Features Associated with Abandoned Underground Mines in the Picher Field Northeastern Oklahoma. Oklahoma Geological Survey. Open File Report.

Manders GC, Aber JS (2014) Tri-State Mining District Legacy in Northeastern Oklahoma. Emporia State Research Studies. 49:2 29-51.

McCauley JR, Brady LL, Wilson FW (1983) Study of Stability Problems and Hazard Evaluation of the Kansas Portion of the Tri-State Mining Area. Kansas Geological Survey. Open File Report.

McKnight ET, Fischer RP (1970) Geology and Ore Deposits of the Picher Field Oklahoma and Kansas. United States Geological Survey. Professional Paper 588.

Missouri Southern State University (2020) Missouri Digital Heritage Collection (MDHC): Tri-State Mining Maps Collection. Accessed online <https://cdm16795.contentdm.oclc.org/digital/collection/tristate>. See appendix A for list of referenced mining maps.

Nairn RW, Beisel T, Thomas RC, LaBar JA, Strevett KA, Fuller D, Strosnider WH, Andrews WJ, Bays J, Knox RC (2009) Challenges in Design and Construction of a Large Multi-Cell Passive Treatment System for Ferruginous Lead-Zinc Mine Waters. Proceedings, 2009 National Meeting of the American Society of Mining and Reclamation, Billings, MT, Revitalizing the Environment: Proven Solutions and Innovative Approaches, May 30 – June 5, 2009. doi: 10.21000/JASMR09010871

O'Connor JA (1952) Germanium Electronic Upsurge. Chemical Engineering. 59:4 pp 15-160.

Oklahoma Department of Environmental Quality (ODEQ) (2006) Oklahoma Plan for Tar Creek. Oklahoma Department of Environmental Quality.

Oklahoma Department of Mines (ODM) (2020) Historic Underground Mining Maps: Oklahoma Department of Mines. Accessed online <https://mines.ok.gov/historic-underground-mining-maps>. See appendix A for list of referenced mining maps.

Oklahoma Office of the Secretary of Environment (OSE): Governor Frank Keating's Tar Creek Task Force (2000) Mine shaft subcommittee final report to Governor Frank Keating's Tar Creek Task Force. Oklahoma Office of the Secretary of Environment.

Oklahoma Water Resources Board (OWRB) (1983) Tar Creek Field Investigation. OWRB.

Playton SJ, Davis RE, McClaflin RG (1980) Chemical Quality of Water in Abandoned Zinc Mines in Northeastern Oklahoma and Southeastern Kansas: Oklahoma Geological Survey. Circular 82.

Reed EW, Schoff SL, Branson CC (1955) Groundwater Resources of Ottawa County, Oklahoma. Oklahoma Geological Survey. Bulletin 72.

Siebenthal CE (1925) Contour Map of the Surface of the Beds Underlying the Cherokee Shale in a Portion of the Picher District, Oklahoma. Showing Relations of Ore Bodies to the Surface Contours. United States Department of the Interior, United States Geological Survey.

Snider LC (1912) Preliminary Report on the Lead and Zinc of Oklahoma. Oklahoma Geological Survey. Bulletin No. 9.

Stepp L. Interview. By Keheley E. and Wood F. October 12, 2004.

Stroup RK, Stroud RB (1967) Zinc-Lead Mining and Processing Activities and Relationship to Land-Use Patterns, Ottawa County, Oklahoma. United States Department of the Interior, Bureau of Mines. Unpublished report.

United States Army Corps of Engineers (2006) Picher Mining Field, Northeast Oklahoma Subsidence Evaluation Report. United States Army Corps of Engineers.

United States Department of the Interior: Bureau of Mines (1936) Minerals Yearbook 1936. United States Department of the Interior.

United States Environmental Protection Agency Region 6 (1994) Five Year Review: Tar Creek Superfund Site: Ottawa County, Oklahoma. United States Environmental Protection Agency Region 6.

United States Environmental Protection Agency Region 6 (2020) Sixth Five Year Review: Tar Creek Superfund Site: Ottawa County, Oklahoma. United States Environmental Protection Agency Region 6.

Weidman S (1932) The Miami-Picher Zinc-Lead District, Oklahoma. Bulletin No. 56. Oklahoma Geological Survey.

Westfield J, Blessing E (1967) Report on Investigation of Surface Subsidence and Safety of Underground Employees in the Picher, Oklahoma, Field of the Tri-State District. United States Department of the Interior, Bureau of Mines.

CHAPTER 5

Evaluating the Water Quantity and Quality of Mine Drainage Discharges in a Hydrologically and Topographically Challenging Location

This chapter has been formatted for submission to *Mine Water and the Environment*

Abstract

Artesian net-alkaline mine drainage (MD) discharges from underground abandoned lead-zinc mining operations in the Picher mining field have been contaminating Tar Creek for over 40 years. Although two existing passive treatment systems (PTS) have been successfully treating MD that historically contaminated Tar Creek, the greatest MD contributions originate further upstream, near Douthat, Oklahoma and remain untreated. The intersecting ground surface elevations and nominal head elevations of the mine pool at Douthat result in highly variable flow rates from multiple discharges, including boreholes and mine shafts. The objective of this study was to evaluate the water quality and quantity of these MD discharges to determine if passive treatment was a viable option. Regular water quality sampling occurred from 2018 through 2021 at five discharges. Weirs with pressure sensors were installed to estimate flow rates at 15-minute time intervals at the three largest discharges. The combined median flow rate was 4,046 lpm with a maximum calculated flow rate of 154,000 lpm. The peak flow rates only occurred for short periods of time, typically less than 37 hours. The flow weighted average totals metals concentrations of the five discharges were 0.022 mg/L Cd, 22.6 mg/L Fe, 0.045 mg/L Pb, and 5.76 mg/L Zn. This study concluded that despite highly variable flow rates, the water quality and quantity of the Douthat discharges is treatable via PTS, in part because the existing PTS remediate MD with greater metals concentrations and treatment wetlands with designed flow rates exceeding the median and maximum flow rates have been successfully implemented elsewhere.

Key Words: Tri-State Mining District, Tar Creek, Passive Treatment

5.1 Introduction

Mine drainage (MD) is a global concern that causes ecological damage to receiving streams (Cravotta III 2007; Byrne et al. 2011). MD can form from both hard and soft rock mining when mining operations expose a surface of a geologic formation that is then subject to biogeochemical processes including dissolution, oxidation, hydrolysis, precipitation, and microbial catalysis reactions (Nordstrom and Alpers 1999; Gagliano 2004). MD often contains elevated concentrations of sulfate, acidity, and metals such as Fe, Zn, Cd, As, and Pb (e.g., Nordstrom and Alpers 1999; Gagliano 2004; Nairn et al. 2009). When metal sulfides in a geologic formation are exposed to oxygen, soluble metals, sulfate, and sulfuric acid are produced (Watzlaf et al. 2004). Acid MD occurs when the host geologic formation does not have sufficient alkalinity to neutralize the mineral acidity, which is the acidity associated with dissolved metals (Watzlaf et al. 2004). However, if alkalinity exceeds the mineral acidity, which often occurs in the presence of carbonate host rock, then net-alkaline MD is produced (Hedin et al. 1994; Watzlaf et al. 2004).

There are multiple methods to treat MD, broadly split into active and passive treatment. However, the high cost and relatively labor-intensive operations often limit active treatment systems at abandoned mine sites (Watzlaf et al. 2004). Conversely, passive treatment has lesser operation and maintenance requirements, and constructed treatment wetlands and similar ecosystems may have the added benefit of creating wildlife habitat (Younger et al. 2002; Watzlaf et al. 2004; Nairn et al. 2009). The most important aspect of selecting, designing, and implementing any type of successful treatment system is proper characterization of the water quality and quantity of the MD (Skousen et al. 2017).

The objective of this research was to evaluate the water quality and quantity of MD discharges in a hydrologically and topographically challenging location to determine if passive treatment was a viable option to remediate these discharges. It was hypothesized that the MD water quality and quantity was treatable via passive methods.

5.2 Materials and Methods

5.2.1 Site Background: Douthat, Oklahoma, USA

This study was conducted near Douthat, Oklahoma, USA, which is in the Oklahoma portion of the abandoned Tri-State Lead-Zinc Mining District, known as the Tar Creek Superfund Site (TCSS). Large pumps were used to dewater the underground mines during the active mining operations that occurred from the early 1900s through the 1970s, with pumping rates reaching at least 136,000 m^3 per day

(McCauley et al. 1983). As mining ceased, and the pumps were shutdown, the underground mine void with an approximate volume of 9,870 hectare-meters began to recharge (Luza at al. 1986; Shepherd et al. 2022). In 1979, the first artesian flowing MD discharges containing elevated concentrations of Cd, Fe, Pb, and Zn were documented (Oklahoma Water Resources Board 1983) and continue to flow to this day.

The majority of the volume of artesian flowing MD within the TCSS occurs at Douthat, OK due to the similar elevations between the nominal head of the mine pool and the ground elevation at approximately 243.8 m above mean sea level (AMSL) (DeHay 2004; CH2M 2011). The intersecting ground and mine pool elevations result in numerous MD discharges in an area covering approximately 30 ha, flowing from existing boreholes, collapse features, and mineshafts (Figure 5.1). Many of these discharges do not flow year-round and are influenced by seasonal fluctuations, rain events, and annual variations from the mean climatic conditions. Within the Douthat study site, there are fourteen mineshafts, four of which are open, at least five surface collapse features, and hundreds of exploratory boreholes. Water quality data at this location date back to the 1980s, with periodic sampling conducted by a variety of agencies, companies, and research groups since then. However, the existing data were inadequate for designing a passive treatment system because of the potential changes in water chemistry that have occurred since the 1980s, and the limited flow data available from each discharge. This was the first study to attempt to identify all sources of artesian flowing MD discharges at Douthat, determine the flow rates, and regularly collect water quality samples from these discharges.

5.2.2 Mine Drainage Water Quality and Quantity Sampling

Potential locations of MD discharges were initially identified using historical sampling locations and aerial imagery, which were then field verified. In total, five MD discharge locations were identified for regular water quality and quantity sampling: Seep Railroad (SRR), Seep 40 road (S40), Admiralty No. 2 (AD2), Seep Blue Barrel (SBB), and Seep Cattails (SCT) (Figure 5.1).

Water quality samples from each MD discharge were collected on a regular basis from 2018-2021. Field analyzed parameters included alkalinity and turbidity using Hach test kits, and a 6-series YSI multiparameter datasonde measuring conductivity, temperature, pH, and dissolved oxygen (Table 5.1). Samples for anions, total metals, and dissolved (<0.45μm) metals were collected and preserved in the field, then analyzed at the University of Oklahoma Center for Restoration of Ecosystems and Watersheds (CREW) laboratories following U.S. EPA standard methods (Table 5.1).

Water quantity data were collected at locations that represented each of the five selected discharges. Flow rates at SRR and S40 were collected using sharp crested, 90-degree, V-notch weirs with 53.3 cm deep and 45.7 cm deep V-notches, respectively. The SRR discharge was originally an exploratory

borehole that occurs approximately 40 m horizontally from known underground mine workings. An attempt to seal this discharge was made in the 1980s, covering the discharge with a mound of dirt approximately 1.5 m high. The discharge eventually began to seep through the mound, resulting in the center of the mound collapsing, creating a bowl shape. Eventually, the MD eroded through one side of the bowl-shaped mound, creating a highly incised channel where the SRR weir was installed. The S40 discharge is a 25 cm (10 inch) diameter, intact-cast iron pipe that connects the underground mine workings approximately 46 m below ground. The water flows into a nearby roadside ditch in which the S40 weir was installed.

The AD2 discharge originates from a partially subsided mine shaft that connects to the underground mine workings approximately 60 m below ground. The MD flows into an old stream channel, referred to as Old Lytle Creek, before it enters Tar Creek (Figure 5.1). The weir was installed in the Old Lytle Creek Channel approximately 15 m above its confluence with Tar Creek. The AD2 weir was a sharp-crested compound weir comprised of a 90-degree, 30.48 cm deep V-notch set into a 152 cm wide by 45.72 cm tall rectangular weir.

Each weir included a deployed pressure sensor, logging pressure and temperature values every 15 minutes. The pressure data from each weir installation were corrected for atmospheric pressure using a barometric pressure sensor located on-site that logged at the same time interval. The corrected pressure data were used to calculate flow rates using the appropriate weir equations. Weir installation was not feasible at SBB and SCT because the flows from these discharges were not channelized. Therefore, water quantity measurements were collected using a calibrated 20 L bucket and stopwatch during the water quality sampling events at these locations.

Historical data showed the mine pool had drastic water elevation fluctuations that occurred over short periods, often less than two days. Based on field observations, the mine pool fluctuations corresponded with elevated discharge flow rates from the discharges. A four-day sampling event was conducted during an elevated discharge event to determine if the water from the discharges during these events was consistent quality MD and not diluted by rainwater. The experiment was conducted by deploying an autosampler at the S40 discharge with a depth sensor set to an elevation of approximately 244.60 m AMSL in a nearby abandoned borehole connected to the underground voids. During a peak discharge event on Dec. 31, 2018, the autosampler was triggered and collected a 1 L discrete sample every four hours for the remaining 96 hours. The samples were retrieved from the field shortly after sampling had ended and were preserved for laboratory analysis of total metals following U.S. EPA standard methods (Table 5.1).

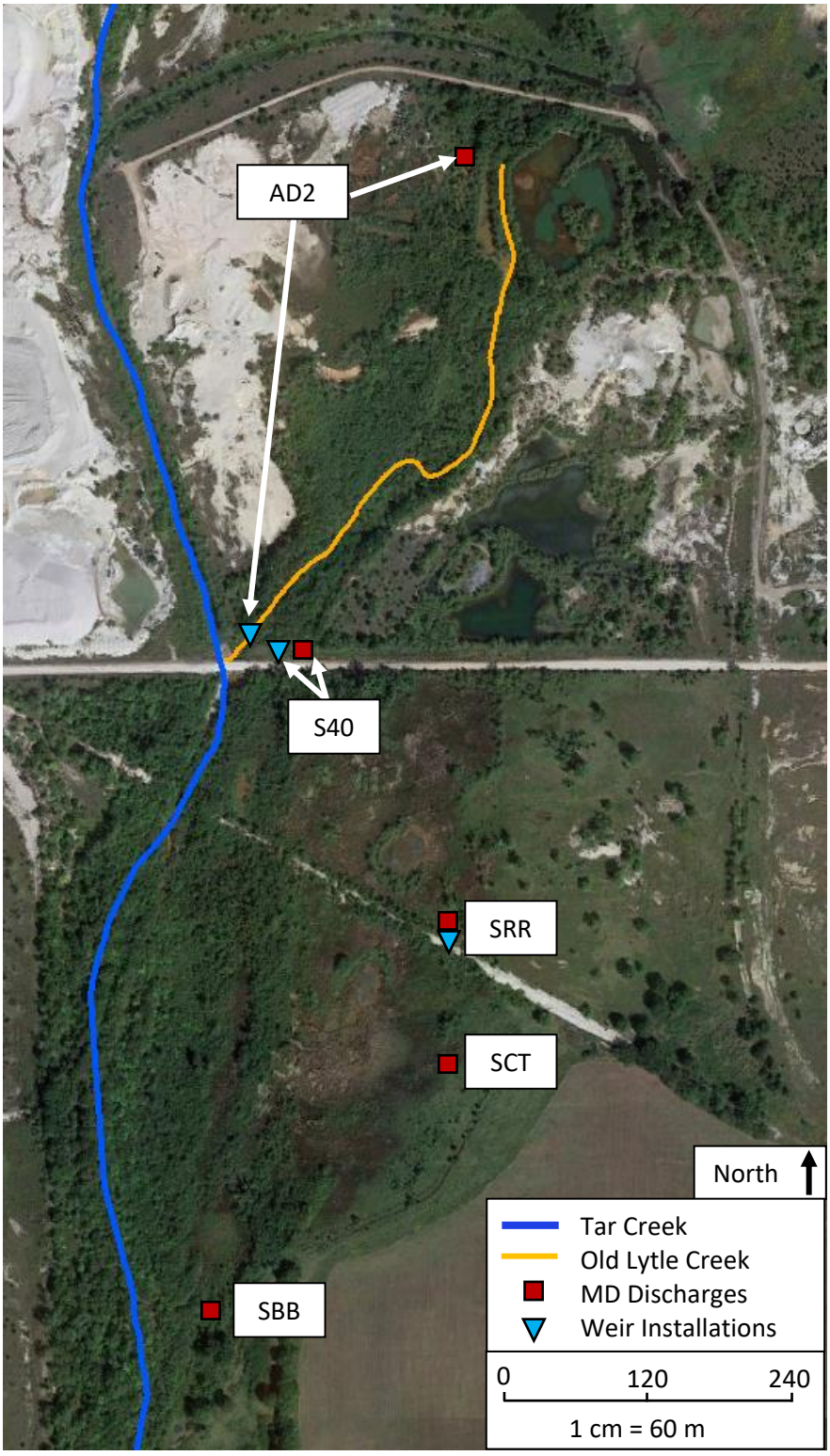

Figure 5.1: Mine Drainage (MD) discharge sampling locations and weir installations at Douthat, Oklahoma, USA, located within the Tar Creek Superfund Site (*Source:* "Douthat, Oklahoma, USA". 36.958292°N, 94.842731°W. Google Earth. Sept. 7, 2021. Jan. 4, 2022.)

Table 5.1: Sampling parameters and methods used to evaluate the water quality and quantity of MD discharges at Douthat, Oklahoma (U.S. EPA 2014; Hach 2015)

	Method/Instrumentation
Water Quality Parameters	
Total Metals	U.S. EPA 3015a and 6010c
Dissolved Metals	U.S. EPA 3015a and 6010c
Sulfate	U.S. EPA 165-D Rev. A
Reactive Phosphorus	U.S. EPA 145-D Rev. A
Nitrite-Nitrate	U.S. EPA 127-D Rev. A
Nitrite	U.S. EPA 115-D Rev. A
Chloride	U.S. EPA 105
Turbidity	Hach 2100P Turbidimeter
Alkalinity	U.S. EPA 310.1
Datasonde Parameters Temperature Specific Conductance Conductivity Resistivity Dissolved Oxygen (DO) (%) DO Concentration (mg/L) Total Dissolved Solids pH	YSI 6-series multiparameter datasonde following CREW and YSI SOPs
Water Quantity	
Captured Discharge Locations	Stopwatch and Calibrated Bucket
Continuous Flow Measurements	Weir and Deployed Pressure Transducers

5.2.3 Data Analyses

The flow values calculated at each weir installation underwent automated and manual quality assurance and quality control (QA/QC) procedures. First, 24 hours of data were automatically excluded from future analyses beginning at the start of a rainfall event that recorded >1.27 cm (0.5 inches) of rainfall in the previous 24 hours, as measured by an onsite rain gauge. The data were excluded to remove uncertainties associated with runoff generated during rainfall events. All data associated with each rainfall and high flow event were then manually inspected to ensure the 24-hour period was a long enough period to remove any artificially elevated flow measurements. Each manually removed data point was determined to be substantially influenced by runoff based on flow measurements that showed an increasing or decreasing trend, with calculated values exceeding 10% of the previous measurement. Temperature data that substantially varied from the 15.8^{o}C MD were also used to verify if water flowing through a weir was influenced by runoff.

Additionally, staff gauge measurements of the stilling area behind the weir were recorded during each water quality sampling event and used to verify the depth recorded by the pressure sensor.

The staff gauge measurements were used to correct the pressure sensor data over the period since the previous field verification, if there were any differences in the depth values. Flow data were also excluded from further analyses if there were any signs during the site visit that the values generated since the previous site visit may be erroneous. An extreme example of this situation occurred during a high-flow event that eroded one side of the weir located at AD2, resulting in all water bypassing the weir.

Once flow data underwent these QA/QC measures, flow rates calculated on 15-minute intervals from the weirs were correlated with mine pool elevation data using the United States Geological Survey (USGS) groundwater monitoring station (365942094504203), known as Slim Jim (Appendix 5A; Figure 5A.1), that has been collecting data since November of 2008. The monitoring well is an abandoned drill hole that is connected to the underground mine workings. The flow data were plotted against the mine pool elevation measured at the Slim Jim monitoring well for each time interval. A trendline with the greatest correlation was plotted, and the resulting equation was used to calculate flow rates at a given mine pool elevation.

Water quality data were evaluated for any temporal trends that occurred for each MD discharge. The minimum, maximum, mean, median, and standard deviation were calculated for each parameter collected at each discharge and were used for the conceptual design of a passive treatment system. The mean metals concentrations and the flow rate trendline equations from each discharge were used to calculate the flow weighted average metals concentrations of the five MD discharges at Douthat and the subsequent metal loading to Tar Creek from these discharges on 30-minute time intervals using the mine pool water elevation data from Slim Jim for 2009-2021.

Additionally, data from the Slim Jim monitoring well, streamflow data from a USGS stream gauge station on Tar Creek (07185090, Tar Creek at US69), and precipitation data from a nearby weather station located in the same county (Ottawa County) that is maintained and operated by the Oklahoma Mesonet were analyzed to determine if drastic increases in mine pool elevation were correlated with rainfall events or elevated streamflow events. Sixty-five events that occurred from 2009 to 2019 were analyzed by determining the amount of precipitation, the maximum discharge of Tar Creek, and the highest mine pool elevation for each event. Then, the relationships of each variable were evaluated using a correlation matrix.

It is important to note that the elevation data presented in this study for the USGS Slim Jim monitoring well (365942094504203) are based on a station elevation of 253.20 m AMSL (830.72 ft AMSL). In early 2022, USGS updated the monitoring station elevation to be 252.96 m AMSL (829.92 ft

above NAVD 1988). Although USGS stated the updated value was a more accurate elevation, the 0.24 m decrease in elevation showed the Slim Jim water elevation well below other mine pool monitoring stations that were surveyed as part of the Operable Unit 4 Study at Tar Creek (Appendix 5A; Figure 5A.2). The new elevation of the monitoring station suggested the mine pool did not flow down gradient towards Douthat, which is incorrect. Therefore, using the previous elevation of 253.20 m AMSL was justified in this study.

5.3 Results and Discussion

5.3.1 Water Quantity

The fluctuations in the mine pool water elevation cause highly variable flow rates at each discharge located at the Douthat study site (Table 5.2). When the mine pool exceeded an elevation of 244.75 m, it only remained above this elevation for a short period, typically less than 37 hours (Table 5.3). It was hypothesized that these short-term, high mine pool elevations, occurred due to water entering open mine features, such as mine shafts, upgradient of Douthat during increased streamflow events (Appendix 5B), not infiltration from precipitation. Comparisons of the highest mine pool elevations, precipitation measurements, and greatest stream flow rate measured during 68 events support this claim, showing a significant correlation between peak mine pool elevation and greatest streamflow, while precipitation and peak mine pool elevation were not significantly correlated (Table 5.4). The increased head pressure from water flowing into open mine features located upgradient created a near-instantaneous pressure increase throughout the mine pool because of the hydraulic connectivity of the underground workings, thus creating a sharp increase in the mine pool water elevation. The head pressure was rapidly relieved by discharging MD via multiple open mine shafts and collapse features at Douthat with critical discharge elevations ranging from 244.54 to 244.75 m AMSL, thus causing an equally sharp decline in the mine pool water elevation. An example of a typical elevated discharge event is shown in Figure 5.2.

Table 5.2: Statistical analyses of the Picher field mine pool as measured at the United States Geological Survey Slim Jim groundwater monitoring station (365942094504203) from Nov. 1, 2008 - Dec. 31, 2020

Parameter	Value
Sample Size (n)	210,504
Min (m AMSL)	242.88
Max (m AMSL)	246.87
Mean (m AMSL)	244.33
St Dev	0.43
St Error	0.0009
1st quartile (m AMSL)	244.07
Median (m AMSL)	244.47
3rd Quartile (m AMSL)	244.63

Table 5.3: Statistical analyses of the duration (in hours) that the Picher field mine pool remains at, or above a given elevation as measured at the USGS Slim Jim groundwater monitoring station (65942094504203), using 68 events occurring from 2009 to 2019

Peak Elevation (m AMSL)	>244.9	>245.1	>245.2	>245.4	>245.5	>245.7	>245.8	>246.0	>246.1	>246.3
Number of Events (n)	68	65	49	39	28	16	12	11	9	9
Mean (hrs)	42.3	23.6	16.7	12.6	11.3	13.3	12.7	10.0	9.1	6.1
Minimum (hrs)	11.0	2.5	2.0	0.5	0.5	3.0	4.5	2.0	6.5	2.0
1st Quartile (hrs)	28.6	15.5	8.5	7.0	5.0	10.1	11.4	9.3	8.5	5.0
Median (hrs)	36.8	22.0	16.5	12.5	9.5	13.5	13.3	11.5	9.0	5.0
3rd Quartile (hrs)	54.1	30.5	22.0	17.5	16.1	17.1	15.4	12.3	10.0	7.0
Maximum (hrs)	102.5	62.5	53.5	41.5	30.0	24.5	16.5	14.0	12.0	11.0
Standard Deviation	18.5	12.7	9.4	8.5	7.6	5.8	3.5	3.7	1.5	2.5

Table 5.4: Correlation matrix comparing the peak mine pool elevation in the Picher mining field, precipitation, and peak stream flow rates of 68 events that occurred from 2009 – 2019

	Peak Mine Pool Elevation	Precipitation	Peak Stream Flow
Peak Mine Pool Elevation[a]	1.00		
Precipitation[b]	0.70	1.00	
Peak Stream Flow[c]	0.96	0.73	1.00

[a]Mine pool elevation data collected from the USGS groundwater monitoring station Slim Jim (365942094504203)
[b]Precipitation data collected from the Oklahoma Mesonet weather station located in Ottawa County
[c]Stream flow data collected from the USGS stream gauge station on Tar Creek (07185090

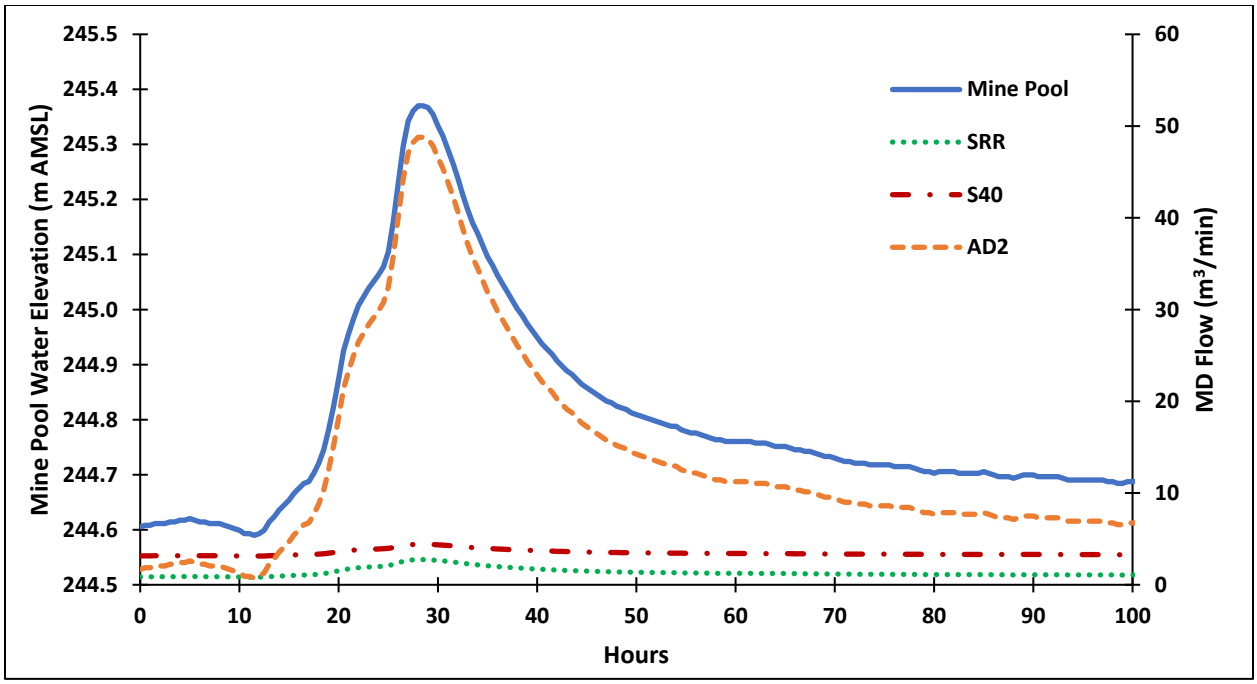

Figure 5.2: Elevated MD discharge event on January 10th, 2020, showing the Picher field mine pool water elevation as measured at the USGS Slim Jim groundwater monitoring station (365942094504203) and the calculated flow rates from SRR, S40, and AD2 MD discharges

The majority of MD discharged during these elevated discharge events flowed down the Old Lytle Creek channel, through the AD2 weir installation location (Figure 5.1). However, the AD2 weir was not able to accurately measure the flow rates of these elevated discharge events. Due to the short time intervals of these elevated discharge events, most of the continuous flow data captured by the AD2 and S40 weirs during these elevated discharge events were removed during the QA/QC process due to interferences with runoff from precipitation at S40, and backwater effects from Tar Creek at AD2 that prevented free flow through the AD2 weir. Therefore, the highest mine pool elevation used to create the flow trendlines at S40 and AD2 was 244.85 m AMSL which was much lower than the highest mine pool elevation that occurred over the same period, 245.74 m AMSL. However, the QA/QC measures were not the only limiting factor. The weirs were not large enough to measure the maximum flow rates of the discharges. Field observations during one of these elevated discharge events that occurred in 2019 noted both the S40 and AD2 weirs were completely submerged from the MD discharges originating on the north side of the project site. Therefore, the uncertainty of the calculated flow values based on the trendlines generated from each discharge increases when mine pool elevation exceeds the maximum mine pool elevation with measured flow values at each discharge.

The AD2 and S40 discharges, located on the north side of the project site, account for 85% of

the combined median flow rates of the five Douthat discharges and 96% of the maximum flow (Table 5.5). The weir installation at AD2 had the greatest range in flow rates because of critical discharge elevation and the large diameter of the AD2 mine shaft. The flow data collected at the AD2 weir were split into two groups based on the critical elevation of the AD2 shaft of 244.54 m AMSL (Figures 5.3 and 5.4). At the median mine pool elevation, below the critical discharge elevation of the AD2 shaft, the MD at the AD2 weir only accounts for a small percentage (12%) of the combined median discharge flow rates. However, the calculated maximum flow rate at the AD2 weir at the peak mine pool elevation account for 91% of the total MD, exceeding 140,000 lpm (Table 5.5).

The AD2 weir had the most issues and inconsistencies in the field that resulted in unusable data. The AD2 weir washed out only a few months after installation due to elevated flow events. Shortly after the AD2 weir was reinstalled with a stronger, stainless steel support structure in June of 2020. The data used to generate the trendlines for AD2 were collected from the reinstalled weir after June of 2020. However, erosion problems resulted in water regularly flowing around the weir and required constant repair. The erosion problems were inescapable because the banks of the old Lytle Creek stream were largely composed of highly erodible mine tailings. The erosion issues eventually led to the weir installation becoming irreparably damaged, and the AD2 weir was removed in December 2020. Additionally, MD periodically and inconsistently seeped from the stream banks and occasionally appeared as overland flow believed to originate from the S40 discharge, creating another source of indeterminate error with the flow data from the AD2 weir. All these challenges resulted in a small sample size compared to the other weirs, and the trendline generated for AD2 at the design mine pool elevation had the weakest coefficient of determination, at 0.38 (Table 5.5 and Figure 5.3).

Table 5.5: Statistical analyses of flow rates, measured in liters per minute, at five discharges near Douthat, Oklahoma, USA, within the Tar Creek Superfund Site. Seep 40 (S40), Seep Railroad (SRR), and Admiralty #2 (AD2) represent calculated flow rates using sharp crested weirs and pressure sensors. Seep Blue Barrel (SBB) and Seep Cattails (SCT) were measured using bucket and stopwatch

Site Name	Sample Size (n)	Mean Measured Flow Rate (lpm)	Median Measured Flow Rate (lpm)	Slim Jim Trendline Equation[a]	R^2	Flow Rate at Median Mine Pool Elevation[2] (lpm)	Flow Rate at Maximum Mine Pool Elevation[b] (lpm)
S40	13,876	2,125	2,073	y = 1,645.0x - 399,235	0.69	2,936	6,877
SRR	53,725	957	952	y = 2,450.8x – 598,616	0.77	547	6,418
SBB	18	55.5	56.8	y = 18.02x – 4,350.6	0.91	55.5	99
SCT	18	10.5	11.6	y = 21.83x – 5,327.3	0.82	9.97	62
AD2 <244.54 m	11,195	326	275	y = 432.34x – 105,205	0.38	497	N/A
AD2 >244.54 m	5,256	3,113	2,408	y = 61,574.x - 15,059,646	0.60	N/A	141,100
					Total Flow Rate	4,046	154,561

[a]x = mine pool elevation as measured at the Slim Jim Monitoring Well in meters above mean sea level and y = calculated flow from each discharge in lpm

[b]Flow rates calculated based on the presented trendline equations at the median and the maximum mine pool elevations of 244.47 m and 246.87 m, respectively. Mine pool elevation statistics based on USGS Slim Jim groundwater monitoring station (65942094504203) from 2008-2020

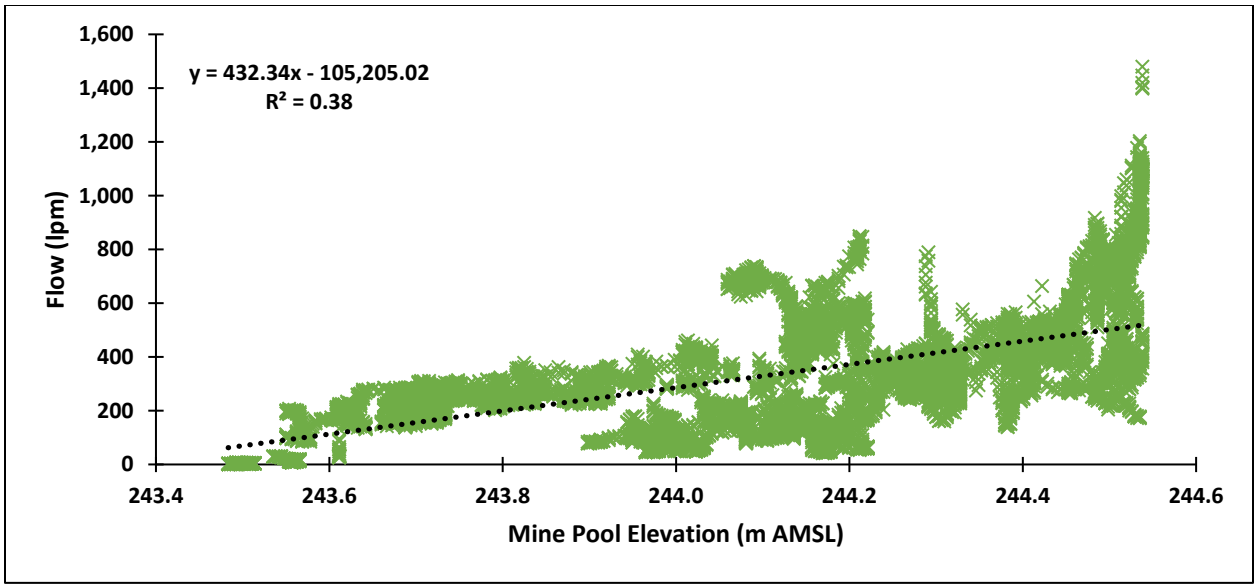

Figure 5.3: Admiralty #2 flow rates calculated using a sharp crested compound weir and pressure sensor versus mine pool elevations below 244.54 m above mean sea level (AMSL), with a linear trendline and equation, and the corresponding correlation coefficient shown

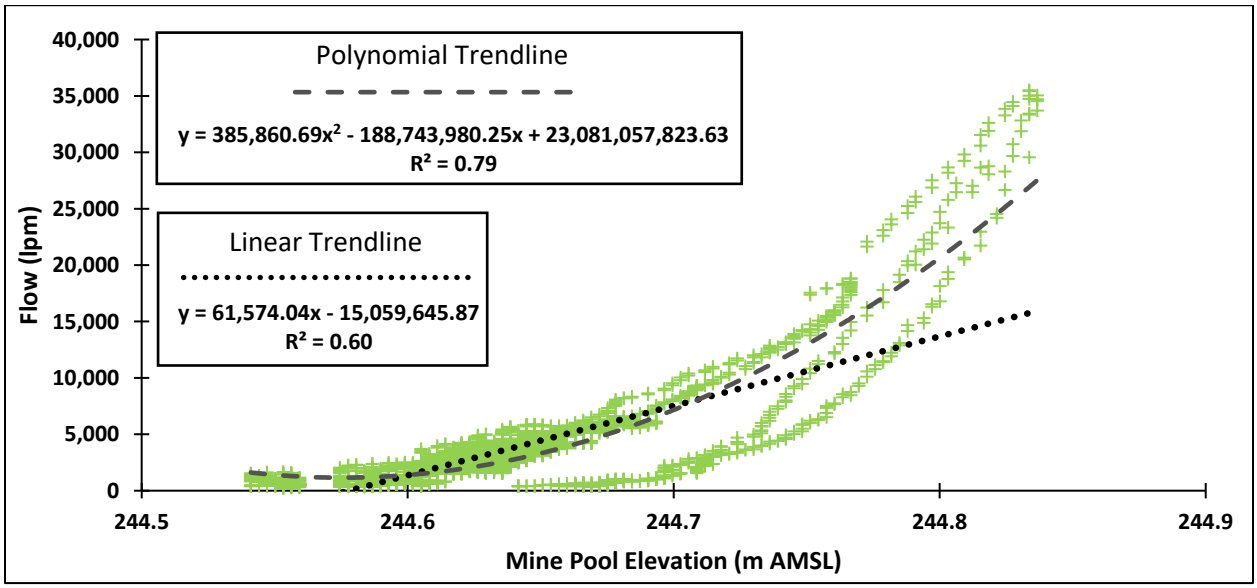

Figure 5.4: Admiralty #2 flow rates calculated using a sharp crested compound weir and pressure sensor versus mine pool elevations exceeding 244.54 m AMSL. Linear and polynomial trendlines with the corresponding equations and correlation coefficient shown

The S40 discharge contributes the majority of the MD volume of the Douthat discharges at the median mine pool elevation, accounting for 73% of combined median flow, while only contributing 4.4% of the maximum combined flow (from Table 5.5). The S40 discharge is a 25 cm (10 inch) diameter, cast iron pipe that was installed in 1935 that was used as an air ventilation-hole for the underground workings during active mining. The pipe was partially obstructed by a concrete cover when the S40 weir was installed. However, the concrete cover was removed in October 2020 to conduct additional experiments at the S40 discharge. Therefore, the data used to generate the trendline for S40 were collected from January 2020 through October 2020, before the removal of the concrete cover (Figure 5.5).

The removal of the concrete cover resulted in an immediate 27% percent increase in the flow rate from 1,250 lpm to 1,586 lpm, but also allowed for a temporary adjustable riser pipe to be attached to the existing cast iron pipe. Although utilizing data before the removal of the concrete cover to evaluate the flow rate at S40 may appear to be a determinate error, the flows collected at the S40 weir since the riser pipe was installed have shown that the flow rate can be manipulated by altering the critical discharge elevation. The top of pipe elevation of the cast iron pipe was estimated to be 242.93 m, based on previous surveys. Then a riser was installed to an estimated elevation of 244.30 m. A comparison of flow data measured at the S40 weir at a mine pool elevation of 244.44 m from these two scenarios, with and without the riser, showed the installation of the riser decreased the flow rate by over 50%, from approximately 3,096 lpm to 1,514 lpm. The possible flow manipulation of S40 potentially allows for some control over the base flow rate and design water elevation for a potential passive treatment system. However, the manipulation of these discharges should occur slowly, with only small adjustments to the discharge elevation each time, to prevent unknown discharges from developing due to a sudden increase in mine pool water elevations.

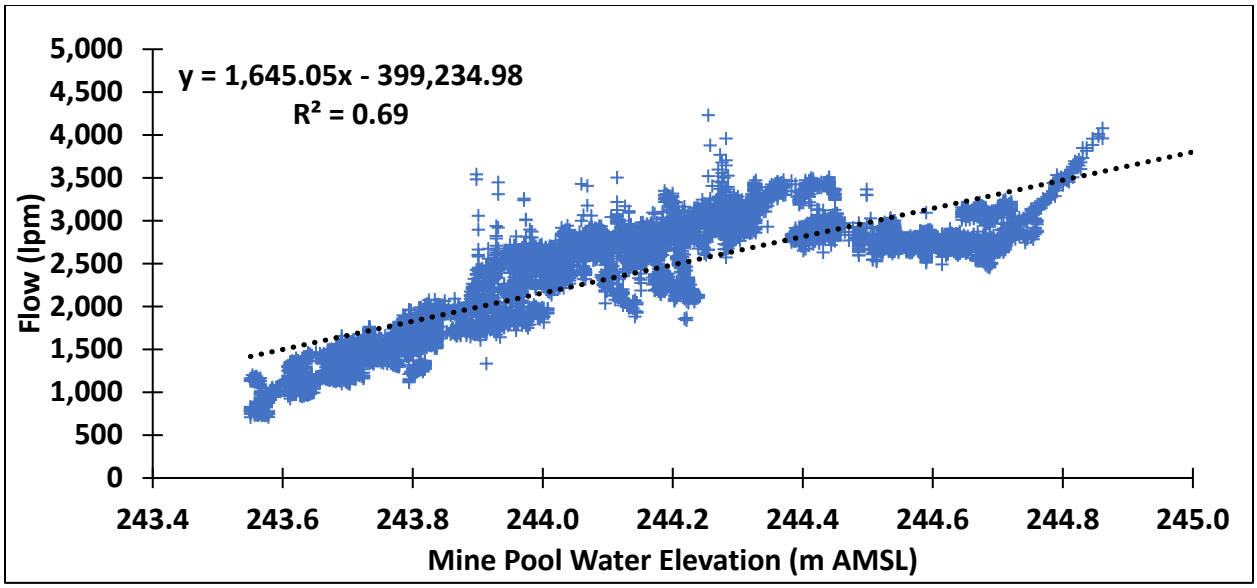

Figure 5.5: Seep 40 Road flow rates calculated using a sharp crested compound weir and pressure sensor versus mine pool elevations, with a linear trendline and equation, and the corresponding correlation coefficient shown; January 2020 through October 2020

The two discharges that used bucket and stopwatch flow rate measurements, SBB and SCT, also contribute the least amount of MD, with combined median flow rates of less than 100 lpm, contributing approximately 1.5% of the median flow rate of the discharges at Douthat (from Table 5.5). These discharges had the smallest sample size, and the smallest range of corresponding mine pool elevations (Figure 5.6). These two discharges are the southernmost Douthat discharges and are not located above any known underground mine voids. It is hypothesized that SBB and SCT are abandoned and partially sealed exploratory boreholes. However, historical mine maps do not show any boreholes at or near their location.

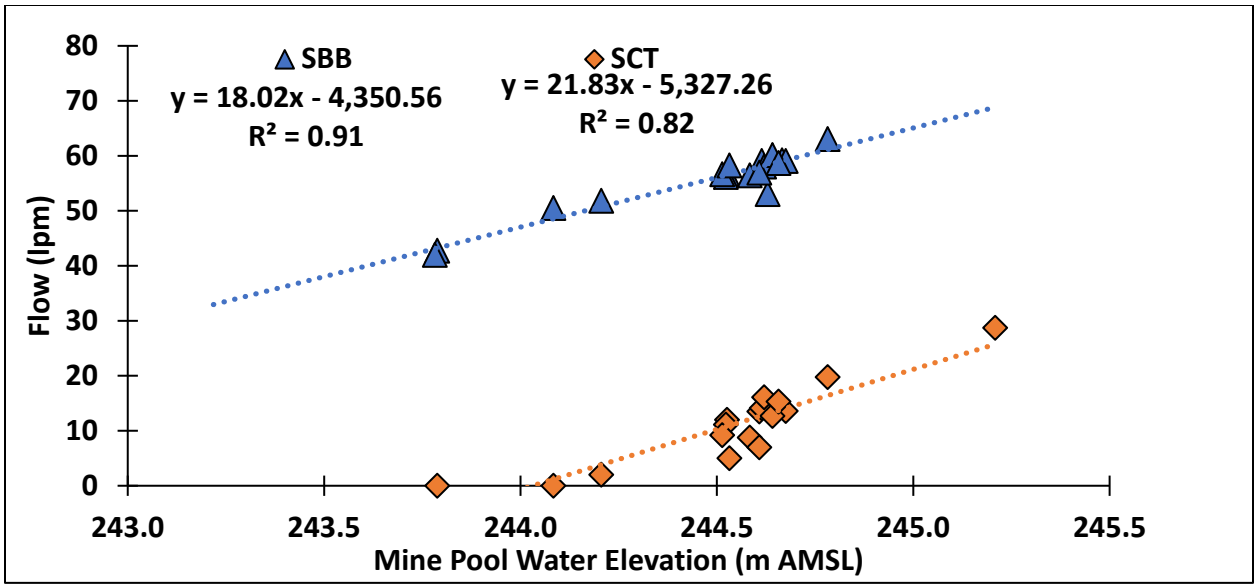

Figure 5.6: Flow rates measured using a bucket and stopwatch at Seep Blue Barrel (SBB) and Seep Cattails (SCT) versus mine pool elevations, with a linear trendline and equation, and the corresponding correlation coefficient shown

SRR contributes 13.5% of the combined median flow rates and 4.2% of the combined maximum flow rates (from Table 5.5). SRR had the strongest coefficient of determination (0.77) of the three weirs at the median mine pool elevation (Figure 5.7) and had the largest sample size because SRR was surrounded by a berm on all sides, limiting outside sources of indeterminate error such as precipitation and runoff.

The discharge elevation of SRR was raised by approximately 0.6 m when the weir was installed. Therefore, the flow rates calculated at SRR are based on the critical elevation of the installed weir at 244.08 m. However, SRR could be captured with an adjustable riser, similar to the riser at S40, which would allow the flow rates and critical discharge elevation to be slightly manipulated if necessary.

Overall, the MD discharges at Douthat have highly variable flows that are driven by fluctuations in the mine pool water elevation. Despite the flow variability, the water quantity is treatable via treatment wetlands. Multiple passive treatment systems have been constructed around the country that have successfully treated flow rates greater than the median flow rate at Douthat of approximately 4,000 lpm, including the West Fork aerobic biotreatment system, located in Missouri, treating 4,500 lpm (Gusek et al. 1998), limestone diversion wells on Lorberry Creek, and wetlands on Lower Rausch Creek, located in Pennsylvania, treating 7,860 lpm and 9,450 lpm, respectively (Cravotta III 2010). Other non-MD treatment wetlands have been constructed to treat flows exceeding the maximum calculated flow at Douthat of 150,000 lpm, such as the East Fork water reuse project in Texas that can divert 290,000

lpm into the 810-hectare treatment wetland (Plummer 2020).

Designing and constructing a passive treatment system at Douthat based on the maximum flow rate would likely be cost-prohibitive and the system would be incredibly large. However, an alternative design approach could be a system to treat everything except the greatest flows. Since the elevated flows only last for a short period, the MD volume of these events could be retained in a large storage basin. Then, the stored MD would be slowly released to be treated in the moderately sized passive treatment system after the flows decrease.

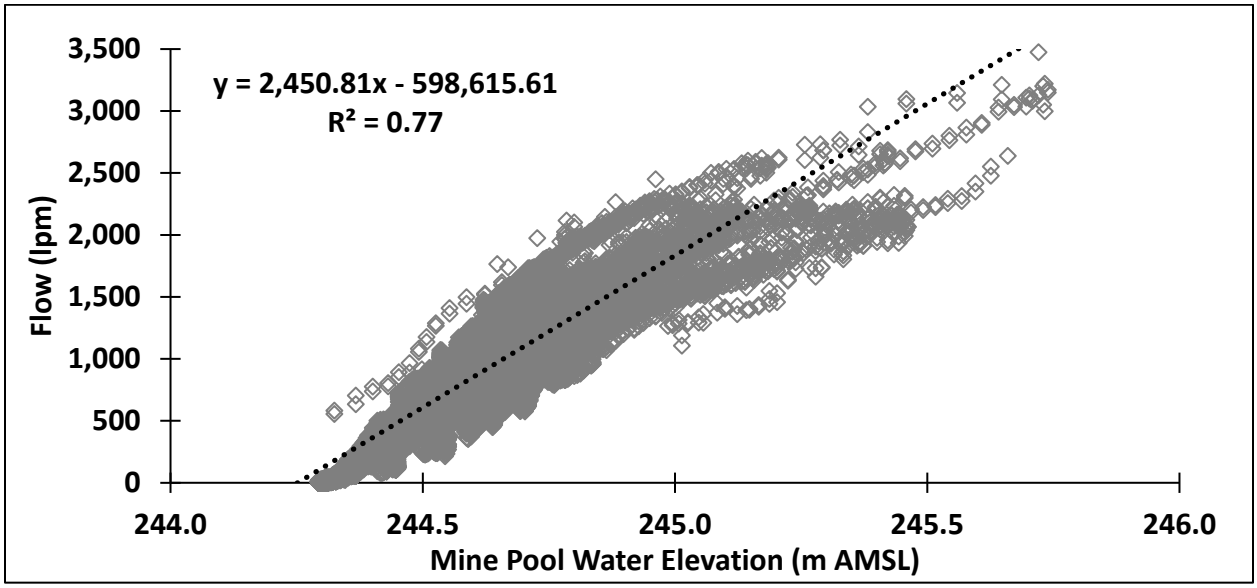

Figure 5.7: Seep Railroad (SRR) flow rates calculated using a sharp crested compound weir and pressure sensor versus mine pool elevations, with a linear trendline and equation, and the corresponding correlation coefficient shown

5.3.2 Water Quality

SBB and SCT discharges had the greatest concentrations of Fe and Pb, with approximately twice the concentrations compared to the other discharges (Table 5.6). Additionally, SBB and SCT had the greatest mean alkalinity and sulfate concentrations, which corresponded with the greatest mean specific conductance of the Douthat discharges. However, the Zn concentrations at SBB were substantially lower than the other discharges at Douthat (Table 5.6).

SRR and AD2 had similar mean metals concentrations and similar trends in metals concentrations over time (Table 5.6 and Figures 5.8-5.11). Both discharges showed a decreasing trend in total Fe throughout 2019 and 2020, with SRR beginning to plateau near 20 mg/L Fe (Figure 5.8). AD2 has less available data to evaluate the trends in metals concentrations because only the data collected while

the discharge was flowing were used in these analyses.

S40 had the most drastic fluctuations in metals concentrations, with a sharp decline in Fe and Pb beginning in 2019 and an inverse trend in Zn and Cd. (Figures 5.8-5.11). Total Fe concentrations were initially near 35 mg/L before a drastic decrease throughout 2019, with total Fe concentrations dropping below 1 mg/L, before a drastic increase starting in November of 2020 and peaking at 24 mg/L in February 2020. Meanwhile, Zn and Cd concentrations peaked in November 2019, with total Zn concentrations nearly doubling compared to 2018 and Cd concentrations increasing eight-fold (Figures 5.10 and 5.11). The causes of the fluctuations in metals concentrations at S40 are unknown. Although the metals concentrations at S40 appear to be stabilizing since early 2021. Additional data should be collected at all of the Douthat discharges to continue to evaluate the long-term trends.

There was a notable increase in rainfall during 2019 compared to previous years with an annual rainfall of 207.36 cm, measured at the Ottawa County, OK Mesonet weather station, compared to the average annual rainfall of 113.06 cm (Kos et al. 2016). The elevated amount of precipitation corresponded with multiple elevated streamflow events in Tar Creek, and the highest mean annual mine pool elevation that was recorded at the USGS monitoring station, Slim Jim of 246.87 m AMSL. However, if the precipitation in 2019 was the cause, the trends in metals concentrations of a similar magnitude would have been expected to occur at AD2 and SRR, since these discharges are hydraulically connected by underground mine voids (Chapter Four). They were not.

S40 was also the only discharge where the underlaying mine pool was sampled because it had an intact cast iron pipe where a riser could be added to temporarily stop the flow and conduct the depth sampling. The total depth of the S40 discharge was 63 m, with the approximate mine void occurring from 46 m to 63 m. Depth sampling showed the water column was homogenous from the surface to a depth of 52 m. The next 3 m, from 52 m to 55 m, showed a heterogenous transition zone. The bottom 8 m were homogenous and contained substantially greater total metals concentrations of 0.043 mg/L Cd, 260 mg/L Fe, 0.43 mg/L Pb, and 35 mg/L Zn (See Chapter Seven for additional discussion). Although the greater aqueous metals concentrations that are found at the bottom of the S40 discharge do not appear to be influencing the discharge water quality when it is flowing, it is worth noting that any subsurface disturbance has the potential to mix the water column resulting in MD at S40 with metals concentrations far greater than reported in this study.

Although the water quality and metals concentrations vary at each of the Douthat discharges, with some discharges showing drastic fluctuations, all the MD discharges at Douthat are treatable via passive treatment. Two other passive treatment systems located within the TCSS have been successfully

treating MD with substantially greater metals concentrations (Table 5.7) compared to those at Douthat. Both the Mayer Ranch PTS and Southeast Commerce PTS, operating since 2008 and 2017, respectively, have continued to show significant decreases in aqueous total metals concentrations of Cd, Fe, Pb, and Zn.

Table 5.6: Mean water quality values and the standard error of selected parameters from each of the five discharges sampled near Douthat, Oklahoma, USA, within the Tar Creek Superfund Site. Flow weighted averages were calculated based on the median flow rates of each discharge

	Sample size (n)	pH	Specific Conductivity (µS/cm)	Alkalinity (mg/L CaCO3 eq.)	Sulfate mg/L	[Cd] mg/L	[Fe] mg/L	[Pb] mg/L	[Zn] mg/L
S40	25	6.11±0.04	2240±34	125.8±5.46	1,428±127	0.027±0.004	20.59±2.29	0.041±0.004	6.16±0.28
SRR	15	6.15±0.03	2,179±22	126.6±3.13	1,596±158	0.004±0.0002	25.64±2.63	0.055±0.006	4.66±0.20
SBB	18	6.40±0.03	2418±25	211.3±6.34	1,572±143	0.007±0.0027	53.47±0.63	0.095±0.004	2.42±0.03
SCT	13	6.23±0.03	2,373±10	175.6±2.89	1,793±154	0.006±0.0005	49.77±1.34	0.091±0.004	4.18±0.05
AD2[a]	7	6.18±0.05	2,240±37	146.4±4.10	1,318±80	0.008±0.0007	24.11±2.44	0.053±0.005	5.05±0.18
Flow Weighted Average		6.13±0.04	2,237±36	129.3±5.69	1,497±173	0.022±0.003	22.61±2.53	0.045±0.005	5.76±0.28

[a]Water quantity samples shown for Admiralty #2 were collected while the discharge was flowing

Table 5.7: Total aqueous metals concentrations and selected physical parameters of the Mayer Ranch (MRPTS) and Southeast Commerce (SECPTS) passive treatment systems using flow weighted averages ± the standard deviations for the inflows of each treatment system

Site Name	Flow (lpm)		Sample Size (n)	pH	Alkalinity (mg/L $CaCO_3$ eq.)	Cd[a] (mg/L)	Fe (mg/L)	Pb[a] (mg/L)	Zn (mg/L)
MRPTS	415±48	In	181	6.00±0.21	385±54.6	0.016.1±0.012	159±38.8	0.110±0.130	7.30±1.88
		Out	57	7.05±0.19	191±45.4	<0.0006 (7)	0.45±0.41	<0.0195 (14)	0.53±0.83
SECPTS	465±35	In	127	5.97±0.23	328±32.3	0.019±0.009	141±20.5	0.268±0.124	6.69±1.14
		Out	54	6.78±0.33	139±43.2	<0.0006 (14)	1.42±1.22	0.021±0.009	0.58±0.99

[a]Values in parentheses indicate the number of samples with concentrations above the detection limit of 0.00064 mg/L for Cd and 0.0195 mg/L for Pb

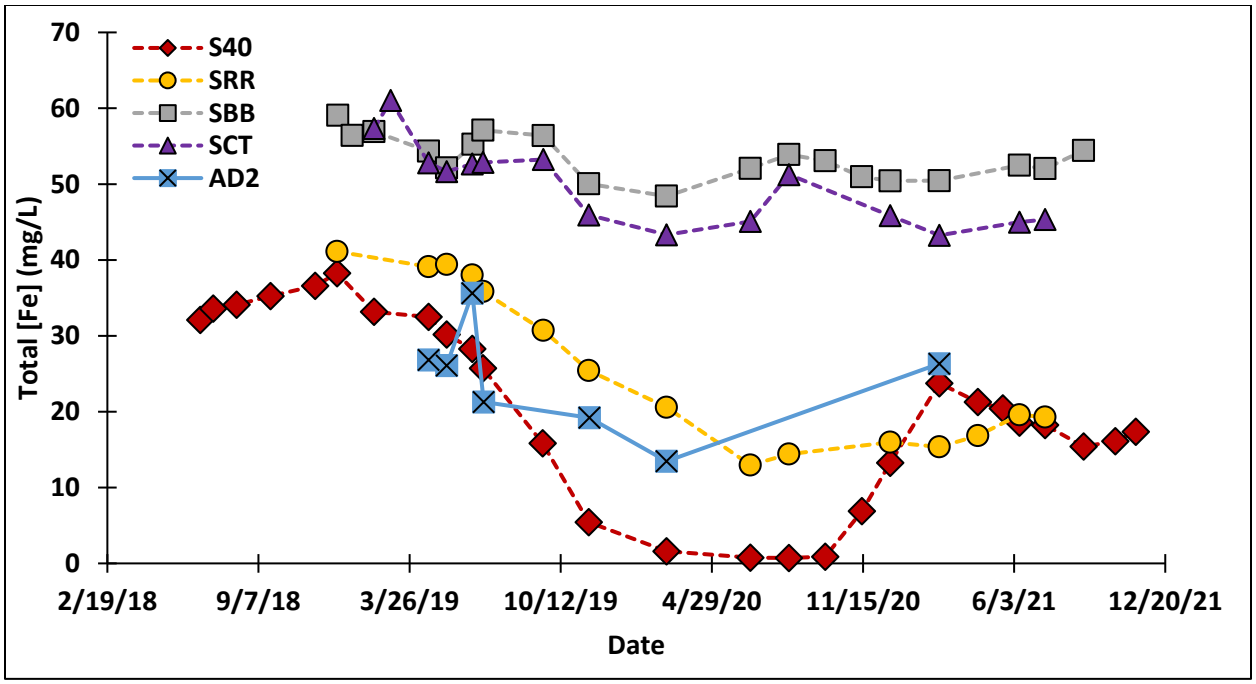

Figure 5.8: Total aqueous Fe concentrations of five mine drainage discharges located near Douthat, Oklahoma, USA

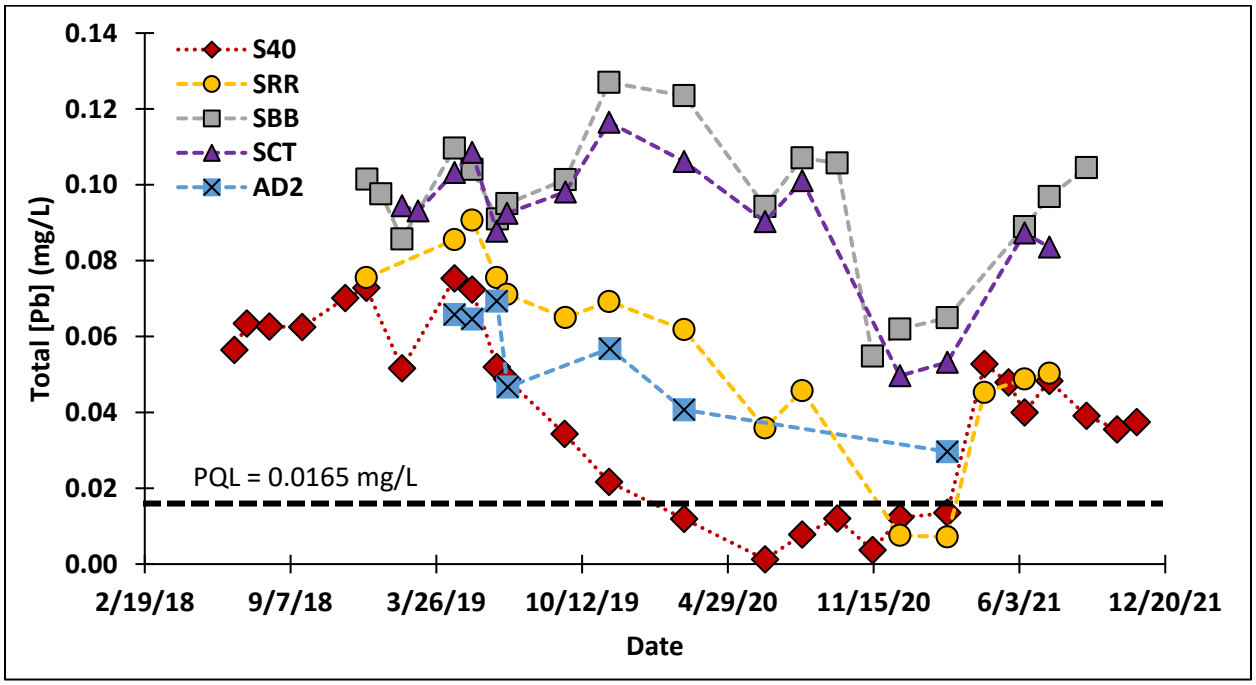

Figure 5.9: Total aqueous Pb concentrations of five mine drainage discharges located near Douthat, Oklahoma, USA with the practical quantitation limit represented by a horizontal black dashed line

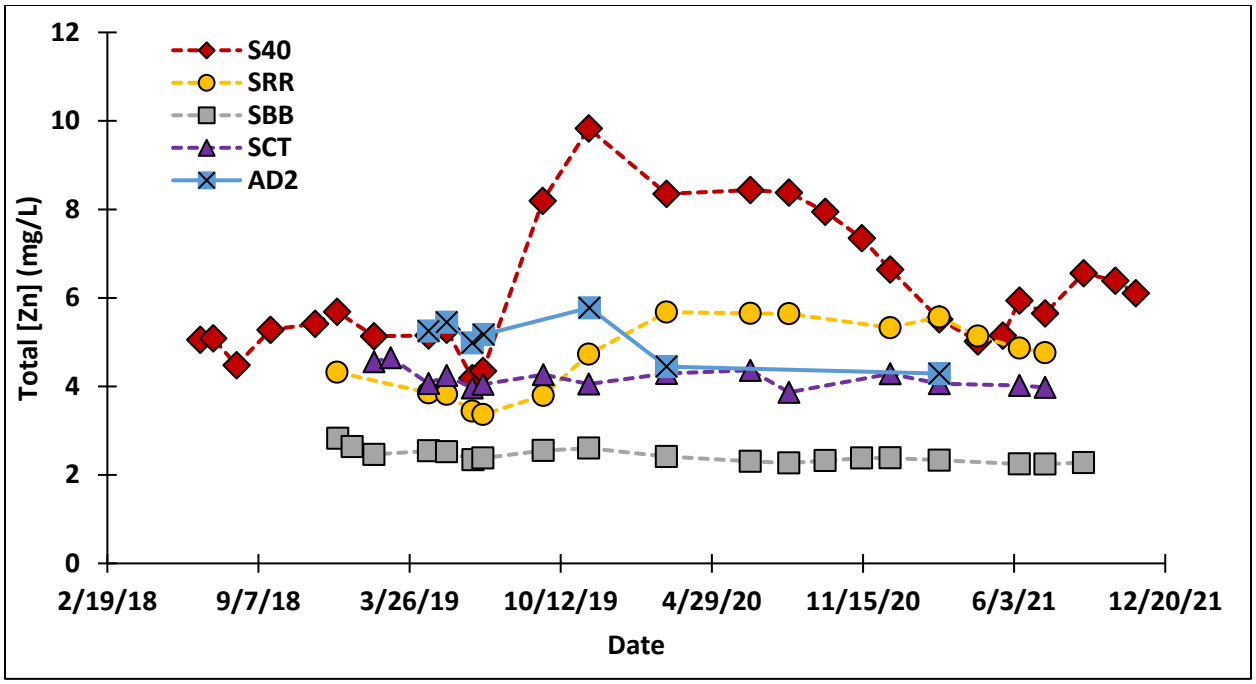

Figure 5.10: Total aqueous Zn concentrations of five mine drainage discharges located near Douthat, Oklahoma, USA

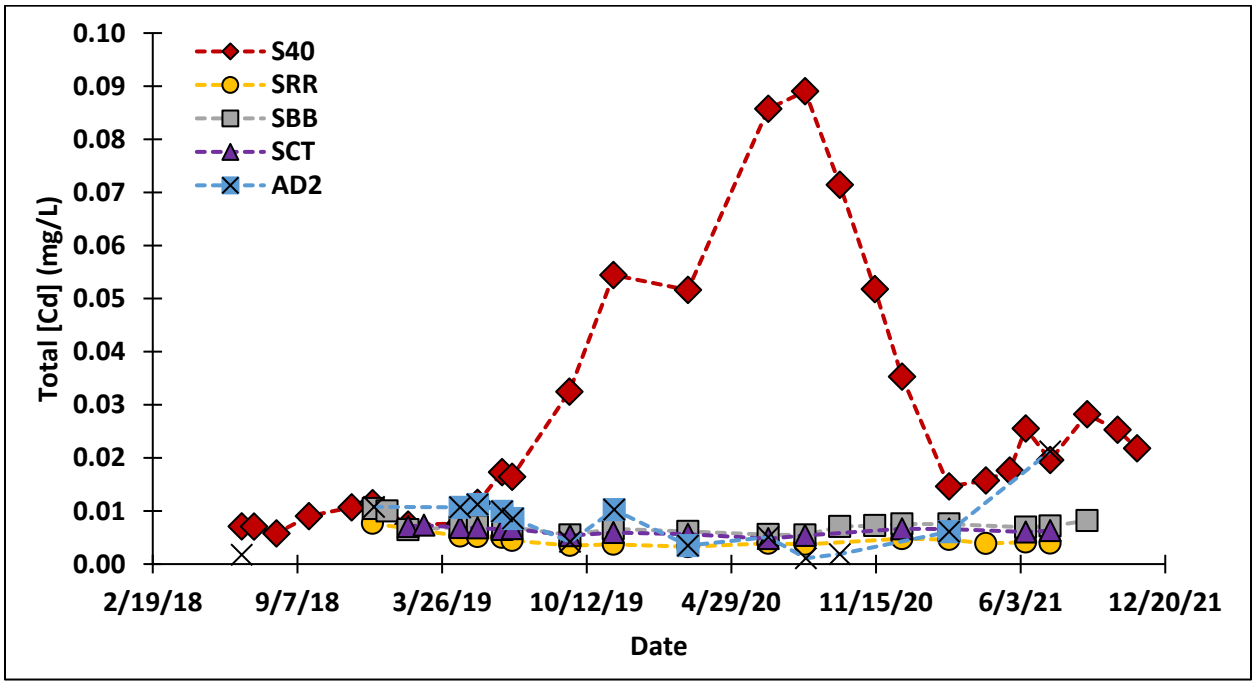

Figure 5.11: Total aqueous Cd concentrations of five mine drainage discharges located near Douthat, Oklahoma, USA

5.3.3 Metals Loadings

S40 and AD2 were the two discharges that contributed the majority of the calculated annual metal loads of Cd, Fe, Pb, and Zn to Tar Creek (Table 5.8). Although AD2 only flowed approximately 44% of the time, the elevated discharge events substantially increased metal loading in a short period. The influence of the metal loading from AD2 during these large discharge events was highlighted by the daily Fe metal loading calculated for each discharge during 2017, with Cd, Pb, and Zn showing similar trends (Figure 5.12).

A four-day sampling event that consisting of total metals samples collected every four hours at S40 during one of the elevated discharge events showed the water from the discharges was undiluted MD. The event began with a 3.6 cm rainfall that resulted in a maximum discharge of 11.5 m^3/sec in Tar Creek. The mine pool elevation increased over 70 cm in 16 hours, peaking at 245.01 m AMSL. There were no substantial changes or trends in metals concentrations of Cd, Fe, Pb, or Zn over the four days (Appendix 5B). The mean and standard deviation of the total metals concentrations during the event were 0.0079 ± 0.00063 mg/L Cd, 29.71 ± 1.32 mg/L Fe, 0.055 ± 0.003 mg/L Pb, and 5.44 ± 0.049 mg/L Zn. Additionally, multiple other elevated discharge events occurred during site visits, and a multiparameter datasonde was used to measure specific conductance at multiple effluent locations from the northern discharges. The specific conductance measured in every instance was consistent with the historical measurements collected during base flow at approximately 2,000 µs/cm, while Tar Creek upstream of the MD discharges had a specific conductance ranging from 300 to 400 µs/cm. A photo was taken during the start of an elevated discharge event that shows precipitated Fe mobilized in Old Lytle Creek due to the increased flow velocities. The precipitated Fe then mixes with Tar Creek (Figure 5.13).

Table 5.8: Annual mean metal loading of five mine drainage discharges located near Douthat, Oklahoma

Site	As kg	Cd kg	Fe kg	Pb kg	Zn kg
S40	0.00	39.6	29,891	58.0	8,686
SRR	5.83	1.12	7,208	15.5	1,310
SBB	1.20	0.19	1,482	2.64	67.4
SCT	0.18	0.03	220	0.40	18.5
AD2	0.00	11.9	35,756	78.6	7,489
Total	7.21	52.8	74,557	155	17,571

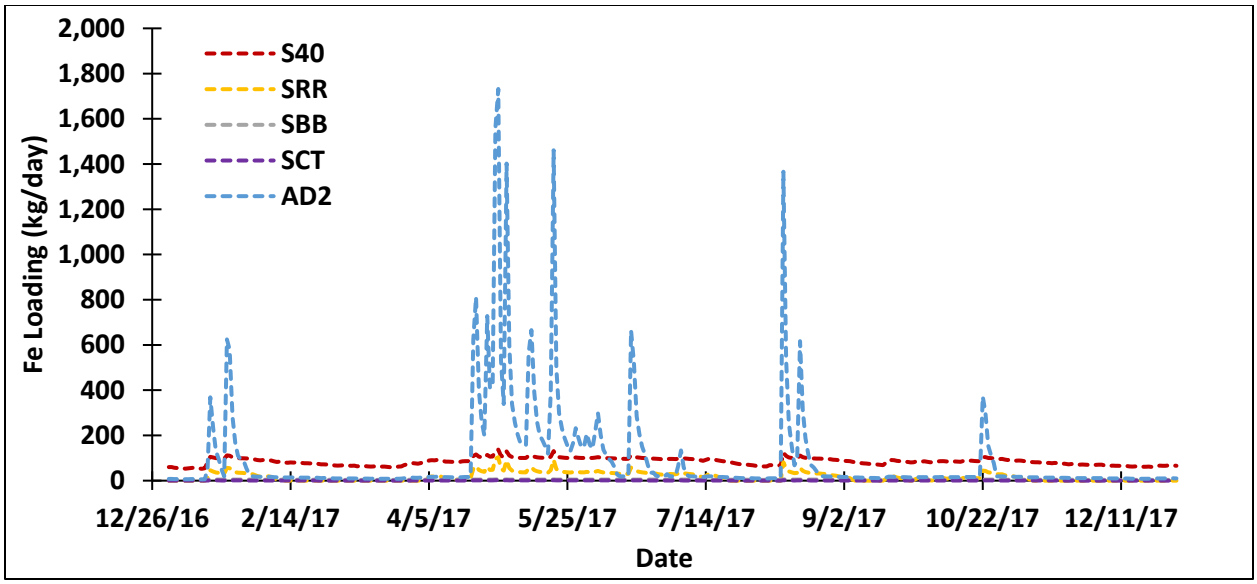

Figure 5.12: Daily Fe loading from five mine drainage discharges located near Douthat, Oklahoma, USA, within the Tar Creek Superfund Site

Figure 5.13: Photo taken during the start of an elevated discharge event on June 17, 2019, showing precipitated Fe being mobilized in Old Lytle Creek (right) as it confluences with Tar Creek (left) near Douthat, OK, USA

It is important to note that the metal loading was based on the calculated flow rates using the equations presented in Table 5.5. The weir installations used in this study were constructed and installed by hand and ultimately were insufficient to accurately measure the maximum flows from AD2, S40, and other open mine features on the north side of the project site. Accurate flow measurements at high mine pool elevations are essential to accurately quantify the metal loadings contributed from these discharges during elevated flow events. Additionally, a flow measuring device capable of measuring the elevated discharge events will also make it possible to quantify the changes in flow rates during these peak mine pool elevations as known inflow locations throughout the Picher mining field are sealed (Appendix 5B). It would be necessary to construct a berm around the remainder of north Douthat; on the west and south side of the site that tied into the existing berm, with a large concrete structure to support an adjustable sharp-crested compound weir to accurately measure the high flow rates. The berm would limit interferences associated with runoff and from Tar Creek and Lytle Creek and would force all known and unknown MD discharges on the north side of the project site to a single, large weir. A conceptual design of this berm is further discussed in Chapter Six.

5.4 Conclusions

This study evaluated the water quantity and quality of five MD discharges located near Douthat. The findings of this study showed that the MD discharges at Douthat are treatable via passive treatment. Although the water quantity was highly variable due to large discharge events, primarily affecting the AD2 discharge, multiple man-made treatment wetlands have been constructed and continue successfully treating water with greater flow rates than the median and maximum flow rates calculated at the Douthat MD discharges. Additionally, two passive treatment systems located within the TCSS are currently remediating MD with greater Cd, Fe, Pb, and Zn total aqueous metals concentrations than those found at the Douthat discharges. The successful implementation of a PTS at Douthat would result in the last of the large MD discharges impacting Tar Creek being remediated and represent the greatest decrease in metal loading to Tar Creek from MD sources. Ultimately, remediating the MD at Douthat has the potential to allow the aquatic ecosystems to recover as was shown after the implementation of MRPTS and SECPTS in an unnamed tributary to Tar Creek.

5.5 References

Byrne PA, Wood PJ, Reid I (2011) The impairment of river systems by metal mine contamination: A review including remediation options. Critical Reviews in Environ Sci Technol. 42(19):2017-2077. ISSN 1064-3389

Cravotta III CA (2007) Passive Aerobic Treatment of Net-Alkaline, Iron-Laden Drainage from a Flooded Underground Anthracite Mine, Pennsylvania, USA. Mine Water Environ. 26:128-149. https://doi.org/10.1007/s10230-007-0002-8

Cravotta III CA (2010) Abandoned Mine Drainage in the Swatara Creek Basin, Southern Anthracite Coalfield, Pennsylvania, USA: 2. Performance of Treatment Systems. Mine Water Environ. 29:200-216. https://doi.org/10.1007/s10230-010-0113-5

CH2M (2011) Tar Creek Superfund Site Operable Unit 4 - Fine Tailings Pond FT011 Injection Work Plan. Prepared for the U.S. EPA.

DeHay KL, Andrews WJ, Sughru MP (2004) Hydrology and Groundwater Quality in the Mine Workings within the Picher Mining District, Northeastern Oklahoma, 2002-03, Report 2004-5043. U.S. Department of the Interior – U.S. Geological Survey.

Gagliano WB (2004) Biogeochemical Characterization of a Constructed Wetland for Acid Mine Drainage Treatment. The Ohio State University, a dissertation.

Gusek J, Wildeman T, Miller A, Fricke J (1998) The challenges of designing, permitting, and building a 1,200 gpm passive bioreactor for metal mine drainage West Fork Mine, Missouri. Journal American Society of Mining and Reclamation. https://doi.org/10.21000/JASMR98010203

Hedin RS, Nairn RW, Kleinmann RLP (1994) Passive Treatment of Coal Mine Drainage. Bureau of Mines, Department of the Interior.

Hach (2015) Phenolphthalein and Total Alkalinity Digital Titrator, Hach Method 8203. Hach Company. Edition 8.

Kos L, Shafer M, Riley R (2016) The Climate of Miami, Oklahoma. Southern Climate Impacts Planning Program. 16 pp.
[Available online at http://www.southernclimate.org/documents/Climate_Miami.pdf.]

Luza KV (1986) Stability problems associated with abandoned underground mines in the Picher field, northeastern Oklahoma. Oklahoma Geological Survey. Circular 88, ISSN 0078-4397.
McCauley JR, Brady LL, Wilson FW (1983) Study of Stability Problems and Hazard Evaluation of the Kansas Portion of the Tri-State Mining Area. Kansas Geological Survey. Open File Report.

Nairn RW, Beisel T, Thomas RC, LaBar JA, Strevett KA, Fuller D, Strosnider WH, Andrews WJ, Bays J, Knox RC (2009) Challenges in Design and Construction of a Large Multi-Cell Passive Treatment System for Ferruginous Lead-Zinc Mine Waters. Proceedings, 2009 National Meeting of the American Society of

Mining and Reclamation. Billings, MT, Revitalizing the Environment: Proven Solutions and Innovative Approaches, May 30 – June 5, 2009. https://doi.org/10.21000/JASMR09010871

Nordstrom DK, Alpers CN (1999) Negative pH, Efflorescent Mineralogy, and Consequences for Environmental Restoration at the Iron Mountain Superfund Site, California. National Academy of Sciences: Proceedings of the National Academy of Sciences of the United States of America. 96:3455-3462.

Oklahoma Water Resources Board (OWRB) (1983) Tar Creek Field Investigation. OWRB.

Plummer (2020) North Texas Municipal Water District East Fork water reuse project.
URL: https://www.plummer.com/projects/north-texas-municipal-water-district-east-fork-water-reuse-project.
Date accessed: January 14, 2022.

Shepherd NL, Keheley E, Dutnell RC, Folz CA, Holzbauer-Schweitzer B, Nairn RW (2022) Picher Field Underground Mine Workings of the Abandoned Tri-State Lead-Zinc Mining District in the United States. J Maps.

Skousen JG, Zipper CE, Rose A, Ziemkiewicz PF, Nairn RW, McDonald LM, and Kleinmann RL (2017) Review of Passive Systems for Acid Mine Drainage Treatment. Mine Water Environ. 36:133–153. https://doi.org/10.1007/s10230-016-0417-1

United States Environmental Protection Agency (2014) Test Methods for Evaluating Solid Waste (SW-846), Update V, Revision 8, U.S. EPA.

Watzlaf GR, Schroeder KT, Kleinmann RLP, Kairies CL, Nairn RW (2004) The Passive Treatment of Coal Mine Drainage. Unites States Department of Energy, National Energy Technology Laboratory.

Younger PL, Banwart SA, Hedin RS (2002) Mine Water: Hydrology, Pollution, Remediation. Kluwer Academic Publishers.

CHAPTER 6

Evaluating Potential Water Quality Changes in a Mine Drainage Impacted Stream Following Simulated Passive Treatment System Implementation

Abstract

Underground mining for lead and zinc occurred in the now-abandoned Picher mining field, located on the border of Oklahoma and Kansas, USA, from the early 1900s until the 1970s. Since mining operations ceased and the last of the underground pumps that kept the mines dry were shut off, the approximately 9,870 hectare-meters (80,000 ac-ft) underground void began recharging with water. In 1979, the first artesian mine drainage (MD) discharges began to flow. The Oklahoma portion of the Picher field became a Superfund site in 1983, known as the Tar Creek Superfund Site, and in 1994, the USEPA ruled that "the impacts to Tar Creek area due to irreversible man-made damages resulting from past mining operations at the site". To date, one of the greatest remaining impacts to Tar Creek is from the MD discharges at Douthat, OK, annually contributing approximately 46 kg Cd, 65,900 kg Fe, 137 kg Pb, and 15,454 kg Zn to Tar Creek. The first objective of this study was to determine if the in-stream water quality downstream of the MD at Douthat would meet the state-designated beneficial use criteria for fish and wildlife propagation more than 50% of the time if the MD remained untreated but all other impacts to Tar Creek were remediated. Eleven years of mine pool water elevation and streamflow data that were collected at 30-minutes intervals from USGS gauge stations were used to simulate the metals loading to Tar Creek from the discharges and the resulting downstream metals concentrations for the metals of concern. The study found that even if the Douthat MD was the only source of metals loading to Tar Creek, the downstream water quality would not meet the beneficial use criteria 82% of the time for acute Zn concentrations and 90% of the time for chronic Cd concentrations. The second objective was to propose conceptual passive treatment system (PTS) designs to remediate the MD at Douthat, then determine if the simulated implementation of PTS would significantly decrease the metals loading to Tar Creek and if the simulated downstream concentrations would meet the state-designated beneficial use criteria more than 50% of the time. The eleven-year simulation of a large conceptual PTS showed a significant decrease in metals loading for all target metals, retaining 95% of Cd, 89% Fe, 89% Pb, and 86% Zn in the PTS, resulting in the downstream water quality beneficial use criteria being met greater than 99.99% of the time. Overall, this study has shown that PTS can successfully be implemented to remediate the MD at Douthat and that the impacts to Tar Creek should not be considered irreversibly

damaged.

Key Words: Tri-State Mining District, Tar Creek, Ecological Engineering, Engineering with Nature

6.1 Introduction

Mine drainage (MD) is a global concern that degrades tens of thousands of km of streams and rivers (Cravotta III, 2007; Simmons, 2010). Much of this MD originates from underground mines. For example, in the eastern United States alone, more than 80% of MD originates from underground coal mines (Skousen et al., 2017). Additionally, many of these underground mines in the United States are abandoned with no company or individual responsible for reclaiming these sites. Therefore, the reclamation of these abandoned mine lands and MD discharges becomes a public responsibility and expense (Skousen et al., 2017).

Passive treatment is often a preferred means to remediate MD at abandoned mine sites because passive treatment systems typically have lower construction, and operation and maintenance costs compared to active treatment (Watzlaf et al., 2004; Nairn et al., 2009). Passive treatment systems (PTSs) utilize a combination of naturally available energy sources and biogeochemical, microbiological, and physical processes to treat MD (Hedin et al., 1994; Younger et al., 2002; Ziemkiewicz et al., 2003; Cravotta III, 2007; Nairn et al., 2009; Zipper and Skousen, 2010; Skousen et al., 2017). Since PTSs rely on natural processes, the reaction time is slower and requires greater land area than ATS options and may require a variety of process units before the desired effluent water quality is achieved (Watzlaf et al., 2004). The primary processes used in PTSs include alkalinity generation, oxidation, reduction, and reaeration. However, in some instances, MD can be net-alkaline and not require initial alkalinity generation.

MD containing metals such as Fe that are easily oxidized under circumneutral pH conditions are typically treated using an oxidation pond and/or aerobic wetlands, which are often the first process units in a PTS for net-alkaline MD (Hedin et al., 1994; Nairn et al., 2009). The Fe retention mechanism is well documented, and these units are often designed using a Fe removal rate of 10 to 20 g Fe m^{-2} day^{-1}, with a retention time based on the initial Fe concentration, acid load, and design life of the unit (Hedin et al., 1994; Younger et al., 2002; Watzlaf et al., 2004; Skousen and Ziemkiewicz, 2005; Nairn et al., 2009; Skousen et al., 2017). The Fe oxidation and hydrolysis reactions for the removal of Fe yields Fe oxyhydroxides and acidity (Reactions 1 and 2) (Younger et al. 2002).

$$4Fe^{2+} + O_2 + 4H^+ \rightarrow 4Fe^{3+} + 2H_2O \quad (1)$$

$$Fe^{3+} + 2H_2O \rightarrow FeOOH\ (s) + 3H^+ \qquad (2)$$

The settling time of the precipitates must be considered when designing these units, whether that takes place in the same oxidation unit, or is achieved through implementing deep-shallow-deep vegetated aerobic wetlands for solids accumulation (Younger et al., 2002). Fe oxides have a reported settling rate of 0.01 to 1.9 cm/min, with decreasing settling rates as the Fe sludge condenses (Dempsey and Jeon, 2001; Dietz and Dempsey, 2002). The maximum sludge density of approximately 0.17 g/cm^3 was achieved after 48 hours (Dempsey and Jeon, 2001; Watzlaf et al., 2005). Utilizing vegetated wetland shelves can assist in solids settling. The meandering flow paths created by the vegetation increase retention time and oxygenate the water (Taylor et al., 2005; Nairn et al., 2009). Studies have also reported trace elements such as As, Cd, Ni, Pb, and Zn have the potential to coprecipitate or sorb to Fe and Mn oxides (Cravotta III, 2007; Nairn et al., 2009; Nairn et al., 2011).

Once the majority of the easily oxidized metals have been removed in the oxidation units, vertical flow systems can be used to remove dissolved metals and generate alkalinity. Vertical flow systems (VFS), including vertical flow ponds (VFP), vertical flow wetlands (VFW), vertical flow bioreactors (VFBR), and reducing and alkalinity producing systems (RAPS), which all rely on an anaerobic environment that generates alkalinity without coating limestone and precipitates metals as metal sulfides, or carbonates (Younger et al., 2002; Watzlaf et al., 2004; Skousen and Ziemkiewicz, 2005; Taylor et al., 2005; Nairn et al., 2009; Skousen et al., 2017).

For vertical flow systems, water is stacked 0.5 to 2.0 m above the substrate and the hydraulic head pressure forces the water vertically downward through an organic layer, often a mixture containing mushroom compost or other forms of organic carbon, ranging from 0.15 to 0.6 m thick, then a drainage layer composed of rock, typically limestone, with a thickness of 0.3 to 1.2 m and into an interbedded piping network (Younger et al., 2002; Watzlaf et al., 2004; Taylor et al., 2005; Skousen et al., 2017; Shepherd and Nairn, 2020). The organic material is decomposed by sulfate-reducing bacteria, reducing sulfate to highly soluble sulfides (Reaction 3) that will react with dissolved metals and precipitate metal sulfides (Reaction 4), where CH_2O represents organic matter and M^{2+} represents divalent cations (Neculita et al., 2007).

$$2CH_2O + SO_4^{2-} \rightarrow H_2S + 2HCO_3^- \qquad (3)$$

$$H_2S + M^{2+} \rightarrow MS + 2\,H^+ \qquad (4)$$

VFS treating AMD typically use design factors of 20 to 35 g acidity m^{-2} day^{-1} removal rate, with an approximate 15 hours of residence time in the stone layer (Younger et al., 2002; Skousen and Ziemkiewicz, 2005; Skousen et al., 2017). Net-alkaline MD treatment is based on the same retention time of 15 hours in the stone layer but uses a sulfate removal rate of 300 mmol m^{-3} day^{-1} for design (URS, 2003; Neculita et al., 2007). However, LaBar and Nairn (2017) found sulfate removal rates ranging from 81 mmol m^{-3} day^{-1} to 691 mmol m^{-3} day^{-1} in a benchtop VFBR experiment comparing high and low ionic strength effluent with circumneutral pH. An additional design parameter for VFS is to achieve a nominal retention time of at least 40 hours (Younger et al., 2002). Following a VFS process unit, the effluent typically flows into a reaeration/oxidation pond to remove any remaining dissolved sulfides as hydrogen sulfide gas, address biochemical oxygen demand, and increase dissolved oxygen concentrations (Skousen and Ziemkiewicz, 2005; Nairn et al., 2009). Lastly, a polishing pond can be an ideal final process unit that can settle solids and act as an ecological buffer before discharging the treated MD to the receiving stream (Nairn et al., 2011). Although MD discharges have a wide range of chemistry, with an equally wide range of treatment options, successful MD treatment has shown to have significant results on the aquatic communities of receiving streams (Cravotta III et al., 2010; Underwood et al., 2014; Williams and Turner, 2015; Chapter Two).

The objective of this study was to propose a conceptual MD treatment system in a hydrologically and topographically challenging location to evaluate the resulting changes in metal loading of the receiving stream if the conceptual treatment system was implemented. It was hypothesized that without the implementation of a passive treatment system to treat net-alkaline MD discharges, the water quality of a second-order stream would not meet the state-designated beneficial use classifications more than 50% of the time, even if all other sources of metals contamination upstream of the discharges were addressed.

6.2 Materials and Methods

6.2.1 Site Background

This study was conducted within the abandoned Picher mining field, located in the Oklahoma and Kansas portion of the abandoned Tri-State Lead-Zinc Mining District (TSMD) in the United States. The Picher field covers approximately 145 km^2 (56 mi^2) of land (Figure 6.1) and was extensively underground mined for lead and zinc ores from the early 1900s through the 1970s, producing approximately 1.5 million metric tons (m-tons) of lead and 8 million m-tons of zinc (Brockie et al., 1968;

Playton et al., 1980; Luza, 1983; ODEQ, 2006). By the end of the mining days, the underground mine void of the Picher field was approximately 9,870 hectare-meters (80,000 ac-ft), covering an area of 1,440 hectares (3,560 ac). Surface features include approximately 1,500 mine shafts and over 100,000 boreholes (Luza, 1983; McCauley et al., 1983; United States Environmental Protection Agency (USEPA), 1994; Luza and Keheley, 2006; Shepherd et al., 2022). Today, at least 200 of the mine shafts in the Picher field remain open, with many of them hydraulically connected by the underground mine workings.

The mine voids began refilling after mining ceased and the dewatering pumps were shut down, resulting in the filling of the voids and generation of contaminated mine water. The first artesian flowing MD discharges were documented in 1979 (Oklahoma Water Resources Board (OWRB), 1983). The metal-laden MD contained elevated concentrations of Cd, Fe, Pb, and Zn. The contamination from the MD and surface contamination from the mine tailings resulted in the Picher field eventually becoming two Superfund sites, with the Oklahoma portion titled the Tar Creek Superfund Site (TCSS) listed on the National Priorities List in 1981, and the Kansas portion titled the Cherokee County Superfund Site listed in 1983 (USEPA, 1994; ODEQ, 2006; Nairn et al., 2009).

To date, two of the MD discharge locations within the TCSS are being successfully treated by two PTSs, Mayer Ranch PTS (MRPTS) and Southeast Commerce PTS (SECPTS). However, the largest MD discharge, measured in terms of both water quantity and metal loading is located further north, near Douthat, OK (Figure 6.2). The Douthat site will be the proposed location of the conceptual PTSs. There are multiple connections to the mine voids at Douthat, including fifteen mineshafts, four of which are open, at least five known surface collapse features (Luza and Keheley, 2006), and hundreds of exploratory boreholes. An attempt was made in the 1980s, as part of Operable Unit 1 (OU1), to stop the MD at Douthat by creating a diversion structure that diverted Lytle Creek around the open mine shafts at Douthat, creating a “new” Lytle Creek channel and an “old” Lytle Creek channel (Figure 6.2) (OWRB, 1983). While the diversion structure did not stop the MD from discharging at Douthat, it did partially isolate the large discharges at north Douthat resulting in flows from the Old Lytle Creek channel being comprised of primarily MD.

Much of the Douthat site is relatively flat, with only a few meters of relief across the one kilometer (0.6 miles) site. Additionally, the approximate ground elevation throughout the site is 244 m above mean sea level (AMSL) (800 ft AMSL), which corresponds to the nominal elevation head of the 9,870 hectare-meters (80,000 ac-ft) mine pool. The overlapping ground elevation and water table result in numerous MD discharges at the site, flowing from existing boreholes, collapse features, and mineshafts. Many of these discharges do not flow year-round and are influenced by seasonal

fluctuations, rain events, and annual variations from the mean climatic conditions (Chapter Five).

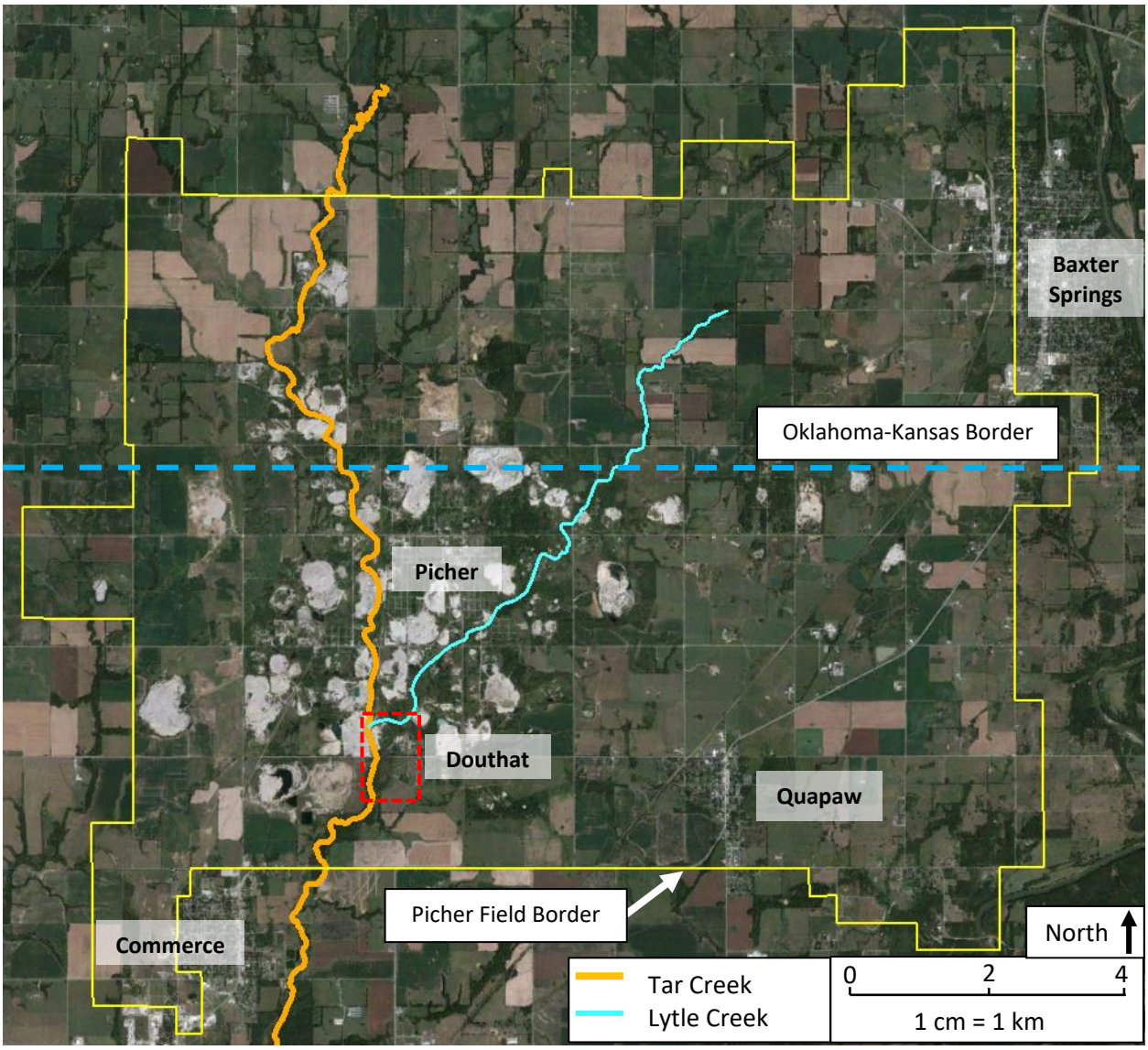

Figure 6.1: Aerial image of the Picher mining field located in Ottawa County, OK and Cherokee County, KS, USA, showing Tar and Lytle Creek, cities, and the study area outline in a dashed-red box (*Source:* "Picher mining field". 36.986864° N, 94.820698° W. Google Earth. Sept. 7, 2021. Jan. 22, 2021.)

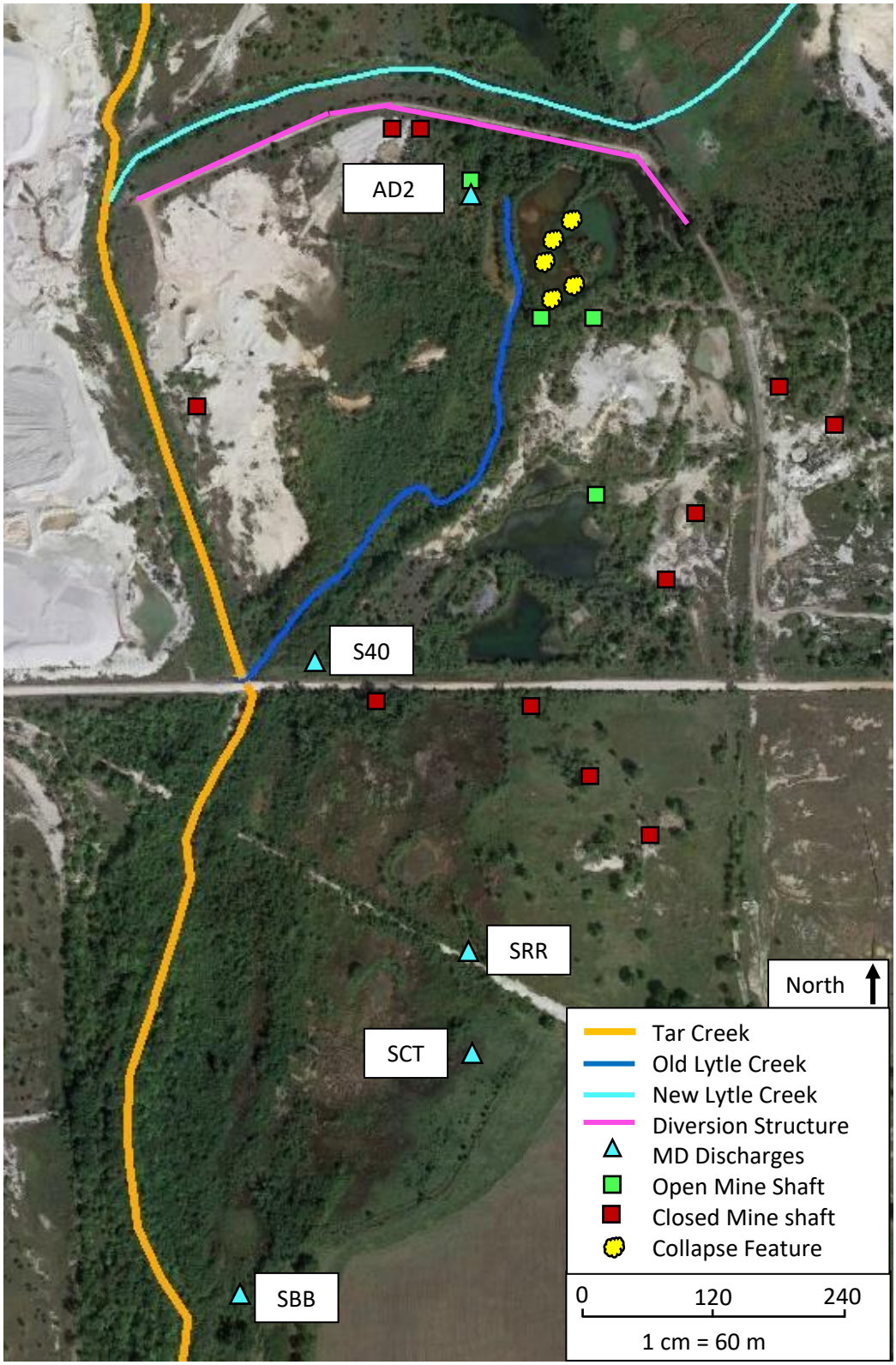

Figure 6.2: Aerial image of Douthat, Oklahoma, USA, showing mine drainage discharges (MD), open and closed mine shafts, collapse features, stream channels, and diversion structure (*Source:* "Douthat, OK". 36.958292°N, 94.842731°W. Google Earth. Sept. 7, 2021. Jan. 4, 2022.)

6.2.2 Conceptual Passive Treatment Design Parameters

Two conceptual PTSs were designed for this study. The first, referred to herein as PTS-1, was designed using the median flow rates from the five MD discharges at Douthat of 4,542 lpm (1,200 gpm). The PTS-1 design assumes that closing known inflow locations (Appendix 5B) will decrease the frequency and volume of MD discharged during the short-term elevated discharge events that are the result of surface mine features connected to the subsurface mine voids that take on water from nearby streams during precipitation events. The second conceptual design, referred to herein as PTS-2, was a much larger system, capable of treating >90% of the MD at Douthat based on flow rates that were calculated using the trendline equations from Chapter Five, summarized in Table 6.1, and mine pool water elevations recorded on 30-minute time intervals from 2010-2021 at the United States Geological Survey (USGS) Slim Jim groundwater monitoring station (65942094504203). The resulting design flow rate for PTS-2 was 8,140 lpm (2,150 gpm). The water quality design parameters remained constant for both designs and were based on the flow weighted average total metals concentrations (Table 6.2). Imperial units will be used throughout this chapter when discussing the conceptual designs or information related to the design. Imperial units, such as design water elevations and earthwork volumes, will be more useful than metric units to those that would use the conceptual design as a proof of concept for a PTS to be implemented in the future at Douthat.

Table 6.1: Trendline equations to calculate flow rates in metric and imperial units for five mine drainage discharges at Douthat, OK based on the mine pool elevation above mean sea level as measured at the United States Geological Surveys Slim Jim monitoring station (365942094504203) using a base elevation of 830.72 ft AMSL

	Slim Jim Trendline Equation		R^2
	Metric (y = lpm, x = m)	Imperial (y = gpm, x = ft)	
S40	y = 1,645x - 399,235	Y = 132.5x - 105,467	0.69
SRR	y = 2,451x – 598,616	y = 197.3x – 158,138	0.77
SBB	y = 18.02x – 4,351	y = 1.451x – 1,149	0.91
SCT	y = 21.83x – 5,327	y = 1.758x – 1,407	0.82
AD2 <244.54 m (<802.3 ft)	y = 432.3x – 105,205	y = 34.81x – 27,792	0.38
AD2 >244.54 m (>802.3 ft)	y = 61,574x - 15,059,646	y = 4,958x - 3,978,358	0.60

Table 6.2: Mean water quality values and the standard error of selected parameters from each of the five discharges sampled near Douthat, Oklahoma, USA, within the Tar Creek Superfund Site. Flow weighted averages were calculated based on the median flow rates of each discharge

	n	pH	Alkalinity mg/L CaCO3 eq.	Sulfate mg/L	[Cd] mg/L	[Fe] mg/L	[Pb] mg/L	[Zn] mg/L
S40	25	6.11±0.04	125.8±5.46	1,428±127	0.027±0.004	20.59±2.29	0.041±0.004	6.16±0.28
SRR	15	6.15±0.03	126.6±3.13	1,596±158	0.004±0.0002	25.64±2.63	0.055±0.006	4.66±0.20
SBB	18	6.40±0.03	211.3±6.34	1,572±143	0.007±0.0027	53.47±0.63	0.095±0.004	2.42±0.03
SCT	13	6.23±0.03	175.6±2.89	1,793±154	0.006±0.0005	49.77±1.34	0.091±0.004	4.18±0.05
AD2[1]	7	6.18±0.05	146.4±4.10	1,318±80	0.008±0.0007	24.11±2.44	0.053±0.005	5.05±0.18
Flow Weighted Average		6.13±0.04	129.3±5.69	1,497±173	0.022±0.003	22.61±2.53	0.045±0.005	5.76±0.28

[1]Water quantity samples shown for Admiralty #2 were collected while the discharge was flowing

The order and function of the process units were the same for both conceptual PTS designs and included a two-phase implementation approach (Figure 6.3). Phase 1 will consist of an initial storage and oxidation pond located on the north side of the county road at the study site. Phase 1 will allow for accurate flow measurements during elevated discharge events, providing necessary information to determine the final design flow and sizing of the Phase 2 PTS that will be on the south side of the study site. The surface flow wetlands (SFWs) and vertical flow bioreactors (VFBRs) were split into three parallel trains to facilitate operation and maintenance. Shutting down one of the three parallel trains during a low flow period will allow the PTS to function at the designed flow rates without overloading the system or bypassing the untreated MD. The targeted design parameters were the same for both conceptual designs (Table 6.3).

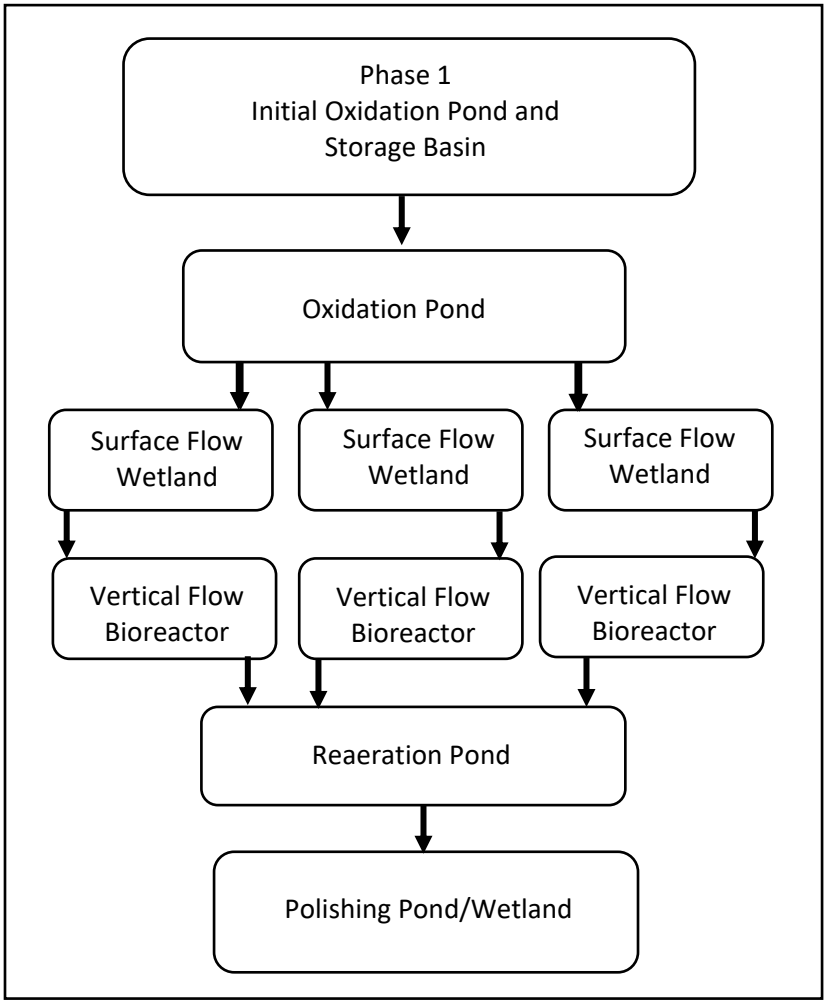

Figure 6.3: Flow chart showing the process units of the conceptual PTS design to remediate mine drainage at Douthat, Oklahoma, USA

Table 6.3: Summary of process units, targeted parameters, design factors, and functions for the conceptual design of the Douthat Passive Treatment Systems

Design Phase	Process Unit	Targeted Parameter	Design Factors	Function
Phase 1	Initial Oxidation and storage pond	• Fe • Water storage	• Phase 1 flow measurements • Maximize storage	• Oxidation, precipitation and settling of Fe precipitates • Trace metal sorption • Storage during elevated discharge events
Phase 2	Oxidation Pond	• Fe	• 20 g Fe m^{-2} day^{-1}	• Oxidation, precipitation and settling of Fe precipitates • Trace metal sorption
	Surface Flow Wetland	• Fe	• 48 hr HRT	• Solids Settling
	Vertical Flow Bioreactor	• Pb and Zn	• 15 hr HRT in media layer • >40 hr total HRT	• Removal of targeted metals as metal sulfides via sulfate reduction
	Reaeration Pond	• Increase O_2 • Sulfide Removal	• 48 hr HRT	• Solar-powered reaeration • Stripping oxygen demand and H_2S • Increase dissolved oxygen
	Final Polishing/Wetland	• Residual solids	• 48 hr HRT or • Maximum HRT based on available space	• Ecological buffer • Solids settling

6.2.3 Metal Loading Calculations

The metal loading of untreated MD was simulated by using the measured mine pool water elevation data collected at the Slim Jim monitoring station at 30-minute intervals from 2010-2021 to calculate MD flow rates based on the linear trendlines of each discharge (Table 6.1). The metal loading of each discharge was calculated for each 30-minute interval by multiplying the mean metals concentrations of each discharge by the flow rate and 30-minute time step (Example Calculation 1).

Example Calculation 1: S40 at a mine pool water elevation of 244.58 m AMSL (802.43 ft AMSL)

Q = 3,112 lpm; Fe = 21.13 mg/L

$$\frac{3{,}112\ L}{min} \times 30\ min \times \frac{21.13\ mg}{L} \times \frac{1\ g}{1{,}000\ mg} = 1{,}974\ g\ of\ Fe$$

The metal loading for each of the five discharges based on the scenario shown in Example Calculation 1 is summarized in Table 6.4.

The simulated metal loading to Tar Creek with the implementation of the conceptual PTSs used the previously calculated metal loading of untreated MD for each discharge multiplied by one minus the expected metals removal efficiencies based on the existing MRPTS removal efficiencies (Example Calculation 2, Table 6.5). During elevated discharge events that would occur when the flow of MD exceeded the design flow rate and storage capacity of each conceptual PTS, the metal loading to Tar Creek from the percentage of the flow that would bypass the system was calculated as 100% untreated (Example Calculation 3).

Example Calculation 2: S40 at a mine pool water elevation of 244.64 m AMSL (802.43 ft AMSL), total flow was less than the design flow of the conceptual PTS-1 (4,542 lpm)

Q_{total} = 4,529 lpm; Q_{S40} = 3,113 lpm; Fe = 21.13 mg/L

$$1{,}974\ g\ Fe \times (1 - 0.997\ removal\ efficiency) = 5.92\ g\ Fe\ effluent\ load$$

Thus, 5.92 g of Fe were loaded to Tar Creek in the 30-minute interval by the S40 discharge, while 1,968.08 g were retained by PTS-1. The metal loading and mass of metals retained by PTS-1 for each of the five discharges in the scenario shown in Example Calculation 2 are summarized in Table 6.4.

Table 6.4: Example calculation of calculated flow rates and metal loading to Tar Creek from five mine drainage discharges at Douthat, Oklahoma USA for a single 30-minute time interval at a mine pool water elevation of 244.58 m (802.44 ft AMSL), under untreated conditions and treated conditions based on the implementation of PTS-1 conceptual design without additional storage

	Flow lpm		Cd[1] g	Fe g	Pb[1] g	Zn g
SBB	57	Untreated	0.012	92.00	0.16	4.19
		PTS-1	0.000	0.25	0.00	0.30
SCT	12	Untreated	0.002	18.40	0.03	1.54
		PTS-1	0.000	0.05	0.00	0.11
SRR	808	Untreated	0.097	621	1.33	113
		PTS-1	0.000	1.69	0.00	7.99
S40	3,112	Untreated	2.610	1,973	3.83	573
		PTS-1	0.000	5.36	0.00	40.50
AD2	538	Untreated	0.130	389	0.86	81.60
		PTS-1	0.000	1.06	0.00	5.77
Total	4,529	Untreated	2.85	3,094	6.21	774
		PTS-1	0.00	8.40	0.00	54.66

[1]Masses of Cd and Pb for PTS-1 were assumed to be zero because the assumed removal efficiency of MRPTS was 100% for Cd and Pb because the metals concentrations at the outflow of MRPTS were below detection limits

Table 6.5: Inflow and outflow total aqueous metals concentrations of samples collected from 2008-2020 and the metals removal efficiencies of the Mayer Ranch Passive Treatment System, located in the Tar Creek Superfund site

	[Cd] mg/L	[Fe] mg/L	[Pb] mg/L	[Zn] mg/L
Inflow	0.0151	169.5	0.0927	7.69
Outflow	<PQL[1]	0.46	<PQL[1]	0.54
% Removed	100	99.7	100	92.9

[1] <PQL indicates value was below the detection limit of 0.00064 mg/L for Cd and 0.0195 mg/L for Pb

Example Calculation 3: S40 at a mine pool water elevation of 245.22 m AMSL (804.53 ft AMSL), total flow was greater than the design flow of the conceptual PTS-1 (4,542 lpm) and storage was full; Q_{total} = 46,224 lpm (12,211 gpm); Q_{S40} = 4,164 lpm (1,100 gpm); Fe = 21.13 mg/L

Metal loading to Tar Creek (untreated)

$$\frac{4{,}164\ L}{min} \times 30\ min \times \frac{21.13\ mg}{L} \times \frac{1\ g}{1{,}000\ mg} = 2{,}639\ g\ of\ Fe$$

Metal loading to Tar Creek with PTS-1 implemented: 3,112 lpm of S40 treated, 1,052 lpm bypassed

$$\left(2{,}639\ g\ Fe \times \frac{3{,}112\ lpm}{4{,}164\ lpm} \times (1 - 0.997)\right) + 2{,}639\ g\ Fe \times \frac{1{,}052\ lpm}{4{,}164\ lpm} = 673\ g\ Fe\ effluent\ load$$

Thus, 673 g of Fe were loaded to Tar Creek in the 30-minute interval by the S40 discharge, while 1,966 g were retained by the PTS. The metal loading and mass of metals retained by PTS-1 for each of the five discharges based on the scenario shown in Example Calculation 3 are summarized in Table 6.6.

Table 6.6: Example of calculated flow rates and metal loading to Tar Creek from five mine drainage discharges at Douthat, Oklahoma USA for a single 30-minute time interval at a mine pool water elevation of 244.22 m AMSL (804.53 ft AMSL), under untreated conditions and treated conditions based on the implementation of the PTS-1 conceptual design without additional storage

	Flow lpm		Cd g	Fe g	Pb g	Zn g
SBB	68.9	Untreated	0.014	110	0.20	5.03
		PTS-1	0.002	18.5	0.04	0.84
SCT	26.3	Untreated	0.005	39.2	0.07	3.30
		PTS-1	0.003	20.8	0.04	1.76
SRR	2,377	Untreated	0.285	1828	3.92	332
		PTS-1	0.188	1,207	2.59	219
S40	4,164	Untreated	3.50	2,640	5.12	767
		PTS-1	0.89	667	1.29	194
AD2	39,586	Untreated	9.50	28,633	62.9	5,997
		PTS-1	9.37	28,244	62.1	5,916
Total	46,224	Untreated	13.3	33,251	72.3	7,105
		PTS-1	10.5	30,157	66.1	6,331

6.2.4 Downstream Metals Concentration Calculations

To test the hypothesis that without the implementation of PTS at Douthat, downstream water quality would not meet the state-designated beneficial use criteria a majority of the time, it was assumed that all other sources of contamination contributing to Tar Creek upstream of the MD discharges were remediated. Therefore, the hypothesis was tested assuming the only source of metals contributing to Tar Creek was from the MD at Douthat. Thus, the percentage of flow in Tar Creek that was not MD was assumed to contain no metals that would dilute the metals concentrations in the percentage of the flow that was MD.

The total flow of the five MD discharges at Douthat was calculated on thirty-minute intervals using the measured mine pool water elevation data collected at the Slim Jim monitoring station from 2010-2021 to calculate each MD discharge based on the linear trendlines (Table 6.1). The flows from each discharge were used to calculate the flow-weighted average metals concentrations of Cd, Fe, Pb, and Zn for all the MD at Douthat. Streamflow data collected on the same 30-minute time intervals from a USGS stream gauge station located 1.6 km downstream of Douthat (Tar Creek near Commerce, OK 07185090) was used to calculate the percentage of MD and the resulting metals concentrations using the mass balance equation (Example Calculation 4).

Example Calculation 4: At a mine pool elevation of 244.57 m AMSL (802.40 ft AMSL), Q_{MD} = 4,459 lpm with a flow weighted average Zn concentration of 5.70 mg/L; measured flow 1.6 km downstream = 10,228 lpm, with the assumption that all non-MD water has a Zn concentration of 0 mg/L.

$$\frac{([Zn]_{md} \times Q_{md})}{Q_{stream}} = [Zn]_{Stream}$$

$$\frac{5.70 \frac{mg}{L} Zn \times 4{,}559\ lpm}{10{,}228\ lpm} = 2.48 \frac{mg}{L} Zn$$

The calculated metals concentrations of Cd, Pb, and Zn were compared to the hardness adjusted acute and chronic Oklahoma water quality criteria to protect beneficial uses for fish and wildlife propagation (Table 6.7) (OWRB (2020). The hardness value of 1,151 mg/L as $CaCO_3$ eq. was calculated using the mean total metals concentrations of 406±15.9 mg/L Ca and 33.3±1.55 mg/L Mg from samples collected at the stream gauge station from 2008 to 2020 by the University of Oklahoma Center for Restoration of Ecosystems and Watersheds (CREW) (sample size = 101).

Table 6.7: Equations used to calculate the acute and chronic beneficial use numerical criteria for fish and wildlife propagation for aqueous metals concentrations of Cd, Pb, and Fe (OWRB 2020)

	Parameter	Equation (µg/L)
Acute	Cadmium (Dissolved)	$e^{(1.0166\times[\ln(\text{hardness})]-3.924)} \times 1.136672 - 0.041838\ln(\text{hardness})]$
	Lead	$e^{(1.273[\ln(\text{hardness})-1.460)]}$
	Zinc (Dissolved)	$e^{(0.8473[\ln(\text{hardness})]+0.884)*0.978}$
Chronic	Cadmium (Dissolved)	$e^{(0.7409[\ln(\text{hardness})]-4.719)} \times [1.101672 - 0.041838\ln(\text{hardness})]$
	Lead	$e^{(1.273[\ln(\text{hardness})]-4.705)}$

6.2.5 Statistical Analyses

A single-tailed, paired T-test was used to determine if the metal loading to Tar Creek on an annual basis was significantly decreased if the conceptual PTS was implemented. The annual metals loading to Tar Creek for each metal under the untreated scenario from 2010 to 2021 was compared to the simulated metals loading to Tar Creek if PTS was implemented over the same period for each conceptual PTS. The metals loading to Tar Creek from the two conceptual PTSs were compared to each other to determine if the increase in the PTS design flow rate and storage basin resulted in a significant decrease in metals loading to Tar Creek using a single-tailed, paired T-test. Similarly, a single-tailed, paired T-test was used to determine if there was a significant decrease in the mean annual percentage of time the calculated metals concentrations downstream of the Douthat discharges did not meet the beneficial use criteria after the implementation of each conceptual PTS compared to the untreated conditions.

6.3 Results and Discussion

6.3.1 Phase 1: Conceptual Passive Treatment System Design Approach

The proposed PTSs presented as part of this study are conceptual and in no way should be considered construction-ready designs (Figures 6.4-6.13, Tables 6.8-6.10, Appendix 6E). The objective of the conceptual PTSs was to determine if it would be feasible to construct a PTS capable of remediating the MD at Douthat and provide a general idea of the footprint and cost of the system.

6.3.1.1 Initial Oxidation Pond and Storage

The initial oxidation and storage pond was designed as the first phase of the conceptual Douthat PTS. **Gathering accurate flow data from all discharges on the northern portion of the study site was the primary design objective of Phase 1.** The objective was achieved by designing a berm at an elevation of 809 ft AMSL around the northern discharges that would tie into the existing OU1 diversion structure to the north that was constructed as a remedial action in the 1980s. The conceptual PTS

designs show the ideal location of the berm (Figures 6.8 and 6.9), however hydraulic modeling needs to be conducted on Tar Creek to compare the current and proposed conditions to ensure the construction of the berm does not impact the bridge located immediately downstream. If the hydraulic modeling shows the bridge will be negatively impacted, the berm may need to be relocated until the modeling shows there are no impacts on the bridge. An alternative option could be to remove the bridge and construct a low water crossing, which would allow the road to be used the great majority of the time and would provide a much greater cross-sectional area for the flow of Tar Creek during rainfall events.

A large concrete outlet structure located near the confluence of Tar Creek and Old Lytle Creek was designed to support a height-adjustable sharp-crested compound weir (Figures 6.4, 6.8, and 6.9). The sharp-crested compound weir was designed to be a 1.5 ft deep, 90-degree V-notch situated in the middle of a 19 ft wide rectangular weir (Figure 6.4). The 90-degree V-notch weir would allow for accurate flow measurements during base and low flow conditions, including the mean and median combined flow rates of AD2 and S40. The V-notch portion of the compound weir was designed to be capable of measuring flows up to 3,090 gpm (6.81 cfs) (Equation 5). The compound weir was designed to measure flow rates exceeding 500 cfs when the invert of the V-notch portion of the weir is installed at the design water elevation of 801 ft AMSL (Equation 6). An emergency spillway was designed on the northwest corner of the constructed berm at an elevation of 807 ft AMSL to bypass any MD that exceeds the flow measuring capabilities of the weir (Figures 6.8 and 6.9).

Sharp-crested 90-degree V-notch weir equation (U.S. Department of the Interior, Bureau of Reclamation, 2001)

$$Q\ (cfs) = 2.49\ \times H^{2.48} \qquad (5)$$

Where H = elevation of the water surface above the crest (ft)

Weir equation when water elevation is higher than the top of the V-notch portion of the weir (U.S. Department of the Interior, Bureau of Reclamation, 2001)

$$Q\ (cfs) = 3.9\ \times h_1^{1.72} - 1.5 + 3.3\ \times L\ \times h_2^{1.5} \qquad (6)$$

Where h_1 = head above the V-notch (ft)
L = Total length of the horizontal portions of the weir (ft)
h_2 = head above the horizontal crest (ft)

The large weir would be capable of measuring flow rates correlated with high mine pool elevations, improving the precision and accuracy of the flow trendlines presented in this study (Table

6.1). As reclamation in the Picher field continues and known inflow locations that influence the mine pool elevation are closed (Appendix 5B), the accurate flow measurements at high mine pool elevations will be able to evaluate the effectiveness of closing a known inflow locations with flow measurements collected before and after the closure. A five-year assessment period following the construction of Phase 1 is recommended to allow time for data collection and to seal all known large inflow locations (Appendix 5B). **It is hypothesized that closing known inflows (Appendix 5B) will significantly decrease the flows during these peak discharge events. However, that hypothesis cannot be tested until Phase 1 is implemented.**

The increased surface area and retention time created by the implementation of Phase 1 will also have the added benefit of partially treating the MD by oxidizing and precipitating Fe. Continued water quality sampling should also occur during the period between Phase 1 and 2 to ensure the manipulation of the northern discharges has not caused a substantial change in the water chemistry. **Any manipulations to the critical discharge elevations of any Douthat discharges should be minimal because altering the discharge elevations at Douthat will influence the entire mine pool** (Appendix 6A).

Once Phase 2 is constructed, the weir would be retrofitted to raise the critical discharge elevation to match the emergency spillway elevation of 807 ft AMSL, creating a large storage basin. The available storage volume was calculated as the available void space from the design water elevation (801 ft AMSL) to the emergency spillway elevation (807 ft AMSL). The flow path of the initial oxidation pond used during Phase 1 (Figures 6.8 and 6.9) was designed to be reversed during Phase 2, (Figures 6.10 and 6.12). MD from the initial oxidation pond would then leave the pond through a second outflow structure that connects to the Phase 2 PTS (Figures 6.10 and 6.12). The second outflow structure would have a restrictor plate to limit the maximum flow rate that could enter the PTS. The excess volume would be temporarily retained in the storage basin. The flow restriction into the PTS from the northern discharges would ensure that the PTS was not inundated, which could lead to operation and maintenance (O&M) issues.

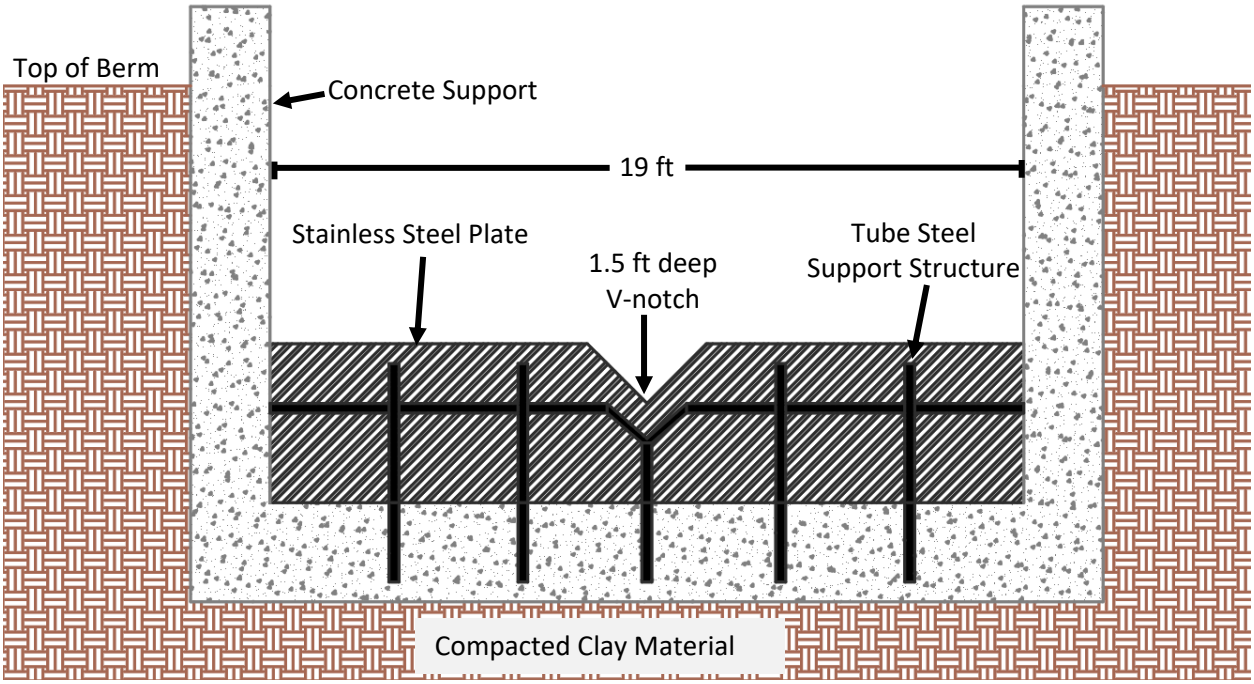

Figure 6.4: Conceptual design of sharp-crested compound weir to measure MD discharge flow rates at Douthat, OK

6.3.2 Phase 2: Conceptual Passive Treatment System Design Approach

6.3.2.1 Oxidation Pond

The oxidation pond was designed to oxidize, hydrolyze, and settle Fe. The inflows into the oxidation pond enter from the northern Phase 1 initial oxidation/storage pond and the SRR discharge (Figures 6.11 and 6.13). SRR would be captured, and an adjustable riser would be installed on the discharge to allow for minor adjustments in the flow rate or to temporarily stop the flow from SRR if needed. The oxidation pond was designed for a 30-year life based on the Fe oxides sludge accumulation and the inflow Fe concentrations. The Fe sludge density was assumed to be 170 kg Fe/m^3 (Dempsey and Jeon, 2001; Watzlaf et al., 2004) with a maximum sludge depth of 4.5 ft after 30 years of accumulation. The oxidation pond minimum depth of seven feet would allow for 2.5 ft of additional storage capacity if the future Fe concentrations increase above the design concentrations. The surface area of the oxidation pond was sized based on the design flow rate, flow weighted average total Fe concentrations, and a Fe removal rate of 20 g Fe m^{-2} day^{-1} (Tables 6.8 and 6.9) (Hedin et al., 1994). Additionally, the oxidation pond design was conservative because it did not consider the partial treatment and subsequent amount of Fe retained in the Phase 1 initial oxidation and storage pond. The oxidation pond design included directional baffle curtains to meander the flow path and decrease dead zones (Figures

6.11 and 6.13). Water flows out of the oxidation ponds via three inlet Agri Drains designed to evenly split the flow into the three parallel SFWs.

SBB and SCT discharges would be captured, and a riser pipe would be added to each discharge to a height that prevents the discharges from flowing. Both conceptual PTSs were designed to ensure SBB and SCT were not located in the wetted area of a process unit. Stopping the flow from these discharges is not expected to cause any issues because these discharges have substantially lesser flow rates compared to the other discharges and are not connected to any subsurface mine voids. However, if the discharges are captured using a riser pipe as opposed to being sealed, then the discharges can be used as monitoring wells. The riser pipe can be periodically lowered if there is any reason or need to sample these discharges or to treat them in the future.

6.3.2.2 Surface Flow Wetlands

A settling process unit is necessary to remove oxidized Fe that did not settle in the oxidation pond (Younger et al., 2002). For the conceptual designs, SFWs were used to facilitate solids settling. Each of the SFWs were designed to have a pool-shelf-pool geometry, with the total area of the SFW evenly split into the three sections (Figure 6.5). The wetland shelf has a design depth of 0.5 ft to facilitate plant growth and would be planted with a mix of native wetland species. The wetland vegetation creates meandering flow paths to facilitate the settling of Fe oxides that did not settle in the oxidation pond. The pools are 5.5 ft deep and serve as sedimentation basins to store the settled solids and increase retention time. The sizing of the SFWs was based on a hydraulic retention time (HRT) of 48-hours. The outflow of each SFW enters a VFBR via open channel flow (Figures 6.11 and 6.13). The SFWs and VFBRs have the same design water elevation to conserve the limited hydraulic head available at the project site (Tables 6.8 and 6.9). The use of three parallel treatment trains for the SFWs and VFBRs was chosen to allow one of the trains to be temporarily shut down for O&M without overwhelming the other two trains.

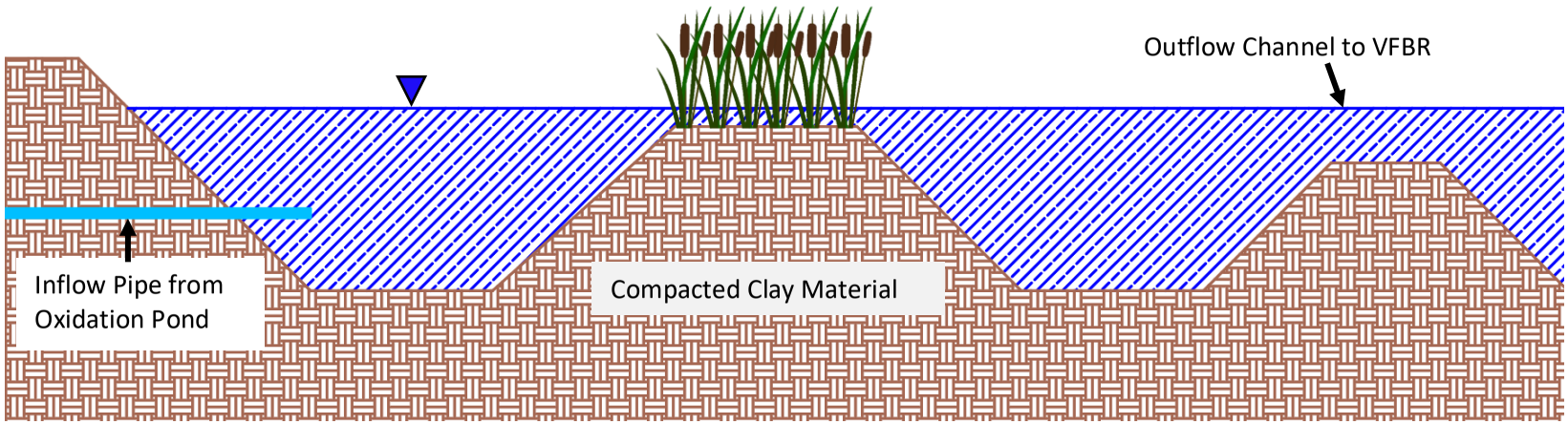

Figure 6.5: Cross-section of the surface flow wetland for the conceptual design of the Douthat passive treatment system

6.3.2.3 Vertical Flow Bioreactors

The VFBRs were designed to promote bacterial sulfate reduction to precipitate and retain Zn and Pb as metal sulfides. The VFBRs have three layers; a water cap, organic media, and a drainage layer (Figure 6.6). The water cap is 2.5 ft deep to provide head pressure to facilitate vertical flow through the bottom layers. The organic media serves as the source of labile carbon for the sulfate-reducing bacteria, consisting of 50% mushroom compost and 50% woodchips. The woodchips will vary in size, with the majority of the wood chips less than 1.5 inches. Larger wood chips typically have a flat face and a study conducted by Cameron and Schipper (2010) found that over time the woodchips will rotate to the flat faces which led to a decrease in hydraulic conductivity. The results showed that the larger the woodchip size, the greater the decrease in hydraulic conductivity over the 22-month study period (Cameron and Schipper, 2010). The drainage layer consists of a 1.5 ft thick layer of inert river rock with lateral perforated PVC pipes spaced every five feet. The perforated pipes collect the water and direct it into a larger gathering pipe that flows into the re-aeration pond. The PVC pipes in the drainage layer are divided into three cells, represented by the different colors in Figures 6.11 and 6.13. The outflow gathering pipe from each cell has an adjustable riser at the inflow of the re-aeration pond. The individual cells and adjustable risers enable more detailed monitoring of the VFBRs. If permeability issues arise in a particular cell, that riser can be raised to preferentially flow water through the other two cells, taking the stress off that cell. The volume and HRT calculations in the drainage and organic media layers were calculated using an estimated porosity of 0.45 (StormTech, 2012; Cameron and Schipper, 2010; Ghane et al., 2016). The system was designed based on a 15-hour HRT in the organic media layer and a 40-hour minimum HRT for the entire unit (Younger et al., 2002). The three VFBRs are connected via an emergency spillway at an elevation two feet above the design water elevation. Therefore, if hydraulic conductivity issues arise in an entire process unit, water will preferentially spill into the neighboring VFBR. If all three VFBRs are stacking water, then the water will be bypassed via an emergency spillway from the center VFBR into the re-aeration pond (Figure 6.11). Additionally, the riprap-lined emergency spillways can be used as access points for a miniature excavator to perform necessary O&M on the VFBRs.

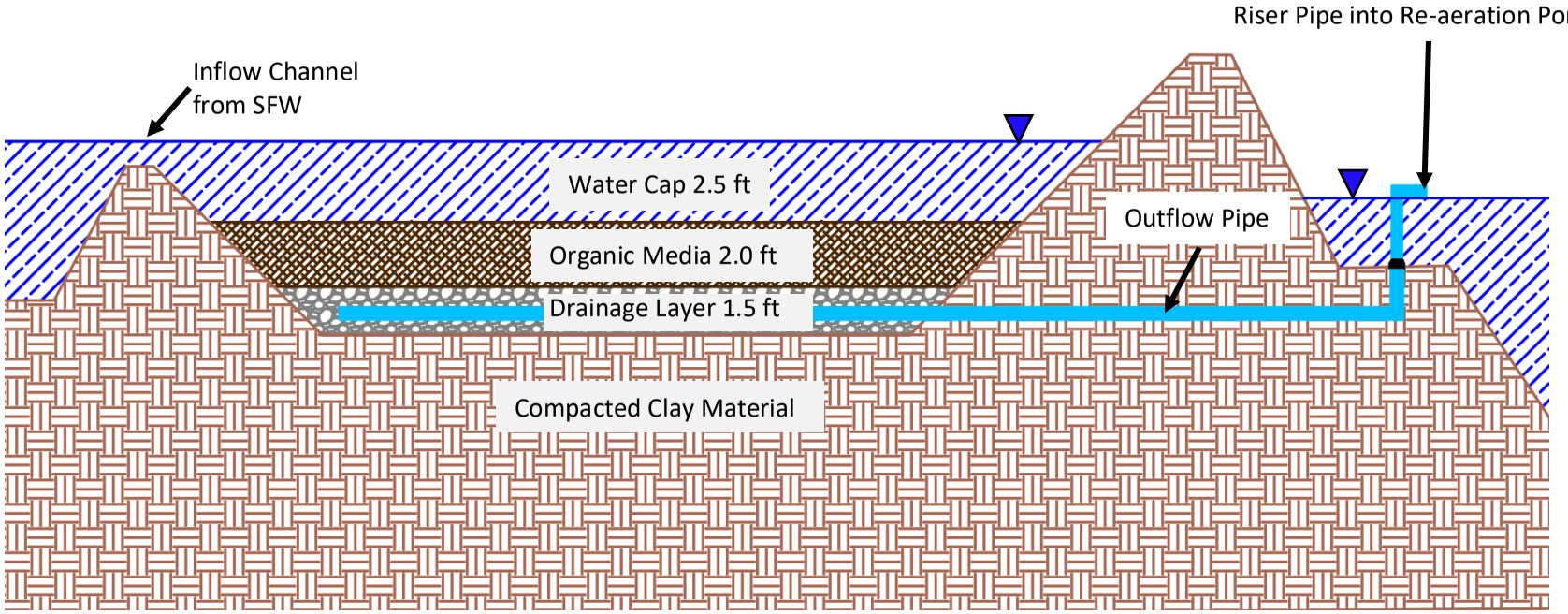

Figure 6.6: Cross-section of the vertical flow bioreactor for the conceptual design of the Douthat passive treatment system

6.3.2.4 Re-aeration Pond

The effluent from the three parallel VFBRs enters a single re-aeration pond to address the oxygen demand of the reduced waters (Porter and Nairn, 2008). The re-aeration pond is seven feet deep to decrease the area required to achieve the design HRT of 48-hours. Directional baffle curtains run lengthwise across the pond to decrease dead zones (Figures 6.11 and 6.13). The pond has active aeration using float mix aerators (FMAs) that are powered by a battery bank and solar energy (Figure 6.7) because the limited topographic relief prevents the use of head-driven re-aeration processes. FMAs have been shown to effectively aerate water (Dorman 2019) and are less likely to clog or be damaged by wildlife compared to traditional bubble diffusers. The water will leave the re-aeration pond and enter the final polishing SWF via open channel flow.

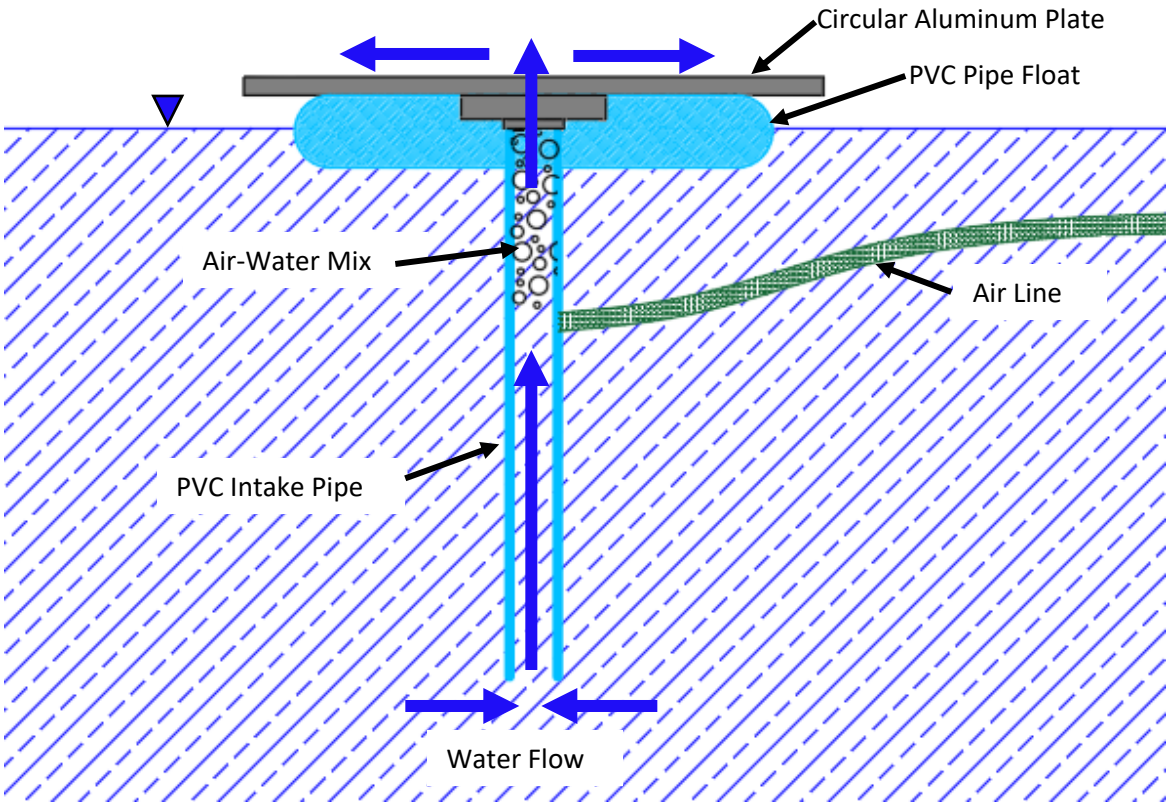

Figure 6.7: Conceptual drawing of the float mix aerators used in the re-aeration pond for the conceptual design of the Douthat passive treatment system

6.3.2.5 Polishing Surface Flow Wetland

The polishing SFW will have a common water surface elevation with the re-aeration pond. The polishing SFW targeted design parameter was a 48-hour HRT or the maximum HRT available based remaining land area. The design objectives of the polishing SFW were to settle and retain residual solids and provide an ecological buffer before discharge to the receiving water body (Nairn et al., 2009). The polishing SFW uses the same deep-shallow-deep design approach as the SFWs that follow the oxidation pond (Figure 6.4). The water leaves the polishing SFW through an inlet Agri Drain structure that conveys the water into a pipe that goes through the outer berm and into the receiving stream (Figures 6.11 and 6.13).

6.3.3 Comparison of the Conceptual Douthat PTS Design Options

6.3.3.1 Phase 1

Both PTS Phase 1 conceptual designs consist of the same berms, weir, and emergency overflow structure that are essential to accurately measure flow rates from the northern discharges at all mine pool elevations. Therefore, the overall disturbed areas for both Phase 1 designs are the same at approximately 65.5 acres. The designs differ when comparing the capacity of the initial oxidation ponds and storage basins during Phase 2 operations. Phase 1 of PTS-1 is a minimalistic approach where the primary objective of the design was measuring flow rates, with less consideration to its function during Phase 2. The proposed excavated area for the PTS-1 initial oxidation pond (Figure 6.8) utilizes the naturally lower land elevations to create the meandering flow path to minimize the amount of cut material. It is expected that the cut material will not meet the remedial goals for soil metals concentrations of Cd 10 mg/kg, Pb 500 mg/kg, and Zn 1,100 mg/kg (CH2M, 2017). Thus, the cut material will likely be hauled to the repository for mining waste material. The storage capacity of PTS-1 was not maximized to further minimize the amount of cut material necessary to complete the project. Although the cost estimate for PTS-1 Phase 1 is approximately half that of the cost for PTS-2 Phase 1 design at $4.4 million, PTS-1 oxidation pond has a pond volume that is approximately a quarter of the size of PTS-2 at the design water elevation, and the storage capacity of PTS-1 is 31% smaller (Tables 6.8-6.10).

PTS-2 Phase 1 design gave far more consideration to the capacity of the initial oxidation and storage pond during Phase 2 operation, resulting in a more resilient design (Figure 6.9). The maximized volume in the PTS-2 initial oxidation pond more than doubles the HRT compared to PTS-1, even with the 80% increase in the design flow rate for PTS-2 (Tables 6.8 and 6.9). Additionally, the larger volume will increase the design life of the initial oxidation pond because of the increased Fe oxide storage capacity.

The greater initial oxidation pond surface area in the PTS-2 design makes the design better suited to handle unforeseen increases in inflow Fe concentrations that may occur after construction. However, both conceptual PTSs initial oxidation ponds have greater surface area and volume compared to the Phase 2 oxidation ponds and will greatly decrease the workload of the Phase 2 oxidation ponds by oxidizing and precipitating most of the Fe from the northern discharges before entering the Phase 2 oxidation ponds.

The primary objective of Phase 1 is flow measurements of the large discharges, primarily mine shafts, which are located within the OU1 berm on the north side of the study site. However, to meet the objective means that any other large discharges or potential discharges that are outside of the berm enclosure proposed in Phase 1 would need to be addressed. To date, two large known discharges are located outside of the proposed berm, known as the Flint Rock discharges (Appendix 6B). The discharges are located 100 feet apart. One is an open mineshaft with an estimated critical discharge elevation of 803.5 ft AMSL, and the other is a non-shaft related collapse. Flow from these discharges can be prevented by reconstructing the failed berms surrounding the discharges (Appendix 6B).

Following construction of Phase 1, the cost estimate includes a five-year assessment period to monitor the water quality and quantity of the MD. However, the assessment period may vary based on multiple factors, including the climate and remediation efforts. If no elevated flow events occur due to a drought period following the completion of Phase 1, then the period may need to be extended. Similarly, if known inflow locations have not been sealed by the end of the five years, then the assessment period should be extended until all known inflow locations have been sealed and the effects on MD flow at Douthat have been evaluated. The cost estimates for the Phase 1 assessment period are the same for both conceptual designs because the monitoring requirements are the same (Table 6.10). The cost estimate includes increased O&M costs in years 2 and 4 to provide the opportunity to hire a contractor to adjust the critical discharge elevation of the weir (Table 6.10).

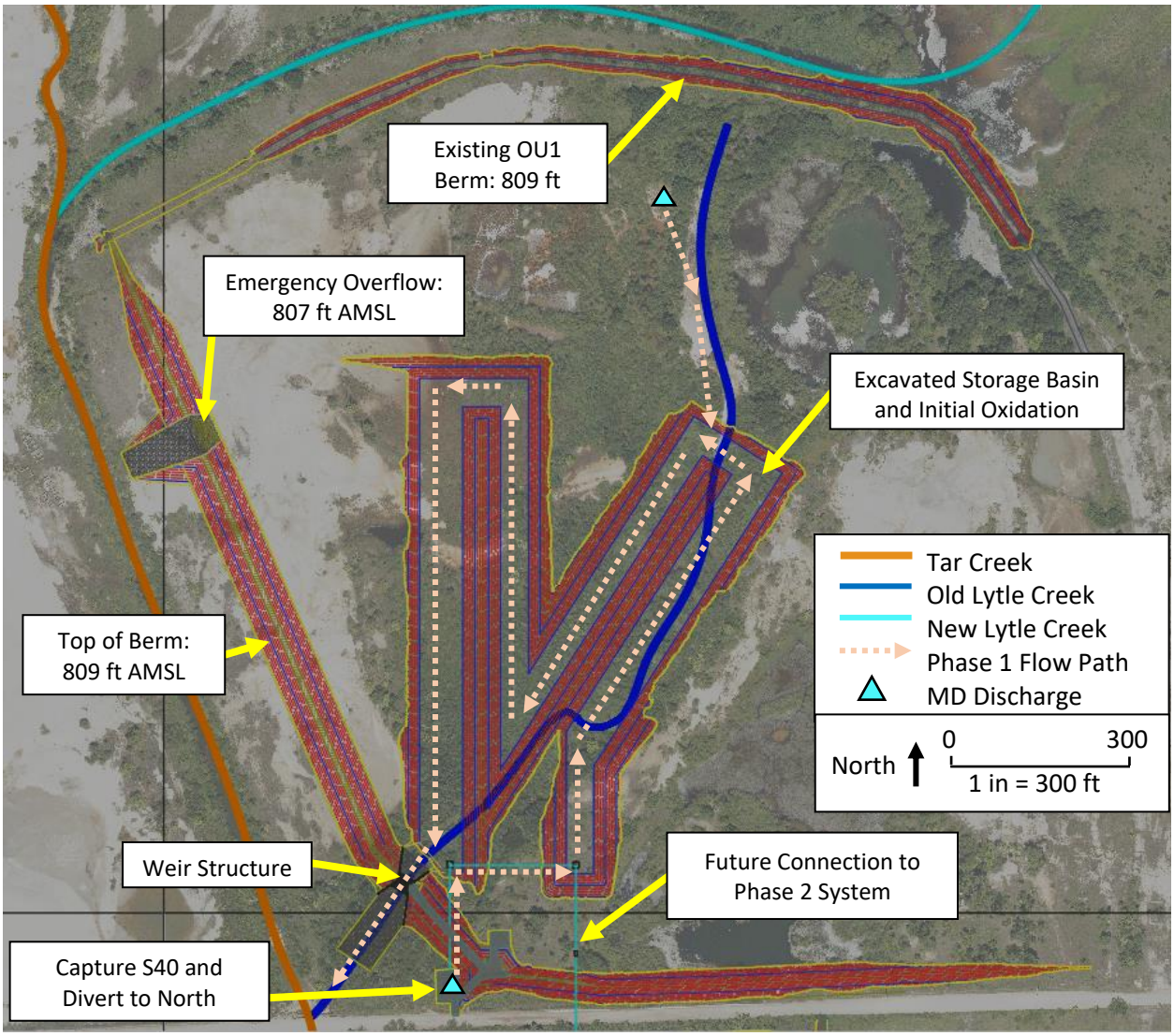

Figure 6.8: Phase 1 of the Option 1 conceptual Douthat passive treatment system design (PTS-1) plan view

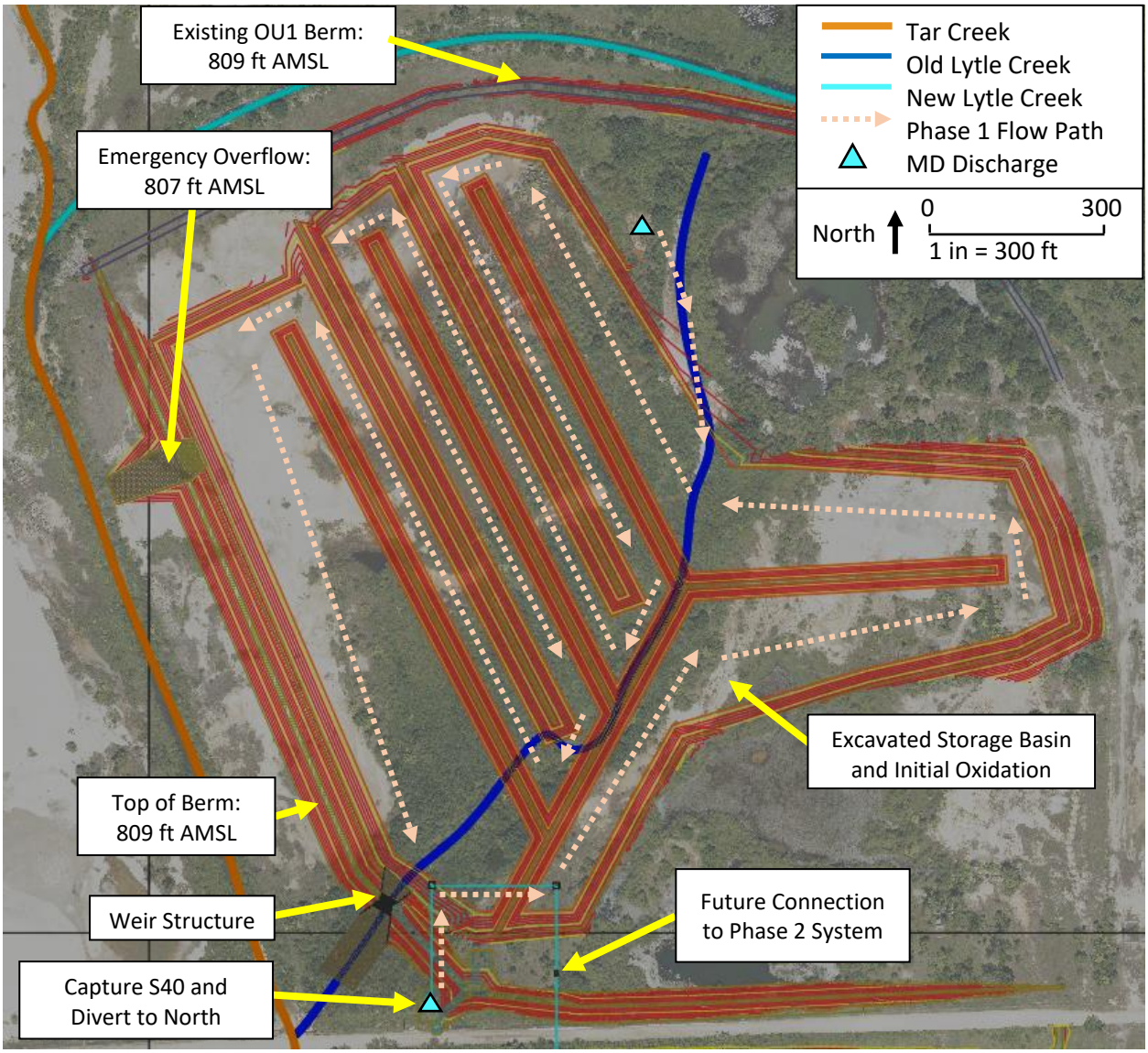

Figure 6.9: Phase 1 of the Option 2 conceptual Douthat passive treatment system design (PTS-2) plan view

6.3.3.2 Phase 2

Both Phase 2 conceptual designs utilize a berm with a top elevation of 807 ft AMSL to prevent Tar Creek from flooding the system during high flow events. It is important to note that the berm location and top elevation have not been evaluated using hydraulic modeling software to determine if the height is sufficient to prevent flooding and the location will not cause adverse effects downstream. The design objective of PTS-1 Phase 2 was to propose a moderately sized PTS that was capable of treating the median flow of MD. The conceptual PTS-1 footprint is approximately 36.6 acres and was limited to the volunteer cattail marsh created by the southern MD discharges. The landowner does currently not utilize this area of land (Figure 6.11). Consequently, the resulting system is much smaller and less resilient compared to the 66.8-acre footprint of PTS-2 (Figure 6.13). The PTS-1 conceptual design relies heavily on managing the mine pool, specifically with respect to preventing or decreasing elevated discharge events.

The design objective of PTS-2 was to treat 90% of the MD volume from the Douthat discharges based on the calculated flow rates from the 2010 to 2021 mine pool elevations, that is, without closing the large inflow locations. PTS-2 was designed without being constrained to the available footprint of the volunteer cattail marsh. Therefore, the PTS-2 design incorporated a more favorable layout of the system compared to the PTS-1 that included doubling the average length to width ratio of the first three SFWs to decrease dead zones, and the polishing SWF was designed in a zig-zag pattern with multiple wetland shelves (Figure 6.13). The increased footprint of PTS-2 resulted in the effluent of the system being discharged into Quapaw Creek, rather than Tar Creek (Figure 6.13), which provided an additional foot of topographic relief compared to PTS-1, with a final discharge elevation of 796 ft AMSL (Tables 6.8 and 6.9).

A sensitivity analysis was used to evaluate the effects of adjusting the storage capacity and the PTS design flow rate of the PTS-1 design to determine which parameter resulted in the greatest increase in metals retention. The 30% increase in storage capacity in the PTS-2 design compared to PTS-1 (Tables 6.8 and 6.9) only resulted in about a 1.5% increase in the annual mean metals retention for the targeted metals. Whereas the 80% increase in the design flow rate of Phase 2 made the greatest difference, increasing the annual mean metals retention for the targeted metals by 20%.

The PTS-1 mean flow rate through the system during the 11-year simulation period was 1,106 gpm, and the system operated at the design flow rate of 1,200 gpm 48% of the time. The simulated PTS-1 treated 66% of the total MD volume over the simulated period. By comparison, the mean flow rate through PTS-2 was 1,521 gpm, and the system operated at the design flow rate of 2,150 gpm 27% of the

time, treating 90% of the MD volume. Therefore, PTS-2 treats an additional 24% of the MD volume at Douthat compared to PTS-1 but comes with a cost estimate of nearly twice that of PTS-1 (Table 6.10). Although PTS-2 does have a substantial increased cost, a larger system can provide necessary safeguards against future unknowns such as changes in water chemistry after construction or new inflow locations occurring in the future because of subsidence or recollapsed mine shafts. The added resiliency provided by implementing a larger system like PTS-2 will also provide longevity because of the extended periods where the system does not have to operate at its maximum capacity.

Additionally, when working with a hydraulically complex system such as Douthat, where there is the possibility of multiple discharges appearing during construction, a larger PTS with resiliency built into the design is preferable over a moderately sized PTS with limited resiliency. An example of how designing for the worst-case scenario still resulted in an undersized system is the SECPTS. The maximum measured flow rate from the available dataset before construction was 112 gpm and was used to design the system. However, during construction, a mine shaft was opened in the bottom of the oxidation pond that created a new preferential flow path for the MD. The median flow rate measured at the VFBR outflows since the system was constructed in 2017 was approximately 10% greater than the designed flow rate at 123 gpm, with a maximum measured flow rate of 171 gpm. Despite the flow rates exceeding the design flow rate, the system has continued to show a significant decrease in Cd, Fe, Pb, and Zn concentrations ($p < 0.05$). However, with SECPTS operating consistently above the design flow rates, there are signs that the VFBR media may be prematurely compacting and the water elevation in the first process units is often above the design water elevation. Although built-in resiliency can decrease the likelihood of either phase requiring a redesign mid-construction, the unknowns that could occur when constructing a large system, such as the proposed conceptual designs in this study, coupled with the hydraulic complexities of Douthat, requires a flexible design and construction approach because unanticipated conditions will occur and may require a partial redesign.

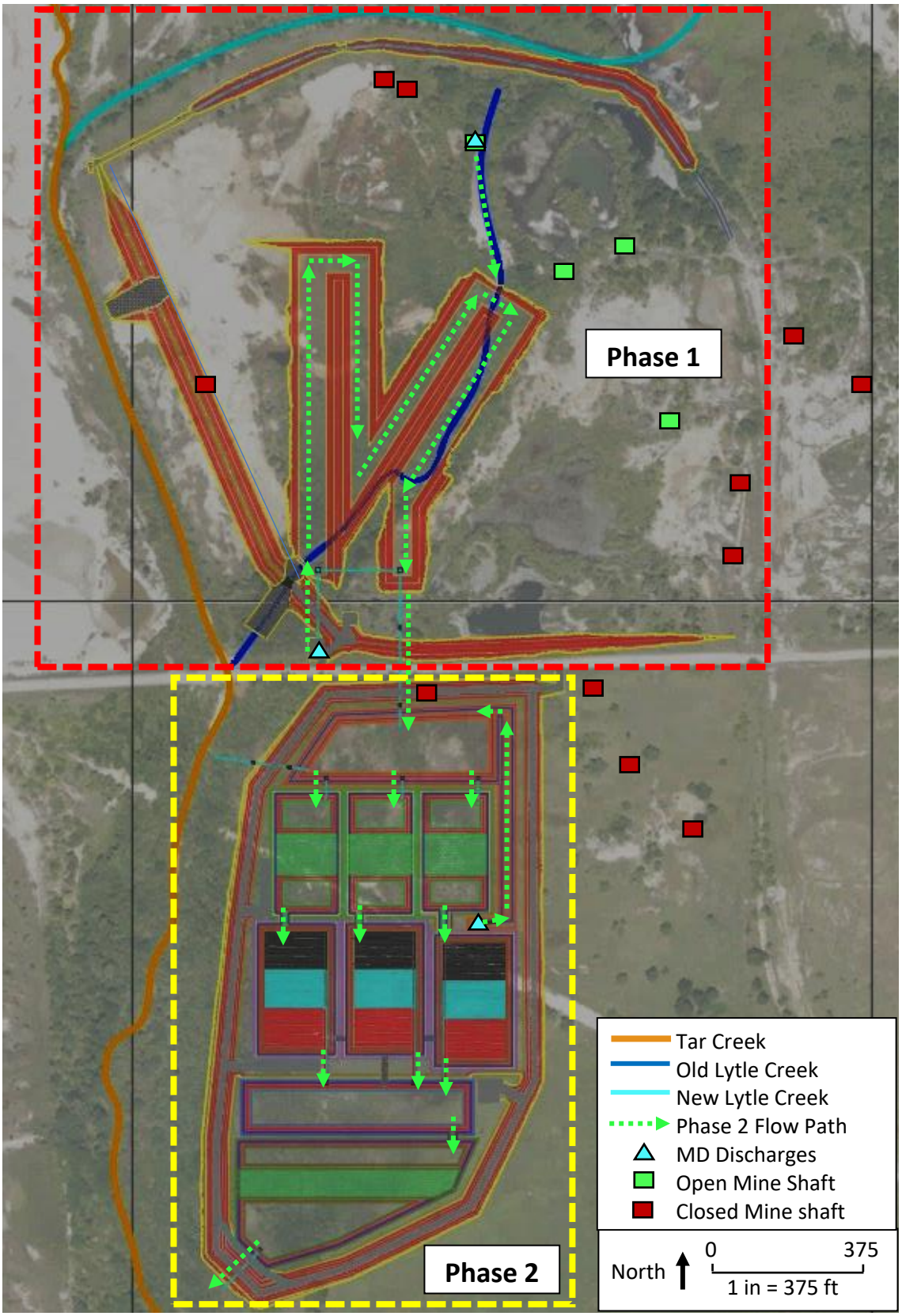

Figure 6.10: Option 1 conceptual Douthat passive treatment system design (PTS-1) plan view

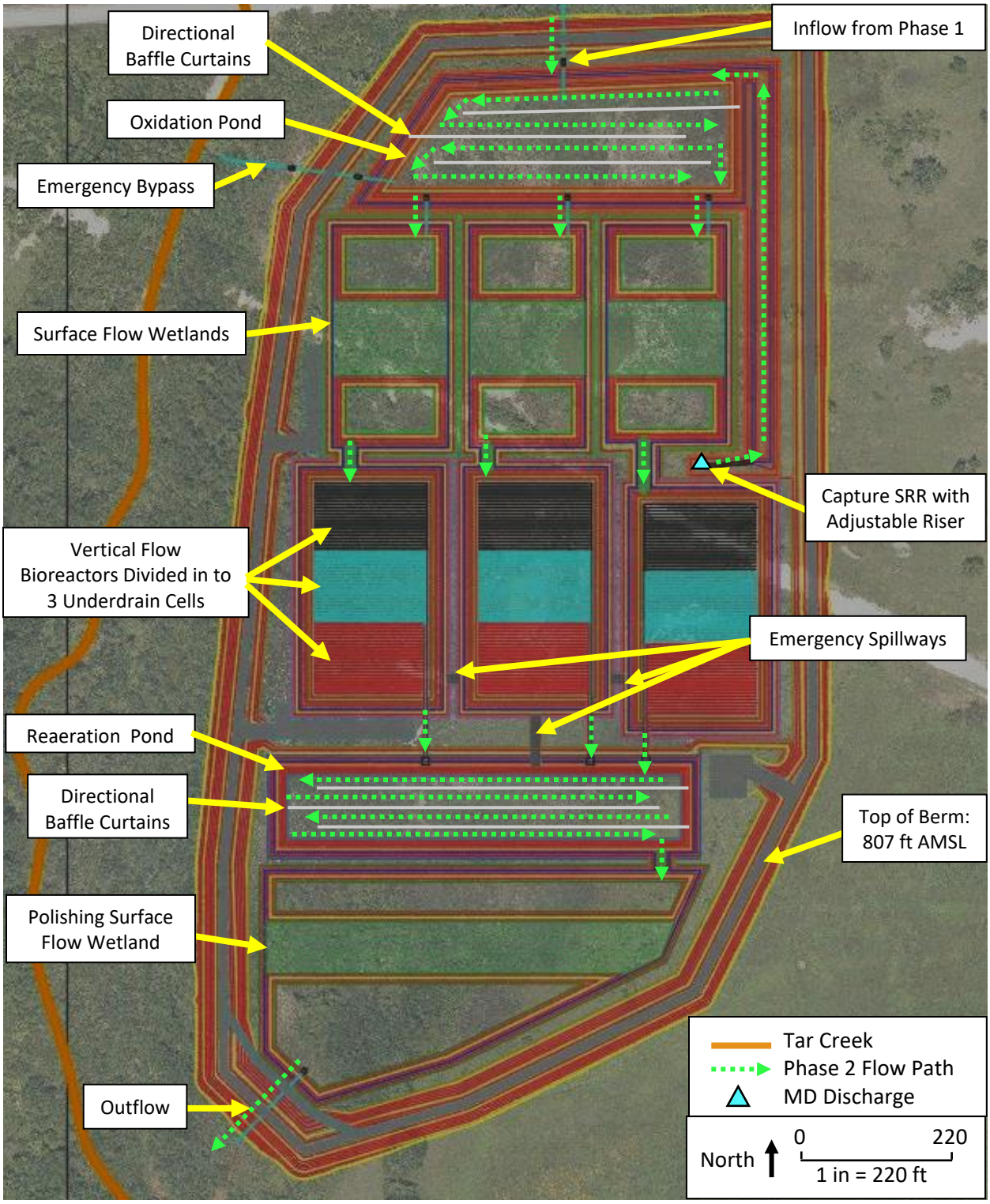

Figure 6.11: Phase 2 of the Option 1 conceptual Douthat passive treatment system design (PTS-1) plan view

Table 6.8: Design highlights of the Option 1 conceptual Douthat passive treatment system design (PTS-1)

Process Unit	Parameter	Elevation ft AMSL	Volume m^3 (ac-ft)	Area m^2 (acres)	HRT Hrs[c]
Phase 1: Initial Oxidation Pond and Storage	Bottom	795.0		19,634 (4.85)	
	Design WE	801.0	49,660 (40.26)	44,480 (10.99)	182.2
	Top of Storage	807.0	274,200 (222.3)	160,000 (39.54)	
	Storage Capacity		224,540 (182.0)		
Oxidation Pond	Bottom	793.5		5,710 (1.41)	
	Design WE	800.0	14,880 (12.07)	10,170 (2.51)	54.6
	Freeboard	803.0	25,630 (20.78)	13,140 (3.25)	
Wetland (Divided into 3 Parallel Units)[a]	Bottom of Settling Basins	793.5		1,394 (0.34)	
	Bottom of Wetland Shelf	798.5		1,625 (0.40)	
	Design WE	799.0	4,293 (3.48)	5,087 (1.26)	47.3
	Freeboard	802.0	9,463 (7.67)	6,240 (1.54)	
Vertical Flow Bioreactor (Divided into 3 Parallel Units)[a]	Bottom	793.0		4,841 (1.20)	
	Top of Drainage Layer	794.5	1,047 (0.85)[b]	5,249 (1.20)	11.52
	Top of Media Layer	796.5	1,517 (1.23)[b]	5,816 (1.30)	16.70
	Top of Water Layer (design WE)	799.0	4,830 (3.92)	6929 (1.44)	53.16
	Freeboard	802.0	6,813 (5.52)	8,013 (1.71)	
Reaeration Unit	Bottom	790.0		4,889 (1.21)	
	Design WE	797.0	13,310(10.79)	7,644 (1.89)	48.84
	Freeboard	799.0	18,310 (14.85)	8,779 (2.17)	
Final Polishing Unit	Bottom of Settling Basins	793.0		6,232 (1.54)	
	Bottom of Wetland Shelf	796.5	8,318 (6.74)	4,057 (1.00)	
	Design WE	797.0	10,400 (8.43)	13,810 (3.41)	38.15
	Freeboard	799.0	19,200 (15.57)	15,090 (3.73)	
Total HRT of System					452.5 (18.85 days)

[a]Volume and area values represent 1 of the 3 units in the parallel treatment train

[b]Volume represents volume of voids using a porosity of drainage and media layer estimated to be 0.45

[c]Hydraulic retention time (HRT) is based on the design flow rate of 1,200 gpm

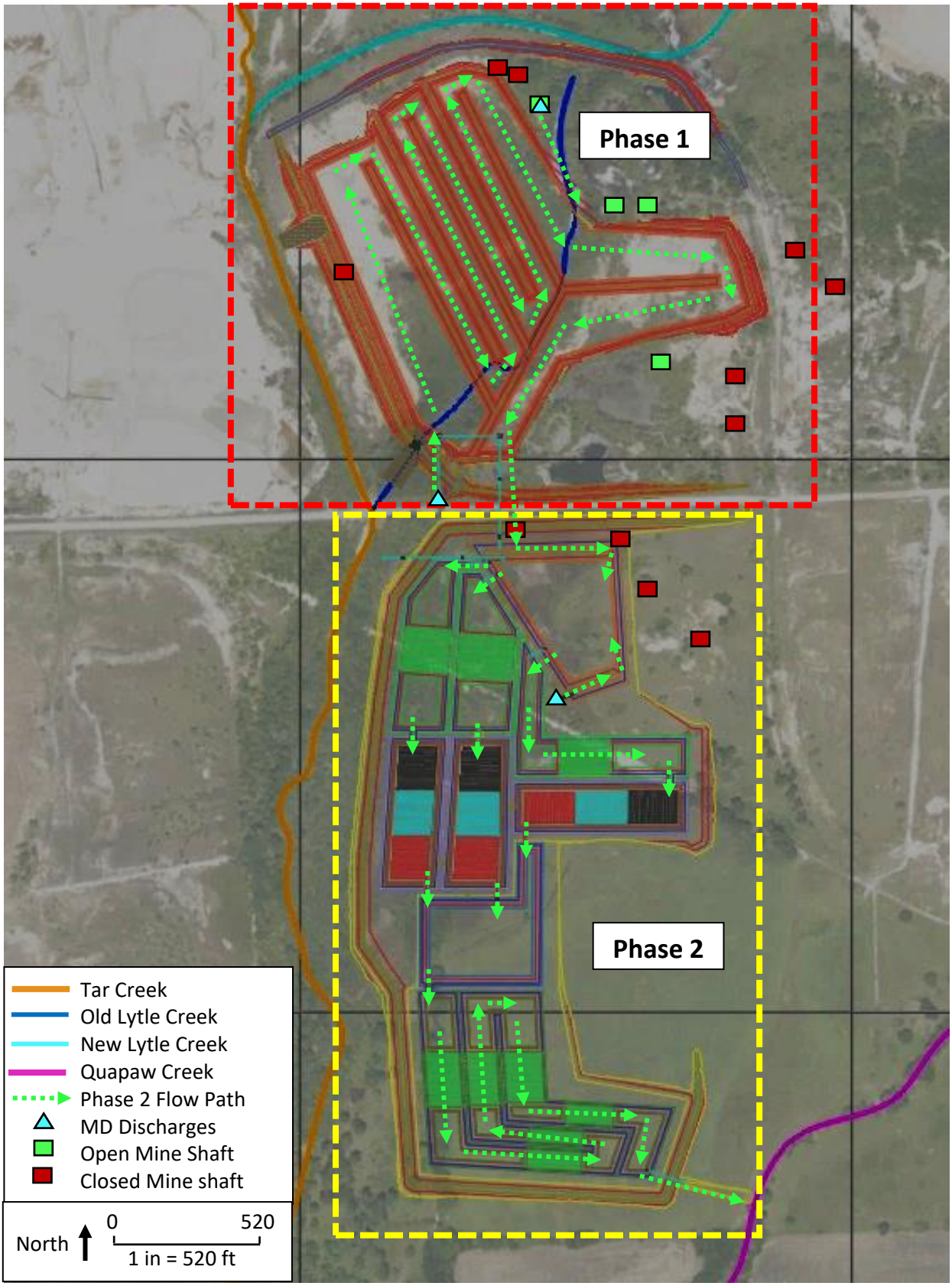

Figure 6.12: Option 2 conceptual Douthat passive treatment system design (PTS-2) plan view

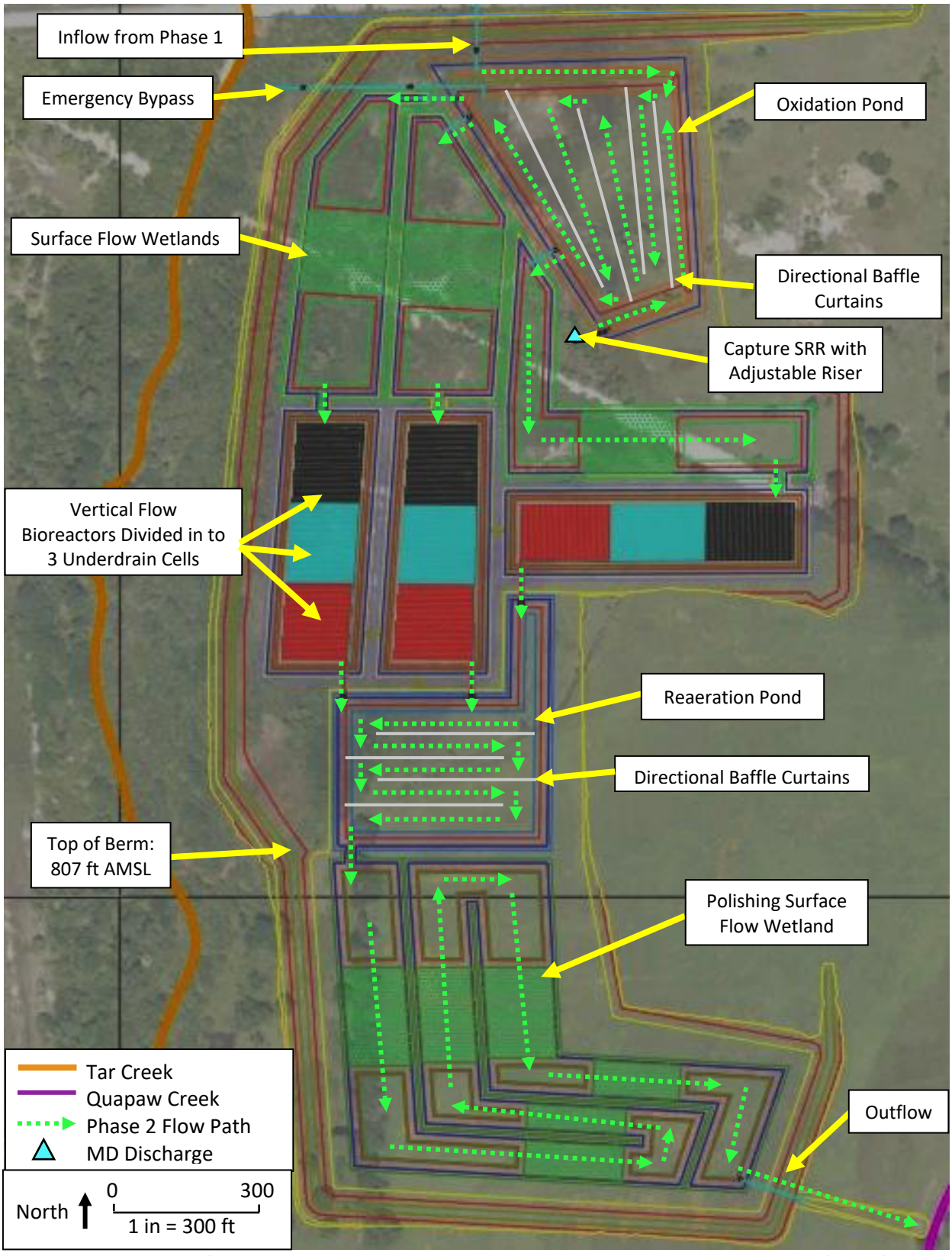

Figure 6.13: Phase 2 of the Option 2 conceptual Douthat passive treatment system design (PTS-2) plan view

Table 6.9: Design highlights of the Option 2 conceptual Douthat passive treatment system design (PTS-2)

Process Unit	Parameter	Elevation ft AMSL	Volume m^3 (ac-ft)	Area m^2 (acres)	HRT[c] hrs
Phase 1: Initial Oxidation Pond and Storage	Bottom	794.0		66,382 (16.4)	
	Design WE	801.0	193,093 (156.5)	135,785 (33.6)	395.4
	Top of Storage	807.0	488,516 (396.1)	160,000 (39.5)	
	Storage Capacity		295,423 (239.6)		
Oxidation Pond	Bottom	793.0		11,416 (2.82)	
	Design WE	800.0	30,447 (24.7)	18,070 (4.47)	62.35
	Freeboard	803.0	47,973 (38.9)	20,225 (5.00)	
Wetland (Divided into 3 Parallel Units)[a]	Bottom of Settling Basins	793.0		3,623 (0.90)	
	Bottom of Wetland Shelf	798.5		2,369 (0.59)	
	Design WE	799.0	9,548 (7.74)	8,953 (2.21)	58.66
	Freeboard	802.0	18,574 (15.1)	10,805 (2.67)	
Vertical Flow Bioreactor (Divided into 3 Parallel Units)[a]	Bottom	792.5		6,850 (1.69)	
	Top of Drainage Layer	794.5	2,011 (1.63)	7,817 (1.93)	12.35
	Top of Media Layer	796.5	2,282 (1.85)	8,832 (2.18)	14.02
	Top of Water Layer (design WE)	799.0	7,234 (5.86)	10,167 (2.51)	44.44
	Freeboard	802.0	10,066 (8.16)	11867 (2.93)	
Reaeration Unit	Bottom	789.0		8,849 (2.19)	
	Design WE	796.0	23,605 (19.1)	13,375 (3.31)	48.34
	Freeboard	798.0	32,183 (26.1)	14,775 (3.65)	
Final Polishing Unit	Bottom of Settling Basins	791.0		10,275 (2.54)	
	Bottom of Wetland Shelf	795.5		10,060 (2.49)	
	Design WE	796.0	24,483 (19.8)	30,439 (7.52)	50.14
	Freeboard	798.0	44,622 (36.2)	35,643 (8.81)	
Total HRT of System					685.7 (28.57 days)

[a]Volume and area values represent 1 of the 3 units in the parallel treatment train

[b]Volume represents volume of voids using a porosity of drainage and media layer estimated to be 0.45

[c]Hydraulic retention time (HRT) is based on the design flow rate of 2,150 gpm

Table 6.10: Summarized cost estimates of the two conceptual passive treatment systems to remediate the Douthat mine drainage discharges. Future values are based on a 3% inflation rate. Appendices 6E and 6F contain detailed cost breakdowns and explanations

Year	Phase	PTS-1		PTS-2	
		Present Value	Future Value	Present Value	Future Value
1	Phase 1 Construction	$4,440,000	$4,440,000	$9,390,000	$9,390,000
2	Phase 1 Assessment Period	$140,000	$150,000	$140,000	$150,000
3		$170,000	$180,000	$170,000	$180,000
4		$140,000	$160,000	$140,000	$160,000
5		$170,000	$190,000	$170,000	$190,000
6		$140,000	$170,000	$140,000	$170,000
7	Phase 2 Construction	$7,550,000	$9,280,000	$16,550,000	$20,350,000
8	Phase 2 Assessment Period	$190,000	$250,000	$190,000	$250,000
9		$190,000	$250,000	$190,000	$250,000
10		$240,000	$320,000	$260,000	$340,000
11		$190,000	$270,000	$190,000	$270,000
12		$320,000	$450,000	$380,000	$540,000
	Phase 1 Total		$5,300,000		$10,260,000
	Phase 2 Total		$10,820,000		$22,000,000
	Project Completion Total		$16,130,000		$32,260,000

6.3.4 Tar Creek Metal Loading and Metal Retention in Conceptual PTS

The Douthat discharges have historically accounted for the majority of the metal loading to Tar Creek from MD and are now the only remaining large MD discharges contaminating Tar Creek since the construction of MRPTS and SECPTS. Both simulated scenarios in this study where passive treatment was implemented showed a significant decrease in metal loading for all metals of interest when compared to the untreated MD ($p < 0.05$) (Table 6.11). The larger PTS-2 conceptual design treated 24% more of the total annual MD volume than PTS-1 in the simulation (Table 6.11). The increased design flow rate and the size of the retention basin showed PTS-2 resulted in significantly less metals loading to Tar Creek compared to PTS-1 ($p < 0.05$).

The conceptual PTS-2 treated 90% of the MD volume over the 11-year simulation (Appendix 6C). Six of the eleven years PTS-2 treated greater than 99% of the MD. The years where the percent of treated MD was lowest correlated to years where there were multiple elevated streamflow events frequently occurring, resulting in a mine pool elevation that was constantly discharging flow rates above the design flow rate of the PTS. For example, 2020 had one of the lowest MD treatment percentages at 75% (Appendix 6C) because 16 elevated streamflow events occurred from January to May that resulted in known inflow locations receiving water and a resulting elevated mine pool. This example reinforces the importance of closing known discharges. Furthermore, a system capable of treating 100% of the MD at Douthat throughout the entire simulation required the Phase 1 storage pond to be doubled to 480 ac-ft and a design flow rate of 3,215 gpm for the Phase 2 system, 50% greater than the conceptual PTS-2

design flow rate.

Table 6.11: Mean annual metal loading to Tar Creek from Douthat mine drainage (MD) discharges under three conditions: 1) untreated MD (current condition) 2) implementation of conceptual PTS-1 3) implementation of conceptual PTS-2 and the mass of metals retained by each conceptual PTS design, where metals removal efficiency of each PTS was based on the removal efficiency of the Mayer Ranch PTS. Mine pool water elevations recorded on 30-minute time intervals from 2010-2021 at a USGS monitoring station were used to calculate discharge flow rates

		Cd	Fe	Pb	Zn	Time a Portion of MD is Bypassed	% Of MD Volume Treated
		kg	kg	kg	kg	(days)	
	Untreated MD	45.6	65,903	137	15,454		
	Metals Retained in PTS	37.5	42,306	86.0	9,907		
PTS-1	Metals Loading to Tar Creek	8.15	23,597	51.5	5,547	90.65	66%
	% Metals Retained	82.1%	64.2%	62.6%	64.1%		
	Metals Retained in PTS	43.2	58,872	122	13,230		
PTS-2	Metals Loading to Tar Creek	2.39	7,031	15.11	2,224	25.34	90%
	% Metals Retained	94.8%	89.3%	89.0%	85.6%		

6.3.5 Downstream Metals Concentrations

The calculated downstream metals concentrations for Zn and Cd under the untreated MD scenario did not meet the hardness adjusted metals criteria for the state-designated beneficial use classifications more than 50% of the time (Table 6.12). The chronic Cd beneficial use criterion was the most frequently unmet value, occurring more than 90% of the time (Table 6.12). Therefore, the hypothesis that without the implementation of a passive treatment system to treat net-alkaline MD discharges, the water quality of a second-order stream would not meet the state-designated beneficial use criteria more than 50% of the time, even if all other sources of metals contamination upstream of the discharges was addressed, was accepted.

The approximately ten percent of the time when the calculated Cd concentrations under the untreated MD scenario met the chronic beneficial use concentration occurred for short periods during elevated streamflow events where the MD was diluted to less than ten percent of the flow rate measured at the downstream gauge station. Although the metals concentrations met the beneficial use criteria during these events, the metal loading was substantial. A single 24-hour event can equate to more than fifteen times the median daily metal loading. For example, the calculated metals concentrations downstream of the MD on April 29th, 2017, met the beneficial use criteria on this day. however, the metal loading of Cd, Fe, Pb, and Zn during the 24 hours was 0.90 kg, 2,360 kg, 5.13 kg, and 500 kg, respectively. By comparison, the overall median daily metal loading of Cd, Fe, Pb, and Zn was 0.02 kg, 131, kg, 0.26 kg, and 33.3 kg, respectively.

The calculated downstream metals concentrations under the two scenarios where PTS was implemented showed significant differences in the percentage of time that the beneficial use concentrations for acute Cd and Zn, and chronic Cd were met ($p < 0.05$). Even though PTS-1 is a much smaller system compared to PTS-2, PTS-1 still had a substantial influence on the calculated downstream water quality, with the beneficial use criteria being met more than 95% of the time (Table 6.12). However, PTS-2 showed further improvement by meeting the beneficial use criteria more than 99.9% of the time (Table 6.12). The periods when downstream calculated metals concentrations did not meet the beneficial use values for PTS-1 and PTS-2 were the result of consecutive rain events occurring in a short period that maintained elevated streamflow and mine pool elevations, generating elevated discharge flow rates that exceeded the design flow capacity and eventually filled the storage pond; bypassing untreated MD. Typically, the storage capacity was exceeded immediately before or immediately after the stream had elevated flow rates. For example, in May 2019, after ten days of rainfall in the previous 19 days the simulated storage capacity of PTS-2 was nearly exceeded. Then another 1.3-inch rainfall occurred and caused a spike in the mine pool elevation, but the rainfall had not yet affected the stream flow rates. A portion of the MD was bypassed, and the beneficial use concentrations were not met for acute Zn and chronic Cd for two hours. The percentage of treated MD at the downstream gauge station was greater than 70%, the percent of untreated MD was approximately 15%, with the remaining 15% non-MD during the two hours. Once the streamflow increased, the untreated MD became diluted enough that it once again met the beneficial use concentrations. The circumstances necessary to create the conditions in the example are very uncommon. The total rainfall during May in 2019 was 18.62 inches, compared to the long-term average measured by the Miami, OK Mesonet station from 1994-2021 of 7.20 inches.

The mean annual percent of time the instream metals concentrations met the beneficial use concentrations in the untreated MD scenario correlated with an increase in total annual rainfall. In 2012, at least one of the beneficial use criteria was not met 96% of the time and the total annual precipitation was 90 cm (35.25 inches) (Appendix 6D). Whereas the wettest year, 2019, had a total annual rainfall of 207 cm (81.64 inches) and at least one of the beneficial use criteria was not met 75% of the time. However, in the scenarios with PTS implemented, the years with the greatest annual rainfall correlated with a decrease in the percent of the time the beneficial use criteria were met because during dry conditions both PTSs were treating the majority of the MD. Whereas a greater volume of MD was bypassed annually during the wet years of the simulation (Appendix 6D).

Overall, the results of the simulated conditions under the three scenarios show that even if all

metals contamination upstream of the Douthat MD discharges is remediated, Tar Creek will remain contaminated, not meeting the state-designated beneficial use criteria the majority of the time (Table 6.12). Additionally, Tar Creek will continue to be stained orange by Fe oxides (Table 6.11). However, implementing a PTS to remediate the Douthat MD can significantly decrease the metal loading to Tar Creek (Table 6.11) and provide the possibility that Tar Creek can meet the state-designated beneficial use criteria the majority of the time for the first time in many decades (Table 6.12).

Table 6.12: Calculated mean metals concentrations and the percent of time calculated metals concentrations downstream of mine drainage discharges at Douthat, OK do not meet beneficial use criteria for fish and wildlife propagation the using data from USGS on 30-minute time intervals from 2010-2021 under three scenarios: 1) untreated MD 2) implementation of conceptual PTS-1 3) implementation of conceptual PTS-2

	% Time Concentrations Did Not Meet Criteria					Mean Metals Conc.		
		Acute		Chronic		Cd (diss)	Pb (tot)	Zn (diss)
	Cd	Pb	Zn	Cd	Pb	µg/L	µg/L	µg/L
Threshold Concentration (µg/L)	21.52	1,831	928.7	1.334	71.34			
Untreated MD	15.28%	0.000%	81.75%	90.05%	0.000%	10.4	20.3	2,640
PTS-1	0.000%	0.000%	3.610%	4.006%	0.000%	0.243	1.530	309
PTS-2	0.000%	0.000%	0.003%	0.001%	0.000%	0.022	0.141	184

6.4 Conclusions

The findings of this study show that the water quality in Tar Creek downstream of Douthat will not meet the Oklahoma state-designated beneficial use criteria for acute Zn and chronic Cd more than 50% of the time if the MD originating from the Douthat site remain untreated (Table 6.12). **Currently, the untreated MD from Douthat is the primary contributor of the metals loading to Tar Creek**, annually loading thousands of kilograms of Fe and Zn to the stream. However, the two conceptual PTSs discussed in this study have shown that **the MD at Douthat can be remediated using PTS** (Table 6.11). The land space required for the conceptual PTSs will fit within a reasonable area, and the conceptual design showed that despite limited topographic relief across the study site, a system can be implemented without requiring the use of pumps to increase the hydraulic head (Figures 6.10 and 6.12; Tables 6.8 and 6.9). The implementation of Phase 1 to accurately measure flow rates from the north Douthat discharges will provide invaluable information about the effects of closing known inflow locations throughout the Picher field and is essential for the future success of any PTS. The implementation of either conceptual PTS discussed in this study provided a significant decrease in metals loading to Tar Creek and a significant increase in the amount of time Tar Creek would meet the

state-designated beneficial use criteria during the 11-year simulation ($p < 0.05$). The increase in the design flow rate and storage capacity of PTS-2 compared to PTS-1 resulted in a significant decrease in metals loading ($p < 0.05$). While PTS-2 is the more expensive system, the resiliency provided by a larger system would increase the longevity because the system would not be required to operate at full capacity as often and has a greater ability to adjust to unforeseen circumstances such as a change in the water chemistry or in the median flow rates from the discharges after the system has been constructed. Overall, the results of this study have shown PTS can be used to remediate the Douthat MD discharges, preventing thousands of kilograms of metals from contaminating downstream environments and Tar Creek would no longer be stained orange for the first time in over forty years.

6.5 References

Brockie DC, Hare EH Jr., Dingess PR (1968) The Geology and Ore Deposits of the Tri-State District of Missouri, Kansas, and Oklahoma. American Institute of Minerals and Metallurgical Engineers. Ch 20 pp. 400-430.

Cameron SG, and Schipper LA (2010) Nitrate removal and hydraulic performance of organic carbon for use in denitrification beds. Ecological Engineering. 36:1588-1595. DOI: 10.1016/j.ecoleng.2010.03.010

CH2M (2017) Remedial Action Report Distal Area Group 4; Tar Creek Superfund Site Source Material Operable Unit 4 Remedial Action. Contract No. EP-W-06-021. Prepared for U.S. EPA, Dallas, TX.

Cravotta III CA (2007) Passive Aerobic Treatment of Net-Alkaline, Iron-Laden Drainage from a Flooded Underground Anthracite Mine, Pennsylvania, USA. Mine Water and the Environment. 26:128-149. DOI: 10.1007/s10230-007-0002-8

Cravotta III CA, Brightbill RA, Langland MJ (2010) Abandoned Mine Drainage in the Swatara Creek Basin, Southern Anthracite Coalfield, Pennsylvania, USA: 1. Stream Water Quality Trends Coinciding with the Return of Fish. Mine Water and the Environment. 29:176–199. DOI: 10.1007/s10230-010-0112-6

Dempsey BA, Jeon B-H (2001) Characteristics of Sludge Produced from Passive Treatment of Mine Drainage. Geochemistry: Exploration, Environment, Analysis. 1:89–94. DOI: 10.1144/geochem.1.1.89

Dietz JM, Dempsey BA (2002) Innovative Treatment of Alkaline Mine Drainage Using Recirculated Iron Oxides in a Complete Mix Reactor. Journal American Society of Mining and Reclamation. 496–516. DOI: 10.21000/JASMR02010496

Dorman DM (2019) The Role of Solar-Powered Float-Mix Aerators on Iron Retention in Passive Treatment Oxidation Ponds. University of Oklahoma, a thesis.

Ghane E, Feyereisen GW, Rosen CJ (2016) Non-linear hydraulic properties of woodchips necessary to design denitrification beds. Journal of Hydrology. 542:463-473. DOI: http://dx.doi.org/10.1016/j.jhydrol.2016.09.021

Hedin RS, Nairn RW, Kleinmann RLP (1994) Passive Treatment of Coal Mine Drainage. Bureau of Mines, Department of the Interior.

LaBar JA, Nairn RW (2017) Evaluation of the Impact of Na-SO4 Dominated Ionic Strength on Effluent Water Quality in Bench-Scale Vertical Flow Bioreactors Using Spent Mushroom Compost. Mine Water and the Environment. 36:572–582. DOI: 10.1007/s10230-017-0446-4

Luza KV (1983) A study of stability problems and hazard evaluation of the Oklahoma portion of the Tri-State Mining Area. U.S. Bureau of Mines Mining Research Contract Report J0100133.

Luza KV, Keheley E (2006) Inventory of Mine Shafts and Collapse Features Associated with Abandoned Underground Mines in the Picher Field Northeastern Oklahoma. Oklahoma Geological Survey Open File Report.

McCauley JR, Brady LL, Wilson FW (1983) Study of Stability Problems and Hazard Evaluation of the Kansas Portion of the Tri-State Mining Area. Kansas Geological Survey. Open-File Report.

Nairn RW, Beisel T, Thomas RC, LaBar JA, Strevett KA, Fuller D, Strosnider WH, Andrews WJ, Bays J, Knox RC (2009) Challenges in Design and Construction of a Large Multi-Cell Passive Treatment System for Ferruginous Lead-Zinc Mine Waters. Proceedings, 2009 National Meeting of the American Society of Mining and Reclamation. Billings, MT, Revitalizing the Environment: Proven Solutions and Innovative Approaches, May 30 – June 5, 2009.
DOI: 10.21000/JASMR09010871

Nairn RW, LaBar JA, Strevett KA (2011) Passive Treatment Opportunities in a Drastically Disturbed Watershed: Reversing the Irreversible?. Journal American Society of Mining and Reclamation. 2011:450–468. DOI: 10.21000/JASMR11010450

Neculita C-M, Zagury GJ, Bussiere B (2007) Passive Treatment of Acid Mine Drainage in Bioreactors using Sulfate-Reducing Bacteria: Critical Review and Research Needs. Journal of Environmental Quality. 63:1-16. DOI: 10.2134/jeq2006.0066

Oklahoma Department of Environmental Quality (ODEQ) (2006) Oklahoma Plan for Tar Creek. ODEQ.

Oklahoma Water Resources Board (OWRB) (1983) Tar Creek Field Investigation. OWRB.

Oklahoma Water Resources Board (OWRB) (2020) Title 785. Oklahoma Water Resources Board Chapter 45. Oklahoma's Water Quality Standards. Oklahoma City, OK.

Playton SJ, Davis RE, McClaflin RG (1980) Chemical Quality of Water in Abandoned Zinc Mines in Northeastern Oklahoma and Southeastern Kansas: Oklahoma Geological Survey. Circular 82.

Porter CM, and Nairn RW (2008) Ecosystem functions within a mine drainage passive treatment system. Ecological Engineering. 32:337-346. DOI: 10.1016/j.ecoleng.2007.12.013

Shepherd NL, Nairn RW (2020) Metals retention in a net alkaline mine drainage impacted stream due to the colonization of the North American Beaver (*Castor canadensis*). Science of the Total Environment. 731(2020) 139203 DOI: https://doi.org/10.1016/j.scitotenv.2020.139203

Shepherd, NL, Keheley E, Dutnell RC, Folz CA, Holzbauer-Schweitzer B, Nairn RW (2022) Picher Field Underground Mine Workings of the Abandoned Tri-State Lead-Zinc Mining District in the United States. Journal of Maps.

Simmons JA (2010) Phosphorus Removal by Sediment in Streams Contaminated with Acid Mine Drainage. Water, Air, & Soil Pollution. 209:123–132. DOI: 10.1007/s11270-009-0185-7

Skousen J, Ziemkiewicz P (2005) Performance of 116 Passive Treatment Systems for Acid Mine Drainage. Journal American Society of Mining and Reclamation. 1100–1133. DOI: 10.21000/JASMR05011100

Skousen JG, Zipper CE, Rose A, Ziemkiewicz PF, Nairn RW, McDonald LM, Kleinmann RL, (2017) Review of Passive Systems for Acid Mine Drainage Treatment. Mine Water and the Environment. 36:133–153. DOI: 10.1007/s10230-016-0417-1

StormTech (2012) Porosity of Structural Backfill; Tech Sheet #1. StormTech, Rocky Hill, CT.

Taylor J, Pape S, Murphy N (2005) A Summary of Passive and Active Treatment Technologies for Acid and Metalliferous Drainage (AMD). Proceedings, Fifth Australian Workshop on Acid Drainage.

Underwood BE, Kruse NA, Bowman JR (2014) Long-term Chemical and Biological Improvement in an Acid Mine Drainage-Impacted Watershed. Environmental Monitoring and Assessment. 186:7539–7553. DOI: 10.1007/s10661-014-3946-8

U.S. Department of the Interior, Bureau of Reclamation (2001) Water Measurement Manual. U.S. Department of the Interior, Bureau of Reclamation. Washington, DC.

United States Environmental Protection Agency Region 6 (1994) Five Year Review: Tar Creek Superfund Site: Ottawa County, Oklahoma. United States Environmental Protection Agency Region 6.
URS (2003) Passive and Semi-Active Treatment of Acid Rock Drainage from Metal Mines—State of the Practice. Prepared for US Army Corps of Engineers, Portland.

Watzlaf GR, Schroeder KT, Kleinmann RLP, Kairies CL, Nairn RW (2004) The Passive Treatment of Coal Mine Drainage. Unites States Department of Energy, National Energy Technology Laboratory.

Williams KM, Turner AM (2015) Acid Mine Drainage and Stream Recovery: Effects of Restoration on Water Quality, Macroinvertebrates, and Fish. Knowledge and Management of Aquatic Ecosystems. 18. DOI: 10.1051/kmae/2015014

Younger PL, Banwart SA, Hedin RS (2002) Mine Water: Hydrology, Pollution, Remediation. Kluwer Academic Publishers.

Ziemkiewicz PF, Skousen JG, Simmons J (2003) Long-Term Performance of Passive Acid Mine Drainage Treatment Systems. Mine Water and the Environment. 22:118–129

Zipper CE, Skousen JG (2010) Influent Water Quality Affects Performance of Passive Treatment Systems for Acid Mine Drainage. Mine Water and the Environment. 29:135–143. DOI: 10.1007/s10230-010-0101-9

CHAPTER 7

Determining Potential Recharge Sources Using Aqueous Light Isotopes and other Water quality Parameters

Abstract

Mine drainage (MD) is a massive source of environmental contamination that negatively impacts thousands of kilometers of streams worldwide. Understanding mine pool hydrology is a critically important factor to manage and potentially decrease flow rates of MD discharges. The objective of this study was to determine if primary mine pool recharge sources could be identified using isotope ratios of ^{2}H and ^{18}O in water and selected water quality parameters to characterize the water chemistry of a mine pool from abandoned underground hard rock mining and, furthermore, to compare the results to three potential mine pool recharge sources that included precipitation entering the mine pool through surface connections like mine shafts, an unconfined aquifer, and a confined aquifer. The findings of this study showed isotope ratios of the three recharge sources were not significantly different. However, conservative ions such as chloride and sodium that had elevated concentrations in the groundwater compared to the rainfall showed the unconfined aquifer and precipitation were both major contributors to mine pool recharge. The unconfined aquifer had mean chloride and sodium concentrations of 23.7 mg/L and 45.4 mg/L, respectively, while rainfall measured <0.15 mg/L for both ions. Comparatively, the mean chloride and sodium concentrations measured in the mine pool were 11.4 mg/L and 30.3 mg/L, respectively. Additionally, the mine pool shows substantial spatial variability in water chemistry, with the most contaminated water being located below the MD discharges, while the mine pool located outside of a 1.6 km radius of the mine pool showed significantly different water quality. The findings of this study indicate that preventing surface connections to the mine pool may substantially decrease the mine pool recharge rate and production of metals-contaminated mine waters.

Key Words: Tar Creek, Deuterium, Isotopes, mine pool characterization

7.1 Introduction

The ratio of deuterium and ^{18}O isotopes in water has been widely used as a natural conservative tracer in precipitation, surface waters, and groundwater (Sharp 2007). Stable isotope ratios have also been used as a tool to characterize mine drainage (MD) (Hazen et al. 2001; Knierim et al. 2013; Corrales et al. 2015; Abu Jabal et al. 2018; Migaszewski et al. 2018; Tomiyama et al. 2019; Wolkersdorfer et al. 2020; Ren et al. 2021). The formation of MD occurs when metal sulfides in the geologic formations are exposed to oxygen during mining operations, which produces sulfate, acidity, and soluble metals (Watzlaf et al. 2004). MD is a global concern that negatively impacts thousands of km of streams around the world (Watzlaf et al. 2004). Therefore, using stable isotopes or other water quality parameters to identify MD recharge sources that can then be managed to decrease the volume of MD can be a substantial benefit to the impacted ecosystems.

A study conducted by Hazen et al. (2001) used stable isotopes to differentiate recharge from two recharge sources, snowmelt, and singular storm events, and estimate water quantity from each recharge source that contributes to a MD discharge at the abandoned Mary Murphy Mine in Colorado, USA. The findings showed over 70% of Zn loading originated from a single stream within the mine and nearly 80% of the flow from the Zn-rich stream was attributed to snowmelt during the melt season (Hazen et al. 2001). These findings were used to justify the installation of a diversion structure resulting in an approximate 90% decreased Zn loading of the MD discharge (Hazen et al. 2001).

Another study published by Walton-Day and Poeter in 2009 used stable isotopes of water to investigate the potential hydraulic connections of a surface water body, Turquoise Lake, and an abandoned underground mine tunnel, Dinero mine tunnel, near Leadville, Colorado, USA. Isotope samples were collected from draining mine tunnels, springs, seeps, five locations on a stream, and Turquoise Lake from 2002 to 2008. The study found that the stable water isotopes identified two distinct meteoric water lines. The first characterized the surface waters which predominantly remained above the Global Meteoric Water Line (GMWL), and the second characterized the groundwater and MD sources, predominantly below the GMWL. The study concluded less than 10% of the water in the Dinero tunnel originated from Turquoise Lake, with the majority of the water originating from deep groundwater (Walton-Day and Poeter 2009). Migaszewski et al. (2018) had similar findings to Walton-Day and Poeter (2009), with stable water isotopes in an acid lake associated with large quarries plotting below the GMWL, which was attributed to the water body being located in a closed drainage basin.

The geologic formation of an aquifer can affect the $\delta^{18}O$ values (Savin and Epstein 1970; Sharp

2007). A study conducted by Savin and Epstein (1970) concluded the differences in $\delta^{18}O$ values of sedimentary rocks and minerals can be used as indicators. Furthermore, the exchange reactions that occur with water and sedimentary rocks often result in enriched $\delta^{18}O$, with values typically in the range of 20-30‰ (Sharp 2007).

Other studies have found pyrite oxidation and Fe hydrolysis associated with mining and acid MD (AMD) in karst aquifers provide a unique isotopic signature of stable isotopes of $\delta^{18}O_{H2O}$, $\delta^{18}O_{SO4}$, and $\delta^{34}S_{SO4}$ that can be used to track the extent of mining contamination in karst aquifers (Sun et al. 2017; Ren et al. 2019; Ren et al. 2021). A study conducted by Sun et al. (2014) investigated the composition of stable water isotopes in karst waters of two similar watersheds in the Guizhou Province, China with one of the watersheds being impacted by AMD generated from coal mining activities. The study found the AMD had a greater $\delta^{2}H$ value than other waters which was attributed to pyrite oxidation and Fe hydrolysis, resulting in the AMD plotting well above the Local Meteoric Water Line (LMWL) and the GMWL (Sun et al. 2014).

Most of the reviewed studies investigated the use of stable water isotopes to characterize AMD that occurs in high altitude locations with snowfall accounting for a substantial amount of the annual precipitation, both of which can provide unique isotopic signatures to trace recharge sources. There is a literature gap investigating the use of stable water isotopes in net alkaline MD generated from karst geology, in a low altitude temperate climate where most of the precipitation is rainfall. Therefore, this study evaluated stable isotope ratios of ^{2}H and ^{18}O and other selected water quality parameters in a net-alkaline mine pool, MD discharges, and potential water sources recharging the mine pool to determine if these parameters could identify the primary recharge contributions to the mine pool. It was hypothesized that 1) Aqueous stable isotope ratios of ^{2}H and ^{18}O measured in rainfall, an unconfined aquifer, and a confined aquifer would be significantly different, and the differences in the isotopic signatures of each potential recharge source could be used to identify distinct sources of water contributing to the mine pool, 2) Selected water quality parameters measured in the mine pool near the MD discharges would be significantly different than the mine pool water quality beyond a 1.6 km radius of the discharges because the upgradient and outer perimeter of the mine pool would have cleaner recharge water that is flushing the more contaminated MD downgradient towards the discharges, and 3) Selected water quality parameters measured in mine pool that were collected during five separate periods from 1976 to present would be significantly different because the highly contaminated mine pool of the past is slowly being flushed and diluted by recharge waters.

7.2 Materials and Methods

7.2.1 Site Background

This study was conducted in the abandoned Picher mining field that is located on the border of Oklahoma and Kansas, USA. Mining operations in the Picher field were conducted from the early 1900s through the 1970s and produced approximately 1.5 million metric tons (m-tons) of lead (Pb) and 8 million m-tons of zinc (Zn) (Playton et al. 1980; Luza 1983). The underground void left behind by the mining operations has an approximate volume of 9,870 hectare-meters, with a surface extent of approximately 1,440 ha (Shepherd et al. 2022). The underground voids had an average height of 6.9 m, with localized heights exceeding 36 m.

The underground mines were continuously pumped to keep the mines dry, reportedly pumping 136,000 m^3 per day during peak mining production in the 1940s (McCauley et al. 1983). Three sources of recharge water were documented during the active mining period, which included groundwater from the Boone and Roubidoux aquifers and surface inflow water (Figure 7.1). The Boone is a shallow partially unconfined aquifer (Branson 1954) with a potentiometric surface elevation often less than ten meters below ground, approximately 250 m above mean sea level (AMSL), with a thickness of 110 m. The Boone is categorized as a minor aquifer by the Oklahoma Water Resources Board (OWRB), yielding less than 190 liters per minute (lpm) (Christenson 1995; Russell and Stivers 2020). The mining occurred in the Boone formation, which is a part of the Mississippian system (Snider 1912; Siebenthal 1925; Fowler and Lyden 1932; Fowler 1942). The Boone formation was originally limestone, but erosion and deformation of the limestone allowed for the ore-bearing inclusions of cotton rock, nodular chert, and fossiliferous dolomite to be deposited (Fowler 1942; Reed et al. 1955; Brockie et al. 1968; McKnight and Fischer 1970; Luza 1983). Historically the Boone discharged under artesian head pressure in natural springs before the mining of the Picher field (Bilharz 1947).

The Roubidoux aquifer is a confined aquifer located below the Boone. The confining layer starts at the bottom of the Boone formation at 140 m AMSL and is approximately 50 m thick (Russell and Stivers 2020). The Roubidoux aquifer is approximately 450 m thick and is categorized as a major aquifer by OWRB (Russell and Stivers 2020). Yields from Roubidoux wells in the study area range from 380 to 3,800 lpm, with hydraulic conductivity values reaching 26 m/day (Adamski 1994; Christenson 1995). In the early 1900s, the wells in the Roubidoux located in the mining region would artesian flow at the land surface at a rate of up to 380 lpm (Siebenthal 1908). Pumps were added to the Roubidoux wells once artesian flow stopped. The withdrawals from the Roubidoux in the mining region have been in the

millions of liters per day since at least 1937, with estimates of 15 million liters per day in 1948 (Reed at al. 1955). During active mining in the 1930s, the Roubidoux had a potentiometric surface elevation higher than the floor elevations of the underground workings, which resulted in water from the Roubidoux recharging portions of the mines when wells that were drilled into the Roubidoux would rust and leak (Williams 1934). Withdrawals from the Roubidoux continued to increase after the mining operations ceased. In the early 1980s, approximately 16 million liters per day were pumped from the Roubidoux by wells located within the study area, with a tire manufacturer being the primary user (Christenson et al. 1990; Christenson 1995). The water usage resulted in a cone of depression in the Roubidoux aquifer that was centered in the Oklahoma portion of the study area. The withdrawal rates substantially decreased after the closure of the tire manufacturing plant in 1986, and the Roubidoux recovered 30 m by 1993 (Christenson 1995). In the early 1990s, the potentiometric surface elevation of the Roubidoux in the mining region ranged from 221 m to 132 m AMSL (Christenson 1995), showing that the range in the potentiometric surface elevations of the Roubidoux overlap with the elevations of the underground voids that can range from approximately 160 to 220 m AMSL (Chapter Four). Therefore, there is potential for the Roubidoux to be a recharge source to the mine pool.

Although both the Boone and Roubidoux were documented recharge sources during active mining, rainfall and the resulting flooding from streams during the active mining period was the most frequently discussed water management concern (Williams 1934; McCuskey 1935, Gray 1938, Bilharz 1947). Surface waters would enter the underground mine workings through open mine shafts, collapse features, and boreholes (Williams 1934; McCuskey 1935, Gray 1938, Bilharz 1947). Once the mining operations ceased and pumps were shut down in the early 1970s, the large underground void began refilling from these recharge sources. Eventually, the mine pool filled, and the first artesian MD discharge was documented in 1979; containing elevated concentrations of cadmium (Cd), iron (Fe), Pb, and Zn (Oklahoma Water Resources Board 1983). The site with the greatest volume of MD discharge is located in Douthat, OK (Figure 7.1).

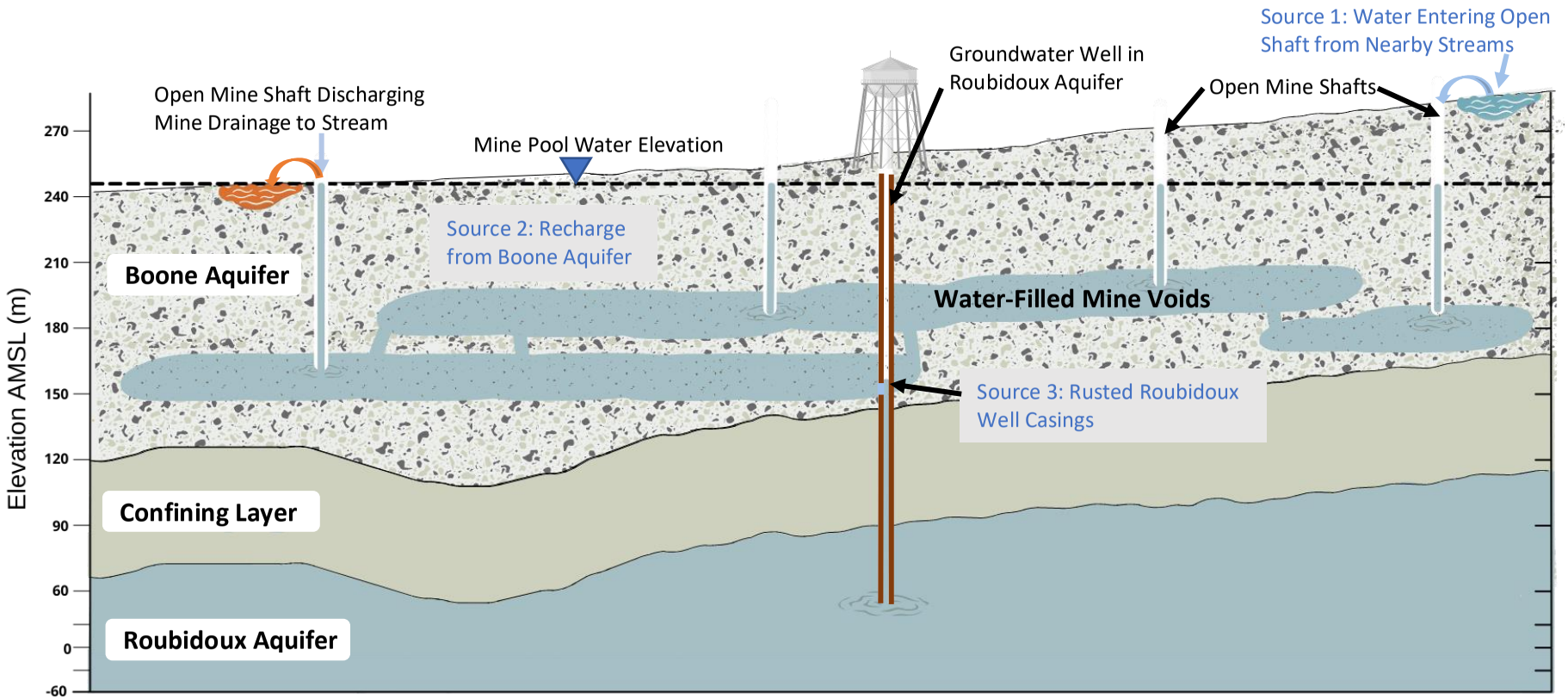

Figure 7.1: Conceptual cross-section of the Picher field mine workings showing the three potential mine pool recharge sources: 1) Precipitation resulting in stream flooding 2) Boone Aquifer 3) Roubidoux Aquifer

7.2.2 Sampling Collection and Analyses

Water samples were collected from three sources: 1) Picher field mine pool using open drill holes, air vents, and mine shafts 2) Boone aquifer existing groundwater wells, and 3) Roubidoux aquifer at existing groundwater wells throughout the Picher field and surrounding areas (Figure 7.2). An Abyss-300 Slimline submersible groundwater pump was used to collect samples from the mine pool and Boone Wells (BW) 3, 4 and 5. The total depth to the bottom of the mine void at each mine pool sampling location was measured using a weight and measuring tape. Mine pool samples were collected approximately 0.5 m from the bottom based on field measurements, and selected sites were profile sampled. Historical mine maps were used to approximate the floor and ceiling heights of the mined void at each location. The void elevations reported on the maps were often deeper than the field measured depth, likely due to collapses or attempts to fill open mine shafts in the past. Boone samples collected using the submersible pump were collected by lowering the pump to the center elevation of the well screen. BW1 and BW2 had newly installed groundwater pumps that were used to sample the wells, and the wells were regularly used by the landowner for irrigation and livestock water. The Roubidoux aquifer was sampled at municipal drinking water wells and a private well that all had functioning submersible pumps. The water quality parameters collected at each location are shown in Table 7.1. At all depth sampling locations, water was pumped until the physical parameters on a YSI multiparameter datasonde were stabilized and consistent for at least a ten-minute interval. The widely accepted practice of purging three well volumes was not used because it was not feasible to pump three mine shaft volumes from mine shafts that measured up to 3.0 m by 3.5 m wide and 60 m deep at a pumping rate of five liters per minute. Samples from four artesian MD discharges at Douthat were periodically collected in 2020 and 2021 and analyzed for the same water quality parameters (Table 7.1).

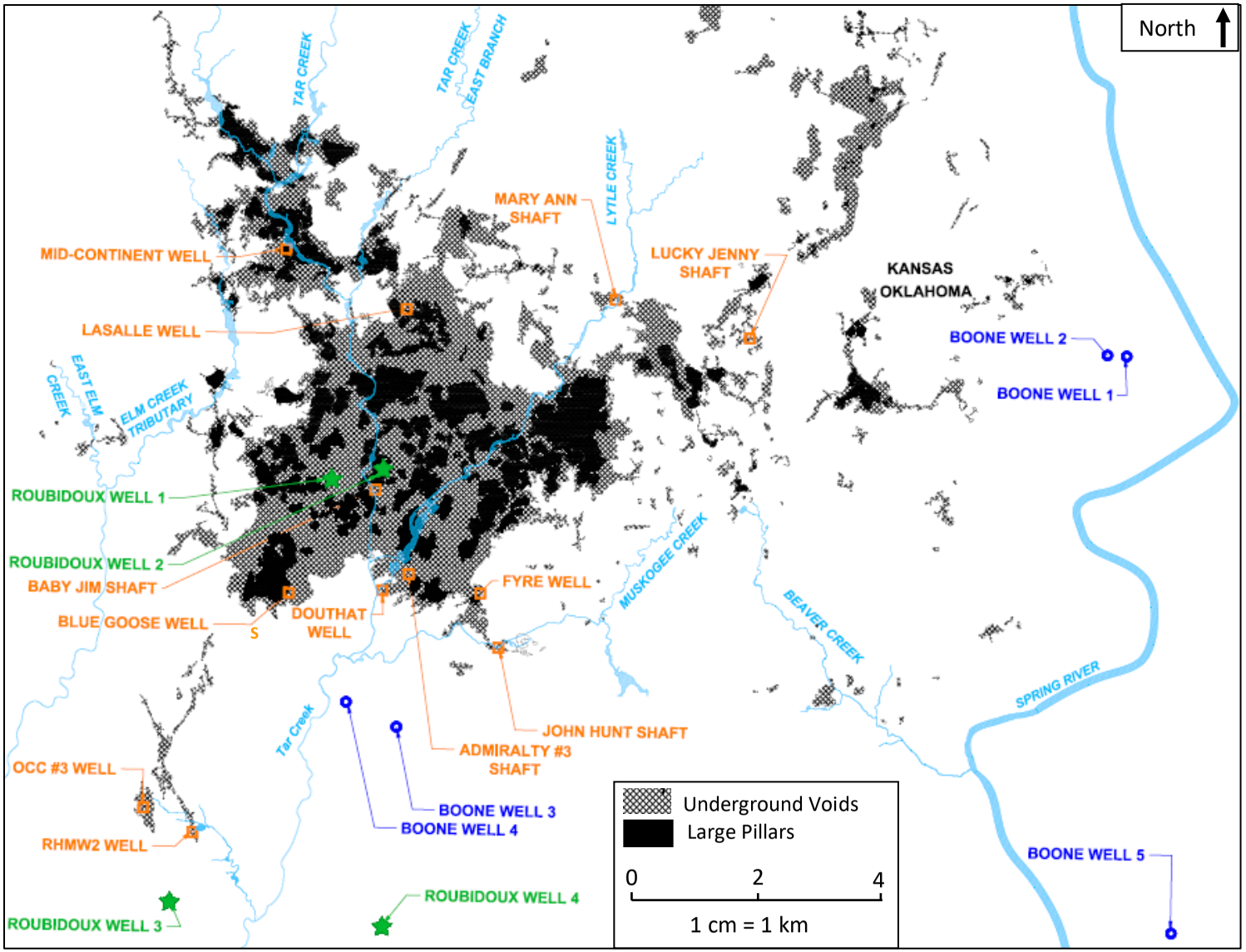

Figure 7.2: Layout of the Picher mining field where the diamond pattern represents underground void spaces and black represents large pillars, with streams overlaid. Color-matched labels for the different types of groundwater sampling locations are shown: Mine pool (orange), Boone samples (blue), and Roubidoux samples (green)

Table 7.1: Sampling parameters and methods used to evaluate the water chemistry of groundwater and mine drainage discharges collected at Douthat, Oklahoma (U.S. EPA 2014; Hach 2015)

	Method/Instrumentation
Water Quality Parameters	
Total Metals	U.S. EPA 3015a and 6010c
Dissolved Metals	U.S. EPA 3015a and 6010c
Sulfate	U.S. EPA 165-D Rev. A
Chloride	U.S. EPA 105
Turbidity	Hach 2100P Turbidimeter
Alkalinity	U.S. EPA 310.1
Datasonde Parameters Temperature Specific Conductance Conductivity Resistivity Dissolved Oxygen (DO) (%) DO Concentration (mg/L) Total Dissolved Solids pH	YSI 6-series multiparameter datasonde following CREW and YSI SOPs
Stable Isotope Ratios ^{2}H ^{18}O	University of Kansas W.M. Keck – NSF Paleoenvironmental and Environmental Stable Isotope Laboratory protocol for the analysis of H and O stable isotopes in water

Water samples that were collected to measure stable isotopes of ^{2}H and ^{18}O were analyzed using a Thermofinnigan High-Temperature Conversion Elemental Analyzer (TC/EA). The stable isotope values were reported as a per mil ratio (‰). The values were calculated as shown in Equation 1, where the δ notation indicates deviation from the Vienna Standard Mean Ocean Water (VSMOW).

$$\delta^2 H = \frac{\left(\frac{^2H}{^1H}\right)_{sample} - \left(\frac{^2H}{^1H}\right)_{VSMOW\ std}}{\left(\frac{^2H}{^1H}\right)_{VSMOW\ std}} \times 1{,}000 \qquad (7.1)$$

Deuterium excess (*d*) expresses the extent that a sample deviates from the GMWL and was calculated for each sample using Equation 2 (Dansgaard 1964).

$$d = \delta^2 H - 8 \times \delta^{18} \qquad (7.2)$$

Rainfall samples for light isotopes were not collected as a part of this study due to the challenges associated with collecting light isotope samples representative of a variety of rainfall events. This study used previously published $\delta^{2}H$ and $\delta^{18}O$ values of rainfall collected in Norman, OK for twelve years from 1996 to 2008 to represent the potential recharge sources associated with rainfall (Jaeschke et al. 2011). The equation for the LMWL published by Jaeschke et al. (2011) is shown in Equation 3.

$$\delta^2 H = 7.32 \times \delta^{18} O + 9.50 \quad (7.3)$$

The rainfall water quality data published by the National Atmospheric Deposition Program (NADP) that were collected in Pittsburg, KS from 1984 to 2020 were used to represent the chemistry of potential recharge sources associated with rainfall (NADP 2022).

7.2.3 Statistical Analyses

7.2.3.1 Stable Isotope Ratios of ^2H and ^{18}O in Potential Recharge Sources

The δ^2H and $\delta^{18}O$ values of samples collected from each of the three potential recharges sources were analyzed to determine if there was a significant difference in isotope ratios between the potential recharge sources. A Welch's ANOVA was used to compare the isotope ratios from each of the three sources because Welch's ANOVA can be used for unequal sample sizes with unequal variances and protects against Type I error. If Welch's ANOVA showed a significant difference among the three potential recharge sources for a particular isotope, then a T-test assuming unequal variance was used to compare the recharge sources in pairs to determine if all sources were different from each other or if two sources were not significantly different ($p>0.05$).

The δ^2H and $\delta^{18}O$ values from rainfall were used to calculate the 0.32 and 0.05 prediction intervals, then these intervals and the LMWL were plotted on a scatterplot. The point data from the Boone, Roubidoux, mine pool, and Douthat MD discharges were then plotted to visually show which data points were within each prediction interval. Box and whisker plots of *d* excess values for the three potential recharge sources were used to summarize and simplify the findings of the δ^2H and $\delta^{18}O$ analyses.

7.2.3.2 Spatial Analysis of the Picher Field Mine Pool

The second hypothesis was evaluated by comparing the water chemistry of the mine pool at the Douthat wells to the combined water chemistry of all mine pool sites located outside of the 1.6 km radius from the Douthat well (Figure 7.2). The Douthat wells used in the spatial analysis include samples collected from a drill hole located approximately 50 m from the most consistent MD discharge at Douthat, and a sample collected 0.5 m from the bottom of the mine void below the discharge itself after a riser was added to the discharge to temporarily stop the flow. Only the data collected from the lowest elevation at each site were used for the spatial analysis because the lowest sampling elevation at multiple sites represented the only sample that was collected within the mine void (Appendix 7A). The selected water chemistry parameters of the Douthat well versus the wells outside of the 1.6 km radius

of the Douthat well were evaluated using a two-sample T-test, assuming unequal variance. The selected parameters included specific conductivity, total hardness, alkalinity, pH, sulfate, dissolved Fe, dissolved Zn, and *d* excess. The selected water chemistry parameters were plotted for each site in the mine pool versus the distance of the site from the Douthat discharges using a scatter plot. The scatterplots were overlaid onto box and whisker plots for each of the three potential recharge sources to show how the chemistry throughout the mine pool related to the water chemistry of the potential recharge sources.

A heat map was created in AutoCAD Civil 3D using the mean values from the selected water quality parameters from each mine pool sampling location to visually represent the spatial variations in the mine pool. A feature line representing the flow path of the mine pool between each sampling location in the primary Picher field mine void was used to create a continuous gradient between sampling locations on the heat map. The feature line was used to accurately represent the preferential flow path of the water through the open mine voids rather than relying on the default option that uses the nearest neighbor method to interpolate between points using linear lines that intersected the outer perimeter of the mine voids. The boundary conditions for the heat map were set 0.5 km outside the outer perimeter of the mine voids and used the mean values of the Boone formation for each parameter.

7.2.3.3 Temporal Analysis of the Picher field Mine Pool

The temporal analysis of the Picher field mine pool compared the water chemistry of the mine pool collected from five separate periods: Period 1) 1976-1977 (Playton et al. 1980), Period 2) 1983-1985 (Parkhurst 1987), Period 3) 2002 (Dehay 2003), Period 4) 2007-2009 (CH2MHill 2010), and Period 5), 2020-2022 (this study). The temporal dataset only included samples that were collected from depths that were within the mine void or the deepest sampling depth from each site. All data from each period for a given parameter were grouped to evaluate how the mine pool chemistry as a whole varied over time. The temporal variations could not be evaluated at individual sites because none of the sites were sampled during all five periods due to remediation efforts sealing open mine features throughout the past 40 years. The spatial distribution of the sampling locations from each period is shown in Figure 7.3. The specific conductivity, pH, alkalinity, sulfate, dissolved Fe, and dissolved Zn from all five periods were compared using Welch's ANOVA. Then Welch's ANOVA was used to compare the same parameters using periods 3-5 to determine if the mine pool has significantly changed over the past two decades. Box and whisker plots were created for each parameter to show the variability of the mine pool chemistry during each period.

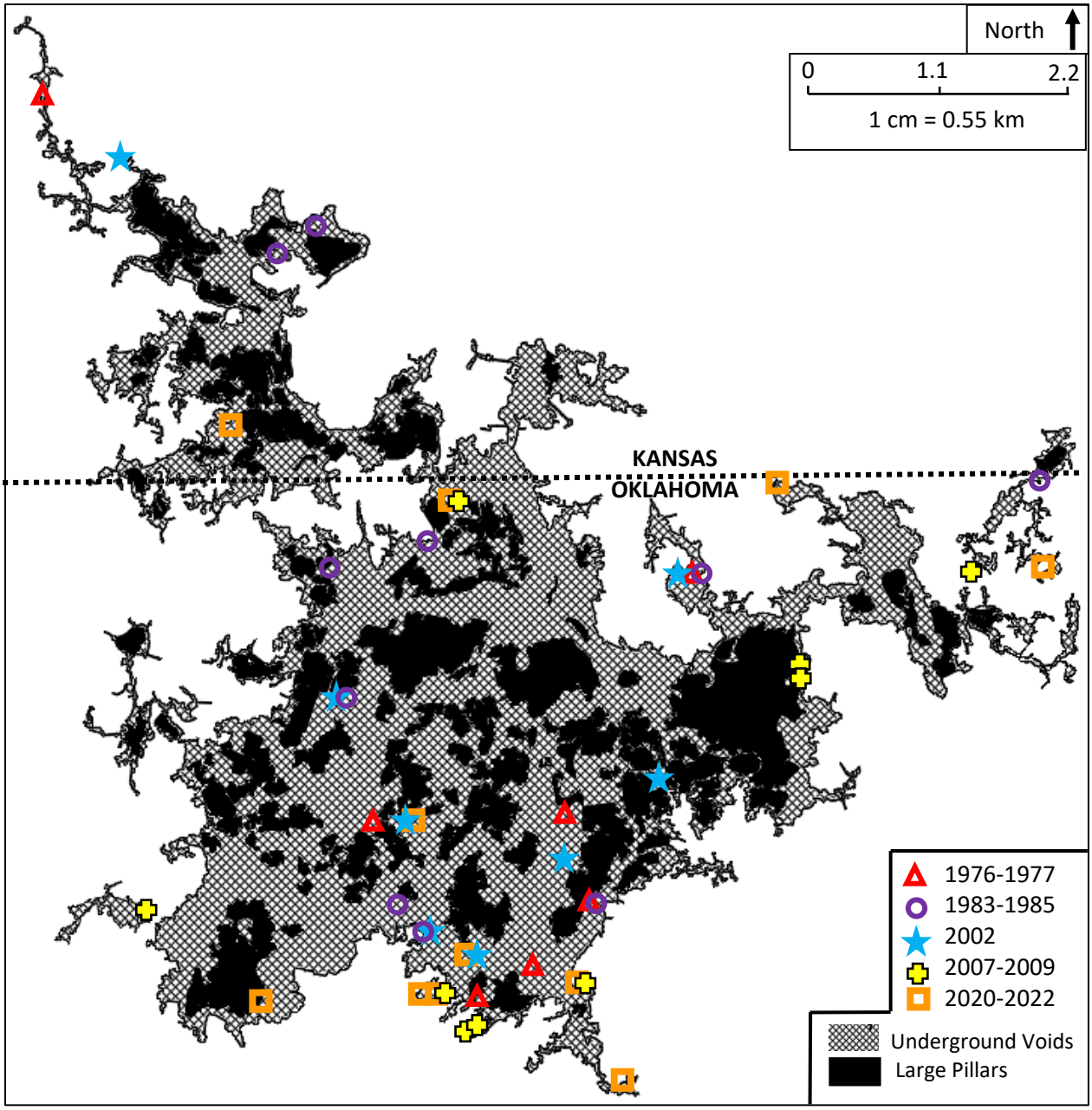

Figure 7.3: Temporal sampling locations within the Picher field mine pool from five time periods. The diamond pattern represents underground void spaces, and the black fill represents large pillars

7.3 Results and Discussion

7.3.1 Stable Isotope Ratios of ^{2}H and ^{18}O in Recharge Sources

The $\delta^{2}H$ and $\delta^{18}O$ values of the rainfall data published by Jaeschke et al. (2011) had a much greater range compared to the Boone and Roubidoux aquifers, resulting in a greater range of *d* excess (Table 7.2 and Figure 7.4). The smaller range of *d* excess values in the Boone and Roubidoux was expected, irrespective of the smaller sample size of the aquifers compared to the rainfall sample size, because groundwater is typically more consistent and representative of the mean isotope ratios of the precipitation that recharged the aquifers (Sharp 2007). Previous studies have shown that the unconfined Boone aquifer is recharged from direct precipitation, resulting in water that was less than 40 years old, with minimum ages near five years (Adamski 2000). The confined Roubidoux formation was shown to be relatively old by comparison (Adamski 2000) and is recharged in geologic outcroppings located in central and south-central Missouri, with minor outcroppings in southeastern Missouri (Adamski 1994). However, a comparison of the $\delta^{2}H$ values in the rainfall and aquifers showed no significant differences ($p > 0.05$), indicating both aquifers were recharged by recent precipitation (Table 7.2). One explanation for the similarities in $\delta^{2}H$ values is the complexity of the hydrogeology in the Roubidoux caused by the varying lithology and multiple faults and nodular chert that can act as localized recharge zones (Adamski 1997). Secondly, the amount of groundwater that has been withdrawn from the Roubidoux since the early 1900s, coupled with hydraulic conductivity values reaching 26 m/day (Adamski 1994), may have resulted in newer water rapidly recharging the Roubidoux formation within the study site.

Although there were no significant differences between $\delta^{2}H$ values in three potential recharge sources, there was a significant difference in $\delta^{18}O$ values ($p < 0.05$; Table 7.2). Comparisons of the paired combinations of potential recharge sources showed the Roubidoux waters were significantly different than rainfall and the Boone ($p < 0.001$), while the Boone and rainfall $\delta^{18}O$ values were not significantly different ($p = 0.36$). The plotted isotope ratios support these findings, where the Boone samples are all inside the 0.32 rainfall prediction interval, while most of the Roubidoux samples plotted lower and to the left of the LMWL because of the depleted $\delta^{18}O$ values (Figure 7.5). The depleted $\delta^{18}O$ values are likely due to interactions with the sandstone found in the Ordovician system of the Roubidoux aquifer. Similar findings from other studies have shown that interactions with carbon dioxide (CO_2) and bicarbonate HCO_3^- found in similar geologic formations can result in depleted $\delta^{18}O$ values (Mickler et al. 2004; Karolytė et al. 2017). However, because the stable isotope ratios of ^{2}H and ^{18}O were not significantly different between all three recharge sources, the second hypothesis that stated the stable

isotopes would identify distinct recharge sources was rejected.

Although the hypothesis was rejected, a few trends were identified from the isotope ratios measured from the potential recharge sources, mine pool, and MD discharges. Samples collected from the Blue Goose well in December 2020 and February 2021 plot to the upper right of the previous Blue Goose sample collected in March 2020 (Figure 7.5). The shift in isotope ratios is indicative of an open surface water source, such as a pond, recharging these workings between March 2020 and December 2021 because as water evaporates from an open water source, the lighter isotopes are preferentially evaporated, leaving behind heavier, enriched isotopes (D'Amore and Panichi 1985, Sharp 2007). It is hypothesized that water used in a wet sieving operation at the nearby Blue Goose well was being pumped from an open surface water pond and the water was then being injected into the Blue Goose underground workings. Furthermore, the Blue Goose sample collected in November 2021 plotted directly above the December 2020 and February 2021 samples, which indicates sulfide exchange may have influenced the isotope ratios of the November sample (Figure 7.5, D'Amore and Panichi 1985). Sulfide exchange can occur when organic matter is broken down under anaerobic conditions by sulfate-reducing bacteria which produce hydrogen sulfide gas. In the case of Blue Goose, algae were present in the mine pool samples collected 90 m below ground in December 2020 and February 2021, which may have entered the mine pool with the water from the open surface water source. A second influence on the December 2020 and February 2021 samples may also be hydrolysis and mineral reactions (Tweed et al. 2005; Sun et al. 2014; Karolytė et al. 2017). The other water chemistry parameters support these claims because the Blue Goose site had the least mean pH and alkalinity values, with elevated specific conductance and dissolved Fe values, indicating MD was being generated at this location (Table 7.3).

Secondly, the Douthat MD discharge samples collected in September 2021 and the mine pool samples collected in November and December 2021 from the sites nearest the Douthat discharges showed increased *d* excess values. These samples plotted directly above previously collected samples, near or outside of the 0.05 rainfall prediction interval (Appendix 7A and Figure 7.5). The enriched deuterium indicates sulfide exchange may be occurring. However, unlike the Blue Goose well, there was no indication that the source of organic material was from an open surface water source. One possibility was the influx of organic material flushed into the mine pool during elevated streamflow events where water enters through open mine shafts (Appendix 5B). Because the elevated streamflow is associated with precipitation events, there would not be the unique open surface evaporation signature that was present in the Blue Goose data.

Table 7.2: Comparison of stable isotope ratios of ^{2}H and ^{18}O in water from three potential sources recharging the Picher field mine pool, rainfall data published by Jaeschke et al. 2011

	$\delta^{2}H$ VSMOW (‰)			$\delta^{18}O$ VSMOW (‰)		
	Boone Aquifer	Roubidoux Aquifer	Rainfall	Boone Aquifer	Roubidoux Aquifer	Rainfall
Sample Size	7	5	264	7	5	264
Mean	-30.89	-35.15	-31.13	-5.79	-6.82	-5.58
Median	-30.70	-33.15	-26.50	-5.64	-6.83	-5.09
Standard Deviation	4.32	4.85	22.02	0.38	0.27	2.93
Welch's ANOVA p-value		0.291			<0.0001	

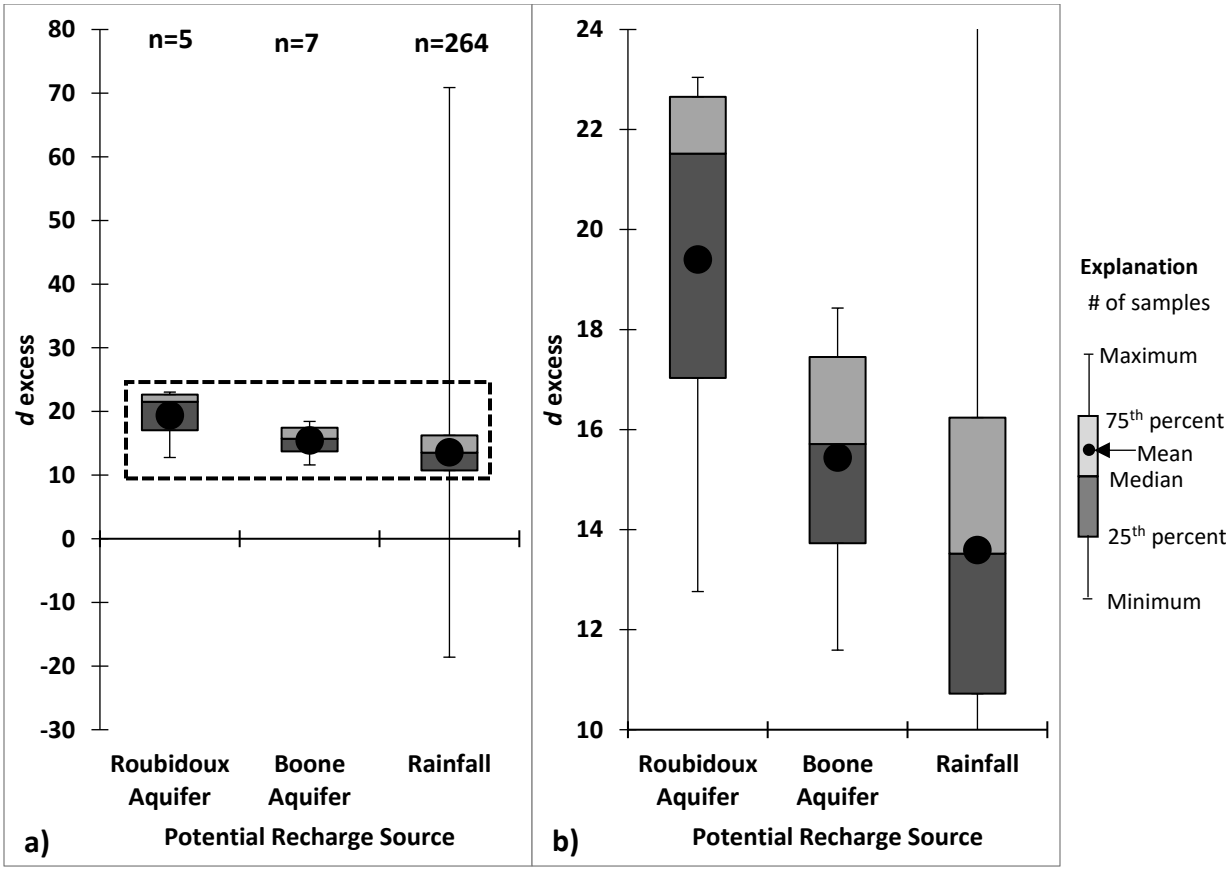

Figure 7.4: a) Box and whisker plot comparing the deuterium excess of three potential recharge sources for the Picher field mine pool: Roubidoux aquifer, Boone aquifer, and rainfall b) shows the smaller y-axis range indicated by the dashed box in figure a. Rainfall data was published by Jaeschke et al. (2011)

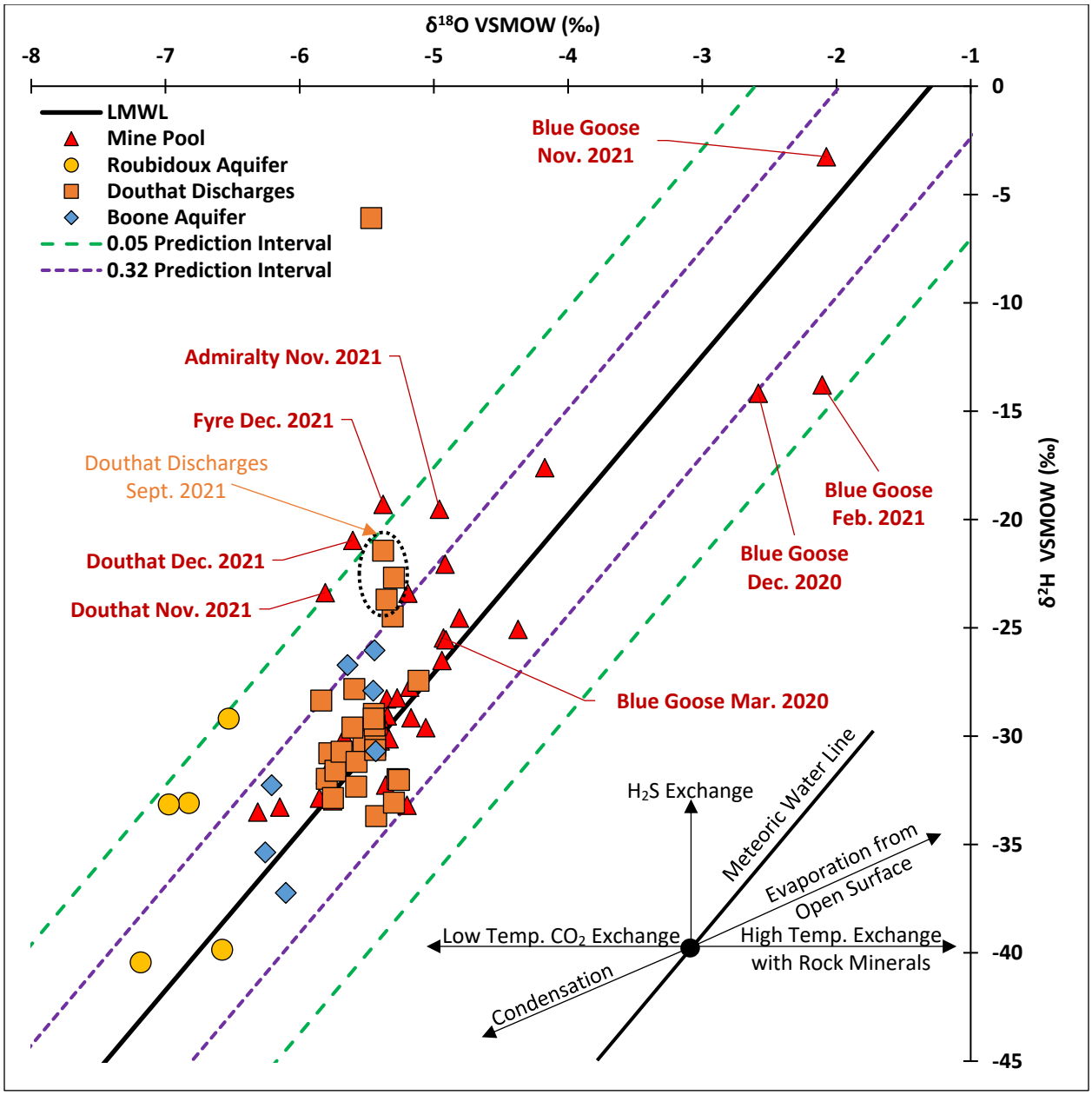

Figure 7.5: Local meteoric water line with 0.05 and 0.32 prediction intervals from isotope ratios of ^{2}H and ^{18}O from rainfall collected in Norman, OK and published by Jaeschke et al. (2011), with plotted data points of $\delta^{2}H$ and $\delta^{18}O$ values from samples collected in 2019-2022 from the Boone and Roubidoux aquifers, the Picher field mine pool, and mine drainage discharges located at Douthat, OK. The isotope explanation for processes that may modify stable isotope content was recreated from D'Amore and Panichi (1985)

Table 7.3: Mean water chemistry of samples collected from the Picher field mine pool from 2020-2022 and the standard deviation. Statistical analyses comparing the Douthat well to sites inside and outside of a 1.6 km radius of the well

Site (Mean Depth [m])	Sample Size	Distance from Douthat	Specific Conductance	pH	Alkalinity	Total Hardness	Sulfate	Dissolved [Zn]	Dissolved [Fe]	*d* excess
	n	km	µS/cm		mg/L CaCO3 eq.	mg/L	mg/L	mg/L	mg/L	
Douthat Wells (59)	5	0.00	3,340±87.0	5.92±0.18	350±6.05	2,225±83.3	2,237±39.7	36.7±1.17	255±21.9	13.9±5.23
Admiralty Shaft (61)	4	0.49	2,281±108	6.23±0.14	133±28.17	1,749±113	1,373±98.2	6.33±1.87	16.2±11.8	13.5±4.87
Blue Goose Well (91)	5	1.39	2,611±77.2	5.36±0.31	61±49.1	1,857±412	1,777±31	0.91±0.63	124±8.96	7.6±5.24
Fyre Well (36)	3	1.47	1,242±392	6.35±0.13	125±29.51	799±281	627±258	2.08±0.1	18.8±8.68	17.1±5.81
Baby Jim Shaft (52)	3	1.55	1,719±131	6.65±0.17	176±17.02	1,207±79.6	841±114	3.39±0.76	5.57±3.25	14.0±3.20
John Hunt Shaft (36)	4	1.92	272±20	6.8±0.24	90±8.81	134±13.9	43±12.1	2.1±0.2	0.04±0.00	15.1±1.24
LaSalle Well (65)	2	4.23	2,328±754	6.41±0.17	161±6.36	1,779±40.6	1,463±50.9	4.98±0.4	41.7±4.47	14.0±0.09
Mid-Continent Well (32)	1	5.30	1,365	6.95	222.5	909.02	607.30	0.01	22.02	9.91
Mary Ann Shaft (45)	4	5.60	596±33.4	6.91±0.12	96±12.58	321±41.8	191±24.9	0.15±0.23	4.24±1.05	15.3±2.43
Lucky Jenny Shaft (55)	3	6.61	1,685±185	6.57±0.33	69±18.59	1,103±156	952±131	6.57±2.65	0.03±0.02	14.6±2.13
Comparison of Douthat Well vs. site inside and outside a 1.6 km radius using t-Test: two-sample assuming unequal variances										
p-value for sites <1.6 km from Douthat			<0.0001	0.29	<0.0001	<0.0001	<0.0001	<0.0001	<0.0001	0.13
p-value for sites >1.6 km from Douthat			<0.0001	<0.0001	<0.0001	<0.0001	<0.0001	<0.0001	<0.0001	0.22

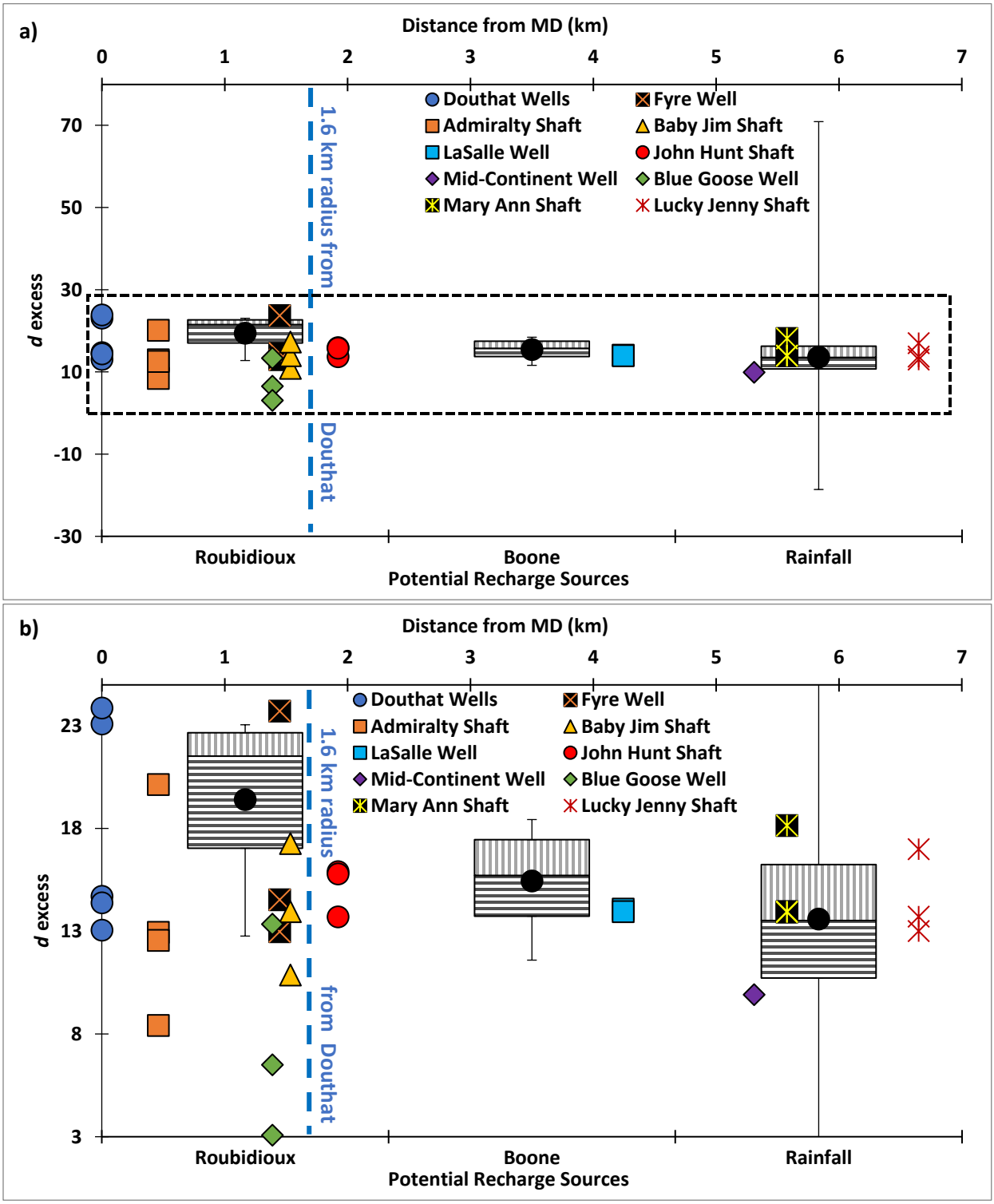

Figure 7.6: a) Scatter plot showing deuterium excess measured the Picher field mine pool versus linear distance (top x-axis) from the Douthat MD discharges from samples collected at 10 locations during three sampling events from 2020-2022 compared to box and whisker plots of potential mine pool recharge sources from samples collected during the same period (bottom x-axis), b) shows the smaller y-axis range indicated by the dashed black box in Figure a. Rainfall data were published by Jaeschke et al. (2011)

7.3.2 Spatial Analyses of the Picher Field Mine Pool

The spatial analyses only evaluated the samples collected from the greatest depth at each site, resulting in a wide range of sampling depths from 32 m to 90 m below the land surface. When comparing sites based on depth, specific conductivity and dissolved Zn show weak trend of increasing values with increased depth, while dissolved Fe and *d* excess show no trends (Figure 7.15). However, the effects of depth on the results of spatial variability were determined to not be a confounding variable because the depth of the Douthat wells of 59 m was within the first standard deviation of the mean depth for sampling locations outside the 1.6 km radius at 48.5±11.5 m and outside the 1.6 km radius at 60.1±20.3 m.

The Picher field mine pool water quality showed substantial spatial variations for nearly all tested parameters (Figures 7.6-7.14 and Table 7.3). The Douthat wells had substantially greater sulfate, alkalinity, Zn and Fe concentrations than the other Picher field mine pool sites (Table 7.3). The spatial water chemistry does show an overall weak trend from the highly contaminated water at the Douthat wells towards water chemistry more representative of the recharge sources with increased distance from the Douthat wells (Figures 7.11-7.14). The statistical analyses of the selected parameters comparing mine pool samples collected outside of the 1.6 km radius of the Douthat wells showed a significant difference in all tested parameters, except for *d* excess which was discussed in Section 7.3.1 (Table 7.3). Thus, the second hypothesis that stated there would be a significant difference in the water quality between the mine pool near the discharges and the mine pool outside a 1.6 km radius was accepted. The analyses only included mine pool samples hydraulically connected to the largest Picher field mine void, excluding OCC3 and RHMW2 wells because they are in distant and isolated mine workings (Figure 7.2).

A second comparison of the mine pool near the Douthat discharges and the wells located within the 1.6 km radius showed they were also significantly different, except for pH and *d* excess (Table 7.3). These findings show that the mine pool near the Douthat wells was significantly different than the rest of the mine pool. The heat maps support the findings, with the Douthat wells often appearing as the hottest (red) area for each parameter (Figures 7.9-7.10).

The specific conductance heat map presents a visual representation of the contamination throughout the mine pool. Specific conductance is a good surrogate parameter since it indicates the number of ions in the water, which in the case of MD indicates greater contamination. The specific conductance was greater in the center of the mine pool compared to the outer edges, with the

exception of the southern edge, inside the 1.6 km radius of the Douthat discharges (Figure 7.7). However, specific conductance was not a good indicator to evaluate potential recharge sources because the mean specific conductance in Boone aquifer and rainwater were less than the majority of the mine pool (Figures 7.7 and 7.11a). It is hypothesized that the elevated specific conductance seen throughout the mine pool compared to the potential recharges sources was due to the recharge water chemically reacting with the exposed geology in the mine pool, creating free ions that increase the specific conductance of the recharge water.

Sodium (Na) and chloride (Cl) are non-reactive in these systems and therefore were shown to be better indicators than specific conductance to determine mine pool recharge sources because both ions are conservative. The Na and Cl data show that rainfall was a substantial contributor to mine pool recharge because the mean concentrations of Cl and total Na in the Boone aquifer were greater than the mean concentrations at all sampling sites, except for the Douthat wells where total Na exceeded the mean concentration of the Boone (Figures 7.9, 7.10, 7.14). The concentrations of Na and Cl in rainfall were substantially lower than the Boone and mine pool samples with both averaging less than 0.15 mg/L. Therefore, rainfall was the only identified recharge source that could generate the low concentrations of Na and Cl in the mine pool. Furthermore, the two mine pool locations with the lowest Cl and Na concentrations, Mary Ann and John Hunt, are both open mine shafts near streams and were identified as potential inflow locations (Appendix 5B).

However, the Na and Cl data suggest rainfall was not the only recharge source. A base flow contribution from the Boone was necessary to explain the Na and Cl concentrations in the mine pool that were much greater than the rainfall concentrations alone. Assuming the two primary recharge sources were rainfall and the Boone, the Cl data showed that both were approximately equal contributors because the mean mine pool Cl concentration was 11.4 mg/L, approximately half of the mean Boone concentration of 23.7 mg/L. The Na data indicated 33% dilution from rainwater based on a mass balance of the mean Na in the mine pool and Boone formation measuring 30.3 mg/L and 45.4 mg/L, respectively. Although preventing recharge from the Boone is not feasible, preventing surface inflows from entering the mine voids is possible by sealing known mine features; the findings of this spatial analysis indicate sealing mine features could substantially decrease the overall mine pool recharge volume.

Although the Roubidoux aquifer had lesser concentrations of Na and Cl compared to the Boone (10.9 mg/L and 7.1 mg/L respectively), it would only have localized effects because it could only impact the mine pool at locations where wells had been drilled through the mine voids and into the Roubidoux

(Williams 1934). These drilled wells were often less than 30 cm diameter, which pales in comparison to a 300 cm diameter mine shaft like the Tulsa Quapaw inflow that receives water from a nearby stream (Appendix 5B), and the potentiometric surface elevation of the Roubidoux has been lower than the Boone or the mine pool.

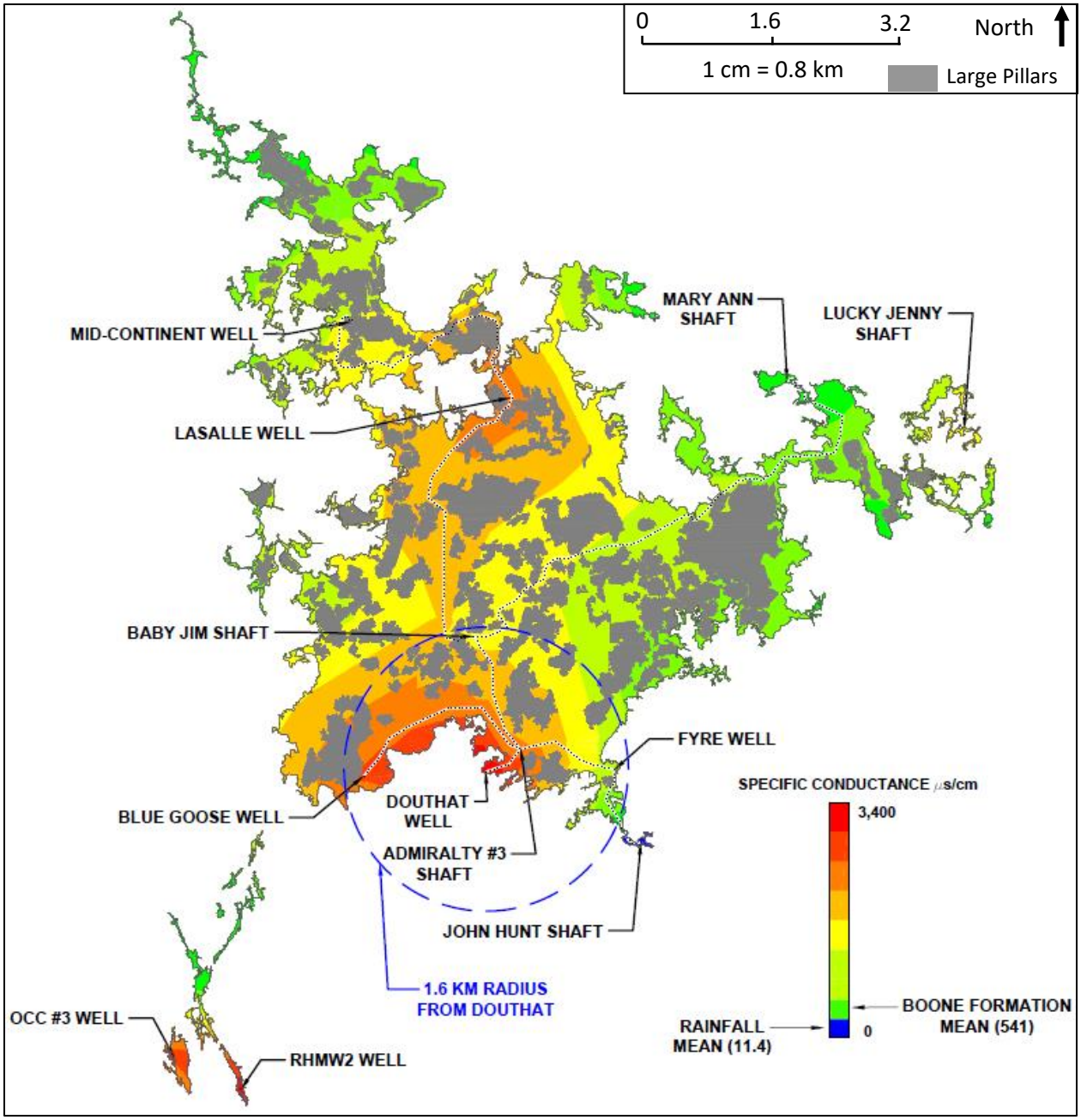

Figure 7.7: Heat map showing mean specific conductance of the mine pool in the Picher field underground mine workings from samples collected at 13 locations during three sampling events from 2020-2022 with boundary conditions set 0.5 km from the workings using the mean value of seven samples collected from the Boone formation during the same period. Rainfall data was published by NADP (2022)

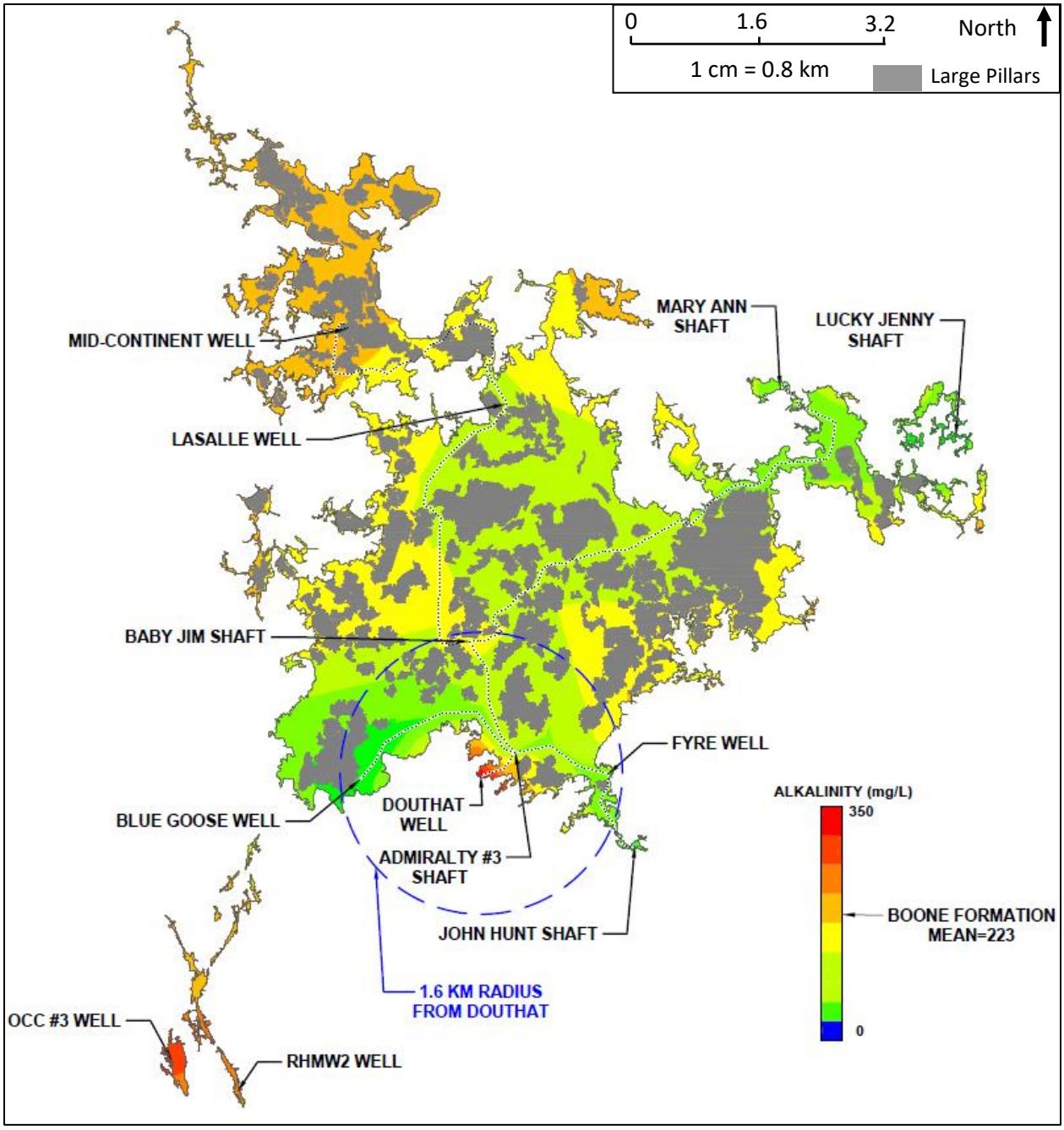

Figure 7.8: Heat map showing mean alkalinity concentrations of the mine pool in the Picher field underground mine workings from samples collected at 13 locations during three sampling events from 2020-2022 with boundary conditions set 0.5 km from the workings using the mean value of seven samples collected from the Boone formation during the same period

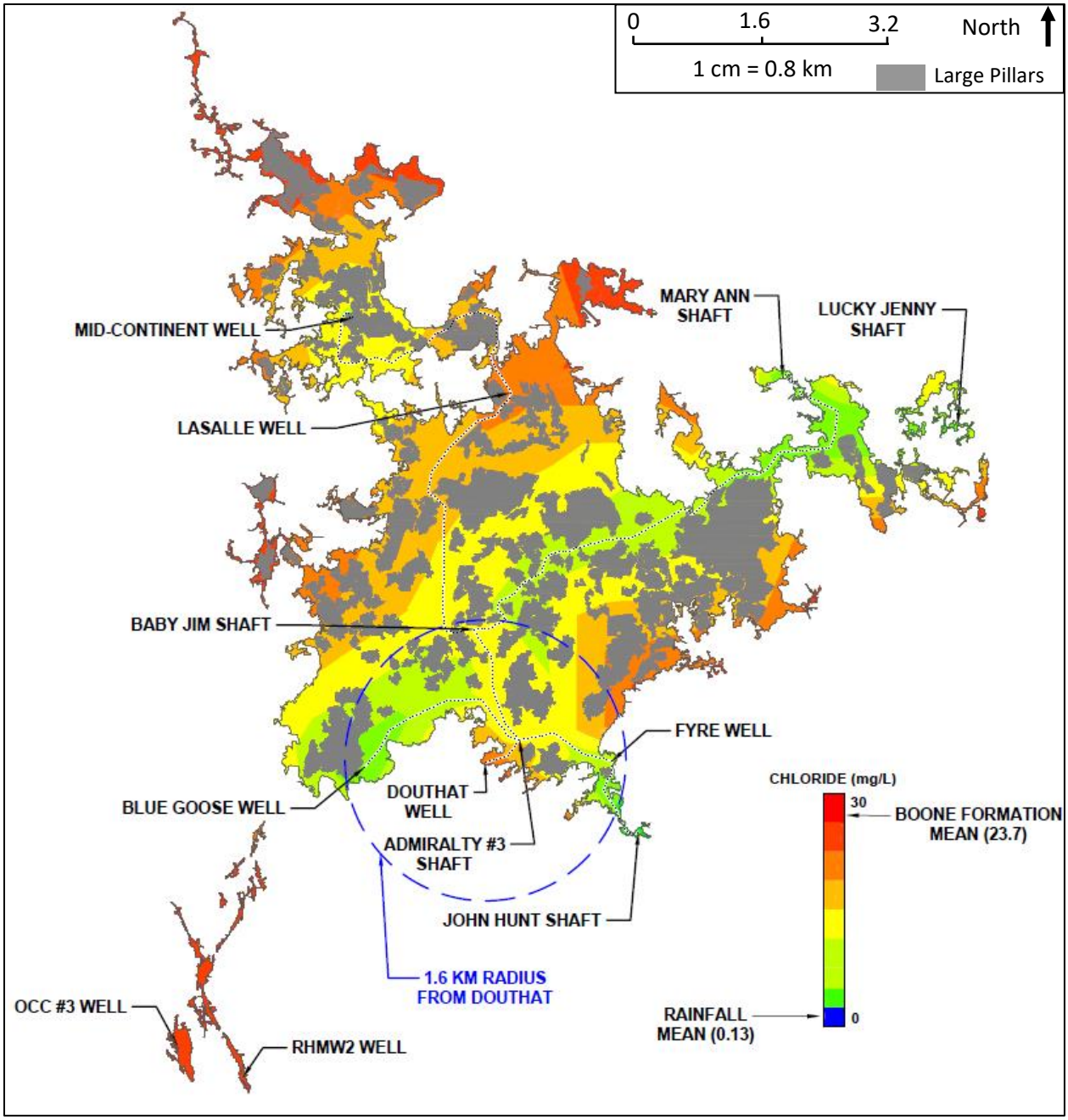

Figure 7.9: Heat map showing chloride concentrations of the mine pool in the Picher field underground mine workings from samples collected at 13 locations during three sampling events from 2021-2022 with boundary conditions set 0.5 km from the workings using the mean value of seven samples collected from the Boone formation during the same period. Rainfall data was published by NADP (2022)

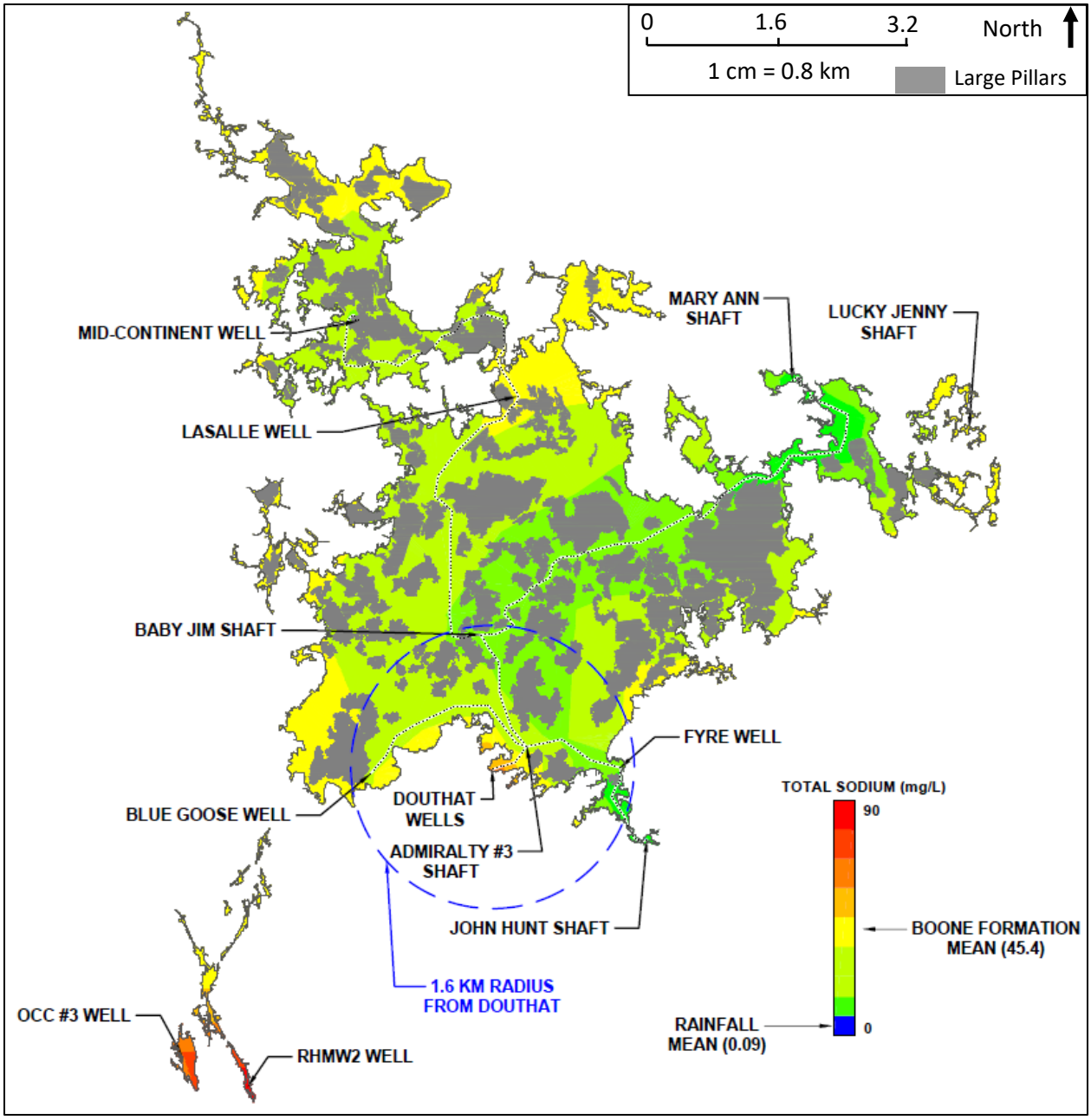

Figure 7.10: Heat map showing total sodium concentrations of the mine pool in the Picher field underground mine workings from samples collected at 13 locations during three sampling events from 2021-2022 with boundary conditions set 0.5 km from the workings using the mean value of seven samples collected from the Boone formation during the same period. Rainfall data was published by NADP (2022)

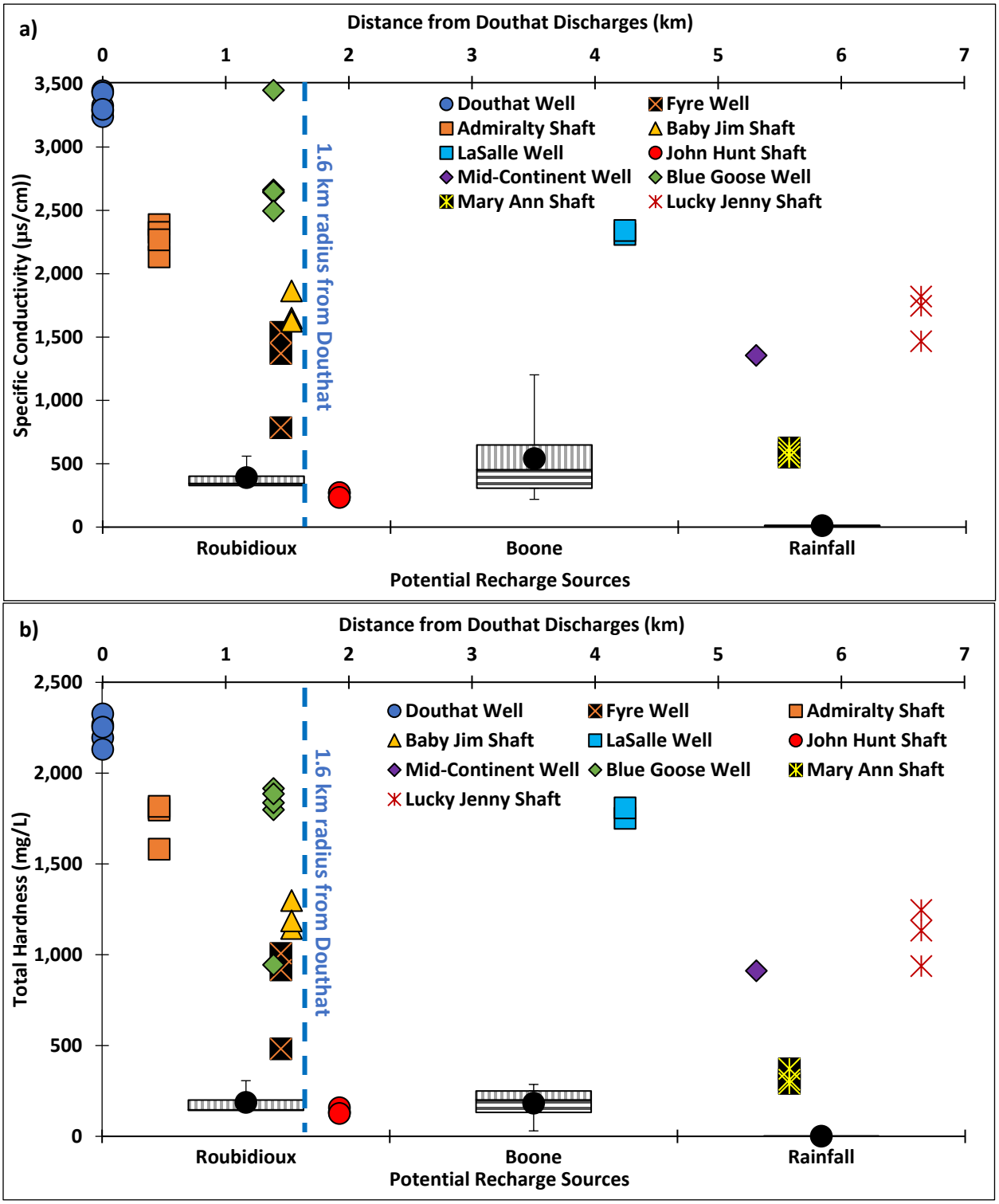

Figure 7.11: Scatter plot showing a) specific conductance and b) total hardness values measured the Picher field mine pool versus linear distance (top x-axis) from the Douthat MD discharges from samples collected at 10 locations during three sampling events from 2020-2022 compared to box and whisker plots of potential mine pool recharge sources from samples collected during the same period (bottom x-axis). Rainfall data was published by NADP (2022)

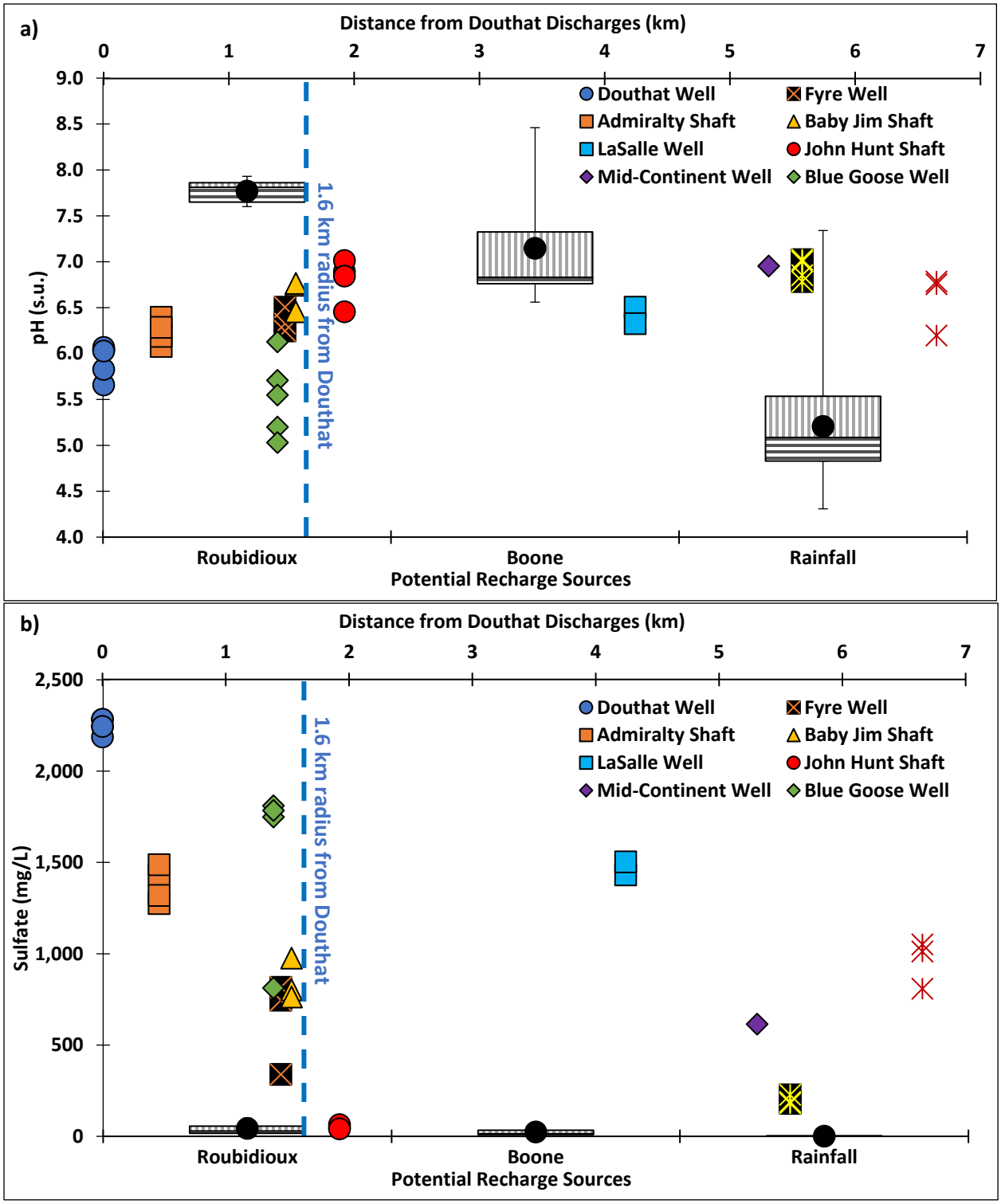

Figure 7.12: Scatter plot showing a) pH and b) sulfate values measured the Picher field mine pool versus linear distance (top x-axis) from the Douthat MD discharges from samples collected at 10 locations during three sampling events from 2020-2022 compared to box and whisker plots of potential mine pool recharge sources from samples collected during the same period (bottom x-axis). Rainfall data was published by NADP (2022)

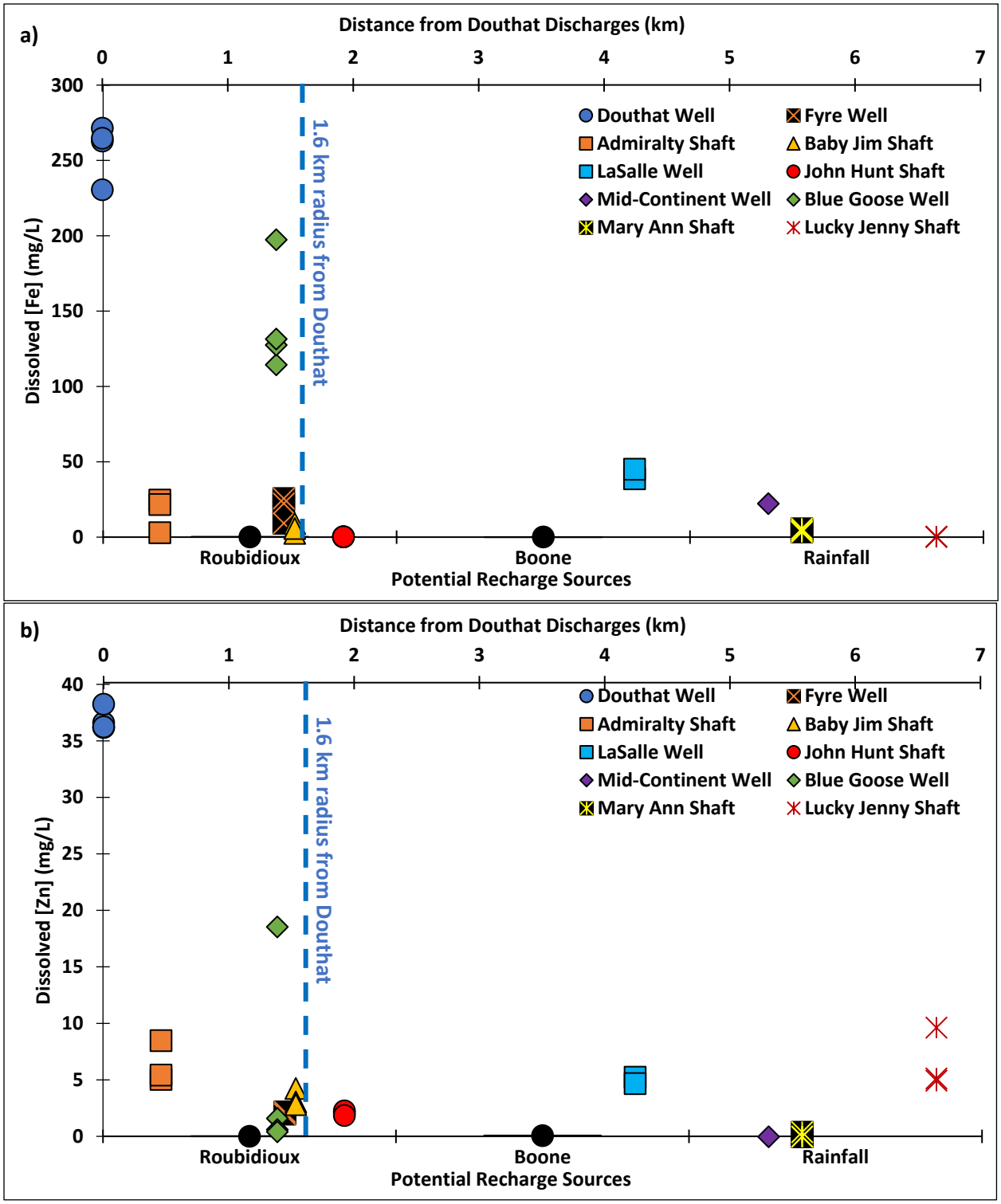

Figure 7.13: Scatter plot showing a) dissolved Fe and b) dissolved Zn values measured the Picher field mine pool versus linear distance (top x-axis) from the Douthat MD discharges from samples collected at 10 locations during three sampling events from 2020-2022 compared to box and whisker plots of potential mine pool recharge sources from samples collected during the same period (bottom x-axis)

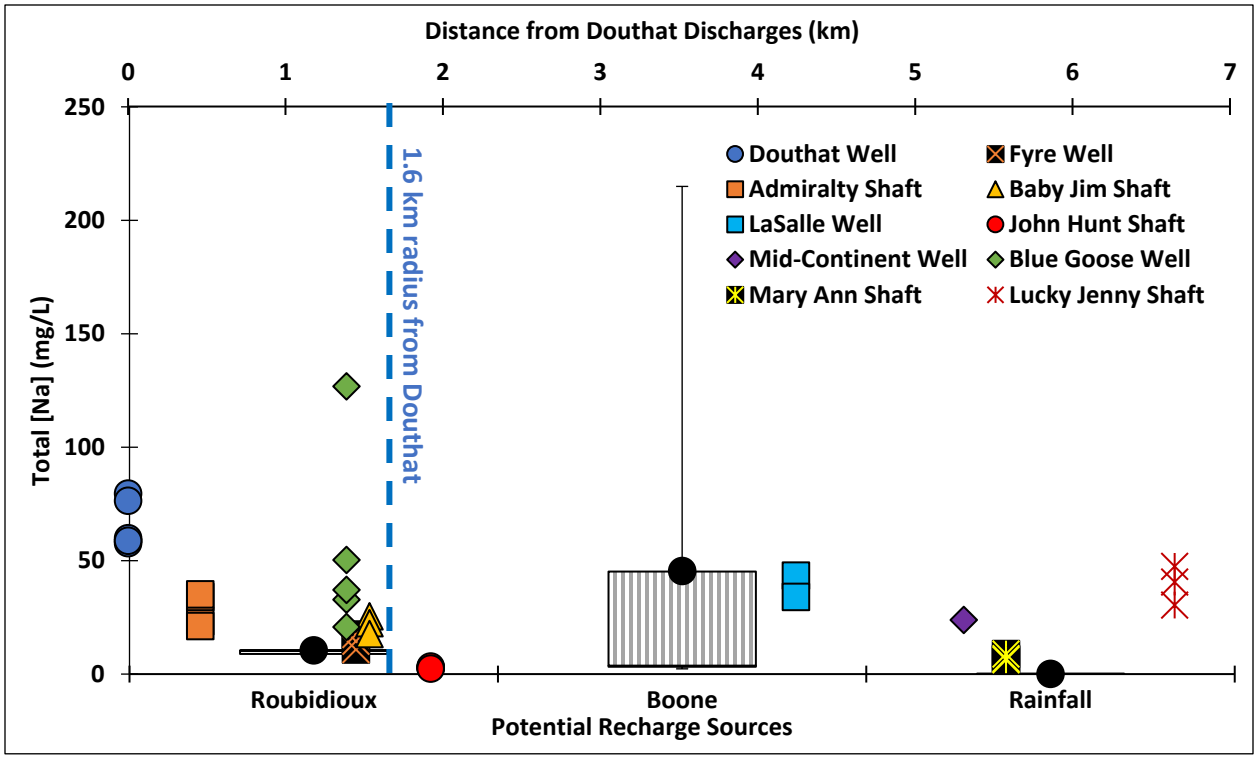

Figure 7.14: Scatter plot showing total Na values measured the Picher field mine pool versus linear distance (top x-axis) from the Douthat MD discharges from samples collected at 10 locations during three sampling events from 2020-2022 compared to box and whisker plots of potential mine pool recharge sources from samples collected during the same period (bottom x-axis). Rainfall data was published by NADP (2022)

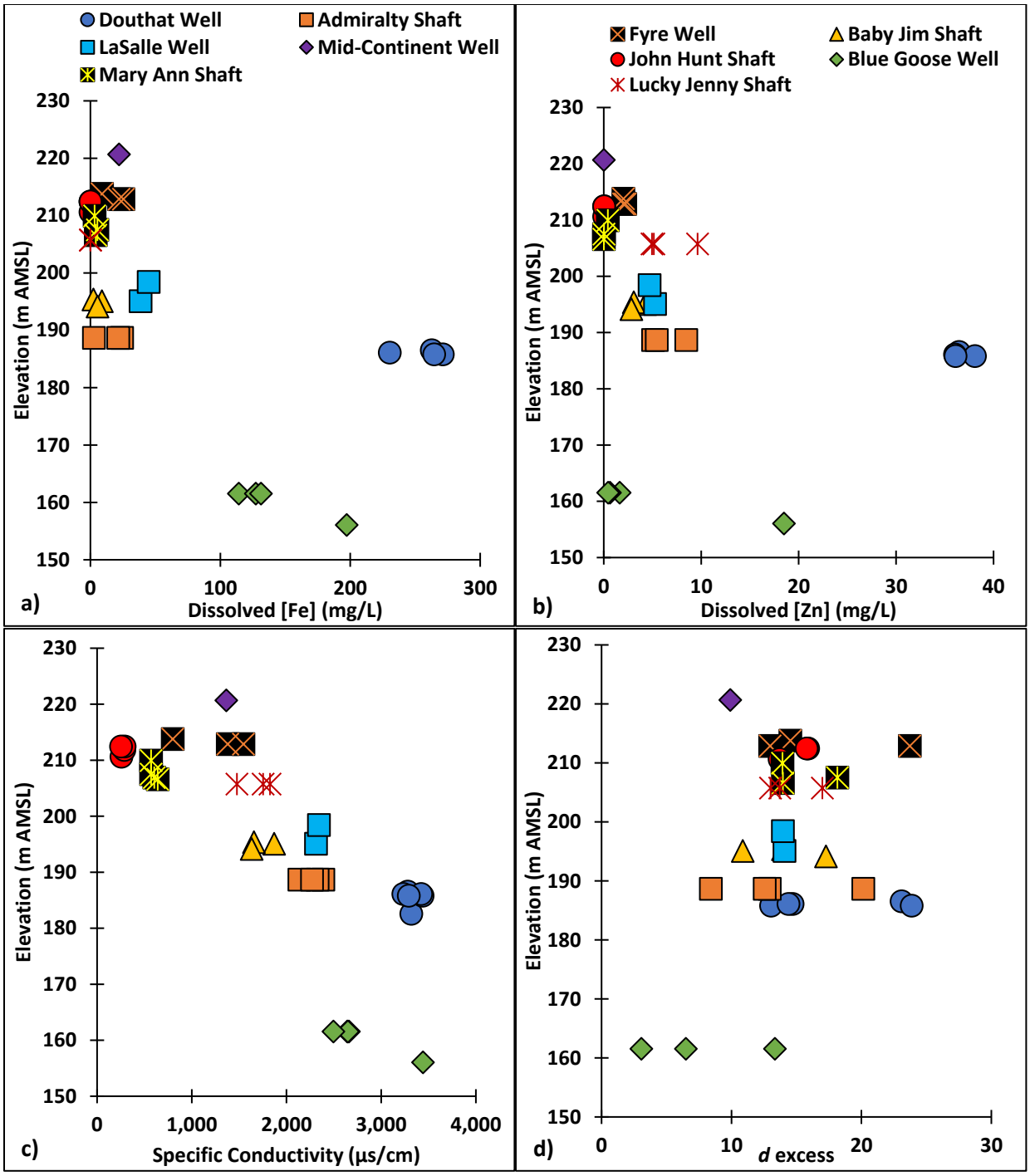

Figure 7.15: Water chemistry in the Picher field mine pool at the lowest sampling elevation at ten sampling locations throughout the mine pool for a) dissolved Fe b) dissolved Zn c) specific conductivity d) *d* excess

7.3.3 Temporal and Depth Analyses of the Picher Field

The temporal analysis of the Picher field mine pool showed that the mine pool has always had a wide range of chemistry because of the spatial variations that can occur as discussed in Section 7.3.2. Overall, the five-time periods fell into two groups, the early mine pool development during Periods 1 and 2, and the later periods since 2002 (Figure 7.16). During Period 1 the mine voids were refilling, and the data show the active formation of MD as the geology on the exposed face of the mine voids reacts with the recharge water, generating low pH measurements, minimal alkalinity, and the greatest dissolved Zn concentrations of the five periods (Figure 7.16). In Period 2, the mine pool remained highly contaminated, shown by the overall elevated specific conductivity. However, there was a substantial decrease in dissolved Zn compared to Period 1 (Figure 7.16). It is hypothesized that the artesian MD discharges which began flowing between Periods 1 and 2 had discharged large quantities of Zn during a first flush event when the discharges began flowing. The ranges in the water chemistry values were substantially smaller beginning in Period 3 compared to Periods 1 and 2. A decrease in the specific conductivity, dissolved Fe, and dissolved Zn during Period 3 indicates that substantial metals loading occurred between Periods 2 and 3 (Figure 7.16). Although it was hypothesized that the decrease in metals concentrations over time was the result of the mine pool being flushed out over time, other factors may have influenced the decrease in metals concentrations, including the stratification of the mine pool. The stratification may result in deeper areas becoming more anoxic over time, hauling pyrite oxidation.

The statistical analyses of all five periods showed that all selected water quality parameters were significantly different ($p < 0.005$; Figure 7.16). Therefore, the third hypothesis that stated selected water quality parameters measured in mine pool that were collected during five separate periods would be significantly different was accepted. However, a comparison of Periods 3-5 showed only the specific conductance and sulfate were significantly different ($p < 0.05$), while there was not a significant difference in the dissolved metals concentrations ($p > 0.05$; Figure 7.16). Dissolved Zn concentrations of the mine pool measured during each period shows exponential decay, with substantial decreases occurring during Periods 1 to 3, but the concentrations have plateaued during Periods 3 to 5 (Figure 7.16). The exponential decay in mine pool contamination and eventual asymptotic level is a common characteristic of mine pool hydrology (Younger et al. 2002). Although the mine pool dissolved metals concentrations in Periods 3 to 5 were not significantly different ($p > 0.05$), there was a substantial difference between the mine pool water chemistry and any of the recharge sources. Since the mine pool metals concentrations appear to be plateauing over the past twenty years, it is hypothesized that the

MD discharges will continue to have elevated metals concentrations for many decades before the metals concentrations in the MD are similar to the recharge sources.

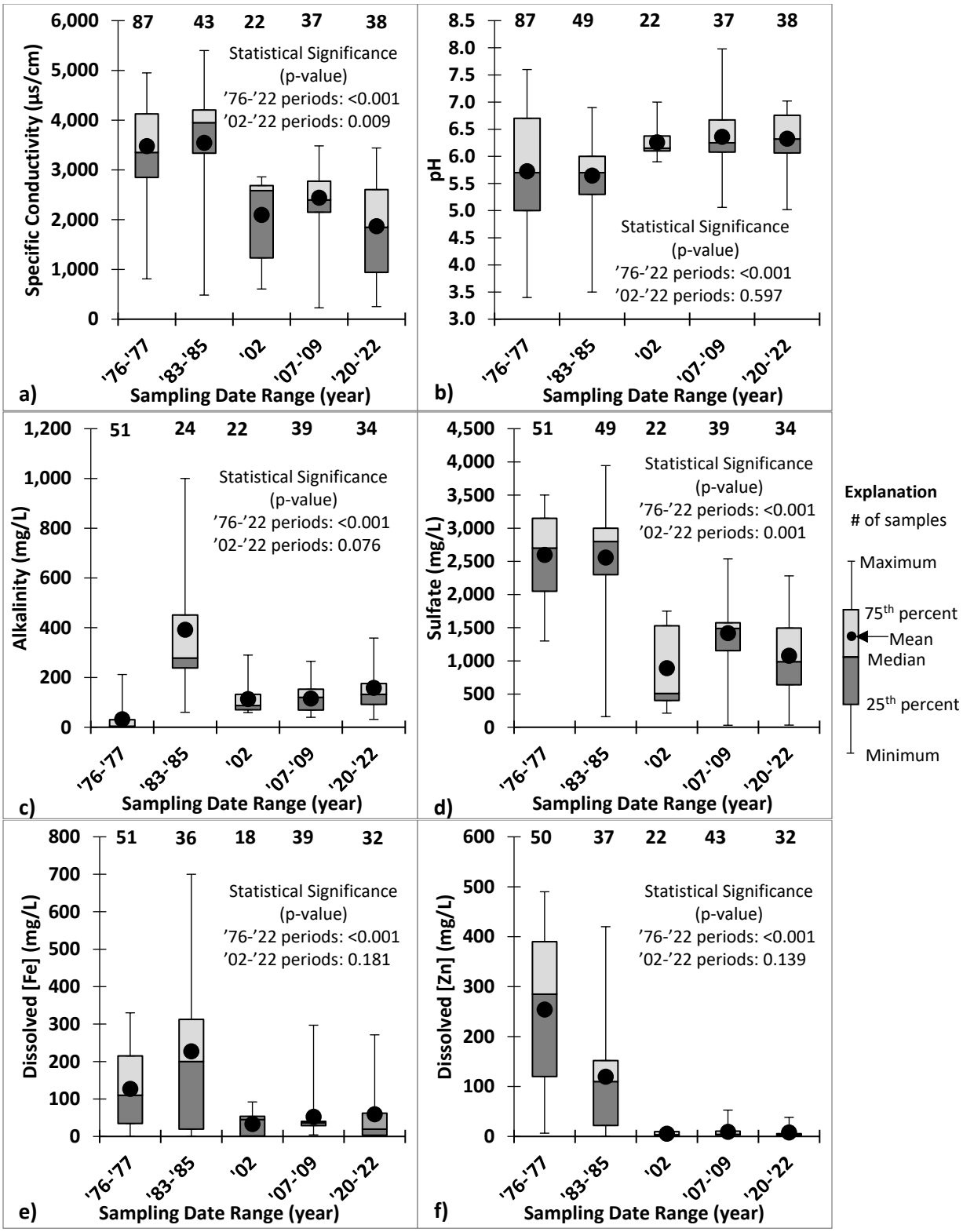

Figure 7.16: Box and whisker plots comparing samples collected from the Picher field mine pool within the mine voids from 1976 to 2022 for a) specific conductivity b) pH c) alkalinity d) sulfate e) dissolved Fe f) dissolved Zn, with statistical significance comparing the five periods and the three most recent periods (2002, 2007-2009, and 2020-2022) using a Welch's ANOVA. 1976-1977 data from Playton et al. (1980), 1983-1985 data from Parkhurst (1987), 2002 data from Dehay (2003), 2007-2009 data from CH2MHill (2010)

7.4 Conclusions

This study evaluated the use of stable light isotopes of ^{2}H and ^{18}O and other water quality parameters to identify potential recharge sources in a low altitude climate where most of the precipitation is rainfall. The first hypothesis that stated $\delta^{2}H$ and $\delta^{18}O$ values would be significantly different in each of the three potential recharge sources was rejected. This study found there was no significant difference in $\delta^{2}H$ values between the three potential recharge sources ($p > 0.05$), but the $\delta^{18}O$ values in the confined Roubidoux aquifer were significantly different than the unconfined Boone aquifer and rainfall. The spatial analysis of the Picher field mine pool showed conservative ions such as Cl and Na can indicate if rainfall is a substantial recharge source for the mine pool. Cl and Na concentrations measured throughout the mine pool were substantially less than the concentrations in the aquifers, and rainfall was the only recharge source that would be capable of diluting these conservative ions.

The second hypothesis that stated the water quality in the mine pool would be significantly different in samples collected at the MD discharge locations compared to samples collected outside of a 1.6 km radius from the discharges was accepted. The mine pool near the Douthat discharges had the greatest Fe and Zn metals concentrations, with weak trends showing a decrease in contamination with increased distance from the discharges. Although there was a significant difference ($p < 0.05$) in the water quality between the mine pool at the discharges and samples collected outside of a 1.6 km radius for all selected parameters except *d* excess, there was also a significant difference in water quality measured in the mine pool at sites within the 1.6 km radius, except for pH and *d* excess.

The temporal analysis of the mine pool showed that the mine pool had a first flush of highly contaminated MD that was discharged in the two decades between Periods 2 and 3, while the water quality of the mine pool in the past two decades from Periods 3 to 5 has plateaued, showing no significant differences in Fe or Zn concentrations ($p > 0.05$). The highly contaminated mine pool that existed as the underground voids were filling and immediately after the MD began to artesian discharge in 1979 resulted in the water chemistry being significantly different when all five periods were analyzed ($p < 0.05$), thus the third hypothesis was accepted. Overall, this study has shown that isotope ratios of ^{2}H and ^{18}O could not be used to identify sources of mine pool recharge in low altitude regions with temperate climates, but other conservative ions that occur in elevated concentrations in the groundwater can be useful to determine if dilution from precipitation is occurring. Lastly, although the Picher field mine pool currently has significantly less Fe and Zn concentrations compared to 40 years ago, the plateauing of the mine pool water chemistry indicates the MD discharges will likely have elevated metals concentrations for many years.

7.5 References

Abu Jabal MS, Abustan I, Rozaimy MR, El Najar H (2018) The deuterium and oxygen-18 isotopic composition of the groundwater in Khan Younis City, southern Gaza Strip (Palestine). Environmental Earth Sciences. 77:155. DOI: https://doi.org/10.1007/s12665-018-7335-4

Adamski JC (1997) Nutrients and Pesticides in Ground Water of Ozark Plateaus in Arkansas, Kansas, Missouri, and Oklahoma. U.S. Geological Survey Water-Resources Investigations Report 96-4313. DOI: https://doi.org/10.3133/wri964313

Adamski JC (2000) Geochemistry of the Springfield Plateau aquifer of the Ozark Plateaus Province in Arkansas, Kansas, Missouri and Oklahoma, USA. Hydrological Processes. 14(5):849-866. DOI: 10.1002/(SICI)1099-1085(20000415)14:5<849:AID-HYP973>3.0.CO;2-7

Adamski JC, Peterson JC, Freiwald DA, Davis JV (1994) Environmental and Hydrologic Setting of the Ozark Plateaus Study Unit, Arkansas, Kansas, Missouri, and Oklahoma. U.S. Geological Survey Water-Resources Investigations Report 94-4022. DOI: https://doi.org/10.3133/wri944022

Bilharz OW (1947) Experiences with acid mine-water drainage in Tri-State field. American Institute of Mining and Metallurgical Engineers. Technical Publication No. 2267.

Branson, CC (1954) Map showing geology of Ottawa County, Oklahoma. Oklahoma Geological Survey, Bulletin 72, Plate 1.

Brockie DC, Hare EH Jr., Dingess PR (1968) The Geology and Ore Deposits of the Tri-State District of Missouri, Kansas, and Oklahoma. American Institute of Minerals and Metallurgical Engineers. Ch 20 pp. 400-430.

CH2MHill (2010) Hydrogeologic Characterization Study Report; Tar Creek Superfund Site, Operable Unit 4. United States Environmental Protection Agency Region 6.

Christenson SC (1995) Contamination of Wells Completed in the Roubidoux Aquifer by Abandoned Zinc and Lead Mines, Ottawa County, Oklahoma. U.S. Geological Survey Water-Resources Investigations Report 95-4150. DOI: https://doi.org/10.3133/ofr90570

Christenson SC, Parkhurst DL, Fairchild RW (1990) Geohydrology and Water Quality of the Roubidoux Aquifer, Northeastern Oklahoma. U.S. Geological Survey Open-File Report 90-570. DOI: https://doi.org/10.3133/ofr90570

Corrales JL, Sánchez-Murillo R, Esquivel-Hernández G, Herrera E, Boll J (2015) Tracking the water fingerprints of Cocos Island: a stable isotope analysis of precipitation, surface water, and groundwater. Revista de Biologia Tropical. 64(1): 105-120. DOI: 10.15517/RBT.V64I1.23420

D'Amore F, and Panichi C (1985) Geochemistry in Geothermal Exploration. International Journal of Energy Research. 9:277-298. DOI: https://doi.org/10.1002/er.4440090307

Dansgaard W (1964) Stable isotopes in precipitation. Tellus. 16:436-468. DOI: https://doi.org/10.1111/j.2153-3490.1964.tb00181.x

DeHay KL (2003) Assessment and Comparison of 1976-77 and 2002 Water Quality in Mineshafts in the Picher Mining District, Northeastern Oklahoma and Southeastern Kansas. U.S. Geological Survey Water-Resources Investigations Report 03-4248.

Fowler GM, Lyden JP (1932) The Ore Deposits of the Tri-State District (Missouri-Kansas-Oklahoma). American Institute of Mining and Metallurgical Engineers. Technical Publication No. 446.

Fowler GM (1942) Ore Deposits in the Tri-State Zinc and Lead District. Princeton University Press. 206-211

Gray HO (1938) Several Picher Area Mines Flooded as rain sends streams on Rampage. Tri-State Zinc & Lead Ore Producers Association. Article Published May 30th, 1938.

Hach (2015) Phenolphthalein and Total Alkalinity Digital Titrator, Hach Method 8203. Hach Company. Edition 8.

Hazen JM, Williams MW, Stover B, Wireman M (2001) Characterisation of Acid Mine Drainage Using a Combination of Hydrometric, Chemical And Isotopic Analyses, Mary Murphy Mine, Colorado. Environmental Geochemistry and Health. 24:1-22. DOI: https://doi.org/10.1023/A:1013956700322

Jaeschke JA, Scholl MA, Cozzarelli IM, Masoner JR, Christenson S, Qi H (2011) Stable-Isotope Ratios of Hydrogen and Oxygen in Precipitation at Norman, Oklahoma, 1996-2008. United States Geological Survey. Scientific Investigations Report 2011-5062.

Karolytė R, Johnson G, Serno S, Gilfillan SM (2017) The influence of water-rock reactions and O isotope exchange with CO_2 on water stable isotope composition of CO_2 springs in SE Australia. Energy Procedia. 114:3832-3839. DOI: 10.1016/j.egypro.2017.03.1515

Knierim KJ, Pollock E, Hays PD (2013) Using Isotopes of Dissolved Inorganic Carbon Species and Water to Separate Sources of Recharge in a Cave Spring, Northwestern Arkansas, USA. Acta Carsologica. 42(2-3):261-276. DOI: 10.3986/ac.v42i2-3.667

Luza KV (1983) A study of stability problems and hazard evaluation of the Oklahoma portion of the Tri-State Mining Area. U.S. Bureau of Mines Mining Research Contract Report J0100133.

McCauley JR, Brady LL, Wilson FW (1983) Study of Stability Problems and Hazard Evaluation of the Kansas Portion of the Tri-State Mining Area. Kansas Geological Survey. Open File Report.

McCuskey EW (1935) Tri-State flood control cuts mine pumping. Engineering and Mining Journal. 136(7):319-322.

McKnight ET, Fischer RP (1970) Geology and Ore Deposits of the Picher Field Oklahoma and Kansas. United States Geological Survey. Professional Paper 588.

Mickler PJ, Banner JL, Stern L, Asmerom Y, Edwards RL, Ito E (2004) Stable isotope variations in modern tropical speleothems: Evaluating equilibrium vs. kinetic isotope effects. Geochimica et Cosmochimica Acta. 68(21):4381-4393. DOI: 10.1016/j.gca.2004.02.012

Migaszewski ZM, Gałuszka A, Dołęgowska S (2018) Stable isotope geochemistry of acid mine drainage from the Wiśniówka area (south-central Poland). Applied Geochemistry. 95:45-56. DOI: https://doi.org/10.1016/j.apgeochem.2018.05.015

National Atmospheric Deposition Program (NRSP-3) (2022) NADP Program Office, Wisconsin State Laboratory of Hygiene, 465 Henry Mall, Madison, WI 53706.

Oklahoma Water Resources Board (OWRB) (1983) Tar Creek Field Investigation. OWRB.

Parkhurst DL (1987) Chemical Analyses of Water Samples from the Picher Mining Area, Northeast Oklahoma and Southeast Kansas. U.S. Geological Survey Open-File Report 87-453.

Playton SJ, Davis RE, McClaflin RG (1980) Chemical Quality of Water in Abandoned Zinc Mines in Northeastern Oklahoma and Southeastern Kansas: Oklahoma Geological Survey. Circular 82.

Reed EW, Schoff SL, Branson CC (1955) Groundwater Resources of Ottawa County, Oklahoma. Oklahoma Geological Survey. Bulletin 72.

Ren K, Pan X, Zeng J, Yuan D (2019) Contaminant sources and processes affecting spring water quality in a typical karst basin (Hongjiadu Basin, SW China): insights provided by hydrochemical and isotopic data. Environmental Science and Pollution Research. 26: 31354-31367. DOI: https://doi.org/10.1007/s11356-019-06272-x

Ren K, Zeng J, Liang J, Yuan D, Jiao Y, Peng C, Pan X (2021) Impacts of acid mine drainage on karst aquifers: Evidence from hydrogeochemistry, stable sulfur and oxygen isotopes. Science of the Total Environment. 761:143223. DOI: https://doi.org/10.1016/j.scitotenv.2020.143223

Russell CA, Stivers JW (2020) Hydrogeologic Units, Contour Maps, and Cross Sections of the Boone and Roubidoux Aquifers, Northeastern Oklahoma. U.S. Geological Survey Water-Resources Investigations Map 3452.

Savin SM, Epstein S (1970) The oxygen isotopic compositions of coarse grained sedimentary rocks and minerals. Geochimica et Cosmochimica Acta. 34(3):323-329. DOI: https://doi.org/10.1016/0016-7037(70)90109-2

Siebenthal CE (1908) Mineral resources of northeastern Oklahoma: U.S. Geological Survey Bulletin 340-C.

Sharp ZD (2007) Principles of Stable Isotope Geochemistry; Chapter 4: The Hydrosphere. Pearson. ISBN: 0130091391.

Shepherd, N. L., Keheley, E., Dutnell, R. C., Folz, C. A., Holzbauer-Schweitzer, B., & Nairn, R. W. (2022). Picher Field Underground Mine Workings of the Abandoned Tri-State Lead-Zinc Mining District in the United States. Journal of Maps.

Siebenthal CE (1925) Contour Map of the Surface of the Beds Underlying the Cherokee Shale in a Portion of the Picher District, Oklahoma. Showing Relations of Ore Bodies to the Surface Contours. United States Department of the Interior, United States Geological Survey.

Snider LC (1912) Preliminary Report on the Lead and Zinc of Oklahoma. Oklahoma Geological Survey. Bulletin No. 9.

Sun J, Tang C, Wu P, Strosnider WHJ (2014) Hydrogen and oxygen isotopic composition of karst waters with and without acid mine drainage: Impacts at a SW China coalfield. Science of the Total Environment. 487:123-129. DOI: http://dx.doi.org/10.1016/j.scitotenv.2014.04.008

Sun J, Kobbayashi T, Strosnider WHJ, Wu P (2017) Stable sulfur and oxygen isotopes as geochemical tracers of sulfate in karst waters. Journal of Hydrology. 551: 245-252. DOI: http://dx.doi.org/10.1016/j.jhydrol.2017.06.006.

Tomiyama S, Igarashi T, Tabelin CB, Tangviroon P, Ii H (2019) Acid mine drainage sources and hydrogeochemistry at the Yatani mine, Yamagata, Japan: A geochemical and isotopic study. Journal of Contaminant Hydrology. 225:103502
DOI: https://doi.org/10.1016/j.jconhyd.2019.103502

Tweed SO, Weaver TR, Cartwright I (2005) Distinguishing groundwater flow paths in different fractured-rock aquifers using groundwater chemistry: Dandenong Ranges, southeast Australia. Hydrogeology Journal. 13:771-786. DOI: 10.1007/s10040-004-0348-y

United States Environmental Protection Agency (2014) Test Methods for Evaluating Solid Waste (SW-846), Update V, Revision 8, *U.S. EPA*.

Walton-Day K, Poeter E (2009) Investigating hydraulic connections and the origin of water in a mine tunnel using stable isotopes and hydrographs. Applied Geochemistry. 24:2266-2282. DOI: 10.1016/j.apgeochem.2009.09.015

Watzlaf GR, Schroeder KT, Kleinmann RLP, Kairies CL, Nairn RW (2004) The Passive Treatment of Coal Mine Drainage. Unites States Department of Energy, National Energy Technology Laboratory.

Williams CF (1934) Bulkheading Abandoned Shafts; A public works project in the Tri-State District. Engineering and Mining Journal. 135(5):204-206.

Wolkersdorfer C, Nordstrom DK, Beckie RD, Cicerone DS, Elliot T, Edraki M, Valente T, França SCA, Kumar P, Lucero RAO, Gil AS (2020) Mine Water and the Environment. 39:204-228.
DOI: https://doi.org/10.1007/s10230-020-00666-x

Younger PL, Banwart SA, and Hedin RS (2002) Mine Water: Hydrology, Pollution, Remediation. Kluwer Academic Publishers.

CHAPTER 8

Conclusions

This dissertation evaluated multiple aspects of mine drainage (MD) including 1) the biological impacts of MD on the receiving stream, and the potential biological recovery following the passive treatment of MD, 2) evaluation of the water quality and quantity of untreated MD discharges from a hydrologically complex mine pool and determination if passive treatment was a viable treatment option, 3) a proposed conceptual treatment system design to remediate the MD, 4) simulation of the effects of implementing passive treatment on the water quality and metals loading of the receiving stream and determination if the stream would meet state-designated beneficial use classifications following the implementation of the proposed treatment system, and 5) investigation of the use of stable isotope ratios of ^{2}H and ^{18}O and other water quality parameters to identify mine pool recharge sources.

Chapter Two investigated the effects of implementing passive treatment to remediate MD on the fish community in the receiving stream. The study site was located in a sub-watershed of Tar Creek. The study findings showed that following the implementation of two passive treatment systems (PTSs) that significantly decrease concentrations of cadmium (Cd), iron (Fe), lead (Pb), and zinc (Zn) ($p < 0.05$) enter the receiving stream results in a significant increase in the species richness and diversity of the fish communities ($p < 0.05$). One site showed an increase in the mean species richness from 1.83 before the implementation of PTS to 6.83 after the implementation of PTS. Notably, no stream or habitat remediation efforts were conducted during the 16-year study, indicating the changes in the fish community were from water quality changes, not habitat restoration. The study concluded that fish will rapidly recolonize a stream that was historically heavily contaminated by MD following the implementation of passive treatment.

The remaining studies in this dissertation occurred in the Tar Creek watershed and surrounding watersheds impacted by abandoned lead-zinc mining operations in the Picher mining field. Chapter Three utilized rapid bioassessment protocols (RBPs) to evaluate the status of the fish and benthic macroinvertebrate communities in a stream impacted by untreated MD and other sources of metals contamination associated with the abandoned mining operations. The data showed that the two sites located within the mining-impacted area had the lowest community metric scores. The fish communities at these two sites had metric scores that were approximately half that of the regional reference conditions for the fish communities and a quarter of the reference conditions for the benthic macroinvertebrate communities. However, the biological communities in the stream improved with

increased distance from the mining-impacted region. The most downstream site was located 11 km from the mining-impacted region and the fish and benthic macroinvertebrate communities at this site showed substantial increases in biological metric scores that were not significantly different than the regional reference conditions ($p > 0.05$). The study concluded that although the upstream sites currently show impairments due to the mining contamination, the downstream fish community can become a source pool for recolonizing the upper reaches if the MD was remediated.

Chapters Four through Seven focused on different aspects of characterizing the mine pool and MD discharges and proposing a conceptual treatment system design in a hydrologically and topographically challenging watershed. The water quality of the MD discharges was shown to be treatable via passive treatment because two existing passive treatment systems located in the same watershed had been successfully treating MD for multiple years that contained greater concentrations of Cd, Fe, Pb, and Zn (Chapter Five). However, the water quantity of the MD had substantial variations with calculated flows that correlated with rapid fluctuations in the mine pool elevation. The flow rate at the median mine pool elevation was estimated to be 4, 000 lpm and increased to a calculated flow rate of over 140,000 lpm for the maximum mine pool elevation. An analysis of 68 elevated mine pool events shows that the rapid spikes in the mine pool were strongly correlated with elevated streamflow during rainfall events ($r = 0.96$). The cause of the fluctuating mine pool elevations was determined to be open mine features near stream channels that would allow water to enter the mine pool during elevated streamflow events (Chapter Five). An in-depth analysis of historical mine maps for the study site showed extensive underground workings that contained a continuous open void up to 11 km long and five kilometers wide, with multiple mine shafts near streams reportedly open (Chapter Four). Further field investigations identified at least three known inflow locations and many other potential inflow locations (Appendix 5B).

An evaluation of the water chemistry of potential mine pool recharge sources in a low altitude, temperate climate showed conservative ions with elevated concentrations in the groundwater system can be used to determine if precipitation driven inflows account for a substantial portion of mine pool recharge. Sodium (Na) and chloride (Cl) data generated from the underground mine pool throughout the abandoned mining area were substantially less than the concentrations in the aquifers. Rainfall was the only recharge source capable of diluting these conservative ions. Dilution from rainfall accounted for approximately 30% to 50% of the mine pool recharge based on a mass balance of the mean Na and Cl concentrations of the mine pool and unconfined groundwater formation (Chapter Seven). Therefore, managing these known inflow locations has the potential to substantially decrease the volume of MD

discharged, and may decrease the frequency and intensity of elevated discharge events.

The findings of Chapters Four and Five were used to propose two conceptual PTS designs to remediate MD in a hydraulically and topographically challenging watershed (Chapter Six). Both conceptual designs used a phased approach, where Phase 1 was designed to accurately measure flow rates during peak discharge events and evaluate the effectiveness of closing known inflow locations. Additionally, Phase 1 would provide partial treatment of MD in the interim, severing as an initial oxidation pond and storage basin. Phase 2 was the construction of a PTS to remediate the MD. PTS-1 was the smaller of the two design options, at an estimated cost of $16.1 million, which included both phases and two five-year assessment periods. An 11-year simulation showed PTS-1 was capable of treating 66% of the total MD volume. PTS-2 was a much larger system with an estimated cost of $32.3 million that was capable of treating 90% of the MD volume during the 11-year simulation. Notedly, the simulation was conducted using current flow rate calculations where the percentage of MD not treated occurred during the short duration, elevated discharge events (Chapter Six).

The simulated analyses of the downstream metals concentrations compared three scenarios (1) untreated MD, 2) implementation of conceptual PTS-1 and 3) implementation of conceptual PTS-2) showed that if all other sources of metals contamination in the watershed were remediated, the untreated MD would result in the downstream metals concentrations not meeting the state of Oklahoma beneficial use criteria for fish and wildlife propagation 82% of the time for acute Zn and 90% of the time for chronic Cd. The simulated implementation of PTS-1, the smaller system, significantly decreased the percentage of time the beneficial use criteria was not met to less than 5% for both acute Zn and chronic Cd ($p < 0.05$). PTS-2 showed an even greater decrease in the percentage of time the beneficial use criteria were not met to less than 0.005% for both acute Zn and chronic Cd (Chapter Six).

In conclusion, this dissertation has shown that fish communities will rapidly recolonize a stream following the implementation of PTS (Chapter Two). The biological communities in the upper portions of the Tar Creek watershed remain impaired due to the impacts of the abandoned mining operations but downstream biota represent a ready source for recolonization (Chapter Three). The characterization of the water quality and quantity of the MD discharges is treatable via PTS, and simulations have shown PTS will significantly decrease downstream metals concentrations (Chapters Five and Six). The analyses of the underground workings and the mine pool have shown that surface inflows are a substantial recharge source that results in short-term elevated discharge events (Chapters Four, Five, and Seven). Therefore, closing known inflow locations may result in a substantial decrease in the elevated discharge events and total MD discharge volume and contaminant mass loading (Chapters Four, Five, and Seven).

APPENDIX 3A
Species and Counts from Fish Collections Conducted on Tar Creek

Table 3A.1: Fish collected at Tar Creek Site 1 in 2018, 2020, and 2021, Ottawa County, OK

	Site		TC1	
	Date	7/6/2018	7/14/2020	8/3/2021
	Unit of Effort (min)	230	165	147
Scientific Name	**Common Name**			
Ameiurus melas	Black Bullhead Catfish			
Aplodinotus grunniens	Freshwater Drum			
Campostoma anomalum	Central Stoneroller	103	2	2
Cyprinus Carpio	Common Carp			
Cyprinella lutrensis	Red Shiner			
Dorosoma cepedianum	Gizzard Shad			
Etheostoma gracile	Slough Darter			
Etheostoma spectabile	Orange Throat Darter			
Etheostoma stigmaeum	Speckled Darter			
Etheostoma whipplei	Redfin Darter			
Fundulus notatus	Blackstripe Topminnow	29	12	60
Gambusia affinis	Mosquito Fish	129	27	69
Ictalurus punctatus	Channel Catfish		1	
Labidesthes sicculus	Brook Silverside			
Lepomis cyanellus	Green Sunfish	9	4	4
Lepomis gulosus	Warmouth sunfish			1
Lepomis humilis	Orangespotted Sunfish			
Lepomis Hybrid	Hybrid Sunfish			
Lepomis macrochirus	Bluegill Sunfish	13	12	8
Lepomis megalotis	Longear Sunfish	46	18	3
Lepomis microlophus	Redear Sunfish			1
YOY Lepomis	Young of Year Sunfish		21	
Lepisosteus platostomus	Shortnose Gar			
Luxilus cardinalis	Cardinal Shiner			
Lythrurus unbratilis	Redfin shiner			
Micropterus punctulatus	Spotted Bass			
Micropterus salmoides	Large Mouth Bass	11	2	13
YOY Micropterus salmoides	Large Mouth Bass (Juvenile)	8		
Moxostoma erythrurum	Golden Redhorse			
Minytrema melanops	Spotted Sucker			
Notropis boops	Bigeye Shiner			
Notemigonus crysocephalus	Golden Shiner			
Notropis percobromus	Carmine Shiner			
Percina caprodes	Logperch			1
Phenacobius mirabilis	Sucker Mouth Minnow			
Pimephales notatus	Bluntnose Minnow			
Pomoxis annularis	White Crappie			
Pomoxis nigromaculatus	Black Crappie			

Table 3A.2: Fish collected at Tar Creek Site 2 in 2018, 2020, and 2021, Ottawa County, OK

	Site		TC2	
	Date	7/7/2018	7/12/2020	8/3/2021
	Unit of Effort (min)	200	163	108
Scientific Name	**Common Name**			
Ameiurus melas	Black Bullhead Catfish		1	3
Aplodinotus grunniens	Freshwater Drum			
Campostoma anomalum	Central Stoneroller	36	16	31
Cyprinus Carpio	Common Carp			
Cyprinella lutrensis	Red Shiner			
Dorosoma cepedianum	Gizzard Shad			
Etheostoma gracile	Slough Darter		1	
Etheostoma spectabile	Orange Throat Darter			
Etheostoma stigmaeum	Speckled Darter			
Etheostoma whipplei	Redfin Darter			1
Fundulus notatus	Blackstripe Topminnow	12		5
Gambusia affinis	Mosquito Fish	130	36	88
Ictalurus punctatus	Channel Catfish			
Labidesthes sicculus	Brook Silverside			
Lepomis cyanellus	Green Sunfish	53	24	58
Lepomis gulosus	Warmouth sunfish	5	9	4
Lepomis humilis	Orangespotted Sunfish			
Lepomis Hybrid	Hybrid Sunfish	2	2	
Lepomis macrochirus	Bluegill Sunfish	20	60	9
Lepomis megalotis	Longear Sunfish	2	40	12
Lepomis microlophus	Redear Sunfish		2	
YOY Lepomis	Young of Year Sunfish			12
Lepisosteus platostomus	Shortnose Gar		1	
Luxilus cardinalis	Cardinal Shiner			
Lythrurus unbratilis	Redfin shiner			
Micropterus punctulatus	Spotted Bass			
Micropterus salmoides	Large Mouth Bass	3		
YOY Micropterus salmoides	Large Mouth Bass (Juvenile)			
Moxostoma erythrurum	Golden Redhorse			
Minytrema melanops	Spotted Sucker			
Notropis boops	Bigeye Shiner			
Notemigonus crysocephalus	Golden Shiner			3
Notropis percobromus	Carmine Shiner			
Percina caprodes	Logperch			1
Phenacobius mirabilis	Sucker Mouth Minnow			
Pimephales notatus	Bluntnose Minnow			
Pomoxis annularis	White Crappie		2	
Pomoxis nigromaculatus	Black Crappie			

Table 3A.3: Fish collected at Tar Creek Site 3 in 2018, 2020, and 2021, Ottawa County, OK

	Site	TC3		
	Date	7/7/2018	8/21/2020	8/5/2021
	Unit of Effort (min)	120	135	116
Scientific Name	**Common Name**			
Ameiurus melas	Black Bullhead Catfish			
Aplodinotus grunniens	Freshwater Drum			
Campostoma anomalum	Central Stoneroller	146	20	19
Cyprinus Carpio	Common Carp			
Cyprinella lutrensis	Red Shiner	9		6
Dorosoma cepedianum	Gizzard Shad			
Etheostoma gracile	Slough Darter	5		
Etheostoma spectabile	Orange Throat Darter			
Etheostoma stigmaeum	Speckled Darter			
Etheostoma whipplei	Redfin Darter			1
Fundulus notatus	Blackstripe Topminnow	29	30	7
Gambusia affinis	Mosquito Fish	104	144	31
Ictalurus punctatus	Channel Catfish			
Labidesthes sicculus	Brook Silverside			
Lepomis cyanellus	Green Sunfish	30	17	63
Lepomis gulosus	Warmouth sunfish		1	
Lepomis humilis	Orangespotted Sunfish			1
Lepomis Hybrid	Hybrid Sunfish			
Lepomis macrochirus	Bluegill Sunfish	7	43	7
Lepomis megalotis	Longear Sunfish	6	125	38
Lepomis microlophus	Redear Sunfish			
YOY Lepomis	Young of Year Sunfish			9
Lepisosteus platostomus	Shortnose Gar			
Luxilus cardinalis	Cardinal Shiner		1	
Lythrurus unbratilis	Redfin shiner	1		
Micropterus punctulatus	Spotted Bass			
Micropterus salmoides	Large Mouth Bass	8	7	10
YOY Micropterus salmoides	Large Mouth Bass (Juvenile)			
Moxostoma erythrurum	Golden Redhorse			
Minytrema melanops	Spotted Sucker			
Notropis boops	Bigeye Shiner			
Notemigonus crysocephalus	Golden Shiner			
Notropis percobromus	Carmine Shiner			
Percina caprodes	Logperch			4
Phenacobius mirabilis	Sucker Mouth Minnow			
Pimephales notatus	Bluntnose Minnow			
Pomoxis annularis	White Crappie			
Pomoxis nigromaculatus	Black Crappie			

Table 3A.4: Fish collected at Tar Creek Site 4 in 2018, 2020, and 2021, Ottawa County, OK

	Site	TC4		
	Date	8/8/2018	8/20/2020	7/15/2021
	Unit of Effort (min)	190	180	195
Scientific Name	**Common Name**			
Ameiurus melas	Black Bullhead Catfish			
Aplodinotus grunniens	Freshwater Drum			1
Campostoma anomalum	Central Stoneroller	9	14	10
Cyprinus Carpio	Common Carp			
Cyprinella lutrensis	Red Shiner			5
Dorosoma cepedianum	Gizzard Shad	7	3	
Etheostoma gracile	Slough Darter			5
Etheostoma spectabile	Orange Throat Darter		2	
Etheostoma stigmaeum	Speckled Darter		1	
Etheostoma whipplei	Redfin Darter			3
Fundulus notatus	Blackstripe Topminnow	127	72	64
Gambusia affinis	Mosquito Fish	587	196	163
Ictalurus punctatus	Channel Catfish			2
Labidesthes sicculus	Brook Silverside		11	1
Lepomis cyanellus	Green Sunfish	3		1
Lepomis gulosus	Warmouth sunfish	2	7	
Lepomis humilis	Orangespotted Sunfish	1	1	
Lepomis Hybrid	Hybrid Sunfish			
Lepomis macrochirus	Bluegill Sunfish	154	150	20
Lepomis megalotis	Longear Sunfish	40	115	121
Lepomis microlophus	Redear Sunfish	4	30	2
YOY Lepomis	Young of Year Sunfish	136		
Lepisosteus platostomus	Shortnose Gar			
Luxilus cardinalis	Cardinal Shiner	1		1
Lythrurus unbratilis	Redfin shiner	16	13	
Micropterus punctulatus	Spotted Bass			
Micropterus salmoides	Large Mouth Bass	14	46	48
YOY Micropterus salmoides	Large Mouth Bass (Juvenile)			35
Moxostoma erythrurum	Golden Redhorse			
Minytrema melanops	Spotted Sucker		2	
Notropis boops	Bigeye Shiner			
Notemigonus crysocephalus	Golden Shiner	13		4
Notropis percobromus	Carmine Shiner	2	1	20
Percina caprodes	Logperch	1	2	5
Phenacobius mirabilis	Sucker Mouth Minnow			
Pimephales notatus	Bluntnose Minnow		7	
Pomoxis annularis	White Crappie			2
Pomoxis nigromaculatus	Black Crappie		2	

Table 3A.5: Fish collected at Tar Creek Site 5 in 2018, 2020, and 2021, Ottawa County, OK

	Site	TC5		
	Date	7/9/2018	8/20/2020	8/4/2021
	Unit of Effort (min)	270	219	258
Scientific Name	**Common Name**			
Ameiurus melas	Black Bullhead Catfish			
Aplodinotus grunniens	Freshwater Drum		1	
Campostoma anomalum	Central Stoneroller	38	13	19
Cyprinus Carpio	Common Carp			
Cyprinella lutrensis	Red Shiner			
Dorosoma cepedianum	Gizzard Shad		2	
Etheostoma gracile	Slough Darter			2
Etheostoma spectabile	Orange Throat Darter	2	5	10
Etheostoma stigmaeum	Speckled Darter		1	
Etheostoma whipplei	Redfin Darter		5	5
Fundulus notatus	Blackstripe Topminnow	27	34	20
Gambusia affinis	Mosquito Fish	230	27	40
Ictalurus punctatus	Channel Catfish			
Labidesthes sicculus	Brook Silverside	11	18	29
Lepomis cyanellus	Green Sunfish	16	3	3
Lepomis gulosus	Warmouth sunfish	1	2	1
Lepomis humilis	Orangespotted Sunfish			
Lepomis Hybrid	Hybrid Sunfish	1		1
Lepomis macrochirus	Bluegill Sunfish	24	74	60
Lepomis megalotis	Longear Sunfish	35	243	59
Lepomis microlophus	Redear Sunfish			18
YOY Lepomis	Young of Year Sunfish			6
Lepisosteus platostomus	Shortnose Gar			
Luxilus cardinalis	Cardinal Shiner			
Lythrurus unbratilis	Redfin shiner			
Micropterus punctulatus	Spotted Bass			2
Micropterus salmoides	Large Mouth Bass	17	8	9
YOY Micropterus salmoides	Large Mouth Bass (Juvenile)			
Moxostoma erythrurum	Golden Redhorse			
Minytrema melanops	Spotted Sucker			
Notropis boops	Bigeye Shiner			
Notemigonus crysocephalus	Golden Shiner			
Notropis percobromus	Carmine Shiner			
Percina caprodes	Logperch			
Phenacobius mirabilis	Sucker Mouth Minnow			
Pimephales notatus	Bluntnose Minnow			
Pomoxis annularis	White Crappie			7
Pomoxis nigromaculatus	Black Crappie		2	2

Table 3A.6: Fish collected at Tar Creek Site 6 in 2018, 2020, and 2021, Ottawa County, OK

	Site		TC6	
	Date	7/11/2018	8/20/2020	8/4/2021
	Unit of Effort (min)	160	195	165
Scientific Name	**Common Name**			
Ameiurus melas	Black Bullhead Catfish			
Aplodinotus grunniens	Freshwater Drum			
Campostoma anomalum	Central Stoneroller	345	13	75
Cyprinus Carpio	Common Carp	1		4
Cyprinella lutrensis	Red Shiner	8		2
Dorosoma cepedianum	Gizzard Shad		3	
Etheostoma gracile	Slough Darter			
Etheostoma spectabile	Orange Throat Darter	3	4	7
Etheostoma stigmaeum	Speckled Darter	1	1	
Etheostoma whipplei	Redfin Darter			
Fundulus notatus	Blackstripe Topminnow	164	49	41
Gambusia affinis	Mosquito Fish	322	37	129
Ictalurus punctatus	Channel Catfish			1
Labidesthes sicculus	Brook Silverside		22	61
Lepomis cyanellus	Green Sunfish	12	4	2
Lepomis gulosus	Warmouth sunfish		4	
Lepomis humilis	Orangespotted Sunfish			
Lepomis Hybrid	Hybrid Sunfish			
Lepomis macrochirus	Bluegill Sunfish	92	56	43
Lepomis megalotis	Longear Sunfish	203	16	73
Lepomis microlophus	Redear Sunfish	4	5	15
YOY Lepomis	Young of Year Sunfish	24		29
Lepisosteus platostomus	Shortnose Gar			
Luxilus cardinalis	Cardinal Shiner		1	
Lythrurus unbratilis	Redfin shiner		6	
Micropterus punctulatus	Spotted Bass	18	2	1
Micropterus salmoides	Large Mouth Bass		3	19
YOY Micropterus salmoides	Large Mouth Bass (Juvenile)	48		
Moxostoma erythrurum	Golden Redhorse			1
Minytrema melanops	Spotted Sucker		1	1
Notropis boops	Bigeye Shiner			
Notemigonus crysocephalus	Golden Shiner			
Notropis percobromus	Carmine Shiner		2	
Percina caprodes	Logperch			4
Phenacobius mirabilis	Sucker Mouth Minnow	1		1
Pimephales notatus	Bluntnose Minnow		7	
Pomoxis annularis	White Crappie		1	11
Pomoxis nigromaculatus	Black Crappie			

APPENDIX 3B
Taxa and Counts from Benthic Macroinvertebrate Collections Conducted on Tar Creek

Table 3B.1: Results of benthic macroinvertebrate samples collected at Tar Creek Site 1 in 2018, 2020, and 2021, Ottawa County, OK

Phylum	Class	Order	Family	Genus	EPT Taxa	HBI Score	TC-1 2018	TC-1 2020	TC-1 2021
PLATYHELMINTHES	Turbellaria	Tricladida	Planariidae	*Dugesia*		4	1		
NEMERTEA	Enopla	Hoplonemertea	Tetrastemmatidae	*Prostoma*		5		1	
MOLLUSCA	Gastropoda	Basommatophora				8	6		
ARTHROPODA	Crustacea	Amphipoda	Talitridae	*Hyalella*		8			
ARTHROPODA	Insecta	Coleoptera	Elmidae	*Stenelmis*		4			
ARTHROPODA	Insecta	Coleoptera	Hydrophilidae	*Berosus*		5	3	36	6
ARTHROPODA	Insecta	Coleoptera	Hydrophilidae	*Enochrus*		5	1		
ARTHROPODA	Insecta	Coleoptera	Hydrophilidae	*Tropisternus*		5			
ARTHROPODA	Insecta	Diptera	Ceratopogonidae	*Bezzia*		6			
ARTHROPODA	Insecta	Diptera	Chironomidae	*Orthocladiinae*		6		9	14
ARTHROPODA	Insecta	Diptera	Chironomidae	*Tanypodinae*		6	97	55	79
ARTHROPODA	Insecta	Diptera	Empididae	*Hemerodromia*		6			
ARTHROPODA	Insecta	Diptera	simuliidae	*Simulium*		6		1	
ARTHROPODA	Insecta	Diptera	Tipulidae	*Tipula*		3	2		
ARTHROPODA	Insecta	Ephemeroptera	Caenidae	*Caenis*	1	7			
ARTHROPODA	Insecta	Hemiptera	Saldidae			0			
ARTHROPODA	Insecta	Megaloptera	Corydalidae	*Corydalus*		0			
ARTHROPODA	Insecta	Megaloptera	Corydalidae	*Negronia*		0			
ARTHROPODA	Insecta	Megaloptera	Sialidae	*Sialis*		4			
ARTHROPODA	Insecta	Odonata	Coenagrionidae	*Argia*		9	12		
ARTHROPODA	Insecta	Odonata	Coenagrionidae	*Enallagma*		9		4	3
ARTHROPODA	Insecta	Odonata	Gomphidae	*Dromogomphus*		1			
ARTHROPODA	Insecta	Odonata	Gomphidae	*Erpetogomphus*		1			
ARTHROPODA	Insecta	Trichoptera	Hydropsychidae	*Cheumatopsyche*		4		7	7
ARTHROPODA	Insecta	Trichoptera	Hydropsychidae	*Hydropsyche*	1	4			
ARTHROPODA	Insecta	Trichoptera	Hydroptilidae	*Hydroptila*	1	4			
ARTHROPODA	Insecta	Trichoptera	Leptoceridae	*Nectopsyche*	1	4		2	
ARTHROPODA	Insecta	Trichoptera	Limnephilidae	*Pycnopsyche*	1	4			
ARTHROPODA	Insecta	Trichoptera	Philopotamidae	*Chimarra*	1	3			
ARTHROPODA	Insecta	Trichoptera	Polycentropodidae	*Cyrnellus*	1	6			
ARTHROPODA	Insecta	Trichoptera	Polycentropodidae	*Polycentropus*	1	6			
ANNELIDA	Oligochaeta	Haplotaxida	Glossoscolecidae	*Sparganophilus*		10			
ANNELIDA	Oligochaeta	Haplotaxida	Tubificidae	*Limnodrilus*		10			

Table 3B.2: Results of benthic macroinvertebrate samples collected at Tar Creek Site 2 in 2018, 2020, and 2021, Ottawa County, OK

Phylum	Class	Order	Family	Genus	EPT Taxa	HBI Score	TC-2 2018	TC-2 2020	TC-2 2021
PLATYHELMINTHES	Turbellaria	Tricladida	Planariidae	*Dugesia*		4	1		
NEMERTEA	Enopla	Hoplonemertea	Tetrastemmatidae	*Prostoma*		5		1	
MOLLUSCA	Gastropoda	Basommatophora				8		1	
ARTHROPODA	Crustacea	Amphipoda	Talitridae	*Hyalella*		8			
ARTHROPODA	Insecta	Coleoptera	Elmidae	*Stenelmis*		4			
ARTHROPODA	Insecta	Coleoptera	Hydrophilidae	*Berosus*		5	16	11	
ARTHROPODA	Insecta	Coleoptera	Hydrophilidae	*Enochrus*		5	5		
ARTHROPODA	Insecta	Coleoptera	Hydrophilidae	*Tropisternus*		5			
ARTHROPODA	Insecta	Diptera	Ceratopogonidae	*Bezzia*		6			
ARTHROPODA	Insecta	Diptera	Chironomidae	*Orthocladiinae*		6		16	1
ARTHROPODA	Insecta	Diptera	Chironomidae	*Tanypodinae*		6	35	82	77
ARTHROPODA	Insecta	Diptera	Empididae	*Hemerodromia*		6			
ARTHROPODA	Insecta	Diptera	simuliidae	*Simulium*		6	1		
ARTHROPODA	Insecta	Diptera	Tipulidae	*Tipula*		3	6	1	
ARTHROPODA	Insecta	Ephemeroptera	Caenidae	*Caenis*	1	7			
ARTHROPODA	Insecta	Hemiptera	Saldidae			0			
ARTHROPODA	Insecta	Megaloptera	Corydalidae	*Corydalus*		0	1	1	
ARTHROPODA	Insecta	Megaloptera	Corydalidae	*Negronia*		0			
ARTHROPODA	Insecta	Megaloptera	Sialidae	*Sialis*		4			
ARTHROPODA	Insecta	Odonata	Coenagrionidae	*Argia*		9			
ARTHROPODA	Insecta	Odonata	Coenagrionidae	*Enallagma*		9		1	
ARTHROPODA	Insecta	Odonata	Gomphidae	*Dromogomphus*		1	2		
ARTHROPODA	Insecta	Odonata	Gomphidae	*Erpetogomphus*		1			1
ARTHROPODA	Insecta	Trichoptera	Hydropsychidae	*Cheumatopsyche*		4		9	32
ARTHROPODA	Insecta	Trichoptera	Hydropsychidae	*Hydropsyche*	1	4			
ARTHROPODA	Insecta	Trichoptera	Hydroptilidae	*Hydroptila*	1	4			
ARTHROPODA	Insecta	Trichoptera	Leptoceridae	*Nectopsyche*	1	4			
ARTHROPODA	Insecta	Trichoptera	Limnephilidae	*Pycnopsyche*	1	4			
ARTHROPODA	Insecta	Trichoptera	Philopotamidae	*Chimarra*	1	3			
ARTHROPODA	Insecta	Trichoptera	Polycentropodidae	*Cyrnellus*	1	6			
ARTHROPODA	Insecta	Trichoptera	Polycentropodidae	*Polycentropus*	1	6			
ANNELIDA	Oligochaeta	Haplotaxida	Glossoscolecidae	*Sparganophilus*		10			
ANNELIDA	Oligochaeta	Haplotaxida	Tubificidae	*Limnodrilus*		10	15		

Table 3B.3: Results of benthic macroinvertebrate samples collected at Tar Creek Site 3 in 2018, 2020, and 2021, Ottawa County, OK

Phylum	Class	Order	Family	Genus	EPT Taxa	HBI Score	TC-3 2018	TC-3 2020	TC-3 2021
PLATYHELMINTHES	Turbellaria	Tricladida	Planariidae	*Dugesia*		4		1	
NEMERTEA	Enopla	Hoplonemertea	Tetrastemmatidae	*Prostoma*		5			
MOLLUSCA	Gastropoda	Basommatophora				8	1		
ARTHROPODA	Crustacea	Amphipoda	Talitridae	*Hyalella*		8			
ARTHROPODA	Insecta	Coleoptera	Elmidae	*Stenelmis*		4			
ARTHROPODA	Insecta	Coleoptera	Hydrophilidae	*Berosus*		5	1	6	1
ARTHROPODA	Insecta	Coleoptera	Hydrophilidae	*Enochrus*		5			
ARTHROPODA	Insecta	Coleoptera	Hydrophilidae	*Tropisternus*		5			
ARTHROPODA	Insecta	Diptera	Ceratopogonidae	*Bezzia*		6			3
ARTHROPODA	Insecta	Diptera	Chironomidae	*Orthocladiinae*		6		12	4
ARTHROPODA	Insecta	Diptera	Chironomidae	*Tanypodinae*		6	56	46	58
ARTHROPODA	Insecta	Diptera	Empididae	*Hemerodromia*		6		2	2
ARTHROPODA	Insecta	Diptera	simuliidae	*Simulium*		6			
ARTHROPODA	Insecta	Diptera	Tipulidae	*Tipula*		3	2	3	1
ARTHROPODA	Insecta	Ephemeroptera	Caenidae	*Caenis*	1	7			
ARTHROPODA	Insecta	Hemiptera	Saldidae			0			
ARTHROPODA	Insecta	Megaloptera	Corydalidae	*Corydalus*		0		8	3
ARTHROPODA	Insecta	Megaloptera	Corydalidae	*Negronia*		0	2		
ARTHROPODA	Insecta	Megaloptera	Sialidae	*Sialis*		4		2	
ARTHROPODA	Insecta	Odonata	Coenagrionidae	*Argia*		9			
ARTHROPODA	Insecta	Odonata	Coenagrionidae	*Enallagma*		9		1	
ARTHROPODA	Insecta	Odonata	Gomphidae	*Dromogomphus*		1			
ARTHROPODA	Insecta	Odonata	Gomphidae	*Erpetogomphus*		1			
ARTHROPODA	Insecta	Trichoptera	Hydropsychidae	*Cheumatopsyche*		4	52	27	40
ARTHROPODA	Insecta	Trichoptera	Hydropsychidae	*Hydropsyche*	1	4			
ARTHROPODA	Insecta	Trichoptera	Hydroptilidae	*Hydroptila*	1	4		1	
ARTHROPODA	Insecta	Trichoptera	Leptoceridae	*Nectopsyche*	1	4			
ARTHROPODA	Insecta	Trichoptera	Limnephilidae	*Pycnopsyche*	1	4	3		
ARTHROPODA	Insecta	Trichoptera	Philopotamidae	*Chimarra*	1	3	5		1
ARTHROPODA	Insecta	Trichoptera	Polycentropodidae	*Cyrnellus*	1	6			
ARTHROPODA	Insecta	Trichoptera	Polycentropodidae	*Polycentropus*	1	6		5	
ANNELIDA	Oligochaeta	Haplotaxida	Glossoscolecidae	*Sparganophilus*		10			
ANNELIDA	Oligochaeta	Haplotaxida	Tubificidae	*Limnodrilus*		10			

Table 3B.4: Results of benthic macroinvertebrate samples collected at Tar Creek Site 4 in 2018, 2020, and 2021, Ottawa County, OK

Phylum	Class	Order	Family	Genus	EPT Taxa	HBI Score	TC-4 2018	TC-4 2020	TC-4 2021
PLATYHELMINTHES	Turbellaria	Tricladida	Planariidae	*Dugesia*		4	1	2	1
NEMERTEA	Enopla	Hoplonemertea	Tetrastemmatidae	*Prostoma*		5			
MOLLUSCA	Gastropoda	Basommatophora				8		1	
ARTHROPODA	Crustacea	Amphipoda	Talitridae	*Hyalella*		8	2		
ARTHROPODA	Insecta	Coleoptera	Elmidae	*Stenelmis*		4			
ARTHROPODA	Insecta	Coleoptera	Hydrophilidae	*Berosus*		5	9		
ARTHROPODA	Insecta	Coleoptera	Hydrophilidae	*Enochrus*		5		1	
ARTHROPODA	Insecta	Coleoptera	Hydrophilidae	*Tropisternus*		5			
ARTHROPODA	Insecta	Diptera	Ceratopogonidae	*Bezzia*		6			1
ARTHROPODA	Insecta	Diptera	Chironomidae	*Orthocladiinae*		6	7	2	
ARTHROPODA	Insecta	Diptera	Chironomidae	*Tanypodinae*		6	61	15	14
ARTHROPODA	Insecta	Diptera	Empididae	*Hemerodromia*		6			
ARTHROPODA	Insecta	Diptera	simuliidae	*Simulium*		6			
ARTHROPODA	Insecta	Diptera	Tipulidae	*Tipula*		3		2	1
ARTHROPODA	Insecta	Ephemeroptera	Caenidae	*Caenis*	1	7			
ARTHROPODA	Insecta	Hemiptera	Saldidae			0			
ARTHROPODA	Insecta	Megaloptera	Corydalidae	*Corydalus*		0	5	1	
ARTHROPODA	Insecta	Megaloptera	Corydalidae	*Negronia*		0			
ARTHROPODA	Insecta	Megaloptera	Sialidae	*Sialis*		4			
ARTHROPODA	Insecta	Odonata	Coenagrionidae	*Argia*		9			
ARTHROPODA	Insecta	Odonata	Coenagrionidae	*Enallagma*		9		1	
ARTHROPODA	Insecta	Odonata	Gomphidae	*Dromogomphus*		1			
ARTHROPODA	Insecta	Odonata	Gomphidae	*Erpetogomphus*		1			
ARTHROPODA	Insecta	Trichoptera	Hydropsychidae	*Cheumatopsyche*		4	23	64	68
ARTHROPODA	Insecta	Trichoptera	Hydropsychidae	*Hydropsyche*	1	4		1	11
ARTHROPODA	Insecta	Trichoptera	Hydroptilidae	*Hydroptila*	1	4			
ARTHROPODA	Insecta	Trichoptera	Leptoceridae	*Nectopsyche*	1	4			
ARTHROPODA	Insecta	Trichoptera	Limnephilidae	*Pycnopsyche*	1	4		11	
ARTHROPODA	Insecta	Trichoptera	Philopotamidae	*Chimarra*	1	3	5	4	5
ARTHROPODA	Insecta	Trichoptera	Polycentropodidae	*Cyrnellus*	1	6			
ARTHROPODA	Insecta	Trichoptera	Polycentropodidae	*Polycentropus*	1	6			1
ANNELIDA	Oligochaeta	Haplotaxida	Glossoscolecidae	*Sparganophilus*		10		2	2
ANNELIDA	Oligochaeta	Haplotaxida	Tubificidae	*Limnodrilus*		10			

Table 3B.5: Results of benthic macroinvertebrate samples collected at Tar Creek Site 5 in 2018, 2020, and 2021, Ottawa County, OK

Phylum	Class	Order	Family	Genus	EPT Taxa	HBI Score	TC-5 2018	TC-5 2020	TC-5 2021
PLATYHELMINTHES	Turbellaria	Tricladida	Planariidae	*Dugesia*		4			2
NEMERTEA	Enopla	Hoplonemertea	Tetrastemmatidae	*Prostoma*		5			
MOLLUSCA	Gastropoda	Basommatophora				8		2	
ARTHROPODA	Crustacea	Amphipoda	Talitridae	*Hyalella*		8		1	
ARTHROPODA	Insecta	Coleoptera	Elmidae	*Stenelmis*		4		3	
ARTHROPODA	Insecta	Coleoptera	Hydrophilidae	*Berosus*		5	3	3	
ARTHROPODA	Insecta	Coleoptera	Hydrophilidae	*Enochrus*		5			
ARTHROPODA	Insecta	Coleoptera	Hydrophilidae	*Tropisternus*		5			
ARTHROPODA	Insecta	Diptera	Ceratopogonidae	*Bezzia*		6			
ARTHROPODA	Insecta	Diptera	Chironomidae	*Orthocladiinae*		6	4		
ARTHROPODA	Insecta	Diptera	Chironomidae	*Tanypodinae*		6	73	29	10
ARTHROPODA	Insecta	Diptera	Empididae	*Hemerodromia*		6			
ARTHROPODA	Insecta	Diptera	simuliidae	*Simulium*		6		1	
ARTHROPODA	Insecta	Diptera	Tipulidae	*Tipula*		3		3	2
ARTHROPODA	Insecta	Ephemeroptera	Caenidae	*Caenis*	1	7			
ARTHROPODA	Insecta	Hemiptera	Saldidae			0			
ARTHROPODA	Insecta	Megaloptera	Corydalidae	*Corydalus*		0		2	1
ARTHROPODA	Insecta	Megaloptera	Corydalidae	*Negronia*		0			
ARTHROPODA	Insecta	Megaloptera	Sialidae	*Sialis*		4			
ARTHROPODA	Insecta	Odonata	Coenagrionidae	*Argia*		9	2	2	
ARTHROPODA	Insecta	Odonata	Coenagrionidae	*Enallagma*		9			
ARTHROPODA	Insecta	Odonata	Gomphidae	*Dromogomphus*		1			
ARTHROPODA	Insecta	Odonata	Gomphidae	*Erpetogomphus*		1			
ARTHROPODA	Insecta	Trichoptera	Hydropsychidae	*Cheumatopsyche*		4	21	46	61
ARTHROPODA	Insecta	Trichoptera	Hydropsychidae	*Hydropsyche*	1	4	2	5	7
ARTHROPODA	Insecta	Trichoptera	Hydroptilidae	*Hydroptila*	1	4			1
ARTHROPODA	Insecta	Trichoptera	Leptoceridae	*Nectopsyche*	1	4			
ARTHROPODA	Insecta	Trichoptera	Limnephilidae	*Pycnopsyche*	1	4			
ARTHROPODA	Insecta	Trichoptera	Philopotamidae	*Chimarra*	1	3	2	1	9
ARTHROPODA	Insecta	Trichoptera	Polycentropodidae	*Cyrnellus*	1	6			1
ARTHROPODA	Insecta	Trichoptera	Polycentropodidae	*Polycentropus*	1	6	14		12
ANNELIDA	Oligochaeta	Haplotaxida	Glossoscolecidae	*Sparganophilus*		10		7	
ANNELIDA	Oligochaeta	Haplotaxida	Tubificidae	*Limnodrilus*		10			

Table 3B.6: Results of benthic macroinvertebrate samples collected at Tar Creek Site 6 in 2018, 2020, and 2021, Ottawa County, OK

Phylum	Class	Order	Family	Genus	EPT Taxa	HBI Score	TC-6 2018	TC-6 2020	TC-6 2021
PLATYHELMINTHES	Turbellaria	Tricladida	Planariidae	*Dugesia*		4			
NEMERTEA	Enopla	Hoplonemertea	Tetrastemmatidae	*Prostoma*		5			
MOLLUSCA	Gastropoda	Basommatophora				8	7		
ARTHROPODA	Crustacea	Amphipoda	Talitridae	*Hyalella*		8			
ARTHROPODA	Insecta	Coleoptera	Elmidae	*Stenelmis*		4			
ARTHROPODA	Insecta	Coleoptera	Hydrophilidae	*Berosus*		5	18		
ARTHROPODA	Insecta	Coleoptera	Hydrophilidae	*Enochrus*		5	2		
ARTHROPODA	Insecta	Coleoptera	Hydrophilidae	*Tropisternus*		5			1
ARTHROPODA	Insecta	Diptera	Ceratopogonidae	*Bezzia*		6		8	7
ARTHROPODA	Insecta	Diptera	Chironomidae	*Orthocladiinae*		6	6		7
ARTHROPODA	Insecta	Diptera	Chironomidae	*Tanypodinae*		6	33	26	55
ARTHROPODA	Insecta	Diptera	Empididae	*Hemerodromia*		6		1	
ARTHROPODA	Insecta	Diptera	simuliidae	*Simulium*		6			3
ARTHROPODA	Insecta	Diptera	Tipulidae	*Tipula*		3	1	2	2
ARTHROPODA	Insecta	Ephemeroptera	Caenidae	*Caenis*	1	7	11		
ARTHROPODA	Insecta	Hemiptera	Saldidae			0	3		
ARTHROPODA	Insecta	Megaloptera	Corydalidae	*Corydalus*		0			
ARTHROPODA	Insecta	Megaloptera	Corydalidae	*Negronia*		0			
ARTHROPODA	Insecta	Megaloptera	Sialidae	*Sialis*		4			1
ARTHROPODA	Insecta	Odonata	Coenagrionidae	*Argia*		9			
ARTHROPODA	Insecta	Odonata	Coenagrionidae	*Enallagma*		9	11	2	
ARTHROPODA	Insecta	Odonata	Gomphidae	*Dromogomphus*		1	2		
ARTHROPODA	Insecta	Odonata	Gomphidae	*Erpetogomphus*		1			
ARTHROPODA	Insecta	Trichoptera	Hydropsychidae	*Cheumatopsyche*		4	29	48	11
ARTHROPODA	Insecta	Trichoptera	Hydropsychidae	*Hydropsyche*	1	4	5	10	4
ARTHROPODA	Insecta	Trichoptera	Hydroptilidae	*Hydroptila*	1	4			3
ARTHROPODA	Insecta	Trichoptera	Leptoceridae	*Nectopsyche*	1	4		7	
ARTHROPODA	Insecta	Trichoptera	Limnephilidae	*Pycnopsyche*	1	4			
ARTHROPODA	Insecta	Trichoptera	Philopotamidae	*Chimarra*	1	3			8
ARTHROPODA	Insecta	Trichoptera	Polycentropodidae	*Cyrnellus*	1	6		2	2
ARTHROPODA	Insecta	Trichoptera	Polycentropodidae	*Polycentropus*	1	6	2		
ANNELIDA	Oligochaeta	Haplotaxida	Glossoscolecidae	*Sparganophilus*		10		1	1
ANNELIDA	Oligochaeta	Haplotaxida	Tubificidae	*Limnodrilus*		10			

APPENDIX 4A
Historical Mine Map Index

Table 4A: Index of historical mine maps used to create the Picher field mine map

Map ID	Map Title	Year	State	T-R-S	Scale	Reference
09-01	Gordon No. 3 Mine (Burnham -T	1970	OK	29N-23E-18	1-50	Keheley (2020)
1_Plate_1_1958	Plate_1	1958	KS	Picher Field	1-300	MDHC (2020)
2_Plate_2_1958	Plate_2	1958	KS	Picher Field	1-300	MDHC (2020)
3_Plate_3_1958	Plate_3	1958	KS	Picher Field	1-300	MDHC (2020)
4_Plate_4_1958	Plate_4	1958	KS	Picher Field	1-300	MDHC (2020)
5_Plate_5_1956	Plate_5	1956	OK	Picher Field	1-300	MDHC (2020)
6_Plate_6_1958	Plate_6	1958	OK	Picher Field	1-300	MDHC (2020)
7_Plate_7_1958	Plate_7	1958	OK	Picher Field	1-300	MDHC (2020)
8_Plate_8_1958	Plate_8	1958	OK	Picher Field	1-300	MDHC (2020)
9_Plate_9_1958	Plate_9	1958	OK	Picher Field	1-300	MDHC (2020)
10_Plate_10_1958	Plate_10	1958	OK	Picher Field	1-300	MDHC (2020)
11_Plate_11_1956	Plate_11	1956	OK	Picher Field	1-300	MDHC (2020)
12_Plate_12_1956	Plate_12	1956	OK	Picher Field	1-300	MDHC (2020)
17-02	Midas Mine	1959	OK	29N-23E-28	1-50	Keheley (2020)
17-04	New Chicago No 2 North half Mine	1959	OK	29N-23E-28	1-50	Keheley (2020)
17-05	New Chicago No 1 Mine	1959	OK	29N-23E-28	1-50	Keheley (2020)
17-06	Buffalo Calf West Half Mine	1959	OK	29N-23E-28	1-50	Keheley (2020)
17-08	Skelton Mine, South Half	1959	OK	29N-23E-28	1-50	Keheley (2020)
17-09	Skelton Mine, North Half	1957	OK	29N-23E-28	1-50	Keheley (2020)
17-10	New Chicago No 2 South half Mine	1957	OK	29N-23E-28	1-50	Keheley (2020)
18-07	Big Chief Mine	1967	OK	29N-23E-17	1-50	Keheley (2020)
18-13	Goodwin Mine	1967	OK	29N-23E-17	1-50	Keheley (2020)
19-01	Baby Jim Mine	1960	OK	29N-23E-29	1-50	Keheley (2020)
19-03	Admiralty No 3 Mine	1966	OK	29N-23E-29	1-100	Keheley (2020)
19-04	Skelton Mine	1957	OK	29N-23E-29	1-50	Keheley (2020)
19-05	Skelton Mine	1957	OK	29N-23E-29	1-50	Keheley (2020)
19-07	Skelton Mine	1959	OK	29N-23E-29	1-50	Keheley (2020)
20-01	M Bed	1959	OK	29N-23E-19	1-100	Keheley (2020)
28N22E1_06	Cactus Mine	ND	OK	28N-22E-1	1-100	Keheley (2020)
28N22E1_10	West Commerce w/ drill logs	ND	OK	28N-22E-1		Keheley (2020)
28N22E1_16	North-Northwest Commerce Area		OK	28N-22E-1	1-40	MDHC (2020)
28N22E1_25	Northwest Commerce Area	ND	OK	28N-22E-1	1-50	Keheley (2020)
28N22E12_01	Lost Trail Mine	ND	OK	28N-22E-12	1-40	Keheley (2020)

Table 4A Continued

Map ID	Map Title	Year	State	T-R-S	Scale	Reference
28N22E12_04	Crowe Mining Tract	1947	OK	28N-22E-12	1-100	Keheley (2020)
28N23E1_02	Mission Mine_Negative of 01	1907	OK	28N-23E-1	1-30	Keheley (2020)
28N23E7_01	Commerce area plan map	1913	OK	28N-23E-7	1-50	MDHC (2020)
28N24E6_01	Valliere Mine	1944	OK	28N-24E-6	1-100	Keheley (2020)
29N22E13_01	Laura Jenny Zheka Wilson	193?	OK	29N-22E-13	1-100	MDHC (2020)
29N22E13_04	Bird Dog Mine	1945	OK	29N-22E-13	1-100	MDHC (2020)
29N22E13_05	Bob White & Mehunka Mine	1948	OK	29N-22E-13	1-100	MDHC (2020)
29N22E14_01	Wild Bull	ND	OK	29N-22E-14		MDHC (2020)
29N22E23_01	Xavier Mine	1933	OK	29N-22E-23	1-50	MDHC (2020)
29N22E24_01	Bob White Mine East 40	1955	OK	29N-22E-24	1-50	Keheley (2020)
29N22E24_02	Bob White Mine West 40	1955	OK	29N-22E-24	1-50	Keheley (2020)
29N22E24_03	Little Greenback Mine	1965	OK	29N-22E-24	1-50	Keheley (2020)
29N22E24_04	Garrett Mine	1957	OK	29N-22E-24	1-50	Keheley (2020)
29N22E24_09	Bird Dog Mine	1951	OK	29N-22E-24	1-100	MDHC (2020)
29N22E24_11	Bird Dog Mine_Similar or same as _10	1945	OK	29N-22E-24	1-100	MDHC (2020)
29N22E24_17	Kitty Mine	1950	OK	29N-22E-24	1-100	MDHC (2020)
29N22E24_19	Kitty Mine	1954	OK	29N-22E-24	1-50	MDHC (2020)
29N22E25_01	Goodeagle Mine	1963	OK	29N-22E-25	1-100	Keheley (2020)
29N22E25_04	Wilson Mine	1942	OK	29N-22E-25	1-100	MDHC (2020)
29N22E25_07	Goodeagle Mine	1945	OK	29N-22E-25	1-100	MDHC (2020)
29N22E25_09	Wilson and Bluebird	ND	OK	29N-22E-25	1-100	MDHC (2020)
29N22E25_14	Blue Bird-Wilson Mine	1949	OK	29N-22E-25	1-100	MDHC (2020)
29N22E25_15	Roanoke Mine	ND	OK	29N-22E-25	1-50	MDHC (2020)
29N22E36_01	Roanoke and Smokey-Hill	1946	OK	29N-22E-36	1-100	Keheley (2020)
29N22E36_07	Roanoke Mine	ND	OK	29N-22E-36	1-100	MDHC (2020)
29N23E13_01	NiDay No. 1	1952	OK	29N-23E-13	1-100	Keheley (2020)
29N23E13_02	Scott	ND	OK	29N-23E-13		MDHC (2020)
29N23E13_03	Scott	ND	OK	29N-23E-13		MDHC (2020)
29N23E13_04	Scott	ND	OK	29N-23E-13		MDHC (2020)
29N23E14_01	Dobson Lease NWSW	1966	OK	29N-23E-14	1-50	Keheley (2020)
29N23E14_03	Dobson Lease	ND	OK	29N-23E-14	1-40	Keheley (2020)
29N23E14_04	Blue Ribbon	1946	OK	29N-23E-14	1-100	Keheley (2020)
29N23E14_06	Farmington	ND	OK	29N-23E-14	1-50	Keheley (2020)

Table 4A Continued

Map ID	Map Title	Year	State	T-R-S	Scale	Reference
29N23E14_07	Lucky Jack Mine	ND	OK	29N-23E-14	1-50	Keheley (2020)
29N23E14_08	Structure Map	1946	OK	29N-23E-14	1-100	Keheley (2020)
29N23E14_09	Farmington	1937	OK	29N-23E-14	1-50	Keheley (2020)
29N23E14_10	Dobson (east side)	1952	OK	29N-23E-14	1-40	MDHC (2020)
29N23E14_11	Dobson (West side)	195?	OK	29N-23E-14	1-40	MDHC (2020)
29N23E15_01	Beck Mining Co	1928	OK	29N-23E-15		MDHC (2020)
29N23E15_03	Brewster Mine	1952	OK	29N-23E-15	1-100	MDHC (2020)
29N23E15_05	Mine No. 2 (North Brewster)	1927	OK	29N-23E-15	1-50	MDHC (2020)
29N23E15_06	Brewster Mine (North)	1952	OK	29N-23E-15	1-100	MDHC (2020)
29N23E15_07	Brewster Mine (northeast)	1927	OK	29N-23E-15	1-50	MDHC (2020)
29N23E15_08	WM&W	ND	OK	29N-23E-15	1-200	MDHC (2020)
29N23E15_11	Mary Ann	ND	OK	29N-23E-15	1-100	MDHC (2020)
29N23E15_13	Mary Ann	1950	OK	29N-23E-15	1-40	MDHC (2020)
29N23E15_14	Mary Ann	ND	OK	29N-23E-15	1-40	MDHC (2020)
29N23E15_15	Mary Ann	ND	OK	29N-23E-15	1-40	MDHC (2020)
29N23E15_18	Golden Eagle	ND	OK	29N-23E-15	1-40	MDHC (2020)
29N23E15_19	Shaffer	ND	OK	29N-23E-15	1-50	MDHC (2020)
29N23E15_21	Crutchfield	1925	OK	29N-23E-15	1-40	MDHC (2020)
29N23E16_01	Swift WNW	ND	OK	29N-23E-16	1-50	Keheley (2020)
29N23E16_03	Swift ENW	1966	OK	29N-23E-16	1-50	Keheley (2020)
29N23E16_04	Commonwealth	ND	OK	29N-23E-16	1-50	Keheley (2020)
29N23E16_05	Cortez Mine	1945	OK	29N-23E-16	1-50	Keheley (2020)
29N23E16_06	Eudora WhiteBird	1966	OK	29N-23E-16	1-50	Keheley (2020)
29N23E16_08	Whitebird Mine	1966	OK	29N-23E-16	1-50	Keheley (2020)
29N23E16_09	Swift-Commonwealth	1965	OK	29N-23E-16	1-50	Keheley (2020)
29N23E16_12	Hunt Mine	ND	OK	29N-23E-16	1-50	MDHC (2020)
29N23E17_03	Crawfish	1966	OK	29N-23E-17	1-50	Keheley (2020)
29N23E17_04	Big Chief	1958	OK	29N-23E-17	1-50	Keheley (2020)
29N23E17_07	Goodwin Mine	1966	OK	29N-23E-17	1-50	Keheley (2020)
29N23E17_08	Howe Mine	1966	OK	29N-23E-17	1-50	Keheley (2020)
29N23E17_09	LaSalle	1964	OK	29N-23E-17	1-50	Keheley (2020)
29N23E17_10	Lucky Syndicate	1965	OK	29N-23E-17	1-50	Keheley (2020)
29N23E17_11	Lucky Syndicate	1966	OK	29N-23E-17	1-50	Keheley (2020)

Table 4A Continued

Map ID	Map Title	Year	State	T-R-S	Scale	Reference
29N23E17_12	Netta White Mine	1965	OK	29N-23E-17	1-50	Keheley (2020)
29N23E17_14	Piokee	1966	OK	29N-23E-17	1-50	Keheley (2020)
29N23E17_16	Otis White	1966	OK	29N-23E-17	1-50	Keheley (2020)
29N23E17_17	Ohimo Mine	1951	OK	29N-23E-17	1-50	Keheley (2020)
29N23E17_18	Slim Jim	1954	OK	29N-23E-17	1-50	Keheley (2020)
29N23E18_03	Gordon No 2 Mine	ND	OK	29N-23E-18	1-50	Keheley (2020)
29N23E18_04	Gordon No 3 Mine NESE	1965	OK	29N-23E-18	1-50	Keheley (2020)
29N23E18_05	Gordon No 3 Mine NESE	1966	OK	29N-23E-18	1-50	Keheley (2020)
29N23E18_07	Gordon No 3 Mine NWSE	1966	OK	29N-23E-18	1-50	Keheley (2020)
29N23E18_09	Gordon No 3 Mine SENE	1966	OK	29N-23E-18	1-50	Keheley (2020)
29N23E18_10	Gordon No 3 Mine SESE	1965	OK	29N-23E-18	1-50	Keheley (2020)
29N23E18_11	Gordon No 3 Mine SESE	1966	OK	29N-23E-18	1-50	Keheley (2020)
29N23E18_15	Pelican Mine	ND	OK	29N-23E-18	1-100	MDHC (2020)
29N23E18_21	Ton-Gah-Hah Beaver	1943	OK	29N-23E-18	1-100	MDHC (2020)
29N23E19_02	Anna Beaver Mine NENE (Quarter of 01)	1963	OK	29N-23E-19	1-50	Keheley (2020)
29N23E19_03	Anna Beaver Mine SENE (Quarter of 01)	1963	OK	29N-23E-19	1-50	Keheley (2020)
29N23E19_04	Anna Beaver Mine SENW (Quarter of 01)	1957	OK	29N-23E-19	1-50	Keheley (2020)
29N23E19_05	Anna Beaver Mine SWNE (Quarter of 01)	1952	OK	29N-23E-19	1-50	Keheley (2020)
29N23E19_06	Anna Beaver Mine NWNE (Quarter of 01)	1963	OK	29N-23E-19	1-50	Keheley (2020)
29N23E19_07	Anna Beaver Mine SENW (Quarter of 01) at 1-100 scale of 04	ND	OK	29N-23E-19	1-100	Keheley (2020)
29N23E19_10	John Beaver Mine NESE (Quarter of 08)	1966	OK	29N-23E-19	1-50	Keheley (2020)
29N23E19_11	John Beaver Mine NWSE (Quarter of 08)	1963	OK	29N-23E-19	1-50	Keheley (2020)
29N23E19_13	John Beaver Mine SWSE (Quarter of 08)	1966	OK	29N-23E-19	1-50	Keheley (2020)
29N23E19_14	Crystal Central	1964	OK	29N-23E-19	1-50	Keheley (2020)
29N23E19_15	Harrisburg Mine	1956	OK	29N-23E-19	1-50	Keheley (2020)
29N23E19_17	Velie Lion Mine	1962	OK	29N-23E-19	1-50	Keheley (2020)
29N23E19_20	Foch Mine	1945	OK	29N-23E-19	1-40	MDHC (2020)
29N23E19_22	Ton Gah Hah Beaver	1939	OK	29N-23E-19	1-100	MDHC (2020)
29N23E19_24	Velie Lion Mine	1954	OK	29N-23E-19	1-50	MDHC (2020)
29N23E19_25	Harrisburg Mine	41953	OK	29N-23E-19	1-50	MDHC (2020)
29N23E19_26	John Beaver Mine	1954	OK	29N-23E-19	1-100	MDHC (2020)
29N23E19_27	Crystal Central	1941	OK	29N-23E-19	1-50	MDHC (2020)
29N23E20_01	Barbara J	1955	OK	29N-23E-20	1-50	Keheley (2020)

Table 4A Continued

Map ID	Map Title	Year	State	T-R-S	Scale	Reference
29N23E20_02	Barbara J	1955	OK	29N-23E-20	1-100	Keheley (2020)
29N23E20_04	Dorothy Bill E40_BW of 03	1955	OK	29N-23E-20	1-50	Keheley (2020)
29N23E20_05	Dorothy Bill E40	1965	OK	29N-23E-20	1-50	Keheley (2020)
29N23E20_06	Dorothy Bill W40	1955	OK	29N-23E-20	1-50	Keheley (2020)
29N23E20_07	Dorothy Bill W40	1965	OK	29N-23E-20	1-50	Keheley (2020)
29N23E20_08	Golden Hawk Mine	1944	OK	29N-23E-20	1-50	Keheley (2020)
29N23E20_09	Golden Hawk Mine	1954	OK	29N-23E-20	1-50	Keheley (2020)
29N23E20_10	Golden Hawk Mine	1965	OK	29N-23E-20	1-50	Keheley (2020)
29N23E20_11	Kenoyer Mine	1955	OK	29N-23E-20	1-100	Keheley (2020)
29N23E20_12	Kenoyer Mine	1966	OK	29N-23E-20	1-100	Keheley (2020)
29N23E20_15	Netta Mine East 40_BW of 14	1955	OK	29N-23E-20	1-50	Keheley (2020)
29N23E20_16	Netta Mine East 40	1965	OK	29N-23E-20	1-50	Keheley (2020)
29N23E20_17	Netta Mine East 40	1967	OK	29N-23E-20	1-50	Keheley (2020)
29N23E20_18	Netta Mine West 40	1954	OK	29N-23E-20	1-50	Keheley (2020)
29N23E20_19	Netta Mine West 40	1965	OK	29N-23E-20	1-50	Keheley (2020)
29N23E20_20	Oko	1966	OK	29N-23E-20	1-50	Keheley (2020)
29N23E20_21	Premier	1955	OK	29N-23E-20	1-50	Keheley (2020)
29N23E20_22	Premier	1965	OK	29N-23E-20	1-50	Keheley (2020)
29N23E20_23	Rialto	1955	OK	29N-23E-20	1-100	Keheley (2020)
29N23E20_24	St. Joe	1955	OK	29N-23E-20	1-50	Keheley (2020)
29N23E20_25	St. Joe	1965	OK	29N-23E-20	1-50	Keheley (2020)
29N23E20_26	Vantage Mine	1953	OK	29N-23E-20	1-50	Keheley (2020)
29N23E20_27	Vantage Mine	1965	OK	29N-23E-20	1-50	Keheley (2020)
29N23E20_29	Rialto No 4Mine L&G	1955	OK	29N-23E-20	1-50	MDHC (2020)
29N23E21_01	Acme	1929	OK	29N-23E-21	1-100	MDHC (2020)
29N23E21_04	Grace Walker Mine K Bed	1954	OK	29N-23E-21	1-100	MDHC (2020)
29N23E21_05	Grace Walker Mine M Bed	1954	OK	29N-23E-21	1-100	MDHC (2020)
29N23E21_07	Black Eagle Mine	1963	OK	29N-23E-21	1-50	Keheley (2020)
29N23E21_08	Black Hawk Mine	1940	OK	29N-23E-21	1-50	Keheley (2020)
29N23E21_11	Eudora WhiteBird NENW	1966	OK	29N-23E-21	1-50	Keheley (2020)
29N23E21_14	Eudora WhiteBird East 40 NWNE	1966	OK	29N-23E-21	1-50	Keheley (2020)
29N23E21_18	Grace Walker NWSE	1966	OK	29N-23E-21	1-50	Keheley (2020)
29N23E21_19	Jeff City West 40	1965	OK	29N-23E-21	1-50	Keheley (2020)

Table 4A Continued

Map ID	Map Title	Year	State	T-R-S	Scale	Reference
29N23E21_20	Jeff City East 40	1964	OK	29N-23E-21	1-50	Keheley (2020)
29N23E21_21	Jefferson	1964	OK	29N-23E-21	1-50	Keheley (2020)
29N23E21_22	Hudson-Bingham Mine	1951	OK	29N-23E-21	1-50	Keheley (2020)
29N23E21_23	New York	ND	OK	29N-23E-21	1-50	Keheley (2020)
29N23E21_24	New York	1966	OK	29N-23E-21	1-50	Keheley (2020)
29N23E21_25	Grace Walker and Royal Mine	1966	OK	29N-23E-21	1-50	Keheley (2020)
29N23E21_26	Royal	1966	OK	29N-23E-21	1-50	Keheley (2020)
29N23E21_28	North Bingham Mine	1956	OK	29N-23E-21	1-50	MDHC (2020)
29N23E21_30	Mahutska	1946	OK	29N-23E-21	1-50	MDHC (2020)
29N23E21_32	Jeff City	1946	OK	29N-23E-21	1-50	MDHC (2020)
29N23E22_01	Dardenne	1939	OK	29N-23E-22	1-50	Keheley (2020)
29N23E22_03	Sam Douthat Land	1930	OK	29N-23E-22	1-100	Keheley (2020)
29N23E22_04	Quapaw District Allotment 7	ND	OK	29N-23E-22	1-100	MDHC (2020)
29N23E22_07	Tulsa	ND	OK	29N-23E-22	1-50	MDHC (2020)
29N23E22_08	Mogul & Aztec	1953	OK	29N-23E-22	1-50	MDHC (2020)
29N23E22_10	Indiana S80	1929	OK	29N-23E-22	1-50	MDHC (2020)
29N23E22_14	Huttig-Beck	ND	OK	29N-23E-22	1-50	MDHC (2020)
29N23E22_15	Indiana N40	1929	OK	29N-23E-22	1-100	MDHC (2020)
29N23E23_01	Blue Bonnett_BW	ND	OK	29N-23E-23	1-50	Keheley (2020)
29N23E23_07	H-K Mine	1924	OK	29N-23E-23	1-20	MDHC (2020)
29N23E23_11	Weiss	1946	OK	29N-23E-23	1-50	MDHC (2020)
29N23E23_12	Weiss Fee	ND	OK	29N-23E-23	1-40	MDHC (2020)
29N23E23_14	Kropp Fee	ND	OK	29N-23E-23	1-40	MDHC (2020)
29N23E23_15	Kropp Fee	ND	OK	29N-23E-23	1-40	MDHC (2020)
29N23E23_16	Kropp Fee	ND	OK	29N-23E-23	1-40	MDHC (2020)
29N23E23_17	Kropp Fee	1935	OK	29N-23E-23	1-40	MDHC (2020)
29N23E23_19	Mission	1939	OK	29N-23E-23	1-40	MDHC (2020)
29N23E23_24	Meteor and Aztec Mines_BW	ND	OK	29N-23E-23	1-100	Keheley (2020)
29N23E23_28	Texas	ND	OK	29N-23E-23	1-50	MDHC (2020)
29N23E23_33	Santa Fe	ND	OK	29N-23E-23	1-40	MDHC (2020)
29N23E23_37	Weiss Land (Mission)	1945	OK	29N-23E-23	1-100	MDHC (2020)
29N23E23_38	Portion of Mission Land	ND	OK	29N-23E-23		MDHC (2020)
29N23E24_01	Crane	ND	OK	29N-23E-24	1-100	MDHC (2020)

Table 4A Continued

Map ID	Map Title	Year	State	T-R-S	Scale	Reference
29N23E24_02	Crane	ND	OK	29N-23E-24	1-100	MDHC (2020)
29N23E24_05	North Imbeau Mine	1955	OK	29N-23E-24	1-100	MDHC (2020)
29N23E24_06	South Imbeau Mine	1941	OK	29N-23E-24	1-100	MDHC (2020)
29N23E24_08	St. Lois No. 4 & Imbeau	1955	OK	29N-23E-24	1-40	MDHC (2020)
29N23E24_11	St. Lois No. 4	1955	OK	29N-23E-24	1-40	MDHC (2020)
29N23E24_13	St. Lois No. 4	1947	OK	29N-23E-24	1-40	MDHC (2020)
29N23E24_14	St. Lois No. 4	ND	OK	29N-23E-24	1-40	MDHC (2020)
29N23E25_01	Mary Jane	ND	OK	29N-23E-25	1-40	MDHC (2020)
29N23E26_06	Minnie Greenback Clabber	ND	OK	29N-23E-26	1-100	MDHC (2020)
29N23E26_08	Allotment 3 - Peck Lease	ND	OK	29N-23E-26	1-100	MDHC (2020)
29N23E27_01	Arthur Buffalo	1951	OK	29N-23E-27	1-100	MDHC (2020)
29N23E27_02	First National	1943	OK	29N-23E-27	1-100	MDHC (2020)
29N23E27_03	Beetho Land (Pat)	ND	OK	29N-23E-27	1-100	MDHC (2020)
29N23E27_04	Pat Mine	1946	OK	29N-23E-27	1-50	MDHC (2020)
29N23E28_02	Skelton Mine_BW of 01	1954	OK	29N-23E-28	1-50	Keheley (2020)
29N23E28_03	Skelton Mine	1954	OK	29N-23E-28	1-50	Keheley (2020)
29N23E28_06	Bull Frog C, D	1943	OK	29N-23E-28	1-50	MDHC (2020)
29N23E28_07	Bull Frog A, B	1953	OK	29N-23E-28	1-50	MDHC (2020)
29N23E28_08	Bull Frog C, D	1943	OK	29N-23E-28	1-50	MDHC (2020)
29N23E28_10	Lawyers Mine	1949	OK	29N-23E-28	1-40	MDHC (2020)
29N23E28_11	Lawyers Mine	1952	OK	29N-23E-28	1-40	MDHC (2020)
29N23E28_13	Midas 40 acres	ND	OK	29N-23E-28	1-200	MDHC (2020)
29N23E28_15	Lawyers Mine	1946	OK	29N-23E-28	1-40	MDHC (2020)
29N23E28_16	Lawyers Mine	ND	OK	29N-23E-28	1-200	MDHC (2020)
29N23E28_17	Frank Buffalo - Bull Frog Lease	ND	OK	29N-23E-28	1-100	Keheley (2020)
29N23E29_02	Admiralty Mines 1,2,4, & 5_BW of 01	ND	OK	29N-23E-29	1-100	Keheley (2020)
29N23E29_05	Admiralty Mine_03 map with elevations	1936	OK	29N-23E-29	1-100	MDHC (2020)
29N23E29_06	Admiralty Mines 1,2,4, & 5	1939	OK	29N-23E-29	1-100	MDHC (2020)
29N23E29_07	AD No 4	1945	OK	29N-23E-29	1-50	MDHC (2020)
29N23E29_09	Admiralty Mines 1,2	1945	OK	29N-23E-29	1-50	MDHC (2020)
29N23E29_11	Baby Jim_With additional drawing	1946	OK	29N-23E-29	1-50	MDHC (2020)
29N23E29_12	Baby Jim	1955	OK	29N-23E-29	1-50	MDHC (2020)
29N23E29_14	Barbara J East	1955	OK	29N-23E-29	1-50	MDHC (2020)

Table 4A Continued

Map ID	Map Title	Year	State	T-R-S	Scale	Reference
29N23E29_18	Domado	1955	OK	29N-23E-29	1-50	MDHC (2020)
29N23E29_19	Domado	1966	OK	29N-23E-29	1-50	Keheley (2020)
29N23E29_20	Douthat	1930	OK	29N-23E-29	1-40	MDHC (2020)
29N23E29_21	Rialto	1966	OK	29N-23E-29	1-50	ODM (2020)
29N23E29_25	Skelton NWSE	1952	OK	29N-23E-29	1-50	Keheley (2020)
29N23E29_26	Skelton SESE	1954	OK	29N-23E-29	1-50	Keheley (2020)
29N23E29_27	Skelton SESE - Color of _26	1954	OK	29N-23E-29	1-50	MDHC (2020)
29N23E29_28	Skelton NESE - Color of _24	1952	OK	29N-23E-29	1-50	MDHC (2020)
29N23E29_33	Barbara J.	1955	OK	29N-23E-29	1-100	MDHC (2020)
29N23E29_35	Barbara J.	1955	OK	29N-23E-29	1-50	MDHC (2020)
29N23E29_36	Skelton and Admiralty Lease	1954	OK	29N-23E-29	1-100	Keheley (2020)
29N23E29_39	Admiralty Mines 1 & 2 upper level circle area	ND	OK	29N-23E-29	1-50	Keheley (2020)
29N23E29_40	Admiralty Mines 1 & 2	1946	OK	29N-23E-29	1-50	Keheley (2020)
29N23E29_41	Admiralty Mine 1	1952	OK	29N-23E-29	1-100	Keheley (2020)
29N23E29_42	Admiralty Mines 1, 2, 4, & 5	ND	OK	29N-23E-29	1-100	Keheley (2020)
29N23E29_45	Rialto No 1 & 2	ND	OK	29N-23E-29	1-50	Keheley (2020)
29N23E29_46	Rialto No 1 & 2	ND	OK	29N-23E-29	1-50	Keheley (2020)
29N23E29_52	Croesus-Domado-Bethel Mines	1919	OK	29N-23E-29	1-40	ODM (2020)
29N23E30_03	Blue Goose No 1	1967	OK	29N-23E-30	1-50	Keheley (2020)
29N23E30_07	Blue Goose No 2 NE corner of 02	1967	OK	29N-23E-30	1-50	Keheley (2020)
29N23E30_08	Blue Goose No 2_M Bed	1954	OK	29N-23E-30	1-100	Keheley (2020)
29N23E30_10	Blue Goose No 2_Sheet Ground	1964	OK	29N-23E-30	1-100	Keheley (2020)
29N23E30_12	Bennie	1964	OK	29N-23E-30	1-50	Keheley (2020)
29N23E30_14	Hum-Bah-Wat-Tah Mine	1967	OK	29N-23E-30	1-50	Keheley (2020)
29N23E30_16	Lottson Blue Goose, & HumBah Mines_M Bed	1954	OK	29N-23E-30	1-100	Keheley (2020)
29N23E30_17	Jaybird Mine	1965	OK	29N-23E-30	1-50	Keheley (2020)
29N23E30_19	Lottson	1958	OK	29N-23E-30	1-50	Keheley (2020)
29N23E30_21	Lucky Bill	1967	OK	29N-23E-30	1-50	Keheley (2020)
29N23E30_22	Ritz Mine - BW of _32	1955	OK	29N-23E-30	1-100	Keheley (2020)
29N23E30_24	See-Sah	1967	OK	29N-23E-30	1-100	Keheley (2020)
29N23E30_25	Shorthorn	1965	OK	29N-23E-30	1-50	Keheley (2020)
29N23E30_27	Tom L Mine	1965	OK	29N-23E-30	1-50	Keheley (2020)
29N23E30_31	Woodchuck Mine	1965	OK	29N-23E-30	1-50	Keheley (2020)

Table 4A Continued

Map ID	Map Title	Year	State	T-R-S	Scale	Reference
29N23E30_32	Ritz Mine	1955	OK	29N-23E-30	1-100	MDHC (2020)
29N23E30_33	Lottson - Blue Goose & Humbah Mines	1954	OK	29N-23E-30	1-100	MDHC (2020)
29N23E31_04	Southside Lower level	ND	OK	29N-23E-31	1-100	Keheley (2020)
29N23E31_06	Southside Upper level	1956	OK	29N-23E-31	1-100	Keheley (2020)
29N23E31_07	DeVilliers Lease	ND	OK	29N-23E-31	1-100	Keheley (2020)
29N23E32_01	Beck	1928	OK	29N-23E-32	1-40	MDHC (2020)
29N23E32_02	Vanpool Lease	1955	OK	29N-23E-32	1-50	MDHC (2020)
29N23E32_03	Montreal Mining Co.	1946	OK	29N-23E-32	1-40	MDHC (2020)
29N23E32_05	Mabon-N80	1939	OK	29N-23E-32	1-50	MDHC (2020)
29N23E32_06	Mabon-N80	ND	OK	29N-23E-32	1-50	MDHC (2020)
29N23E32_07	Montreal and Quebec	1943	OK	29N-23E-32	1-40	MDHC (2020)
29N23E32_08	Montreal and Quebec	ND	OK	29N-23E-32	1-50	Keheley (2020)
29N23E33_02	Craig East Half	ND	OK	29N-23E-33	1-100	MDHC (2020)
29N23E33_03	Waxahatchie	1945	OK	29N-23E-33	1-40	MDHC (2020)
29N23E33_08	Craig West Half	1954	OK	29N-23E-33	1-100	MDHC (2020)
29N23E33_09	Big Jim, Plumb	1954	OK	29N-23E-33	1-50	MDHC (2020)
29N23E33_10	Big Jim Mine	1945	OK	29N-23E-33	1-40	MDHC (2020)
29N23E33_11	Big Jim Mine_10 with contours	1945	OK	29N-23E-33	1-40	MDHC (2020)
29N23E34_03	Ruth Goodeagle Allotment	ND	OK	29N-23E-34		MDHC (2020)
29N23E35_02	Buckeye Mine	ND	OK	29N-23E-35	1-100	MDHC (2020)
29N23E36_03	Silver Streak	1953	OK	29N-23E-36	1-50	Keheley (2020)
29N24E17_04	Discard	1929	OK	29N-24E-17	1-40	MDHC (2020)
29N24E17_05	Clark and Discard	ND	OK	29N-24E-17		MDHC (2020)
29N24E17_07	Warren Lease	ND	OK	29N-24E-17		MDHC (2020)
29N24E17_08	Clark	1929	OK	29N-24E-17	1-40	MDHC (2020)
29N24E18_02	Bingham Lease	ND	OK	29N-24E-18	1-40	MDHC (2020)
29N24E18_04	Diamond Joe (Blue Streak)	ND	OK	29N-24E-18	1-40	MDHC (2020)
29N24E19_02	Campbell	1938	OK	29N-24E-19	1-40	Keheley (2020)
29N24E19_03	Campbell	1940	OK	29N-24E-19	1-40	Keheley (2020)
29N24E19_06	Malsbury	1943	OK	29N-24E-19	1-40	Keheley (2020)
29N24E19_07	Malsbury	1928	OK	29N-24E-19	1-40	MDHC (2020)
29N24E19_08	Malsbury	1943	OK	29N-24E-19	1-40	MDHC (2020)
29N24E19_11	Bendene Lease	1926	OK	29N-24E-19	1-40	MDHC (2020)

Table 4A Continued

Map ID	Map Title	Year	State	T-R-S	Scale	Reference
29N24E19_14	Campbell	ND	OK	29N-24E-19	1-40	MDHC (2020)
29N24E30_03	Patty C Mine (Pearl Mine)	ND	OK	29N-24E-30	1-40	MDHC (2020)
29N24E30_04	120 Acres	ND	OK	29N-24E-30	1-100	MDHC (2020)
29N24E30_05	Abrams Land	ND	OK	29N-24E-30	1-200	MDHC (2020)
29N24E30_06	Kaw Lead Co	1926	OK	29N-24E-30	1-40	MDHC (2020)
29N24E31_03	Waxahachie and Red Eagle Lease	1948	OK	29N-24E-31	1-40	MDHC (2020)
29N24E31_04	Old Abe Mine	ND	OK	29N-24E-31	1-40	MDHC (2020)
29N24E32_01	Black Snake	ND	OK	29N-24E-32	1-40	MDHC (2020)
34S23E34_02	Karcher Land	ND	KS	34S-23E-34	1-100	Keheley (2020)
34S23E34_03	Karcher	ND	KS	34S-23E-34	1-50	Keheley (2020)
34S24E26_01	HHH Lease	1945	KS	34S-24E-26	1-40	MDHC (2020)
34S24E26_03	HHH Lease	1945	KS	34S-24E-26	1-40	MDHC (2020)
34S24E31_01	Sparlin	1949	KS	34S-24E-31	1-50	MDHC (2020)
34S24E33_01	Paxson Mine w/ ore blocks	1947	KS	34S-24E-33	1-100	MDHC (2020)
34S24E33_04	Abel Swalley Land	1937	KS	34S-24E-33	1-100	MDHC (2020)
34S24E34_01	Brugger 160 Acres	ND	KS	34S-24E-34	1-200	MDHC (2020)
34S24E34_03	Brugger 160 Acres	ND	KS	34S-24E-34	1-100	MDHC (2020)
34S24E34_04	Brugger 160 Acres_Variation of _03	ND	KS	34S-24E-34	1-100	MDHC (2020)
34S24E35_10	Beck	1929	KS	34S-24E-35	1-50	MDHC (2020)
34S24E35_12	Old M&H Mine	1944	KS	34S-24E-35	1-50	MDHC (2020)
35-01	Cactus Mine	1959	OK	29N-22E-1	1-100	Keheley (2020)
35S23E10_01	Athletic Chubb (A.D. Chubb)	1943	KS	35S-23E-10	1-100	MDHC (2020)
35S23E10_02	Grace B	1939	KS	35S-23E-10	1-50	MDHC (2020)
35S23E10_04	Big John-Black Eagle	1946	KS	35S-23E-10	1-100	MDHC (2020)
35S23E10_08	Big John-Black Eagle	1946	KS	35S-23E-10	1-100	MDHC (2020)
35S23E10_09	Big John	1946	KS	35S-23E-10	1-100	MDHC (2020)
35S23E10_12	Jarrett Lease	ND	KS	35S-23E-10	1-100	MDHC (2020)
35S23E10_18	Big John D&E and Black Eagle A,B & F (K Bed)	1950	KS	35S-23E-10	1-100	MDHC (2020)
35S23E10_19	Big John D&E and Black Eagle A,B & F (M Bed)	1950	KS	35S-23E-10	1-100	MDHC (2020)
35S23E10_20	Big John D, E,H, &I and Black Eagle F&J (M Bed)	1942	KS	35S-23E-10	1-100	MDHC (2020)
35S23E10_21	Big John D&E and Black Eagle A,B & F (GH Bed)	1950	KS	35S-23E-10	1-100	MDHC (2020)
35S23E10_22	Big John-Black Eagle (GH and E Bed)	1950	KS	35S-23E-10	1-100	MDHC (2020)
35S23E11_01	Bendelari	1942	KS	35S-23E-11	1-50	MDHC (2020)

Table 4A Continued

Map ID	Map Title	Year	State	T-R-S	Scale	Reference
35S23E11_02	DeArmand Mine	1929	KS	35S-23E-11	1-40	MDHC (2020)
35S23E11_04	Tulsa-Quapaw	1950	KS	35S-23E-11	1-50	MDHC (2020)
35S23E11_05	Tulsa-Quapaw_M	ND	KS	35S-23E-11	1-100	MDHC (2020)
35S23E11_09	Fox Mine	1948	KS	35S-23E-11	1-50	MDHC (2020)
35S23E11_14	Robinson (East side)	1944	KS	35S-23E-11	1-40	MDHC (2020)
35S23E11_16	Robinson (West side)	ND	KS	35S-23E-11	1-40	MDHC (2020)
35S23E11_18	Bendelari	1947	KS	35S-23E-11	1-50	MDHC (2020)
35S23E11_21	King Brand	1939	KS	35S-23E-11	1-50	MDHC (2020)
35S23E11_23	King Brand	ND	KS	35S-23E-11	1-50	MDHC (2020)
35S23E11_25	Longacre Mine	ND	KS	35S-23E-11	1-50	MDHC (2020)
35S23E11_26	Longacre Mine	1945	KS	35S-23E-11	1-50	MDHC (2020)
35S23E11_27	Wilbur Mine	1950	KS	35S-23E-14	1-100	MDHC (2020)
35S23E11_29	Wilbur Mine (K bed)	1950	KS	35S-23E-14	1-100	MDHC (2020)
35S23E11_32	Lawyers Mine	1929	KS	35S-23E-14	1-40	MDHC (2020)
35S23E11_34	Boska Mine	1929	KS	35S-23E-14	1-40	MDHC (2020)
35S23E11_36	Boska Mine	1929	KS	35S-23E-14	1-40	MDHC (2020)
35S23E12_01	Jarrett Mine	1946	KS	35S-23E-12	1-100	MDHC (2020)
35S23E12_02	Jarrett Mine	1946	KS	35S-23E-12	1-100	MDHC (2020)
35S23E12_04	Jarrett Mine_Variation of _03	ND	KS	35S-23E-12	1-100	MDHC (2020)
35S23E12_08	Webber Mine	1950	KS	35S-23E-12	1-100	MDHC (2020)
35S23E12_10	Kansouri Mine_Variation of _09	1945	KS	35S-23E-12	1-100	MDHC (2020)
35S23E12_11	Cherokee Mine	1950	KS	35S-23E-12	1-100	MDHC (2020)
35S23E13_01	Blue Diamond Mine	1949	KS	35S-23E-13	1-50	MDHC (2020)
35S23E13_02	Blue Mound Mine (middle and upper levels)	1949	KS	35S-23E-13	1-50	MDHC (2020)
35S23E13_03	Blue Mound Mine	1945	KS	35S-23E-13	1-50	MDHC (2020)
35S23E13_04	Chubb Mine	1942	KS	35S-23E-13	1-100	MDHC (2020)
35S23E13_05	Chubb Mine_colored pencil outlines	1942	KS	35S-23E-13	1-100	MDHC (2020)
35S23E13_06	Blue Diamond Mine	1945	KS	35S-23E-13	1-50	MDHC (2020)
35S23E2_02	Bilharz Mining Co. Sec 2 and 11_Sections hand drawn on _01	ND	KS	35S-23E-2,11	1-100	MDHC (2020)
35S23E2_08	Northern	1953	KS	35S-23E-2	1-50	MDHC (2020)
35S23E3_05	Big John-Lucky Jew Mines	1946	KS	35S-23E-3	1-100	MDHC (2020)
35S23E3_08	Lucky Jew-Parmenter "40"	1945	KS	35S-23E-3	1-100	MDHC (2020)
35S23E3_09	Big John-Lucky Jew Mines (upper beds)	1947	KS	35S-23E-3	1-100	MDHC (2020)

Table 4A Continued

Map ID	Map Title	Year	State	T-R-S	Scale	Reference
35S23E3_10	Stebbins Fee	ND	KS	35S-23E-3	1-100	MDHC (2020)
35S23E3_11	Karcher Mining Tract	1947	KS	35S-23E-3	1-100	MDHC (2020)
35S23E3_13	Stebbins - Lucky Jew	ND	KS	35S-23E-3	1-100	Keheley (2020)
35S24E10_07	Part of Ballard Area	1949	KS	35S-24E-10	1-100	MDHC (2020)
35S24E10_09	Bailey Part of Ballard Area	1940	KS	35S-24E-10	1-100	MDHC (2020)
35S24E10_13	Ballard and Slaughter Part of Ballard Area	1949	KS	35S-24E-10	1-100	MDHC (2020)
35S24E13_02	Harrington Mine	1943	KS	35S-24E-13	1-50	MDHC (2020)
35S24E13_03	Harrington Mine	1951	KS	35S-24E-13	1-100	MDHC (2020)
35S24E13_06	Commonwealth No. 2	ND	KS	35S-24E-13	1-40	MDHC (2020)
35S24E13_09	Hunter Land	ND	KS	35S-24E-13	1-100	MDHC (2020)
35S24E16_01	Lucky OK Mine	1952	KS	35S-24E-16	1-40	MDHC (2020)
35S24E16_02	Lucky OK Mine	1937	KS	35S-24E-16	1-50	MDHC (2020)
35S24E16_03	Lucky OK Mine	ND	KS	35S-24E-16	1-50	MDHC (2020)
35S24E17_01	Kansas Line Mine	ND	KS	35S-24E-17	1-100	MDHC (2020)
35S24E17_02	Kansas Line Mine_West portion	1947	KS	35S-24E-17	1-50	MDHC (2020)
35S24E17_03	John Stoskopf	1943	KS	35S-24E-17	1-100	MDHC (2020)
35S24E2_01	Homestake	ND	KS	35S-24E-2	1-50	MDHC (2020)
35S24E2_05	Racetrack Mine	ND	KS	35S-24E-2	1-40	MDHC (2020)
35S24E2_06	Racetrack Mine	1948	KS	35S-24E-2	1-40	MDHC (2020)
35S24E2_09	Clara Jane	ND	KS	35S-24E-2	1-50	MDHC (2020)
35S24E2_10	Clara Jane	ND	KS	35S-24E-2	1-50	MDHC (2020)
35S24E2_11	Beck No. 3 (Wakeman and Hocker Leases)	1929	KS	35S-24E-2	1-50	MDHC (2020)
35S24E2_16	Leopard_similar to _15	1947	KS	35S-24E-2	1-100	MDHC (2020)
35S24E2_19	North Ballard Area	1949	KS	35S-24E-2	1-50	MDHC (2020)
35S24E2_22	Portion of Ballard Area	1946	KS	35S-24E-2	1-100	MDHC (2020)
35S24E3_01	Hartley	ND	KS	35S-24E-3		MDHC (2020)
35S24E3_02	Portion of Ballard Area	1957	KS	35S-24E-3	1-100	MDHC (2020)
35S24E3_03	English 'O	1952	KS	35S-24E-3	1-40	MDHC (2020)
35S24E3_04	Smith	1947	KS	35S-24E-3	1-50	MDHC (2020)
35S24E3_05	English 'O	1946	KS	35S-24E-3	1-100	MDHC (2020)
35S24E4_01	Swalley "D" Mine	1947	KS	35S-24E-4	1-100	MDHC (2020)
35S24E6_01	MacArthur	1951	KS	35S-24E-6	1-50	MDHC (2020)
35S24E6_04	MacArthur	ND	KS	35S-24E-6		MDHC (2020)

Table 4A Continued

Map ID	Map Title	Year	State	T-R-S	Scale	Reference
35S24E7_01	Foley	1950	KS	35S-24E-7	1-100	MDHC (2020)
35S24E7_04	Westside Mine	1950	KS	35S-24E-7	1-100	MDHC (2020)
35S24E7_06	Westside Mine (Upper levels)	1944	KS	35S-24E-7	1-100	MDHC (2020)
35S24E7_07	Harris Old Lease No. 24 (Big Yank)	1947	KS	35S-24E-7	1-40	MDHC (2020)
35S24E7_09	Big Yank	ND	KS	35S-24E-7	1-40	MDHC (2020)
35S24E7_11	Blue Mound Mine	ND	KS	35S-24E-7	1-40	MDHC (2020)
35S24E7_12	Harris Mine Lease 24	1946	KS	35S-24E-7	1-40	MDHC (2020)
35S24E7_14	Lease No. 24	ND	KS	35S-24E-7	1-40	MDHC (2020)
37-02	Blue-Bird Wilson Mine	1968	OK	29N-22E-25	1-100	Keheley (2020)
409-N	Half Section Maps_Brichta	1957	OK	29N-23E-32	1-200	Keheley (2020)
413-S	Half Section Maps_Brichta	1958	OK	29N-23E-36	1-200	Keheley (2020)
434-Na	Half Section Maps_Brichta	1956	OK	29N-23E-29	1-200	Keheley (2020)
434-Nb	Half Section Maps_Brichta	1956	OK	29N-23E-29	1-200	Keheley (2020)
434-Nc	Half Section Maps_Brichta	1956	OK	29N-23E-29	1-200	Keheley (2020)
434-Nd	Half Section Maps_Brichta	1956	OK	29N-23E-29	1-200	Keheley (2020)
434-S	Half Section Maps_Brichta	1956	OK	29N-23E-29	1-200	Keheley (2020)
DM10	Picher_Workings	1944	OK, KS	Picher Field		MDHC (2020)

APPENDIX 4B
Mine Map of the Picher Field Underground Workings

Picher Field Underground Mine Workings of the Abandoned Tri-State Lead-Zinc Mining District in the United States

Nicholas L. Shepherd[1*], Ed Keheley[2] Russell C. Dutnell[3], Carlton A. Folz[1], Brandon Holzbauer-Schweitzer[1], and Robert W. Nairn[1]

[1]Center for Restoration of Ecosystems and Watersheds
School of Civil Engineering and Environmental Science, University of Oklahoma,
202 W. Boyd St. Room 334, Norman, OK 73019-1024

[2]Keheley and Associates Inc,
220 S 640 Rd, Quapaw, OK 74363

[3]Riverman Engineering, PLC.
1504 Ann Arbor, Norman, OK 73069

*Corresponding author: Nick.Shepherd@ou.edu

CREW Center for Restoration of Ecosystems and Watersheds
University of Oklahoma

The UNIVERSITY of OKLAHOMA
Gallogly College of Engineering
School of Civil Engineering and Environmental Science

94° 54' W · 94° 51' W · 94° 48' W · 94° 45' W
37° 3' N · 37° 0' N · 36° 57' N

Baxter Springs
Kansas (Cherokee Co.)
Oklahoma (Ottawa Co.)
Treece
Monarch
Mound City
Hockerville
Picher
Cardin
Whitebird
Douthat
Century
New Joplin
Quapaw
Zincville
Commerce
Hattenville
North Miami
Mission City
Lincolnville
Happy Hollow
Sunny Side

E and Chester Beds[1]	*Mining Lease (Alternate Mining Lease)*[2]
G-H Beds[1]	**Surviving Camps**
K Bed[1]	~~***Abandoned Camps***~~
M Bed[1]	
Sheet Ground Workings (O-P-Q Beds)[1]	
Natural Caves	
Lease Boundaries	
State Line	
Open Mine Shafts	
Closed or Status Unknown Mine Shafts	

[1]Bedding layers represent best approximations based on available data from historical mine maps and drill logs.

[2]Lease names based on Eagle Picher 1958 plate maps with alternate names representing previous naming that was shown on historical maps found in Appendix A.

Explanation of Informal Bedding Layer Classifications[1]

Series	Member	Informal Letter Classification	Thickness (m)
Meramec	Moccasin Bend Member	Chester Beds, E, and G-H Beds	0-43
	Baxter Springs Member	K Bed	0-1.5
			0-15
			0-18
Osage	Short Creek Oolite Member	M Bed	0-3
	Joplin Member		0-30
	Grand Falls Chert Member	Sheet Ground Workings (O-P-Q Beds)	7.5-30

Disconformity

[1]Modified from Fowler 1942; Reed et al. 1955; Brockie et al. 1968; McKnight and Fischer 1970; Luza, 1986.

N
Scale Ratio 1:35,000
1,400 0 1,750 3,500 Meters

Coordinate Reference System
NAD83 Oklahoma State Plane, North Zone, US Foot

Base Map Data Sources
United States Bureau of Land Management, Public Land Survey System: Oklahoma and Kansas Quarter-Quarter Sections;
See appendix A for historic mine map data sources

APPENDIX 5A
Slim Jim Monitoring Well Gage Height Comparison

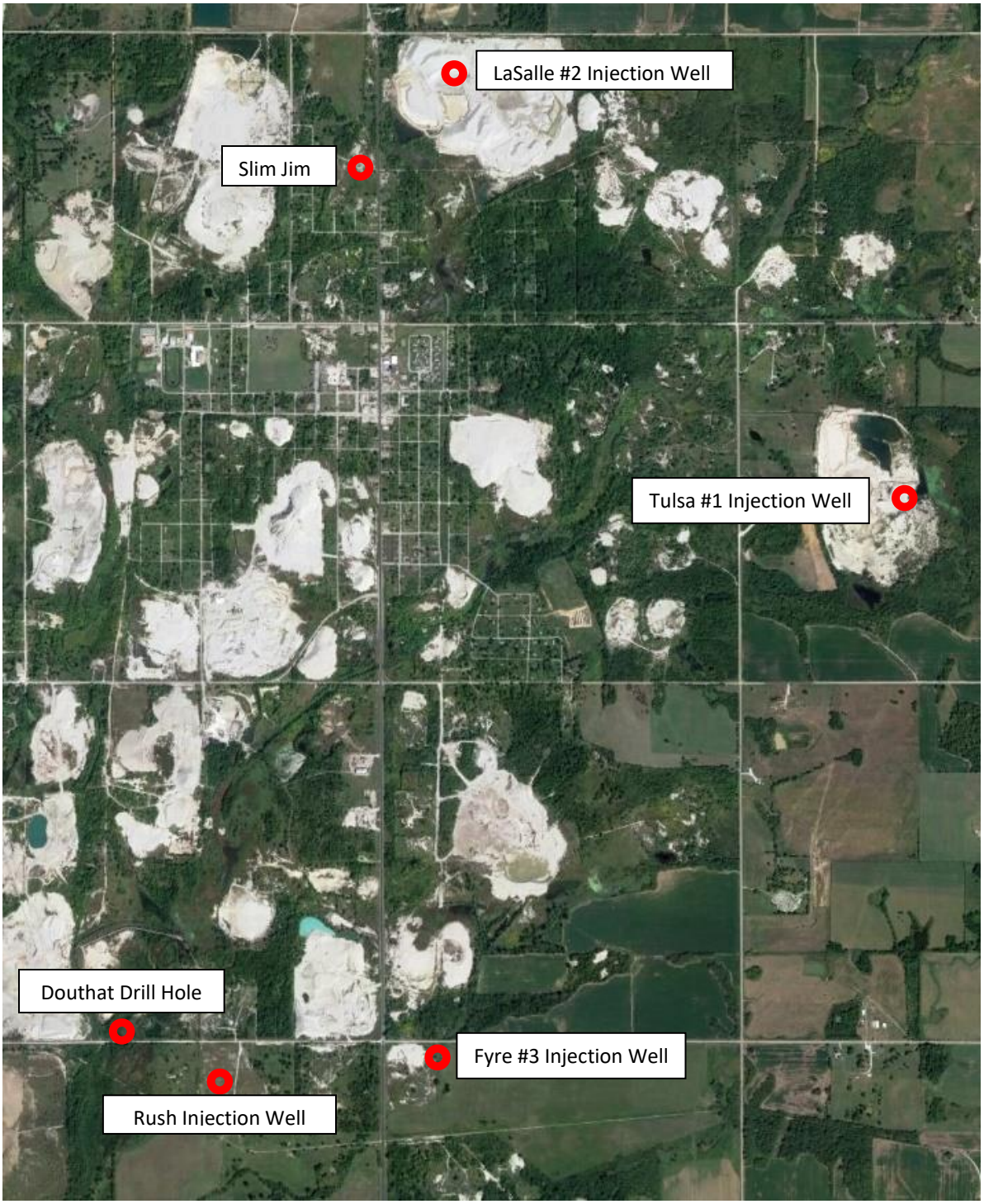

Figure 5A.1: Aerial image of the Picher mining field, showing locations of mine pool monitoring stations that were surveyed during the Tar Creek Operable Unit #4 and the USGS gage station, Slim Jim (Google Earth Image, September 2021)

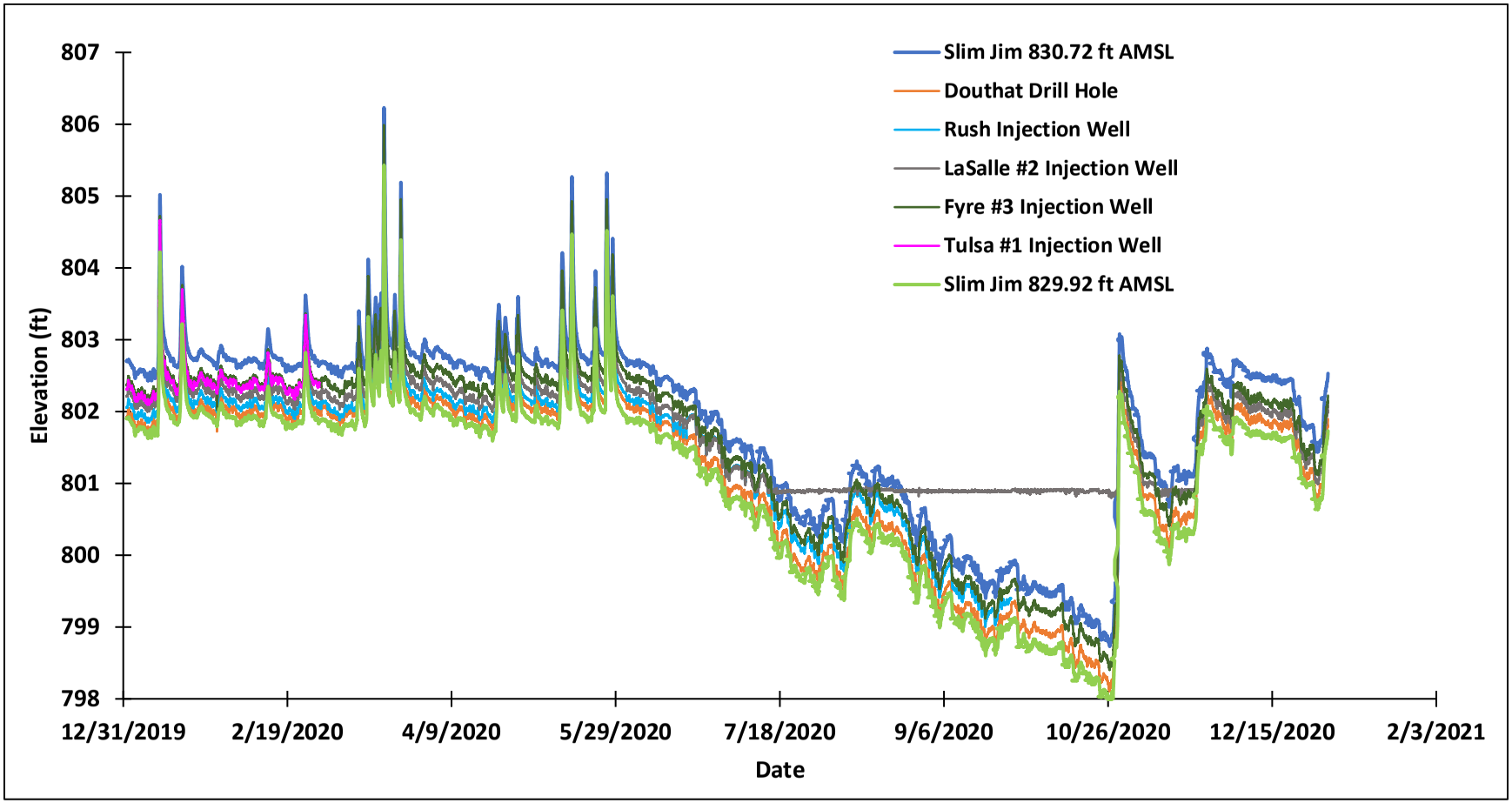

Figure 5A.2: Mine pool water elevations at multiple locations throughout the Picher mining field, comparing the USGS gage station heigh of 830.72 ft AMSL to the recently updated height of 829.92 ft AMSL in relation to other mine pool gage stations

APPENDIX 5B
Known Inflow Locations

5B.1 Explanation

For this appendix, a known inflow location is defined as an open mine shaft that is within close proximity of a stream channel and has been field verified to receive water from the nearby stream. Potential inflow locations are defined as open mine features that have shown signs of receiving water, such as eroded channels into the shaft or flowing water subsurface into the shaft. Approximate inflow locations are defined as general areas where a groundwater elevation monitoring location has recorded data where the mine pool elevation at the location is higher than the majority of the mine pool.

5B.2 Known Inflow Locations

Tulsa-Quapaw

Name: Tulsa-Quapaw
Location: 37.0072, -94.8572
Claim: Tulsa-Quapaw
Description: Tulsa-Quapaw is an open mine shaft in Kansas that is estimated to be 8 to 10 ft in diameter around which the surrounding soil has been eroded down to bed rock (Figure 5B.2). There appear to be two channels that flow into this mine shaft. The first channel that enters from the south is estimated to be 30 ft wide and incised 10 to 12 ft down to bedrock and appears to be connected to Tar Creek. The second channel that enters from the north appears to be more recent and anthropogenically made. A reclamation project was conducted on the land to the north of the mine shaft in 2009-2010. During this period, the aerial imagery indicates a channel was excavated that leads from the land reclamation site directly into the mine shaft (Figures 5B.3- 5B.4). The underground workings have cavernous connections from the mine shaft to the Douthat discharges (Chapter 4), located 3.45 miles to the south. Additional photos of Tulsa-Quapaw are shown in Figures 5B.5-5B.7.

Figure 5B.1: Aerial image of known inflow locations in relation to the Douthat discharges, with a mine pool water elevation monitoring station shown (Google Earth Image, March 2015)

Figure 5B.2: Tulsa-Quapaw: Tulsa-Quapaw surface inflow to Picher Field mine pool during low flow conditions. Nick is standing in the southern inflow channel (Tar Creek connection). The northern inflow channel (channel excavated during land reclamation) is at the top of the image, with small amounts of water flowing into the mine shaft (Photo Credit: Robert Nairn)

Figure 5B.3: Pre-land reclamation near Treece, KS, with the Tulsa-Quapaw: Tulsa-Quapaw mine shaft identified by a star (Google Earth image – June 15, 2009)

Figure 5B.4: Post-land reclamation near Treece, KS, with the Tulsa-Quapaw: Tulsa-Quapaw mine shaft identified by a star and the red box identifies the zoomed location for Figures 8 and 9 (Google Earth image – March 29, 2015)

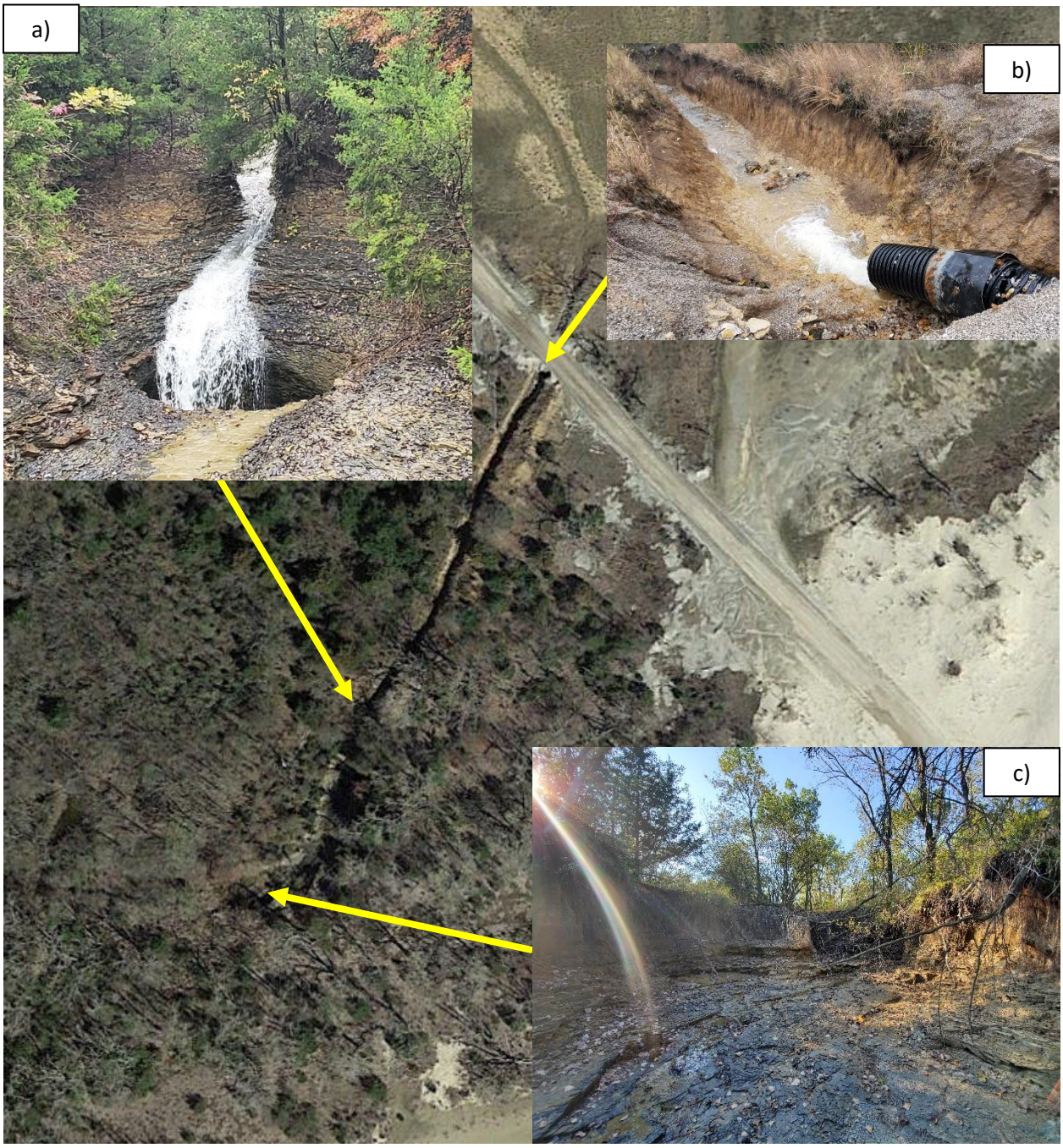

Figure 5B.5: Post-land reclamation, Google Earth image (March 29, 2015): a) 8'-10' diameter mineshaft, with surrounding material eroded down to bedrock with surface runoff from the land reclamation flowing into the shaft from the north. b) Excavated channel entering from the north from land reclamation on site between 2009-2010. c) Eroded/blown out channel where Tar Creek overtops its berms during flooding and flows into the mineshaft

Figure 5B.6: Photo of Tulsa-Quapaw taken using a drone in October 2019

Figure 5B.7: Photo of Tulsa-Quapaw taken during dry conditions in August 2020

Lytle 8th

Name: Lytle 8th
Location: 36.9775, -94.8234
Claim: Acme
Description: Lytle 8th is an open mine shaft in Oklahoma and is estimated to have been a 5 ft by 7 ft shaft. The shaft receives surface water from nearby Lytle Creek when the creek flows outside of its banks. The substantial flow was seen entering the collapse then swirling and disappearing into the mine pool, suggesting the shaft has no blockage and essentially acts as a 5 ft by 7 ft conduit into the mine workings (Figure 5B.8). The concrete that is shown in Figure 5B.8 (b) and Figure 5B.9 is believed to be the original cap of the mineshaft that has rotated into the void and is lodged at an angle. The underground workings have cavernous connections from the mine shaft to the Douthat discharges (Chapter 4), located 1.6 miles to the southwest. There was a mine pool monitoring station located between the Lytle 8th and Douthat (Figure 5B.1**;** MP14 New York) that appear to show evidence of the influence of the Lytle 8th inflow, increasing the localized mine pool elevation one to two feet above the mine pool water elevations measured throughout the Picher field (Figures 5B.13 and 5B.14). Additionally, the data show that Lytle 8th only receives water during larger storm events, where the events on 5/4/21 (Figure 5B.13) and 3/11/20 (Figures 5B.14) did not generate streamflow elevated enough to spill into the open shaft. The Lytle 8th inflow has been known to flood the subsurface mines for decades. The article in Figure 5B.9 discusses the shaft on the Acme claim near Lytle Creek that was responsible for flooding a nearby claim, New York, during a flood event in 1938.

Figure 5B.8: Lytle 8th St. (Acme) surface inflow connection to Picher Field mine pool during a high flow event on September 26th, 2019. a) Water from Lytle Creek entering the eroded collapse b) Water swirling into the mine shaft located below the concrete pads covered in moss

Figure 5B.8: Lytle 8th St. inflow location during dry conditions, showing the rotated concrete cap and the mine pool water elevation under the cap. Photo taken in August 2021

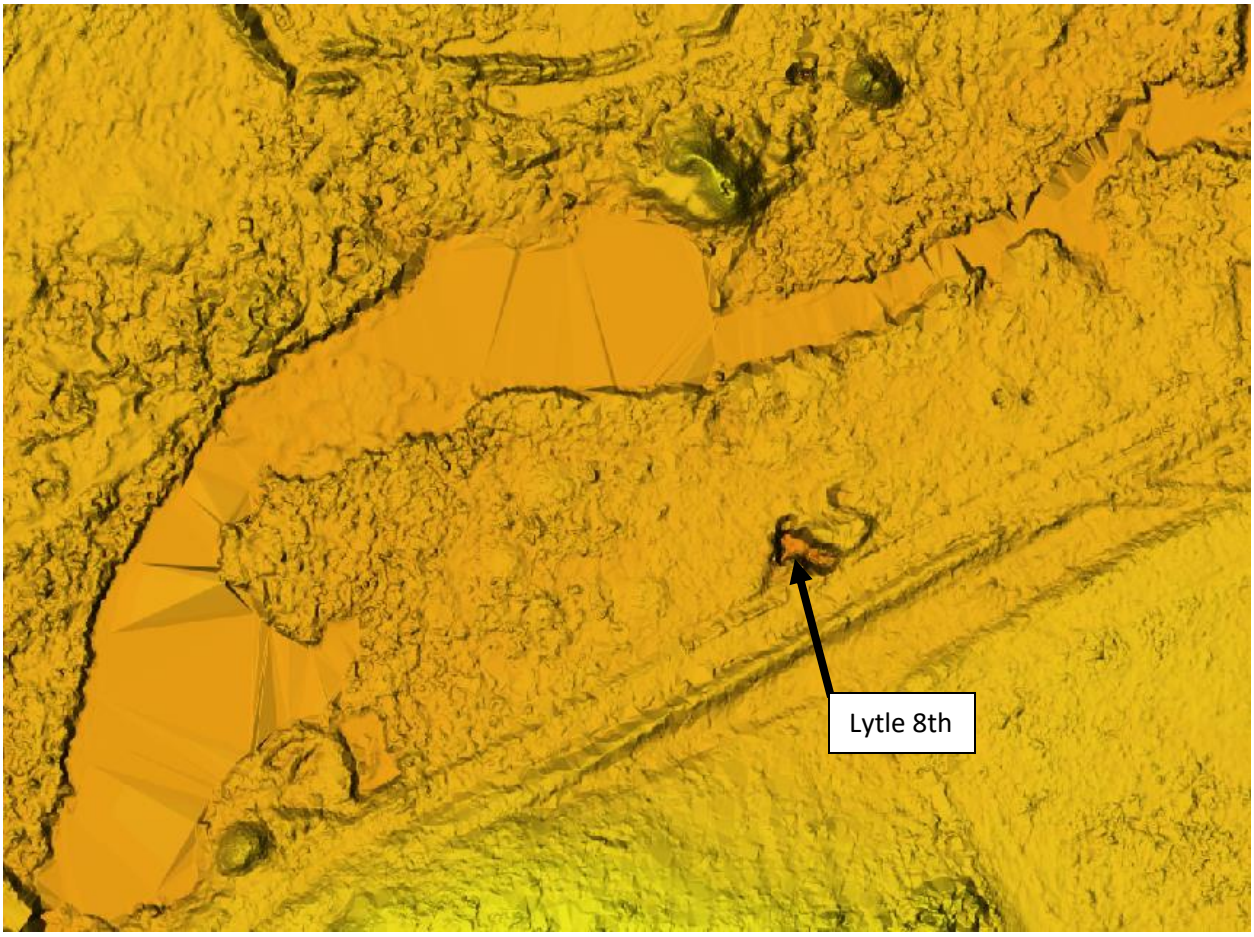

Figure 5B.10: Lytle 8th St. inflow shown on LiDAR digital elevation model flown in July 2020.

May 30, 1938

MINES AND MINING

HOWARD O. GRAY, Editor.

Several Picher Area Mines Flooded As Rain Sends Streams on Rampage

An avalanche of water caused by torrential rains early Sunday morning over the Tar creek watershed later in the day rushed violently down the channels of the small stream and its tributaries to overflow and flood several of the zinc and lead mines situated along its course. It was one of the worst floods in the history of the famous Kansas-Oklahoma mining area of the Tri-State district.

Fortunately, mines affected by the floods were closed for Sunday and there was no loss of human life. However, two of eight mules left underground at one mine were drowned. Hundreds of dollars' damage was done by the water to mining properties, principally shafts, but the chief damage will be entailed later through extensive pumping operations of dewatering the underground workings of several mines.

New York Hard Hit.

The New York mine of the Cortez-King Brand Mines Company, in the southeast part of Picher, was the hardest hit. A roadway across Lytle branch, a tributary of Tar creek, with several steel boilers forming a culvert, held the water back at that point and soon rose to swirl down the old Acme field shaft on the east side above the New York property.

More than 100 men worked frantically most of the day Sunday in an effort to block the water off by use of bags of tailings from a nearby tailing pile. Water flowed at a tremendous rate into the shaft for more than 12 hours, beginning at 6 o'clock Sunday morning, according to W. T. Landrum of Baxter Springs, manager of the Cortez-King Brand Company.

At the decision of Mayor J. H. Klinefelter of Picher, G. C. Niday of the Eagle-Picher Mining and Smelting Company and Landrum, several blasts of dynamite were discharged to loosen three of the boilers, which were pulled out to open a larger spillway for the water. By midnight Sunday, the crews of workmen had blocked the water from the Acme shaft. The roadway over the branch connects Picher for residents of Mineral Heights addition, the southeast part of town. It will be rebuilt.

Six mules were hoisted alive yesterday from the New York mine, after being rescued from the flood waters on the 235-foot level. It was in this mine that two mules were drowned. Mining operations had been carried on at the 285-foot level as late as Saturday. The property was to have been closed some time this week due to low ore prices. The flood water rose to around the 225-foot level in parts of the mine. It will require several months to dewater the lower level, Landrum said.

At Zincville, northeast of Picher, Lytle branch spread out of its banks several hundred feet, flooding shafts and underground workings in that area, including those kept the water out of the shaft. Sam Ashe, secretary of the Rialto Mining Corporation, said the swollen waters of Tar creek at this point were the highest he had seen in a period of many years. Further to the south, the creek flooded the roadway leading to the No. 3 tailing plant of the Cardin Mining and Milling Company, where an electric motor was damaged by the storm. Mules in the ground at the Lavrion mine on the Ramage lease were pulled for fear of the rising waters, Ashe said.

At the Big Jim mine on the Craig lease, east of Douthat, water rose underground to a depth of 11 feet in the east part of the workings. Mine operations are expected to get under way today in the west end of the mine workings, where the water rose only about two feet.

A mile further to the east, lightning struck the Muskogee pump station, owned and operated jointly by several mining companies, which was destroyed by fire. A 250-horsepower electric motor, which powered the 14-inch Pomona turbine pump, was a total loss. The extent of damage to the large pump was not learned. The total loss was estimated at $5,000. The large pump drains a greater part of the southeast Picher area. Workmen yesterday had started the construction of a new building, preparatory to placing the pump again in operation as soon as possible.

At the No. 4 property of the St. Louis Smelting and Refining Company, a mile and a half north of Quapaw, the deluge of water in that area broke the dikes of the mill pond at two places. The dikes were repaired, but it probably will be several days before sufficient water can be pumped from the mine to fill the pond in order to operate the mill.

Hailstones, which accompanied the storm, broke the window panes in several mills and derricks, including the mills of the Iron Mountain Lead and Zinc Company and the Andrews Mining and Milling Company.

Paxson Is Flooded.

Two miles west of Baxter Springs, the head waters of Willow creek flooded the Paxson property of the Commerce company. The water ran into both the mill and pump shafts, and the change house at the mine was flooded nearly two feet, according to S. S. Chapel, mine superintendent. The large power plant of the company, west of Cardin, was shut down two hours during the storm, with no damage reported. An oil switch was burned out at the company's Webber mill north of Picher in Kansas, but the plant was placed in operation yesterday. Ground pump electric motors were damaged some at the Commerce Sea Sah, and an old dummy elevator of the Jay Bird was blown down.

TARIFF REDUCTION THREATENS MINING

No Let-up in Fight to Maintain Necessary Protection, Journal Says.

The American Mining Congress Journal recently pointed out editorially that any reduction in the moderate but vitally necessary duties on lead and zinc items would be a "serious blow to our mining industry." The editorial, entitled "A Threat to Mining," follows:

"Inclusion of a number of mineral commodities among the items to be considered in pending negotiations for a trade agreement with the United Kingdom and Canada constitutes an alarming threat to the industries engaged in their extraction and processing in this country.

"As an outstanding example, and without minimizing the importance of other minerals involved, any reduction in the moderate but vitally necessary duties on the lead and zinc items on the list would be a serious blow to our mining industry.

"Any action tending to lower prices for these metals or ores in the United States would almost certainly result in loss of employment for many thousands of men; lower the tax revenues of federal, state and local governments; seriously jeopardize the income of many more tens of thousands of people dependent on the welfare of the mining industry; and actually threaten seriously to make the United States dependent in part on foreign countries for supplies of these metals—termed by the war department as 'critical minerals'—thus destroying the self-sufficiency in these materials built up by means of our moderate tariff protection.

"A plentiful supply of relevant factual information has been submitted to members of congress and the state department, and there will be no let-up in the fight to maintain the vitally necessary protection now afforded to American mining."

Figure 5B9: Article from Tri-State Zinc & Lead Ore Producers Association published on May 30th, 1938, describing the Acme shaft flooding workings on adjacent claims

Wesley Smith

Name: Wesley Smith
Location: 36.953, -94.8329
Claim: Wesley Smith
Description: Wesley Smith is a partially open mine shaft in Oklahoma. There is an eroded channel that directs water from Quapaw Creek (Figure 5B.12) and ends at the mine shaft (Figures 5B.10 and 5B.11). The underground workings have cavernous connections from the mine shaft to the Douthat discharges (Chapter 4), located 0.7 miles to the northwest.

Figure 5B.10: Wesley Smith inflow location where the channel ends at the edge of the shaft. Photo taken in October 2020

Figure 5B.10: Wesley Smith inflow location close-up of the partially open mine shaft, with large pieces of concrete lodged into portions of the opening. Photo taken in October 2020

Figure 5B.11: Inflow channel that directs water into the Wesley Smith inflow shaft. Photo taken in October 2020

5B.3 Potential and Approximate Inflow Locations

Mid-Continent

Location: 37.0047, -94.8603
Claim: Mid-Continent
Description: Mid-continent is an open mine shaft in KS, located a few hundred meters west of Tulsa-Quapaw, across Tar Creek (Figures 5B.1 and 5B.12). The shaft has an approximate depth to water of 28 ft and appears to be partially filled with debris at 33 ft. The shaft does have a decent amount of runoff water from the landscape that flows into the shaft (Figures 5B.15 and 5B.16). The runoff water, while contributing to the mine pool, did not contribute a substantial amount of water that would show a localized increase in the mine pool water elevations. The nearby Mid-Continent drill hole had a deployed pressure sensor in 2020 and 2021 and the data show that the mine pool at Mid-Continent does fluctuate with the mine pool, it does not drastically exceed the mine pool elevations of other measuring stations (Figures 5B.13 and 5B.14). However, given the shaft's proximity to Tar Creek and that the opening is flush with the ground, it is possible that the Mid-continent shaft could take on water from Tar Creek in extremely elevated flooding events that did not occur during the deployment of the pressure sensors at this site.

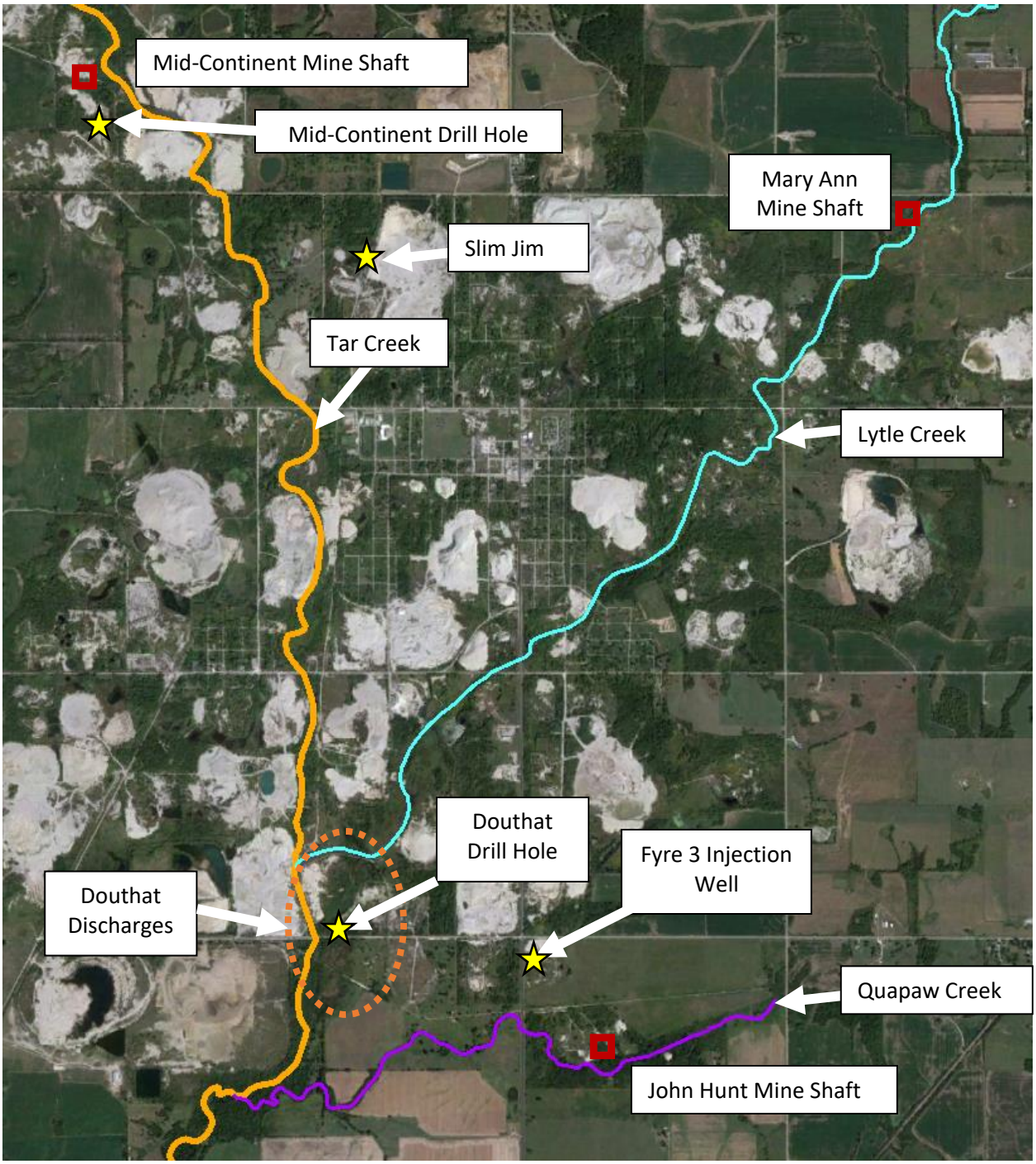

Figure 5B.12: Aerial image of the Picher mining field, showing potential and approximate inflow locations and selected mine pool monitoring locations (Google Earth Image, September 2021)

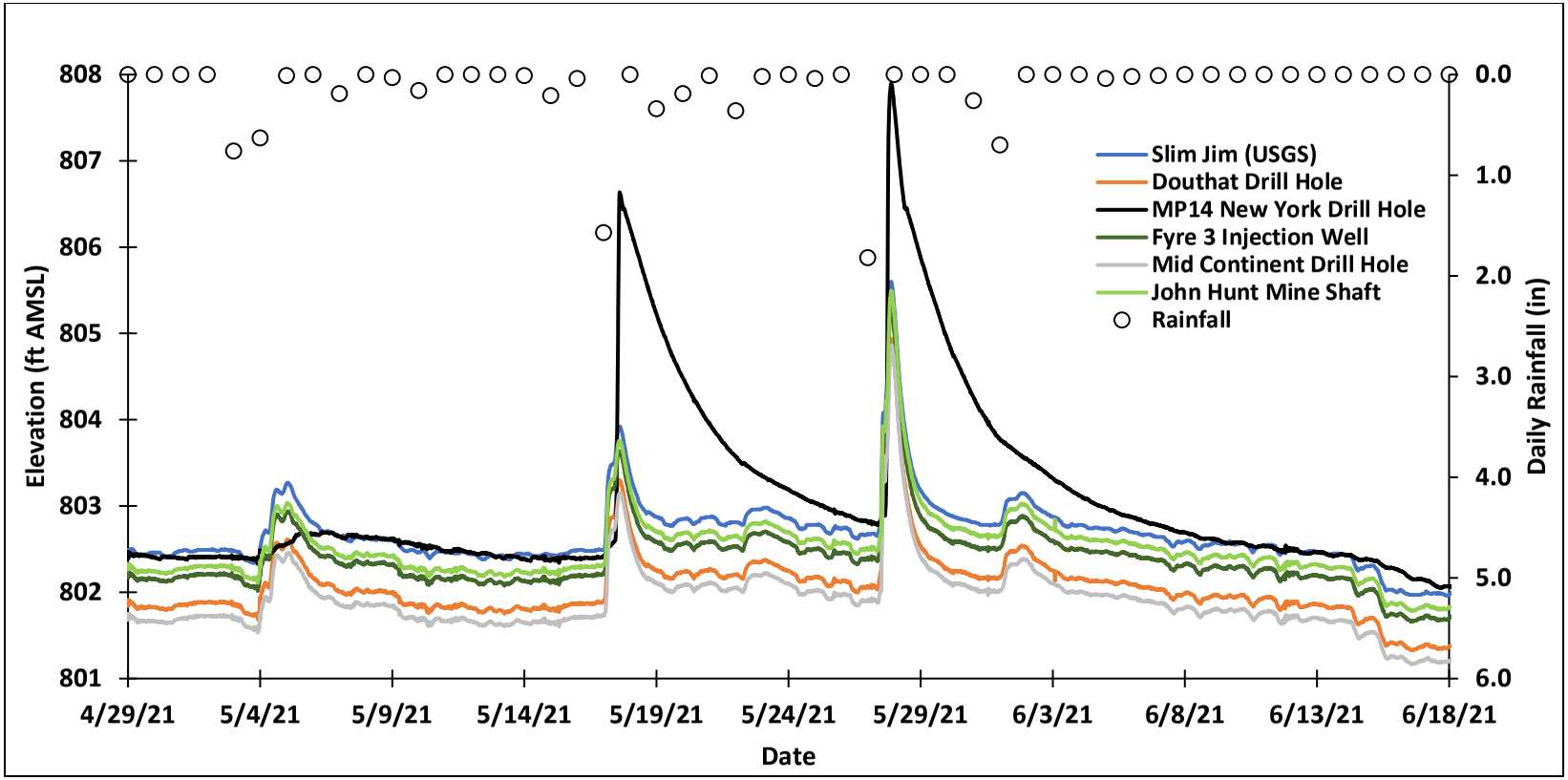

Figure 5B.13: Water elevations of the Picher field mine pool in spring of 2021 at stations located throughout the Picher field, with daily rainfall inversely plotted

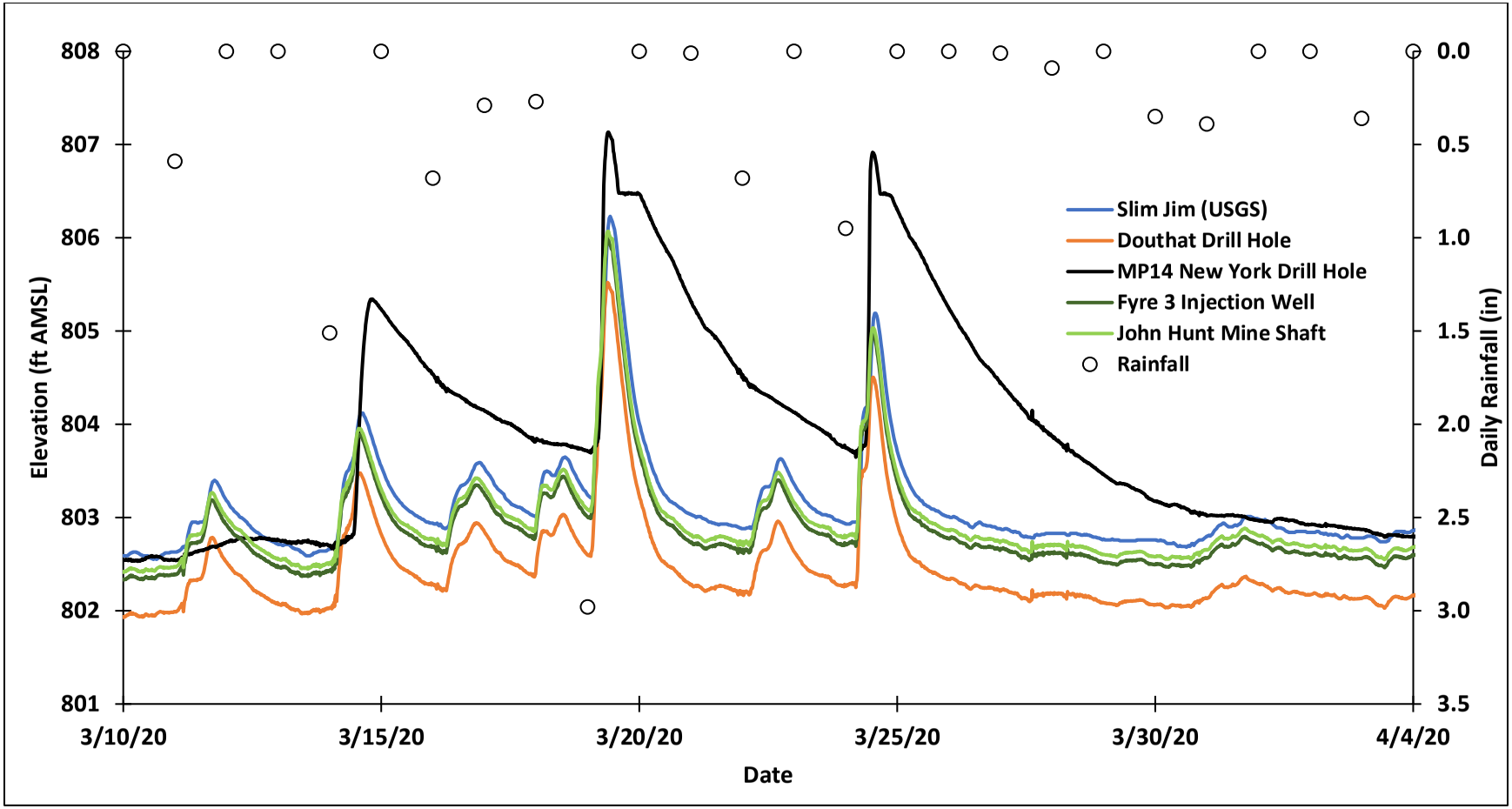

Figure 5B.14: Water elevations of the Picher field mine pool in spring of 2020 at stations located throughout the Picher field, with daily rainfall inversely plotted

Figure 5B.15: Mid-Continent open mineshaft receiving runoff water during a rain event. Photo taken October 2019

Figure 5B.16: Mid-Continent open mineshaft receiving runoff water during a rain event. Photo taken October 2019

Mary Ann

Location: 36.9969, -94.8042
Claim: Mary Ann
Description: Mary Ann is an open equipment mine shaft measuring 8 ft x 12 ft nearby Lytle Creek (Figures 5B.12, 5B.17, 5B.18). The depth to water (DTW) at this shaft is typically greater than 20 ft deep. The total shaft depth is currently 155 ft, with the ceiling/floor depth of the mine voids on the historical mine maps recorded at 141/157 ft below the surface. On occasion the water elevation sharply increases during rainfall events, plateaus well above the mine pool elevation recorded in the rest of the Picher Field, then sharply falls a few days later (Figure 5B.19). As shown in Figure 5B.17, the water level is only a few feet below the ground surface, but the water was not actively flowing into the shaft from the surface, nor did there appear to be turbulent flow where water might have been entering from the walls of the shaft. However, if the open shaft itself is not the inflow location, that suggests there might be another unknown inflow location that is hydraulically connected to the same mine voids as Mary Ann that is causing the increased water elevation. Although the Mary Ann mine workings are hydraulically connected to the larger Picher mining field, the connection is small (Chapter 4). The incredibly high mine pool elevation recorded at Mary Ann might be because the hydraulic connection to the Douthat discharges, located 3.3 miles to the southwest, is partially obstructed. Additionally, the depth samples collected at Mary Ann have also been consistently low conductivity samples that are more representative of rainwater than the mine pool, further suggesting that the water in this area of the mine pool originates from the surface and not groundwater recharge.

Figure 5B.17: Mary Ann open equipment mine shaft showing high water elevations following a rainfall event. Photo taken September 2019

Figure 5B.18: Mary Ann open equipment mine shaft on a typical day. Photo taken February 2021 during a sampling event

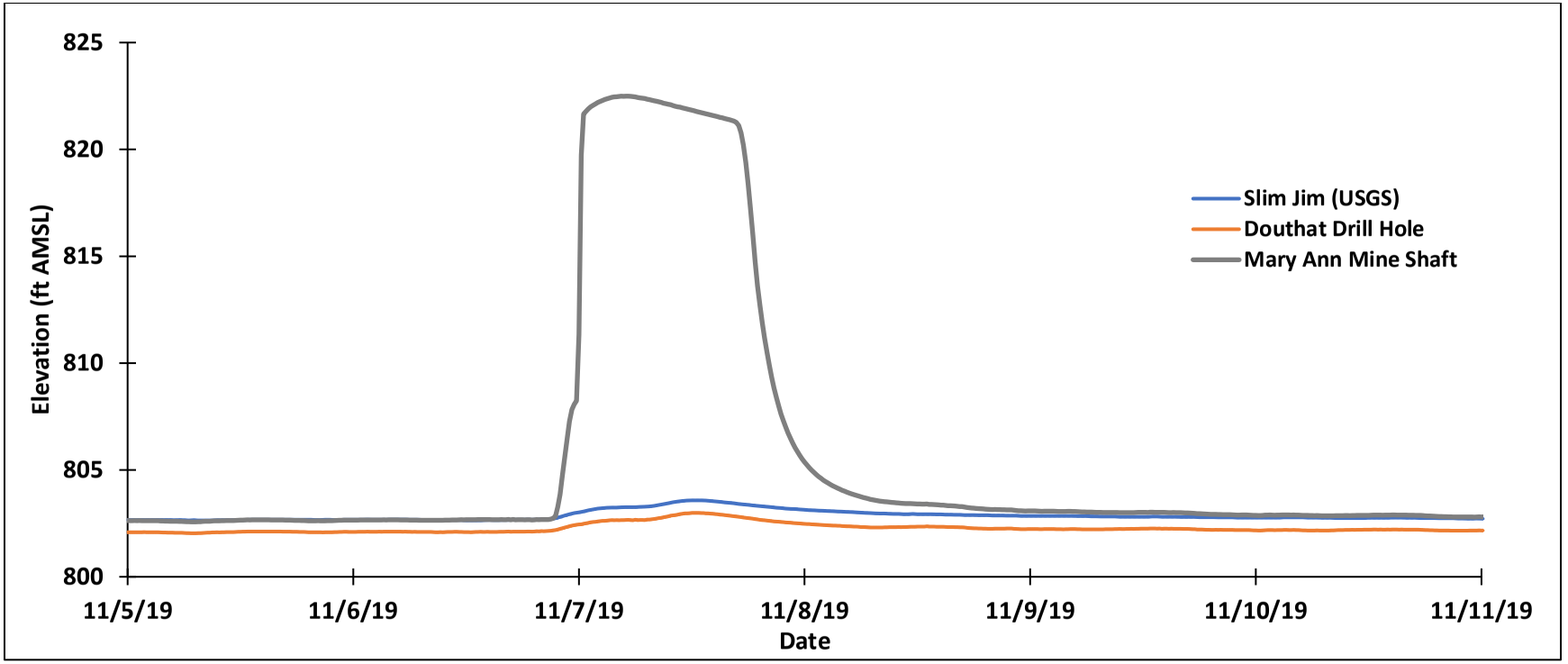

Figure 5B.19: Water elevations of the Picher field mine pool in November 2019, showing a single event where one measuring station (Mary Ann) substantially exceeded the mine pool water elevations at two other monitoring stations

John Hunt

Location: 36.9505, -94.8246
Claim: John Hunt
Description: John Hunt is an open mine shaft in close proximity to Quapaw Creek in OK (Figure 5B.12). The shaft is 5 ft by 7 ft and has an intact concrete collar that extends approximately 3 ft above the ground level (Figures 5B.20 and 5B.21). The current depth of the shaft is 121 ft, but the mine void ceiling/floor depths recorded on the historical maps were 181/194 ft below the surface. The mine pool water elevation data collected inside the John Hunt shaft and at the nearby Fyre injection well suggest the John Hunt shaft has not been a major inflow location during the period of data collection in 2020 and 2021. However, the site has the potential to become a major inflow location. It is only a matter of time until the shaft collar collapses since it has been documented that a decent amount of water is already entering the shaft through the failing concrete collar. The John Hunt mine workings have a direct hydraulic connection to the Douthat Discharges (Chapter 4).

Figure 5B.20: John Hunt open mine shaft near Quapaw Creek. Photo taken September 2019

Figure 5B.21: Inside the John Hunt open mine shaft near Quapaw Creek, showing water entering through the concrete cracks on the corner of the shaft. Photo taken September 2019

APPENDIX 5C
Figures of Mine Pool Elevation Vs. Metals Concentrations

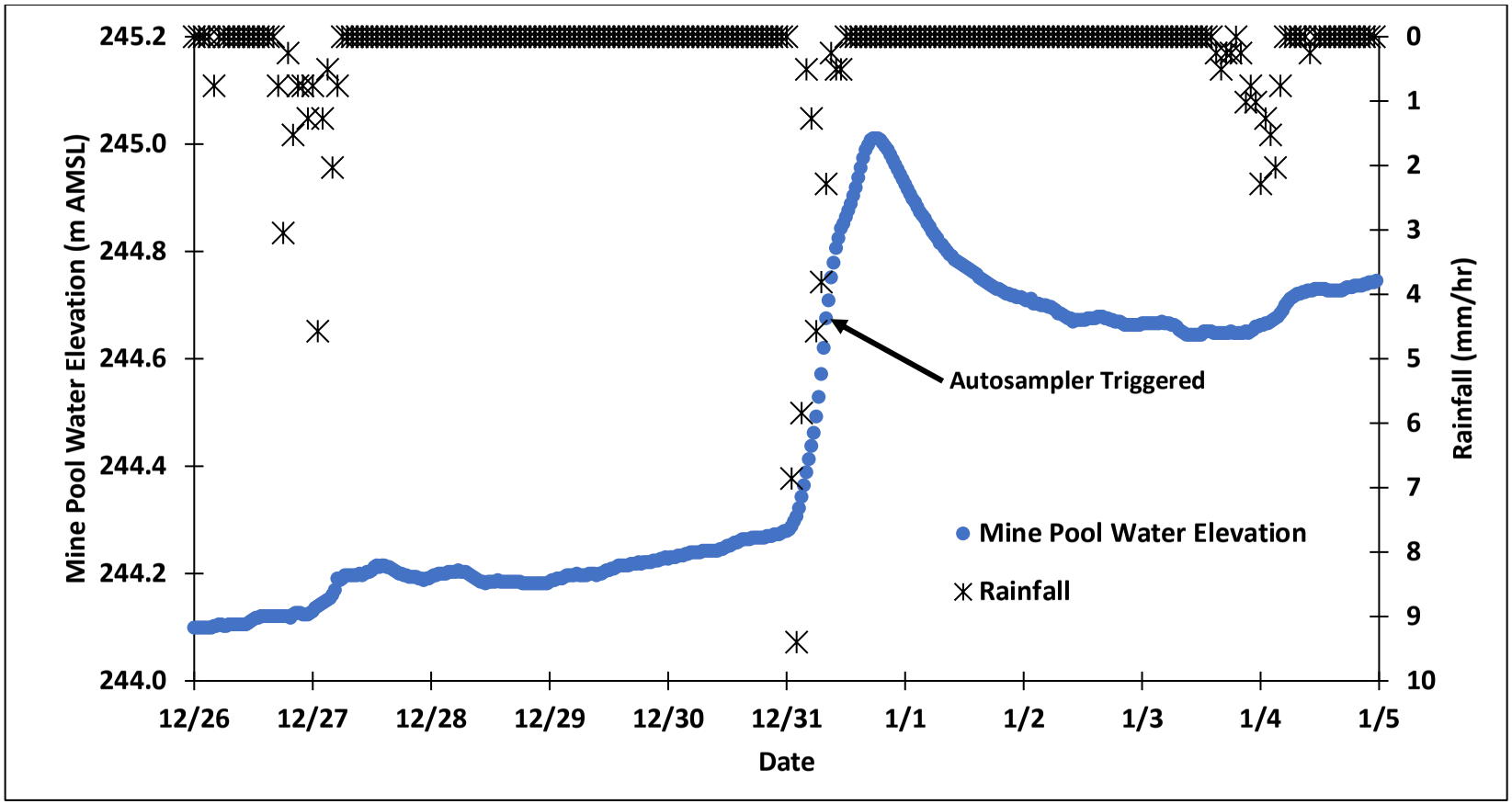

Figure 5C.1: Picher mining field mine pool water elevations, as measured by the USGS Slim Jim groundwater monitoring station (65942094504203), versus rainfall intensity measured using an on-site rain gage at Douthat, OK from December 26th, 2018, to January 5th, 2019

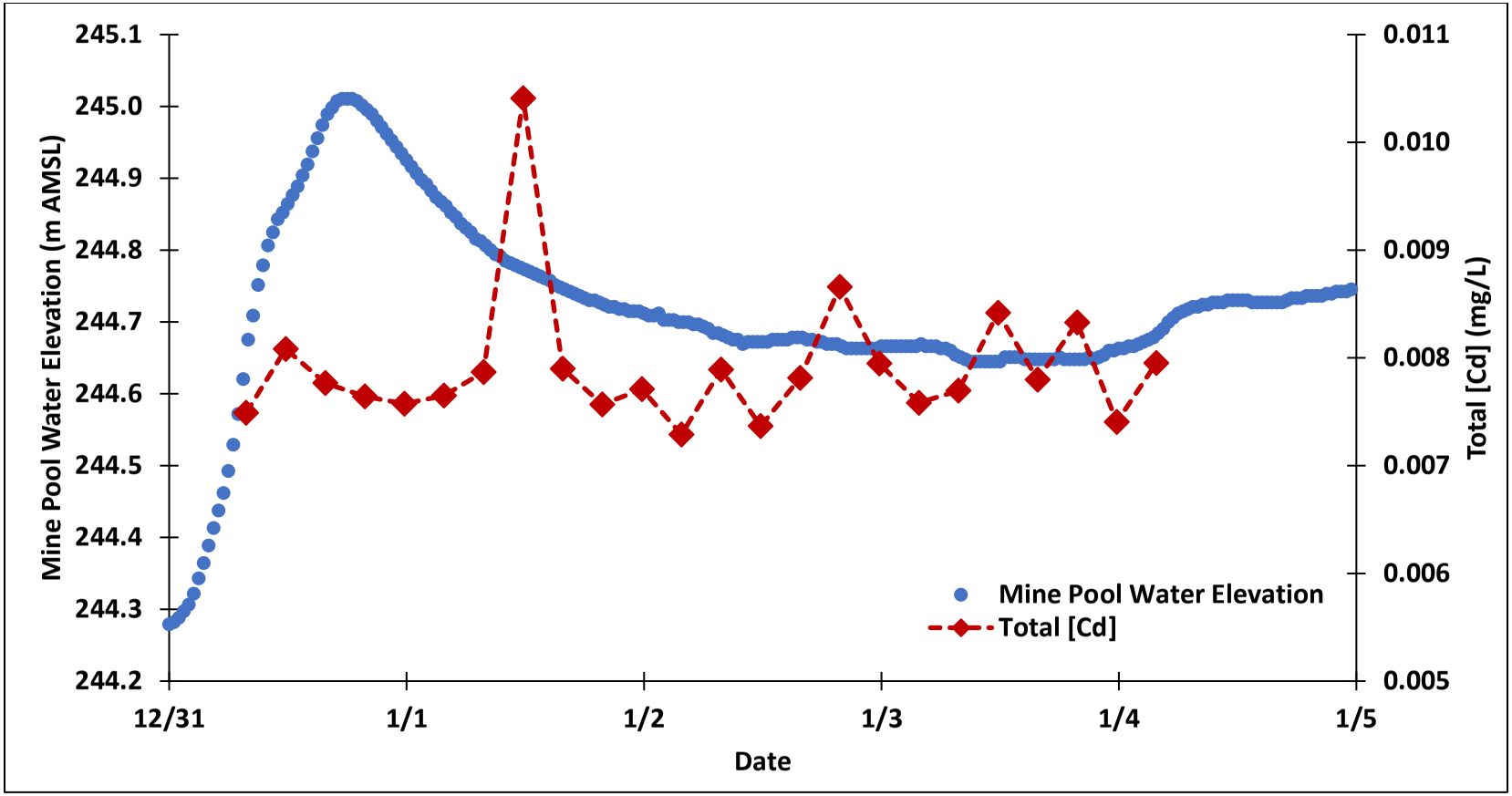

Figure 5C.2: Picher mining field mine pool water elevations during a rainfall event occurring on December 31st, 2018, as measured by the USGS Slim Jim groundwater monitoring station (65942094504203), versus total cadmium concentrations of the Seep 40 Road mine drainage discharge, collected on 30-minute intervals using an autosampler

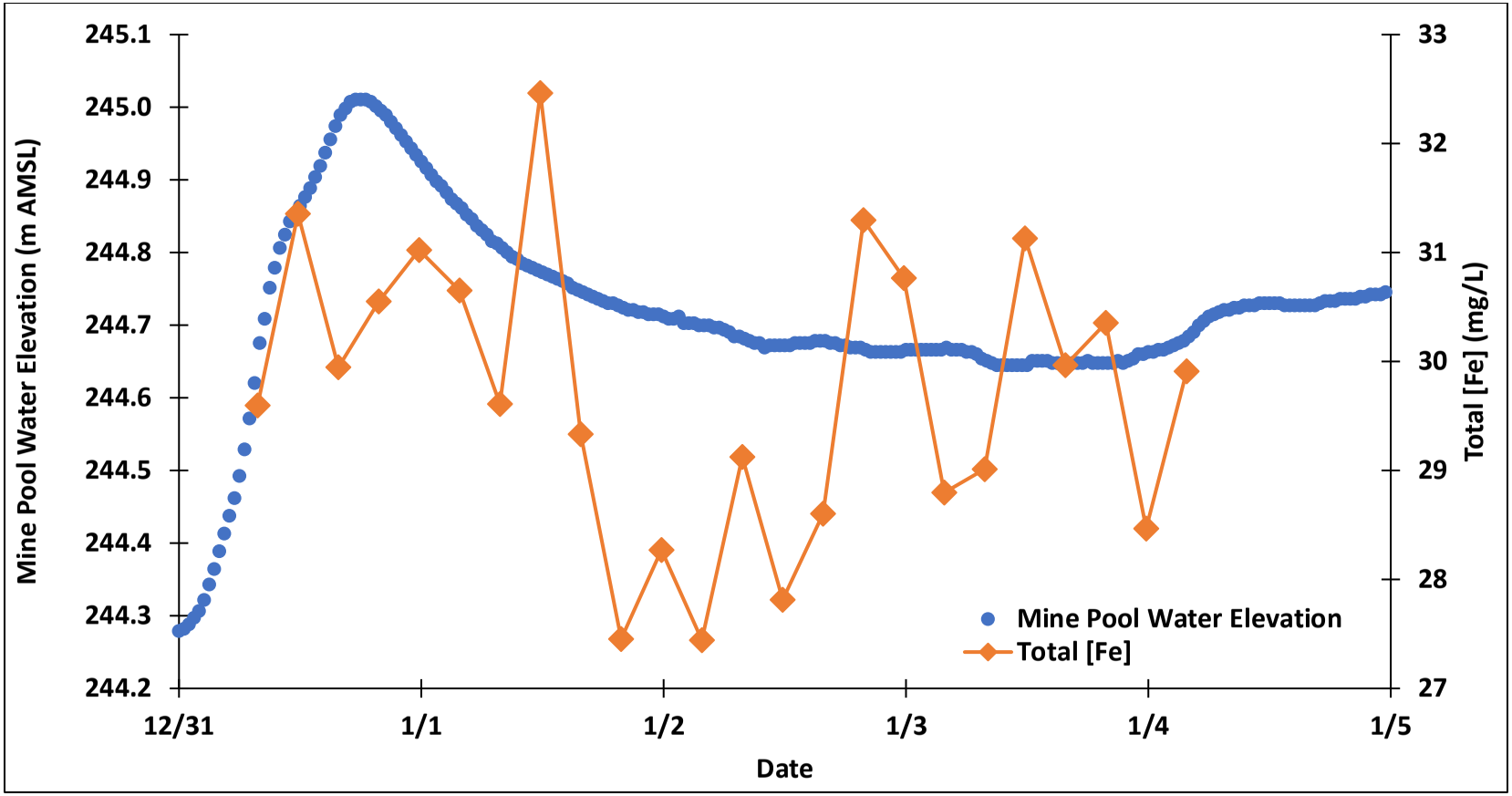

Figure 5C.3: Picher mining field mine pool water elevations during a rainfall event occurring on December 31st, 2018, as measured by the USGS Slim Jim groundwater monitoring station (65942094504203), versus total iron concentrations of the Seep 40 Road mine drainage discharge, collected on 30-minute intervals using an autosampler

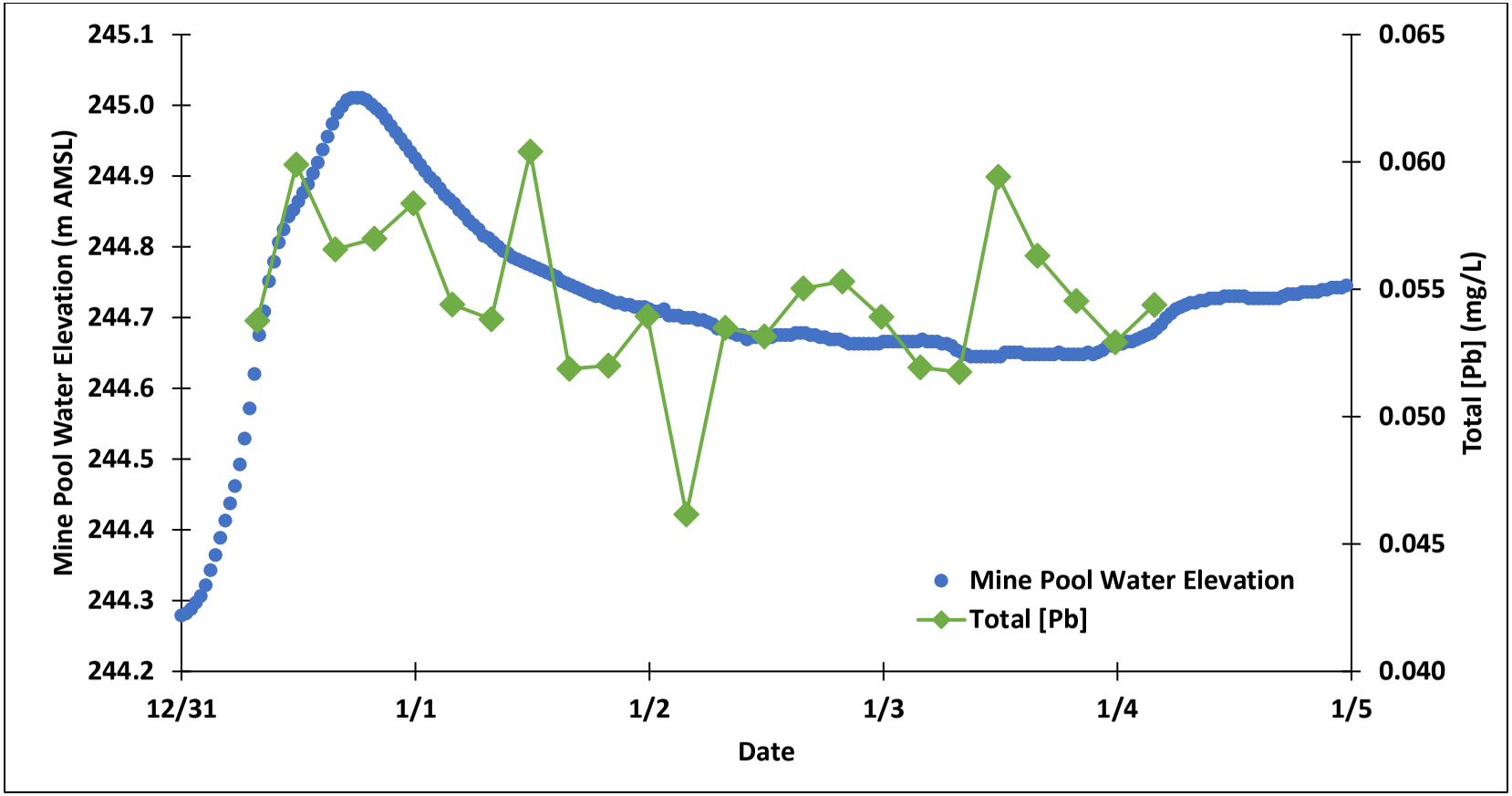

Figure 5C.4: Picher mining field mine pool water elevations during a rainfall event occurring on December 31st, 2018, as measured by the USGS Slim Jim groundwater monitoring station (65942094504203), versus total lead concentrations of the Seep 40 Road mine drainage discharge, collected on 30-minute intervals using an autosampler

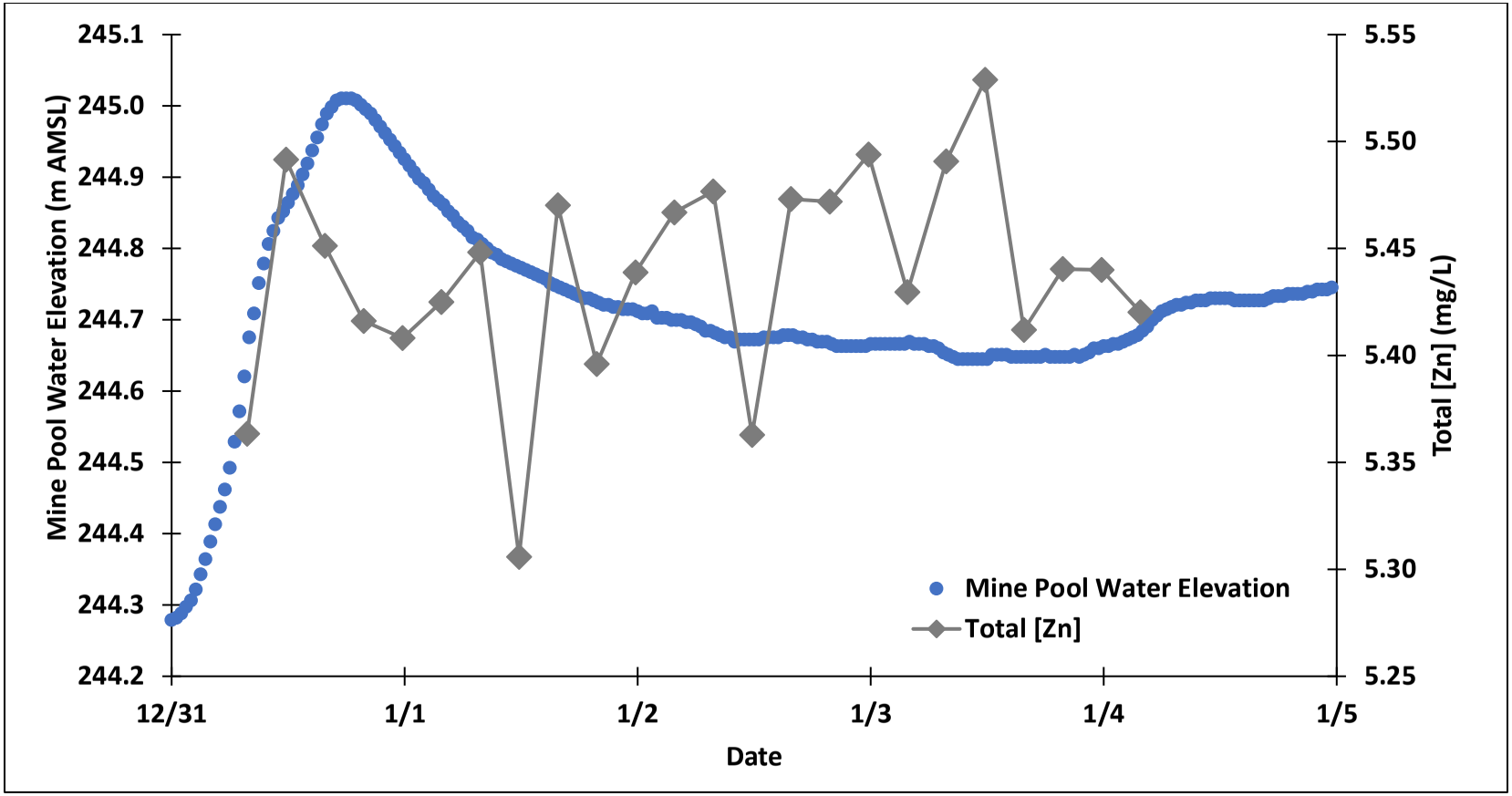

Figure 5C.5: Picher mining field mine pool water elevations during a rainfall event occurring on December 31st, 2018, as measured by the USGS Slim Jim groundwater monitoring station (65942094504203), versus total zinc concentrations of the Seep 40 Road mine drainage discharge, collected on 30-minute intervals using an autosampler

APPENDIX 6A
Mine Pool Hydraulic Head Test

The Douthat Seep 40 Road discharge was originally covered by a concrete cap that forced the water out from the bottom and sides of the cap. The cap was removed in October of 2020 (Figure 6A.1). On September 3rd, 2021, the Douthat Seep 40 Road discharge was captured by installing an 8-inch riser pipe inside the 10-inch air vent connected by a rubber Fernco reducer (Figure 6A.2). The riser was set to an approximate discharge elevation of 801.5 ft AMSL, whereas the original discharge elevation of the ten-inch air vent was approximately 798.5 ft AMSL. The riser remained at this elevation until November 11th, 2021, where it was then lowered to a discharge elevation of approximately 800 ft AMSL where it has remained through the duration of this study. Multiple mine pool monitoring stations were used to track the response of the mine pool (Figure 6A.3). The locations of each monitoring station are shown in Figure 6A.4. The elevations of the John Hunt and Mid-Continent monitoring stations are approximate and have not been professionally surveyed. The USGS Slim Jim monitoring station uses a monitoring height of 830.72 ft AMSL. The remaining monitoring stations have been surveyed during the Tar Creek Operable Unit 4 study.

The mine pool showed a near-instantaneous response once the riser was installed. All the monitoring stations located within the hydraulically connected workings, which are all stations except Red Hole Monitoring Well #2 (RHMW2), increased approximately 2.5 ft over a period of two months after the riser was installed (Table 6A.1). While some precipitation events can be seen in the mine pool elevation data, the mine pool showed a logarithmic trend as it approached its peak elevation on November 11th. The mine pool again began to fall once the riser was lowered by 1.5 ft on November 11th, dropping approximately a foot over the next month through December 15th. (Table 6A.1, Figure 6A.3). The well that is not connected to the larger Picher field workings, RHMW2, still showed an increase of 1.19 ft approximately half of the magnitude of the other wells after the riser was installed. Similarly, once the riser was lowered to 800 ft AMSL, RHMW2 decreased by approximately half of the magnitude by 0.45 ft (Table 6A.1). This hydraulic head test shows that attempting to substantially increase the head of the mine pool elevation at Douthat by manipulating the discharges will affect the entire Picher field. Maintaining an elevated mine pool elevation will result in increased flow rates at Mayer Ranch and Southeast Commerce passive treatment systems

Figure 6A.1: Seep 40 discharge showing the original 10” air ventilation pipe shortly after the concrete cover was removed. Photo taken October 23rd, 2020

Figure 6A.2: Eight-inch riser installed on the S40 discharge. Photo taken September 4th, 2021

.

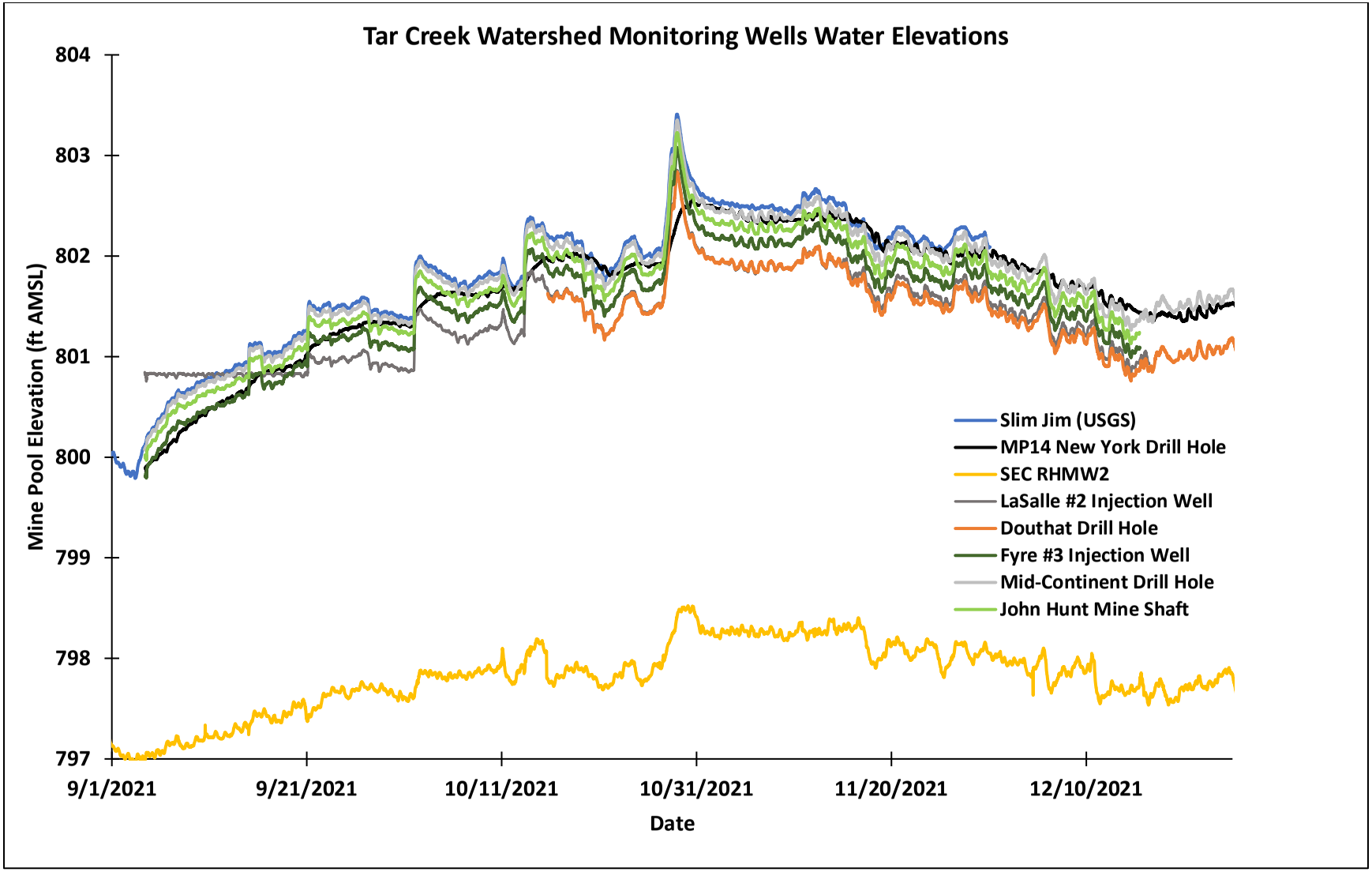

Figure 6A.3: Mine pool water elevations at multiple locations throughout the Picher mining field from September 1st, 2021, to December 31st, 2021, during a hydraulic head test where a riser was installed on the S40 discharge, changing the discharge elevation

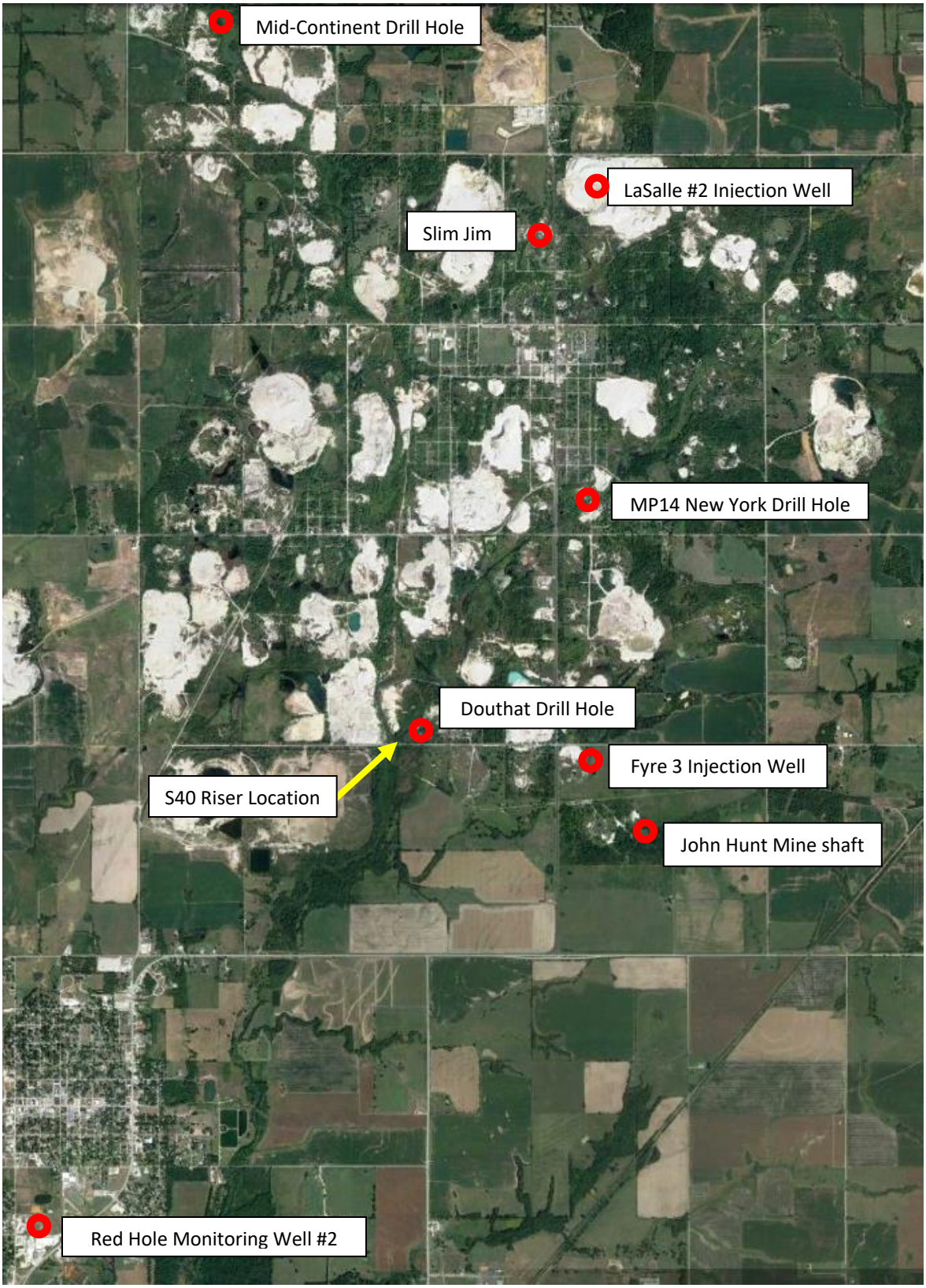

Figure 6A.4: Aerial image of the Picher mining field, showing locations of mine pool monitoring stations (Google Earth Image, September 2021)

Table 6A.1: Mine pool water elevation at multiple monitoring stations throughout the Picher mining field after a riser was installed on S40 discharge on September 4th at an approximate elevation of 801.5 ft AMSL, then lowered to 800 ft AMSL on November 11th

		September 4th		November 11th		December 15th
Riser Elevation (ft AMSL)		801.50		801.50	800.00	800.00
	Mine Pool Elevation (ft AMSL)	800.10		802.50		801.37
Mid-Continent Drill Hole	Δ Water Elevation (ft)		2.40		-1.13	
	Mine Pool Elevation (ft AMSL)	800.15		802.57		801.44
Slim Jim	Δ Water Elevation (ft)		2.42		-1.13	
	Mine Pool Elevation (ft AMSL)	-		802.01		800.96
LaSalle #2 Injection Well	Δ Water Elevation (ft)		-			-1.05
	Mine Pool Elevation (ft AMSL)	799.83		802.24		801.09
Fyre #3 Injection Well	Δ Water Elevation (ft)		2.41		-1.15	
	Mine Pool Elevation (ft AMSL)	800.01		802.38		801.24
John Hunt Mine Shaft	Δ Water Elevation (ft)		2.37			-1.14
	Mine Pool Elevation (ft AMSL)	799.89		802.41		801.44
MP14 New York Drill Hole	Δ Water Elevation (ft)		2.52		-0.97	
	Mine Pool Elevation (ft AMSL)	-		802.00		800.88
Douthat Drill Hole	Δ Water Elevation (ft)		-		-1.12	
	Mine Pool Elevation (ft AMSL)	797.04		798.23		797.78
Red Hole Monitoring Well #2	Δ Water Elevation (ft)		1.19		-0.45	

APPENDIX 6B
Known Discharge Locations Outside the Douthat Study Area

Name: Flint Rock Discharges
Location: 36.9645, -94.8473
Claim: Douthat
Description: The Flint Rock discharges are the only known potentially large discharge that is not located within the OU1 Berm at the primary study site. The discharges are located approximately 1,000 ft to the northwest of the study site (Figures 6B.1-6B.4). These discharges are only a few feet apart. One is an open mine shaft that has partially collapsed, and the surface feature is now a 40 ft x 100 ft ellipse (Figure 6B.2). It is estimated that the critical mine pool elevation that will result in discharging water at this site is 803.5 ft AMSL. The mine pool was 803.2 ft AMSL on the day the photo in Figure 6B.5 was taken. Where minimal MD was flowing, and the Fe had already been oxidized. However, the water chemistry confirmed the water from this shaft was mine drainage (Table 6B.1). The majority of the feature is surrounded by chat berm that likely prevented the shaft from discharging in the past. However, a portion of the berm has been blown out. The blowout through the berm was trapezoidal-shaped, approximately 8 ft wide on the bottom and 15 ft on top. The blowout was approximately 6 ft deep (Figure 6B.5). The channel from the blowout leads directly to Tar Creek. The berm around this shaft must be reconstructed to prevent this discharge from flowing to get accurate flow rates from the Douthat discharges.

The second Flint Rock discharge is located approximately 100 ft to the east of Flint Rock Discharge #1 (FRD #1) and is approximately 25 ft in diameter (Figures 6B.2-6B.4). FRD #2 is a non-shaft related collapse feature that has opened between FRD #1, and a shaft located 50 ft to the north of FRD #2 that was closed in 2005 by the US Army Corps of Engineers (Luza, 2006). The closed shaft is referred to as the Douthat Shaft #72 in the report. Imagery confirmed the collapse, FRD #2, opened between 2015 and 2020. While on-site observations have not confirmed FRD #2 to be a discharge, there is an eroded channel to the north of this shaft that leads towards Tar Creek (Figure 6B.6). Secondly, the orange color of the collapse shown in Figure 6B.4 indicates FRD #2 is hydraulically connected to the contaminated mine pool below. The orange coloration is likely from the collapse recently discharging, then the Fe oxidized once the discharge stopped flow. It is recommended that the berm around the collapse be reconstructed to prevent the shaft from discharging in the future. Since this collapse occurs between two mine shafts, the best practice would likely be to construct a large retaining structure around both open features and the closed shaft because there is the possibility that the collapse will expand to encompass both shafts.

Table 6B.1: Water quality of Flint Rock Discharge #1 collected immediately after flow rates had decreased following an elevated discharge event

Date	Temp	Specific Conductivity	[DO]	pH	Alkalinity	Turbidity	Tot. Cd	Tot. Fe	Tot. Pb	Tot. Zn
M/D/Y	C	µS/cm	mg/L		mg/L	NTU	mg/L	mg/L	mg/L	mg/L
2/29/2020	14.84	2,036	0.98	6.23	117.00	63.63	0.002	9.08	0.031	4.59

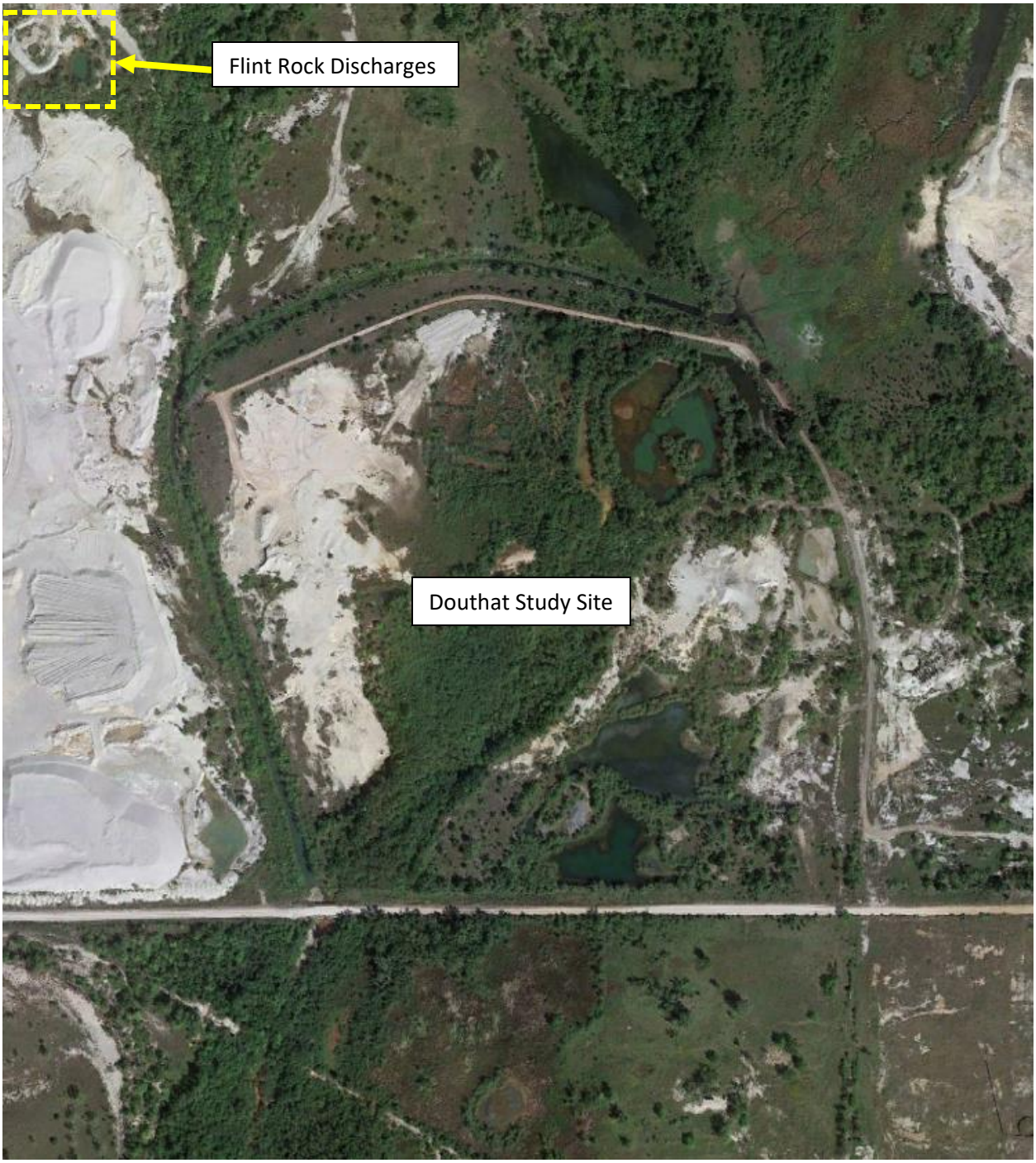

Figure 6B.1: Aerial image of the Douthat study site in proximity to the Flint Rock Discharges (Google Earth Image, September 2021)

Figure 6B.2: Aerial image of the Flint Rock Discharges (Google Earth Image, September 2021)

Figure 6B.3: Drone image of the Flint Rock Discharges. Photo taken November 2019 facing south.

Figure 6B.4: Drone image of the Flint Rock Discharge #2 collapse. Photo taken November 2019 from the north, facing south.

Figure 6B.5: Photo of the berm blowout at Flint Rock Discharge #1, with a student standing in the blown-out berm for size comparison. Photo taken February 2020

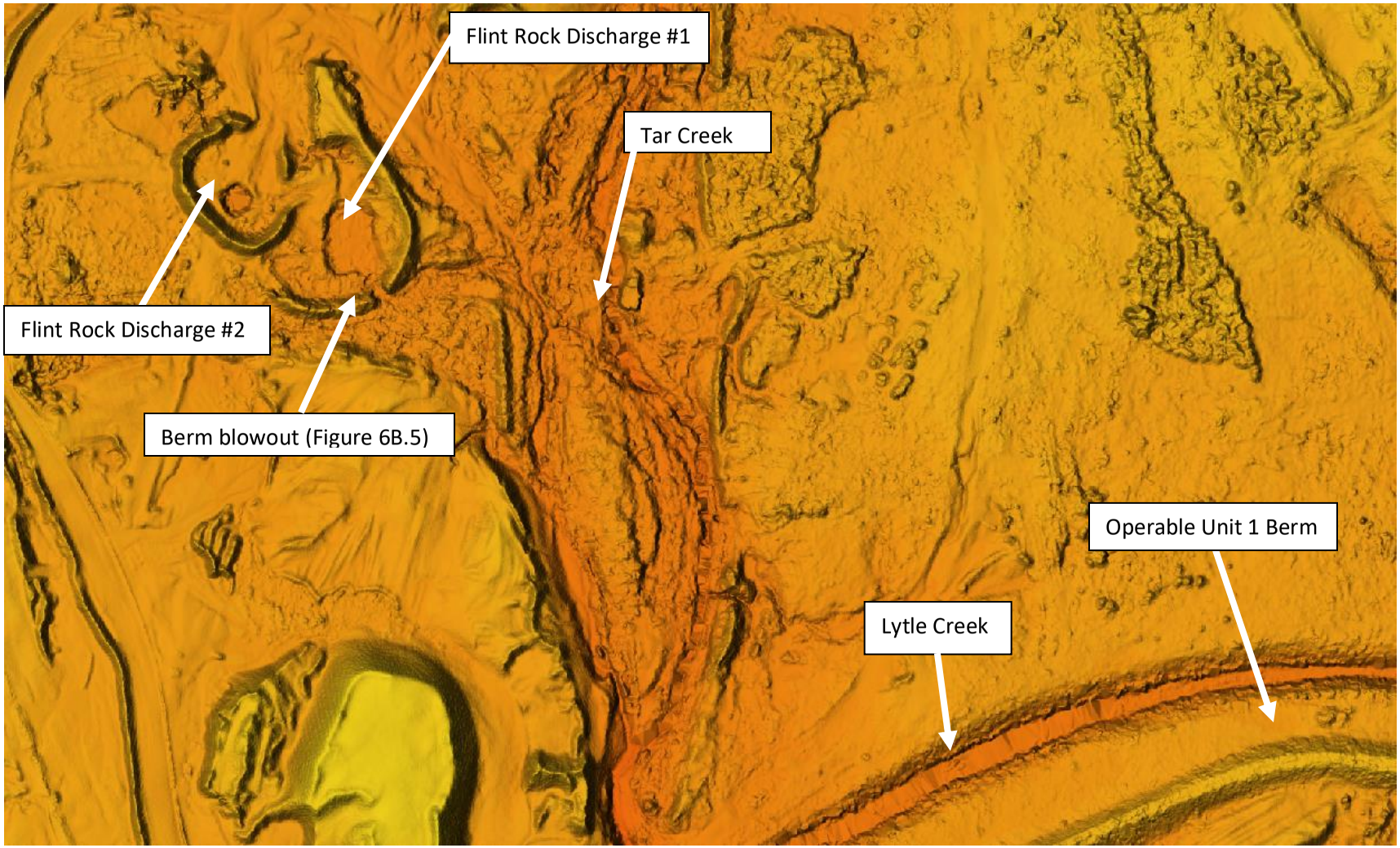

Figure 6B.6: LiDAR Imagery flown July 2020 of Flint Rock Discharges

APPENDIX 6C
Calculated Annual Metal Loading to Tar Creek

Table 6C.1: Annual metals loading to Tar Creek with untreated MD

Year	Site	As kg	Cd kg	Fe kg	Pb kg	Zn kg	Total MD Volume cu ft
	S40	0.00	33.76	25,473	49.43	7,402	100,516,873
	SRR	5.70	1.10	7,052	15.13	1,282	
	SBB	0.99	0.16	1,217	2.17	55	
	SCT	0.17	0.02	207	0.38	17	
2010	AD2	0.00	10.71	32,273	70.94	6,760	
	S40	0.00	35.74	26,972	52.33	7,837	95,408,433
	SRR	4.45	0.86	5,509	11.82	1,001	
	SBB	1.12	0.18	1,378	2.45	63	
	SCT	0.13	0.02	164	0.30	14	
2011	AD2	0.00	9.45	28,475	62.59	5,964	
	S40	0.00	25.62	19,332	37.51	5,617	58,381,055
	SRR	2.24	0.43	2,772	5.95	504	
	SBB	0.92	0.15	1,130	2.01	51	
	SCT	0.08	0.01	95	0.17	8	
2012	AD2	0.00	4.86	14,634	32.17	3,065	
	S40	0.00	20.16	15,211	29.51	4,420	54,159,909
	SRR	2.50	0.48	3,090	6.63	562	
	SBB	0.65	0.11	802	1.43	36	
	SCT	0.08	0.01	95	0.17	8	
2013	AD2	0.00	5.41	16,303	35.84	3,415	
	S40	0.00	27.64	20,860	40.48	6,062	64,566,132
	SRR	3.16	0.61	3,906	8.38	710	
	SBB	0.86	0.14	1,057	1.88	48	
	SCT	0.11	0.02	132	0.24	11	
2014	AD2	0.00	5.33	16,062	35.31	3,364	
	S40	0.00	34.35	25,918	50.29	7,531	133,729,465
	SRR	6.78	1.31	8,388	17.99	1,525	
	SBB	0.99	0.16	1,217	2.16	55	
	SCT	0.19	0.03	235	0.43	20	
2015	AD2	0.00	17.64	53,168	116.88	11,136	
	S40	0.00	37.84	28,554	55.41	8,297	85,239,652
	SRR	4.32	0.83	5,344	11.46	971	
	SBB	1.15	0.19	1,414	2.51	64	
	SCT	0.15	0.02	186	0.34	16	
2016	AD2	0.00	6.59	19,856	43.65	4,159	
	S40	0.00	30.66	23,138	44.90	6,724	91,988,695
	SRR	4.33	0.84	5,358	11.49	974	
	SBB	0.91	0.15	1,125	2.00	51	
	SCT	0.14	0.02	169	0.31	14	
2017	AD2	0.00	10.21	30,768	67.64	6,445	

Table 6C.1 Continued

Year	Site	As kg	Cd kg	Fe kg	Pb kg	Zn kg	Total MD Volume cu ft
	S40	0.00	33.12	24,993	48.50	7,262	80,587,014
	SRR	3.90	0.75	4,825	10.35	877	
	SBB	1.04	0.17	1,279	2.28	58	
	SCT	0.13	0.02	161	0.29	14	
2018	AD2	0.00	7.07	21,304	46.83	4,462	
	S40	0.00	42.01	31,699	61.51	9,211	184,212,346
	SRR	10.10	1.95	12,488	26.79	2,270	
	SBB	1.17	0.19	1,446	2.57	66	
	SCT	0.27	0.04	332	0.61	28	
2019	AD2	0.00	25.56	77,030	169.33	16,135	
	S40	0.00	39.55	29,845	57.91	8,672	132,668,830
	SRR	6.52	1.26	8,058	17.29	1,465	
	SBB	1.18	0.19	1,455	2.59	66	
	SCT	0.19	0.03	233	0.43	20	
2020	AD2	0.00	15.98	48,168	105.89	10,089	
	S40	0.00	42.01	31,705	61.52	9,213	119,340,259
	SRR	7.00	1.35	8,654	18.56	1,573	
	SBB	1.22	0.20	1,505	2.68	68	
	SCT	0.21	0.03	267	0.49	22	
2021	AD2	0.00	12.06	36,347	79.90	7,613	
	S40	0.00	402.44	303,699	589.29	88,250	1,200,798,665
	SRR	61.00	11.77	75,445	161.84	13,712	
	SBB	12.18	1.97	15,025	26.72	684	
Total	SCT	1.83	0.27	2,277	4.16	191	

Table 6C.2: Annual metal loading to Tar Creek if PTS-1 conceptual design were implemented

Year	Parameter	As kg	Cd kg	Fe kg	Pb kg	Zn kg	Days of water bypassing Annually	% of MD Treated
2010	Total Mass	6.86	45.75	66223	138.04	15516	113.4	66%
	Metals Retained	6.08	37.86	43366	88.21	10105		
	Metals Lost	0.78	7.89	22857	49.83	5411		
	% Retained	88.67	82.75	65	63.90	65		
2011	Total Mass	5.70	46.25	62498	129.50	14879	79.25	72%
	Metals Retained	5.07	39.79	43773	88.71	10330		
	Metals Lost	0.63	6.46	18725	40.79	4549		
	% Retained	88.90	86.04	70	68.51	69		
2012	Total Mass	3.23	31.06	37963	77.81	9246	34.35	82%
	Metals Retained	2.98	28.53	30574	61.78	7271		
	Metals Lost	0.25	2.54	7389	16.03	1975		
	% Retained	92.29	91.83	81	79.40	79		
2013	Total Mass	3.23	26.16	35502	73.58	8441	18.60	80%
	Metals Retained	2.99	23.79	28585	58.56	6647		
	Metals Lost	0.23	2.38	6916	15.02	1794		
	% Retained	92.84	90.91	81	79.58	79		
2014	Total Mass	4.12	33.74	42016	86.28	10195	28.17	93%
	Metals Retained	4.02	32.69	38920	79.67	9070		
	Metals Lost	0.11	1.05	3097	6.61	1125		
	% Retained	97.43	96.89	93	92.34	89		
2015	Total Mass	7.96	53.48	88927	187.76	20268	130.2	48%
	Metals Retained	6.36	37.05	41401	83.90	9668		
	Metals Lost	1.60	16.44	47527	103.85	10599		
	% Retained	79.93	69.26	47	44.69	48		
2016	Total Mass	5.62	45.47	55354	113.37	13507	51.40	87%
	Metals Retained	5.34	42.64	47094	95.52	11117		
	Metals Lost	0.28	2.83	8260	17.85	2391		
	% Retained	95.01	93.78	85	84.25	82		
2017	Total Mass	5.38	41.87	60558	126.34	14207	66.71	69%
	Metals Retained	4.72	35.13	41020	83.74	9570		
	Metals Lost	0.66	6.74	19539	42.60	4637		
	% Retained	87.77	83.90	68	66.28	67		
2018	Total Mass	5.07	41.13	52562	108.25	12673	28.50	90%
	Metals Retained	4.88	39.21	46938	96.14	10926		
	Metals Lost	0.19	1.92	5624	12.11	1747		
	% Retained	96.27	95.34	89	88.81	86		
2019	Total Mass	11.54	69.74	122995	260.81	27709	268.5	41%
	Metals Retained	9.05	44.30	49476	100.09	11477		
	Metals Lost	2.49	25.44	73519	160.71	16232		
	% Retained	78.46	63.52	40	38.38	41		
2020	Total Mass	7.88	57.01	87759	184.10	20312	154.4	54%
	Metals Retained	6.39	41.76	43667	87.79	10348		
	Metals Lost	1.49	15.25	44092	96.30	9964		
	% Retained	81.12	73.25	50	47.69	51		
2021	Total Mass	8.43	55.65	78478	163.15	18490	114.4	68%
	Metals Retained	7.56	46.81	52857	107.32	12349		
	Metals Lost	0.87	8.84	25621	55.83	6140		
	% Retained	89.71	84.11	67	65.78	67		

Table 6C.3: Annual metal loading to Tar Creek if PTS-2 conceptual design were implemented

Year	Parameter	As kg	Cd kg	Fe kg	Pb kg	Zn kg	Days of water bypassing Annually	% of MD Treated
2010	Total Mass	6.86	45.75	66,223	138.04	15,516	11.90	98%
	Metals Retained	6.80	45.20	64,504	134.59	14,355		
	Metals Lost	0.05	0.55	1,719	3.45	1,161		
	% Retained	99.24	98.81	97	97.50	93		
2011	Total Mass	5.70	46.25	62,498	129.50	14,879	25.13	94%
	Metals Retained	5.58	44.93	58,553	121.15	13,285		
	Metals Lost	0.13	1.32	3,946	8.35	1,594		
	% Retained	97.79	97.14	94	93.55	89		
2012	Total Mass	3.23	31.06	37,963	77.81	9,246	7.50	100%
	Metals Retained	3.23	31.06	37,880	77.81	8,740		
	Metals Lost	0.00	0.00	83	0.00	506		
	% Retained	100.00	100.00	100	100.00	95		
2013	Total Mass	3.23	26.16	35,502	73.58	8,441	0.00	100%
	Metals Retained	3.22	26.13	35,339	73.38	7,990		
	Metals Lost	0.00	0.03	163	0.20	451		
	% Retained	99.91	99.88	100	99.73	95		
2014	Total Mass	4.12	33.74	42,016	86.28	10,195	0.00	100%
	Metals Retained	4.12	33.74	41,924	86.28	9,633		
	Metals Lost	0.00	0.00	93	0.00	561		
	% Retained	100.00	100.00	100	100.00	94		
2015	Total Mass	7.96	53.48	88,927	187.76	20,268	0.00	81%
	Metals Retained	7.44	48.08	73,186	153.60	16,148		
	Metals Lost	0.52	5.40	15,741	34.16	4,119		
	% Retained	93.51	89.90	82	81.81	80		
2016	Total Mass	5.62	45.47	55,354	113.37	13,507	28.88	99%
	Metals Retained	5.61	45.35	54,898	112.66	12,656		
	Metals Lost	0.01	0.11	456	0.72	851		
	% Retained	99.81	99.75	99	99.37	94		
2017	Total Mass	5.38	41.87	60,558	126.34	14,207	7.44	89%
	Metals Retained	5.16	39.58	53,820	111.83	12,134		
	Metals Lost	0.22	2.29	6,739	14.51	2,073		
	% Retained	95.92	94.52	89	88.51	85		
2018	Total Mass	5.07	41.13	52,562	108.25	12,673	33.17	100%
	Metals Retained	5.07	41.13	52,448	108.25	11,986		
	Metals Lost	0.00	0.00	114	0.00	687		
	% Retained	100.00	100.00	100	100.00	95		
2019	Total Mass	11.54	69.74	122,995	260.81	27,709	0.00	75%
	Metals Retained	10.54	59.32	92,697	194.91	20,175		
	Metals Lost	1.00	10.42	30,298	65.90	7,534		
	% Retained	91.36	85.06	75	74.73	73		
2020	Total Mass	7.88	57.01	87,759	184.10	20,312	103.54	75%
	Metals Retained	7.08	48.60	63,331	130.96	14,216		
	Metals Lost	0.80	8.40	24,428	53.13	6,095		
	% Retained	89.81	85.26	72	71.14	70		
2021	Total Mass	8.43	55.65	78,478	163.15	18,490	113.88	99%
	Metals Retained	8.42	55.50	77,883	162.20	17,440		
	Metals Lost	0.01	0.15	595	0.95	1,050		
	% Retained	99.83	99.73	99	99.42	94		

APPENDIX 6D
Calculated Mean Metals Concentrations Downstream of the Douthat Mine Drainage Discharges

Table 6D.1: Calculated mean metals concentrations and the percent of time calculated metals concentrations do not meet beneficial use criteria for fish and wildlife propagation due to mine drainage discharges at Douthat, OK using data from USGS on 30-minute time intervals from 2010-2021 with untreated MD, and annual rainfall

	Acute			Chronic		Cd (diss)	Pb (tot)	Zn (diss)	Annual Rainfall
Year	Cd	Pb	Zn	Cd	Pb	µg/L	µg/L	µg/L	cm
2010	2.9%	0.0%	79.1%	88.8%	0.0%	7.41	16.05	2007	123
2011	15.5%	0.0%	87.4%	92.9%	0.0%	11.61	21.81	2874	109
2012	46.4%	0.0%	92.4%	96.0%	0.0%	16.68	28.40	3865	90
2013	25.4%	0.0%	75.1%	91.5%	0.0%	11.52	20.61	2762	122
2014	20.4%	0.0%	89.3%	95.6%	0.0%	11.28	20.61	2744	97
2015	0.7%	0.0%	76.7%	85.2%	0.0%	6.90	15.29	1896	163
2016	15.4%	0.0%	92.6%	96.8%	0.0%	11.67	22.45	2933	N/A
2017	0.5%	0.0%	80.3%	89.4%	0.0%	7.83	15.78	2026	N/A
2018	20.6%	0.0%	86.9%	94.0%	0.0%	12.00	22.02	2924	116
2019	1.7%	0.0%	62.4%	75.3%	0.0%	5.32	14.69	1693	207
2020	19.4%	0.0%	74.0%	85.1%	0.0%	10.57	21.09	2717	140
2021	11.9%	0.0%	81.2%	89.8%	0.0%	10.86	22.57	2863	121
All	15.3%	0.0%	81.8%	90.1%	0.0%	10.41	20.34	2637	

Table 6D.2: Calculated mean metals concentrations and the percent of time calculated metals concentrations do not meet beneficial use criteria for fish and wildlife propagation due to mine drainage discharges at Douthat, OK using data from USGS on 30-minute time intervals from 2010-2021 with the implementation of conceptual PTS-1, and annual rainfall

	Acute			Chronic		Cd (diss)	Pb (tot)	Zn (diss)	Annual Rainfall
Year	Cd	Pb	Zn	Cd	Pb	µg/L	µg/L	µg/L	cm
2010	0.00%	0.00%	6.13%	6.13%	0.00%	0.336	2.119	320	123
2011	0.00%	0.00%	0.96%	4.33%	0.00%	0.212	1.339	307	109
2012	0.00%	0.00%	1.99%	2.26%	0.00%	0.095	0.597	307	90
2013	0.00%	0.00%	0.25%	0.34%	0.00%	0.069	0.437	217	122
2014	0.00%	0.00%	0.02%	0.04%	0.00%	0.064	0.405	214	97
2015	0.00%	0.00%	3.85%	4.78%	0.00%	0.353	2.224	323	163
2016	0.00%	0.00%	1.99%	2.20%	0.00%	0.134	0.842	266	N/A
2017	0.00%	0.00%	1.72%	2.27%	0.00%	0.185	1.167	236	N/A
2018	0.00%	0.00%	1.12%	1.44%	0.00%	0.079	0.499	233	116
2019	0.00%	0.00%	13.71%	14.09%	0.00%	0.740	4.665	532	207
2020	0.00%	0.00%	4.94%	5.78%	0.00%	0.356	2.248	380	140
2021	0.00%	0.00%	2.36%	2.86%	0.00%	0.232	1.461	318	121
All	0.00%	0.00%	3.61%	4.01%	0.00%	0.243	1.530	309	

Table 6D.3: Calculated mean metals concentrations and the percent of time calculated metals concentrations do not meet beneficial use criteria for fish and wildlife propagation due to mine drainage discharges at Douthat, OK using data from USGS on 30-minute time intervals from 2010-2021 with the implementation of conceptual PTS-2, and annual rainfall

	Acute			Chronic		Cd (diss)	Pb (tot)	Zn (diss)	Annual Rainfall
Year	Cd	Pb	Zn	Cd	Pb	µg/L	µg/L	µg/L	cm
2010	0.000%	0.000%	0.000%	0.000%	0.000%	0.006	0.041	133	123
2011	0.000%	0.000%	0.000%	0.000%	0.000%	0.005	0.028	190	109
2012	0.000%	0.000%	0.000%	0.000%	0.000%	0.000	0.000	253	90
2013	0.000%	0.000%	0.000%	0.000%	0.000%	0.002	0.015	181	122
2014	0.000%	0.000%	0.000%	0.000%	0.000%	0.000	0.000	179	97
2015	0.000%	0.000%	0.000%	0.000%	0.000%	0.028	0.177	138	163
2016	0.000%	0.000%	0.000%	0.000%	0.000%	0.004	0.026	194	N/A
2017	0.000%	0.000%	0.000%	0.000%	0.000%	0.034	0.213	151	N/A
2018	0.000%	0.000%	0.000%	0.000%	0.000%	0.000	0.000	191	116
2019	0.000%	0.000%	0.033%	0.013%	0.000%	0.089	0.560	160	207
2020	0.000%	0.000%	0.000%	0.000%	0.000%	0.088	0.555	229	140
2021	0.000%	0.000%	0.000%	0.000%	0.000%	0.003	0.017	187	121
All	0.000%	0.000%	0.003%	0.001%	0.000%	0.022	0.141	184	

APPENDIX 6E
Conceptual Designs of the Douthat Passive Treatment Systems and the Associated Cost Estimates

DOUTHAT PASSIVE TREATMENT SYSTEM
CONCEPTUAL DESIGNS
TAR CREEK SUPERFUND SITE
OTTAWA COUNTY, OKLAHOMA
APRIL 2022

SHEET LIST TABLE	
SHEET NO.	SHEET TITLE
C001	COVER PAGE
C100	EXISTING CONDITIONS NORTH DOUTHAT
C101	EXISTING CONDITIONS NORTH DOUTHAT AERIAL IMAGERY
C102	EXISTING CONDITIONS NORTH DOUTHAT UNDERGROUND MINE WORKINGS
C103	EXISTING CONDITIONS SOUTH DOUTHAT
C104	EXISTING CONDITIONS SOUTH DOUTHAT UNDERGROUND MINE WORKINGS
C300	PTS-1 SITE LAYOUT
C301	PTS-1 PHASE 1 INITIAL OXIDATION POND AND RETENTION BASIN
C302	PTS-1 PHASE 2 PASSIVE TREATMENT SYSTEM GRADING
C303	GRADING PROFILE
C304	PTS-2 SITE LAYOUT
C305	PTS-2 PHASE 1 INITIAL OXIDATION POND AND RETENTION BASIN
C306	PTS-2 PASSIVE TREATMENT SYSTEM GRADING

SCALE 1"=250'
DESIGN OVERVIEW MAP

SCALE 1"=1,000'
LOCATION MAP

CONCEPTUAL DESIGN
NOT FOR CONSTRUCTION

CREW
Center for Restoration of Ecosystems and Watersheds
University of Oklahoma

NICHOLAS SHEPHERD DISSERTATION
DOUTHAT PASSIVE TREATMENT SYSTEM
CONCEPTUAL DESIGNS
OTTAWA COUNTY, OKLAHOMA

COVER PAGE

DATE:
DRAWING SCALE: SEE DRAWING
DRAWN BY: NLS

DRAWING NO.:
C001

288

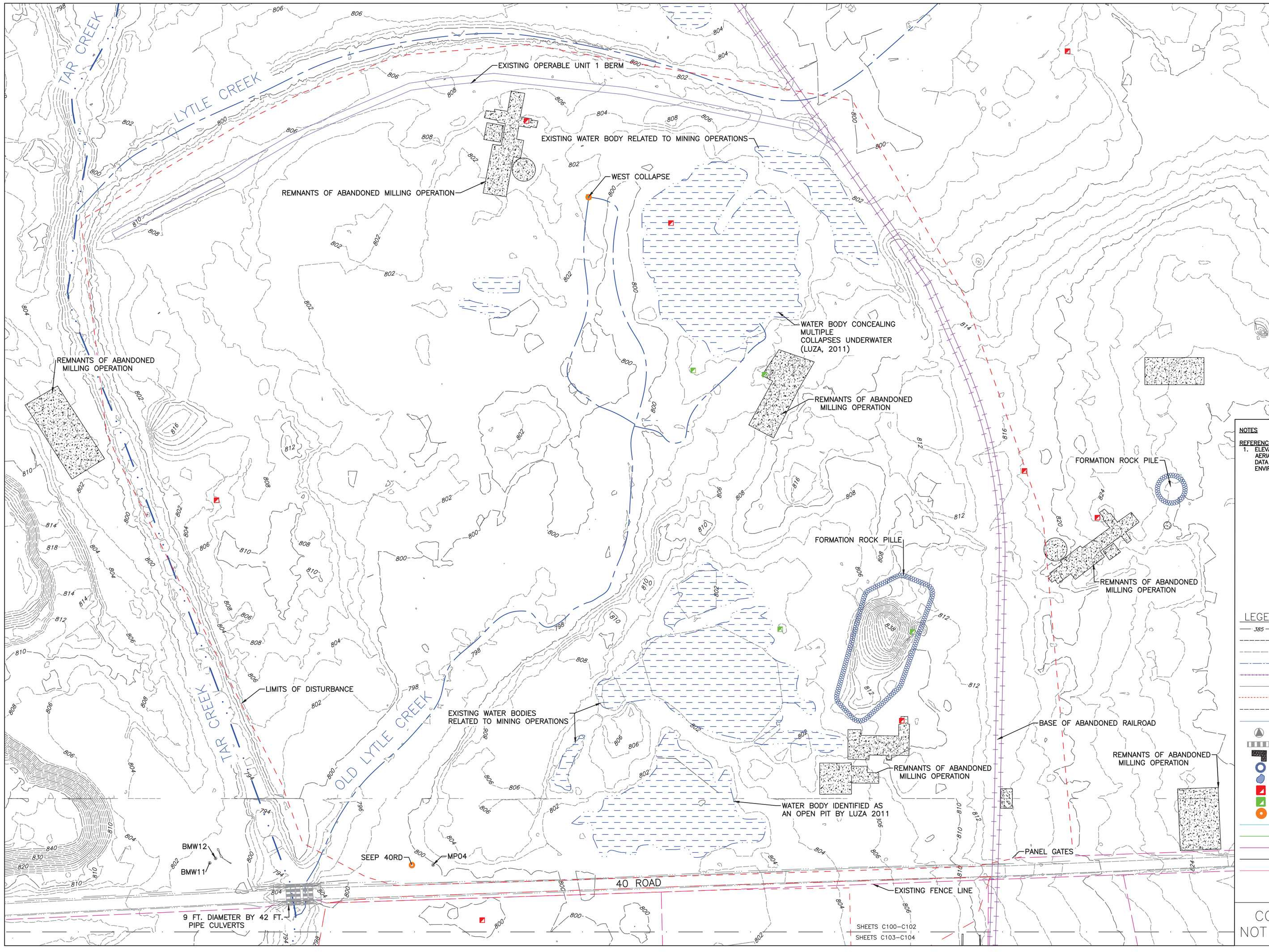

NORTH

SCALE IN FEET

0 100 200

NOTES

REFERENCES

1. ELEVATION CONTOURS AND IMAGERY DERIVED FROM AERIAL LIDAR DATA PERFORMED ON JULY 12, 2020. DATA WAS PROVIDED BY OKLAHOMA DEPARTMENT OF ENVIRONMENTAL QUALITY.

LEGEND

- EXISTING MAJOR CONTOURS
- EXISTING MINOR CONTOURS
- EXISTING DRAINAGE CHANNEL
- EXISTING STREAM CHANNEL
- ABANDONED RAIL LINE
- EXISTING GRAVEL ROAD
- EXTENT OF DISTURBED AREA
- EXISTING FENCE LINE
- EXISTING OPERABLE UNIT 1 BERM
- EXISTING MONITORING WELL
- EXISTING BRIDGE CULVERT
- ABANDONED MINING STRUCTURES
- FORMATION ROCK PILE
- EXISTING WATER BODY
- CLOSED MINE SHAFT
- OPEN MINE SHAFT
- MINE DRAINAGE DISCHARGE
- E BED MINE WORKINGS
- GH BED MINE WORKINGS
- K BED MINE WORKINGS
- M BED MINE WORKINGS
- NATURAL CAVES MINE WORKINGS

CONCEPTUAL DESIGN
NOT FOR CONSTRUCTION

CREW
Center for Restoration of Ecosystems and Watersheds
University of Oklahoma

NICHOLAS SHEPHERD DISSERTATION

DOUTHAT PASSIVE TREATMENT SYSTEM CONCEPTUAL DESIGNS

OTTAWA COUNTY, OKLAHOMA

EXISTING CONDITIONS
NORTH DOUTHAT

DATE:
DRAWING SCALE: SEE DRAWING
DRAWN BY: NLS

DRAWING NO.:
C100

289

NORTH
SCALE IN FEET
0 100 200

NOTES

REFERENCES
1. ELEVATION CONTOURS AND IMAGERY DERIVED FROM AERIAL LIDAR DATA PERFORMED ON JULY 12, 2020. DATA WAS PROVIDED BY OKLAHOMA DEPARTMENT OF ENVIRONMENTAL QUALITY.

LEGEND
- EXISTING MAJOR CONTOURS
- EXISTING MINOR CONTOURS
- EXISTING DRAINAGE CHANNEL
- EXISTING STREAM CHANNEL
- ABANDONED RAIL LINE
- EXISTING GRAVEL ROAD
- EXTENT OF DISTURBED AREA
- EXISTING FENCE LINE
- EXISTING OPERABLE UNIT 1 BERM
- EXISTING MONITORING WELL
- EXISTING BRIDGE CULVERT
- ABANDONED MINING STRUCTURES
- FORMATION ROCK PILE
- EXISTING WATER BODY
- CLOSED MINE SHAFT
- OPEN MINE SHAFT
- MINE DRAINAGE DISCHARGE
- E BED MINE WORKINGS
- GH BED MINE WORKINGS
- K BED MINE WORKINGS
- M BED MINE WORKINGS
- NATURAL CAVES MINE WORKINGS

CONCEPTUAL DESIGN
NOT FOR CONSTRUCTION

CREW
Center for Restoration of Ecosystems and Watersheds
University of Oklahoma

NICHOLAS SHEPHERD DISSERTATION

DOUTHAT PASSIVE TREATMENT SYSTEM CONCEPTUAL DESIGNS

OTTAWA COUNTY, OKLAHOMA

EXISTING CONDITIONS NORTH DOUTHAT AERIAL IMAGERY

DATE:
DRAWING SCALE: SEE DRAWING
DRAWN BY: NLS

DRAWING NO.:
C101

290

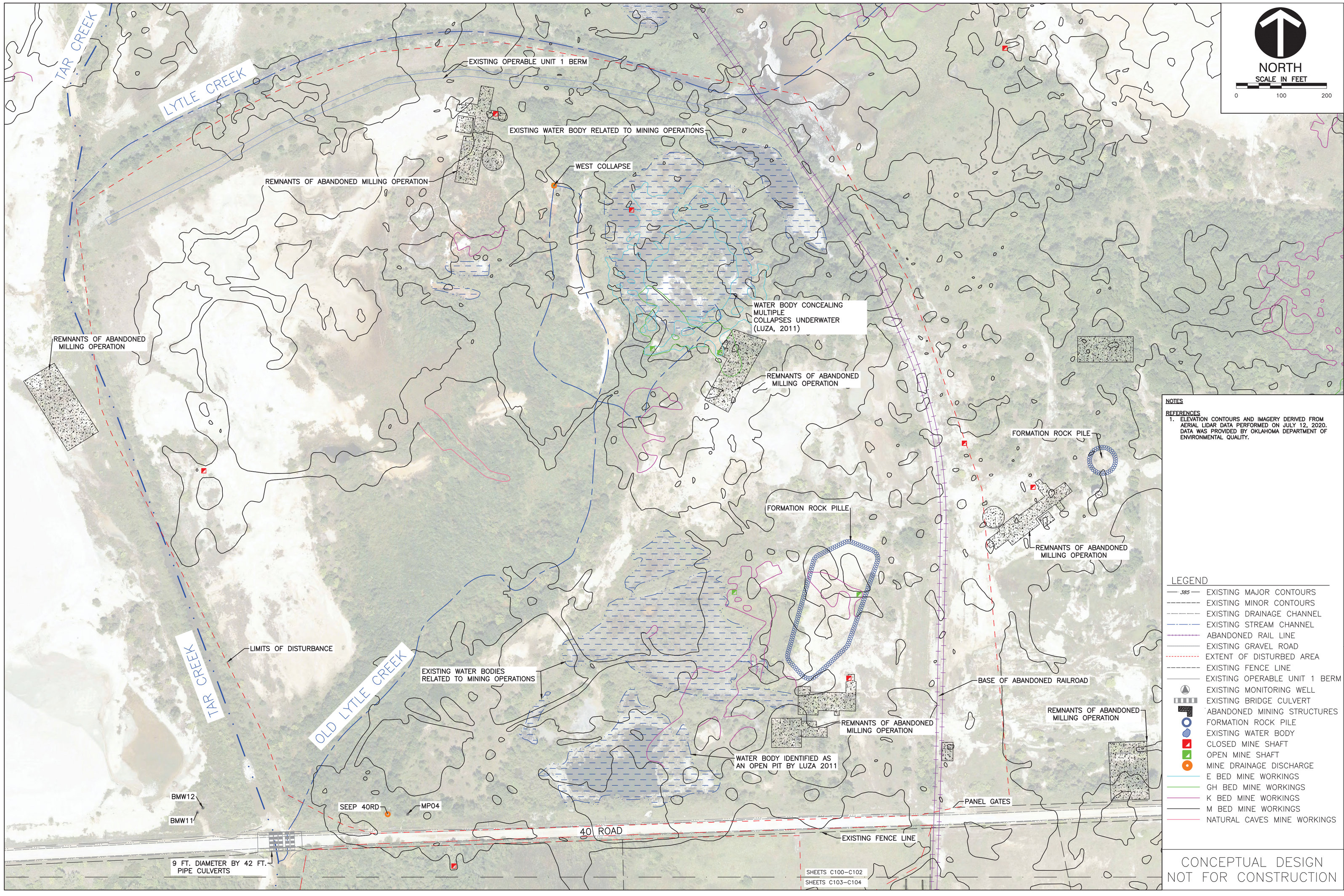

NOTES

REFERENCES

1. ELEVATION CONTOURS AND IMAGERY DERIVED FROM AERIAL LIDAR DATA PERFORMED ON JULY 12, 2020. DATA WAS PROVIDED BY OKLAHOMA DEPARTMENT OF ENVIRONMENTAL QUALITY.

LEGEND

- EXISTING MAJOR CONTOURS
- EXISTING MINOR CONTOURS
- EXISTING DRAINAGE CHANNEL
- EXISTING STREAM CHANNEL
- ABANDONED RAIL LINE
- EXISTING GRAVEL ROAD
- EXTENT OF DISTURBED AREA
- EXISTING FENCE LINE
- EXISTING OPERABLE UNIT 1 BERM
- EXISTING MONITORING WELL
- EXISTING BRIDGE CULVERT
- ABANDONED MINING STRUCTURES
- FORMATION ROCK PILE
- EXISTING WATER BODY
- CLOSED MINE SHAFT
- OPEN MINE SHAFT
- MINE DRAINAGE DISCHARGE
- E BED MINE WORKINGS
- GH BED MINE WORKINGS
- K BED MINE WORKINGS
- M BED MINE WORKINGS
- NATURAL CAVES MINE WORKINGS

CONCEPTUAL DESIGN
NOT FOR CONSTRUCTION

CREW
Center for Restoration of Ecosystems and Watersheds
University of Oklahoma

NICHOLAS SHEPHERD DISSERTATION

DOUTHAT PASSIVE TREATMENT SYSTEM CONCEPTUAL DESIGNS

OTTAWA COUNTY, OKLAHOMA

EXISTING CONDITIONS NORTH DOUTHAT UNDERGROUND MINE WORKINGS

DATE:
DRAWING SCALE: SEE DRAWING
DRAWN BY: NHS

DRAWING NO.:
C102

291

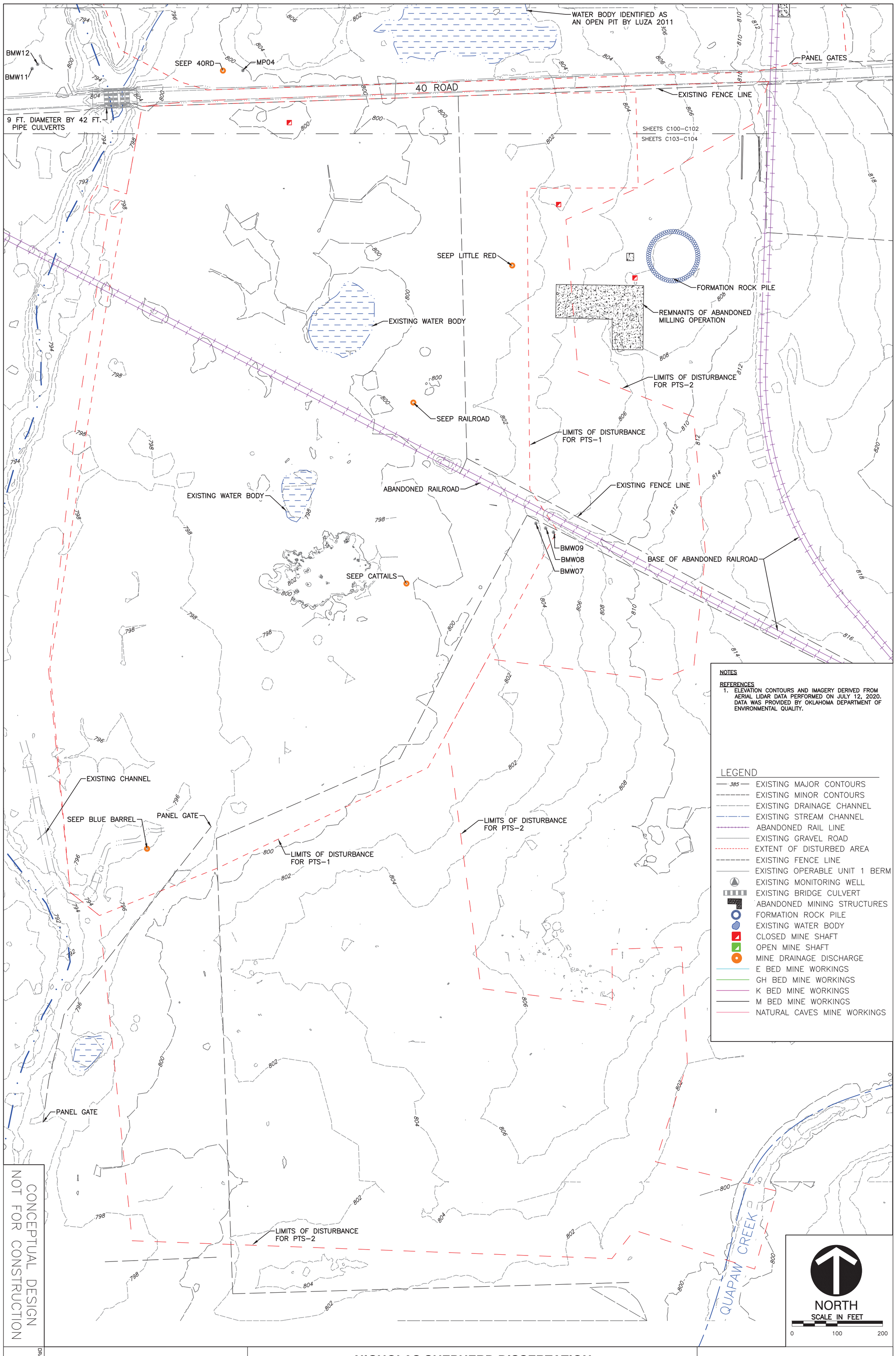

CONCEPTUAL DESIGN
NOT FOR CONSTRUCTION

DRAWING NO.: C103

EXISTING CONDITIONS
SOUTH DOUTHAT

DATE:
DRAWING SCALE: **SEE DRAWING**
DRAWN BY: **NLS**

NICHOLAS SHEPHERD DISSERTATION

DOUTHAT PASSIVE TREATMENT SYSTEM CONCEPTUAL DESIGNS

OTTAWA COUNTY, OKLAHOMA

CREW
Center for Restoration of Ecosystems and Watersheds
University of Oklahoma

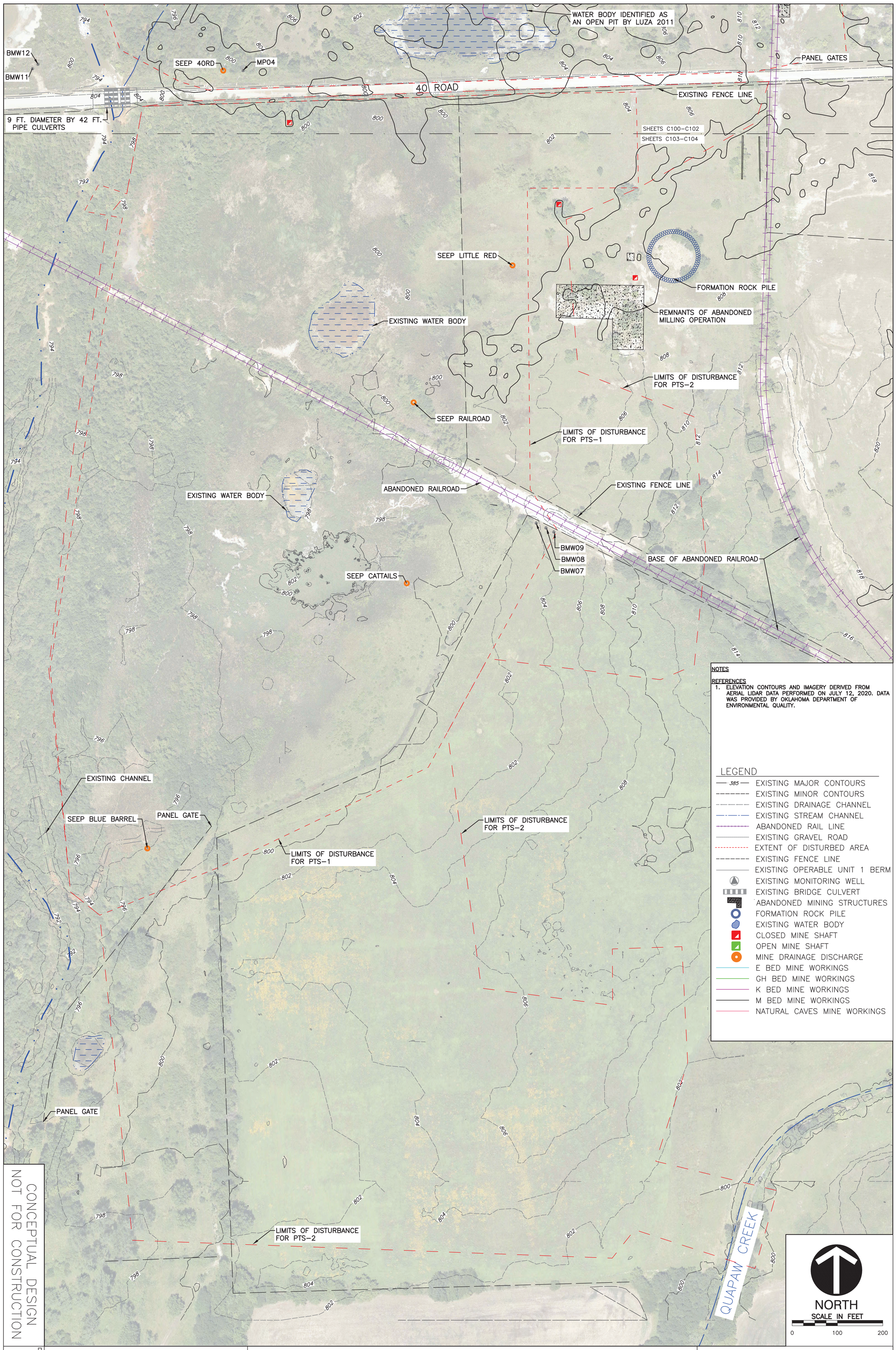

NOTES

REFERENCES

1. ELEVATION CONTOURS AND IMAGERY DERIVED FROM AERIAL LIDAR DATA PERFORMED ON JULY 12, 2020. DATA WAS PROVIDED BY OKLAHOMA DEPARTMENT OF ENVIRONMENTAL QUALITY.

LEGEND

- EXISTING MAJOR CONTOURS
- EXISTING MINOR CONTOURS
- EXISTING DRAINAGE CHANNEL
- EXISTING STREAM CHANNEL
- ABANDONED RAIL LINE
- EXISTING GRAVEL ROAD
- EXTENT OF DISTURBED AREA
- EXISTING FENCE LINE
- EXISTING OPERABLE UNIT 1 BERM
- EXISTING MONITORING WELL
- EXISTING BRIDGE CULVERT
- ABANDONED MINING STRUCTURES
- FORMATION ROCK PILE
- EXISTING WATER BODY
- CLOSED MINE SHAFT
- OPEN MINE SHAFT
- MINE DRAINAGE DISCHARGE
- E BED MINE WORKINGS
- GH BED MINE WORKINGS
- K BED MINE WORKINGS
- M BED MINE WORKINGS
- NATURAL CAVES MINE WORKINGS

CONCEPTUAL DESIGN
NOT FOR CONSTRUCTION

DRAWING NO.: C104

EXISTING CONDITIONS SOUTH DOUTHAT UNDERGROUND MINE WORKINGS

DATE:

DRAWING SCALE: **SEE DRAWING**

DRAWN BY: **NLS**

NICHOLAS SHEPHERD DISSERTATION

DOUTHAT PASSIVE TREATMENT SYSTEM CONCEPTUAL DESIGNS

OTTAWA COUNTY, OKLAHOMA

CREW
Center for Restoration of Ecosystems and Watersheds
University of Oklahoma

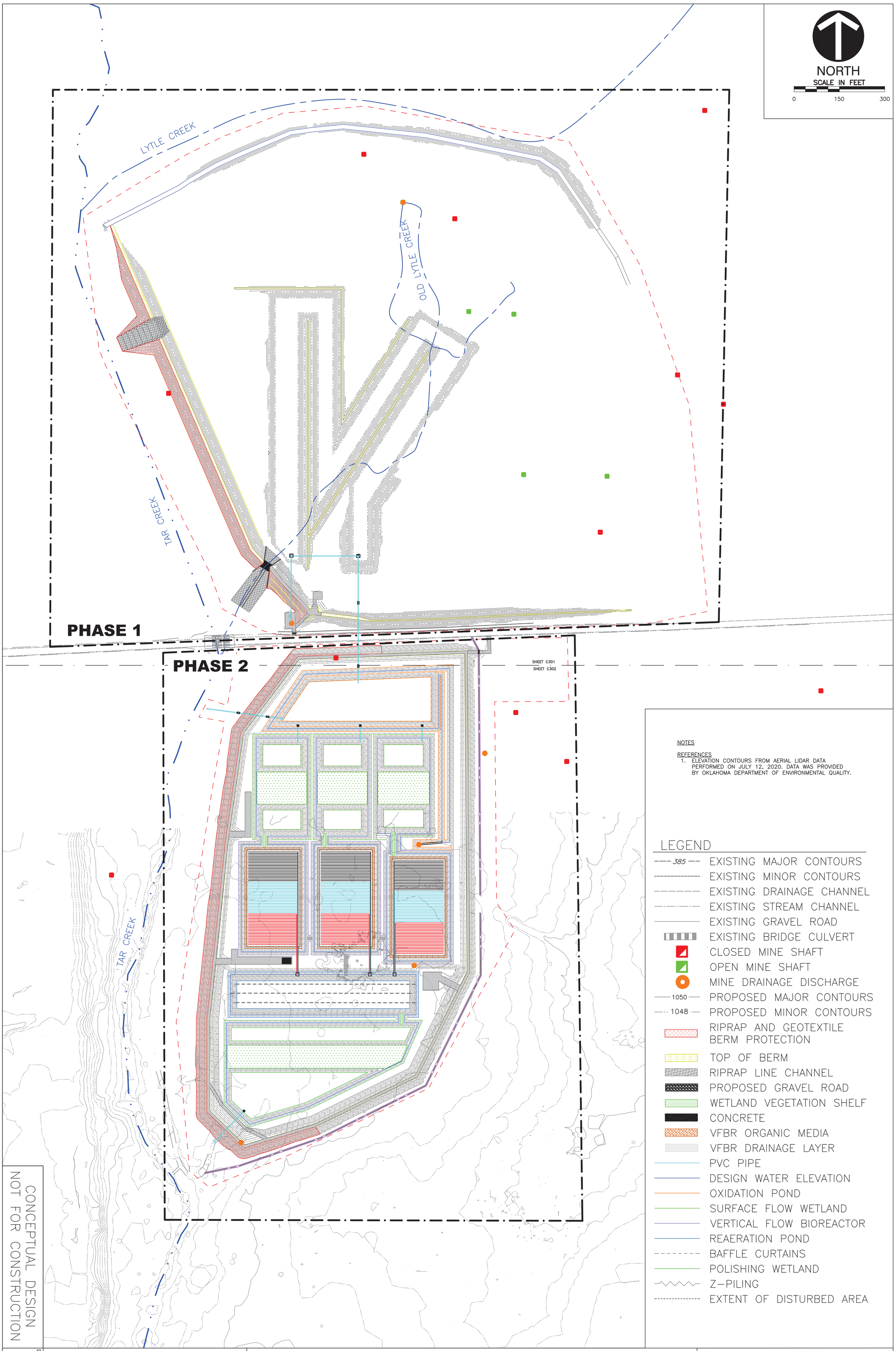

CONCEPTUAL DESIGN
NOT FOR CONSTRUCTION

DRAWING NO.: C300

PTS-1 SITE LAYOUT

DATE:

DRAWING SCALE: **SEE DRAWING**

DRAWN BY: **NLS**

NICHOLAS SHEPHERD DISSERTATION

DOUTHAT PASSIVE TREATMENT SYSTEM CONCEPTUAL DESIGNS

OTTAWA COUNTY, OKLAHOMA

CREW
Center for Restoration of Ecosystems and Watersheds
University of Oklahoma

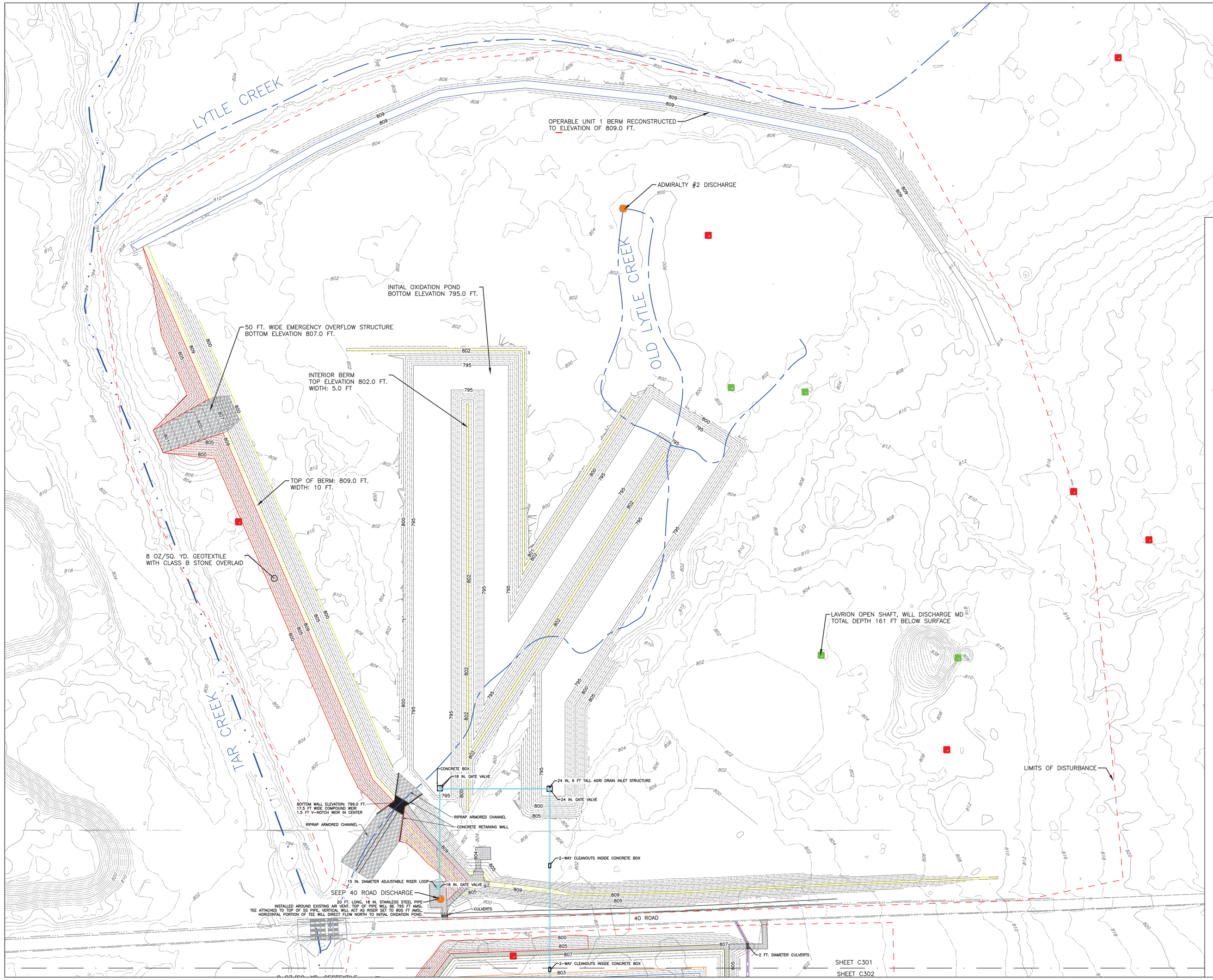

NORTH

SCALE IN FEET

0 100 200

CREW
Center for Restoration of Ecosystems and Watersheds
University of Oklahoma

NOTES

REFERENCES
1. ELEVATION CONTOURS FROM AERIAL LIDAR DATA PERFORMED ON JULY 12, 2020. DATA WAS PROVIDED BY OKLAHOMA DEPARTMENT OF ENVIRONMENTAL QUALITY.

LEGEND

- 385 EXISTING MAJOR CONTOURS
- EXISTING MINOR CONTOURS
- EXISTING DRAINAGE CHANNEL
- EXISTING STREAM CHANNEL
- EXISTING GRAVEL ROAD
- EXISTING BRIDGE CULVERT
- CLOSED MINE SHAFT
- OPEN MINE SHAFT
- MINE DRAINAGE DISCHARGE
- 1050 PROPOSED MAJOR CONTOURS
- 1048 PROPOSED MINOR CONTOURS
- RIPRAP AND GEOTEXTILE BERM PROTECTION
- TOP OF BERM
- RIPRAP LINE CHANNEL
- PROPOSED GRAVEL ROAD
- WETLAND VEGETATION SHELF
- CONCRETE
- VFBR ORGANIC MEDIA
- VFBR DRAINAGE LAYER
- PVC PIPE
- DESIGN WATER ELEVATION
- OXIDATION POND
- SURFACE FLOW WETLAND
- VERTICAL FLOW BIOREACTOR
- REAERATION POND
- BAFFLE CURTAINS
- POLISHING WETLAND
- Z-PILING
- EXTENT OF DISTURBED AREA

CONCEPTUAL DESIGN
NOT FOR CONSTRUCTION

NICHOLAS SHEPHERD DISSERTATION

DOUTHAT PASSIVE TREATMENT SYSTEM CONCEPTUAL DESIGNS

OTTAWA COUNTY, OKLAHOMA

PTS-1 PHASE 1 INITIAL OXIDATION POND AND RETENTION BASIN

DATE:
DRAWING SCALE: SEE DRAWING
DRAWN BY: NLS

DRAWING NO.:
C301

295

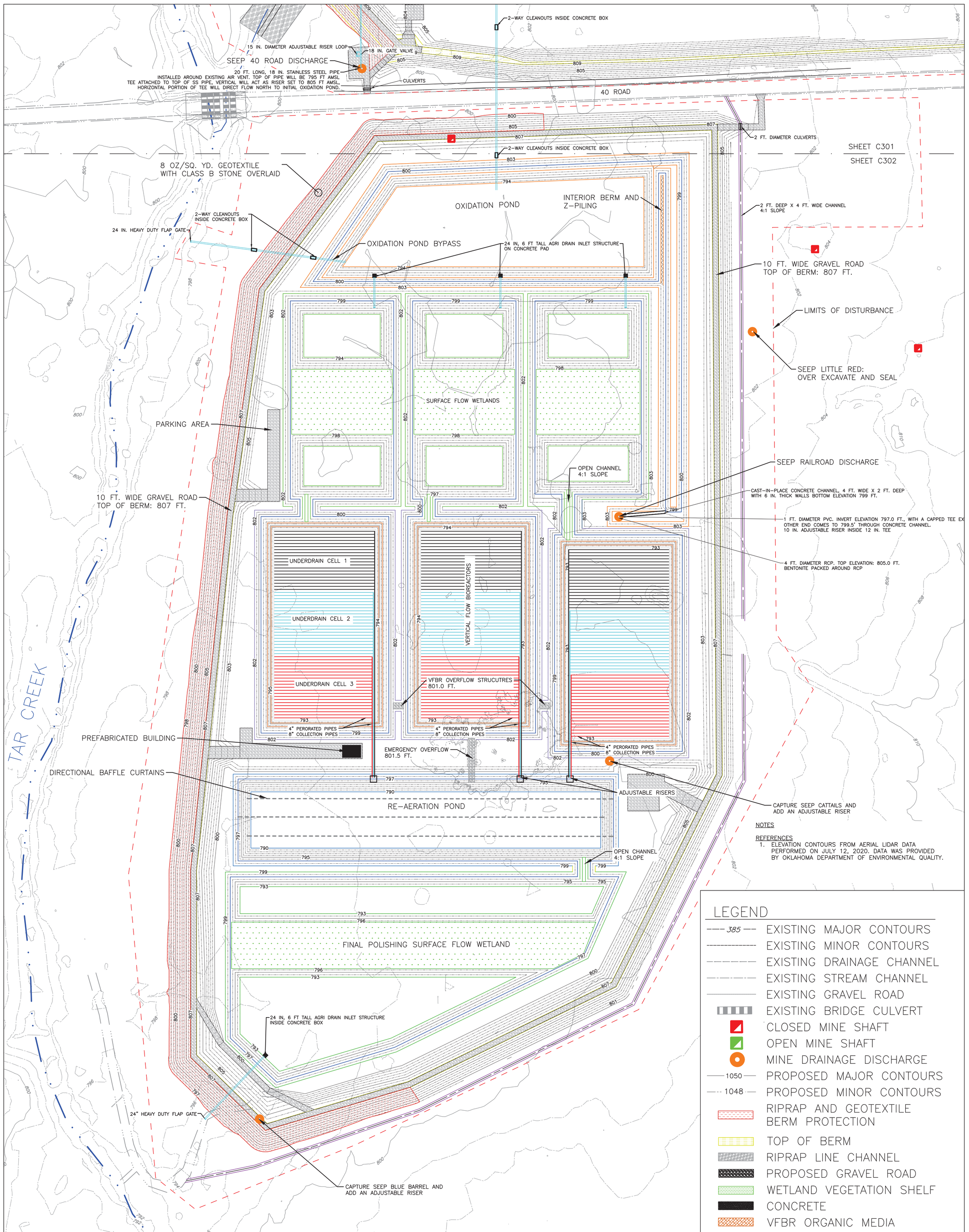

NOTES

REFERENCES

1. ELEVATION CONTOURS FROM AERIAL LIDAR DATA PERFORMED ON JULY 12, 2020. DATA WAS PROVIDED BY OKLAHOMA DEPARTMENT OF ENVIRONMENTAL QUALITY.

LEGEND

- EXISTING MAJOR CONTOURS
- EXISTING MINOR CONTOURS
- EXISTING DRAINAGE CHANNEL
- EXISTING STREAM CHANNEL
- EXISTING GRAVEL ROAD
- EXISTING BRIDGE CULVERT
- CLOSED MINE SHAFT
- OPEN MINE SHAFT
- MINE DRAINAGE DISCHARGE
- PROPOSED MAJOR CONTOURS
- PROPOSED MINOR CONTOURS
- RIPRAP AND GEOTEXTILE BERM PROTECTION
- TOP OF BERM
- RIPRAP LINE CHANNEL
- PROPOSED GRAVEL ROAD
- WETLAND VEGETATION SHELF
- CONCRETE
- VFBR ORGANIC MEDIA
- VFBR DRAINAGE LAYER
- PVC PIPE
- DESIGN WATER ELEVATION
- OXIDATION POND
- SURFACE FLOW WETLAND
- VERTICAL FLOW BIOREACTOR
- REAERATION POND
- BAFFLE CURTAINS
- POLISHING WETLAND
- Z-PILING
- EXTENT OF DISTURBED AREA

NORTH

SCALE IN FEET

0 80 160

CONCEPTUAL DESIGN
NOT FOR CONSTRUCTION

DRAWING NO.: C302

PTS-1 PHASE 2 PASSIVE TREATMENT SYSTEM GRADING

DATE:

DRAWING SCALE: **SEE DRAWING**

DRAWN BY: **NLS**

NICHOLAS SHEPHERD DISSERTATION

DOUTHAT PASSIVE TREATMENT SYSTEM CONCEPTUAL DESIGNS

OTTAWA COUNTY, OKLAHOMA

CREW
Center for Restoration of Ecosystems and Watersheds
University of Oklahoma

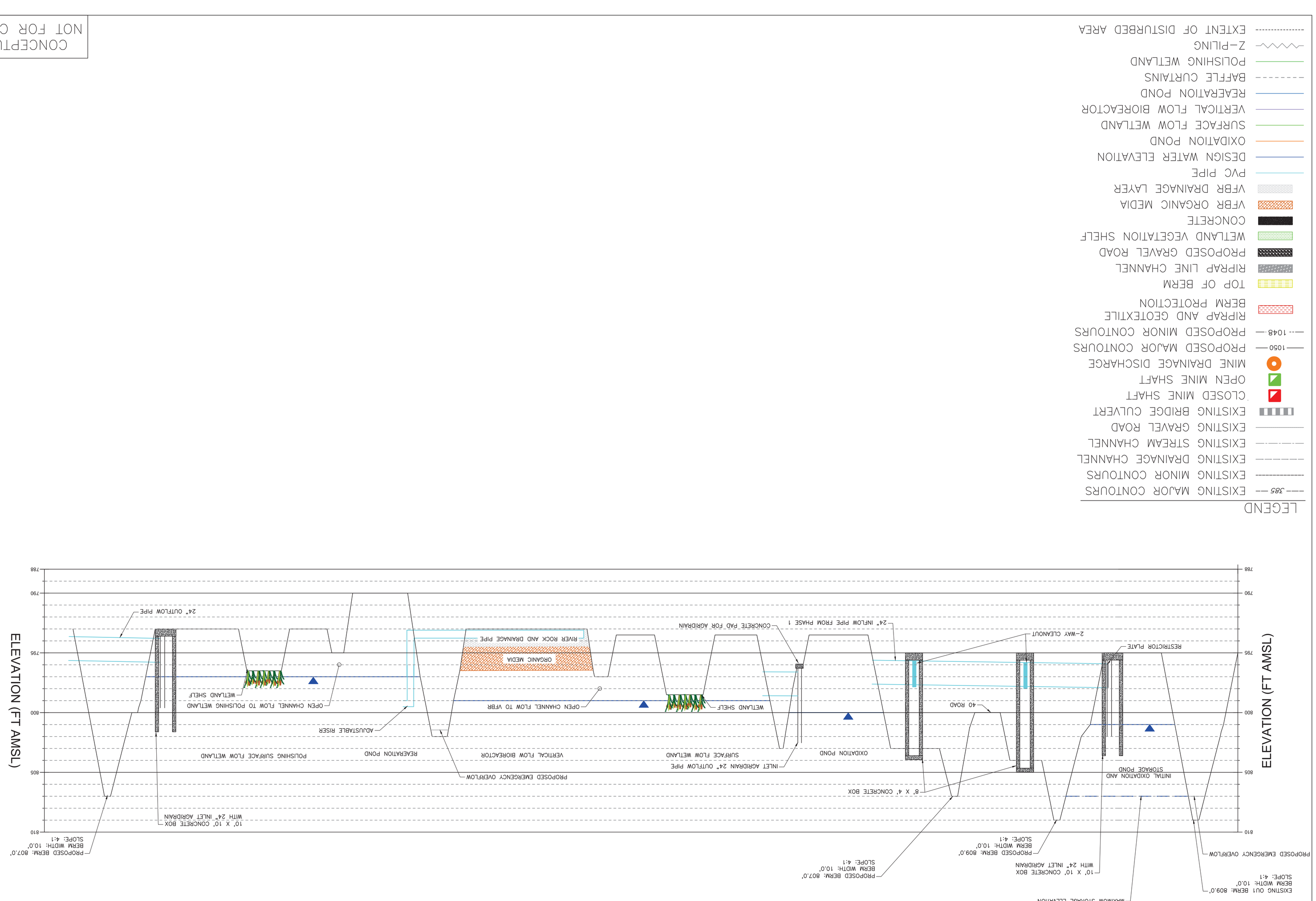

CONCEPTUAL DESIGN
NOT FOR CONSTRUCTION

GRADING PROFILE

DRAWING NO.: **C303**

DATE:
DRAWING SCALE: **SEE DRAWING**
DRAWN BY: **NLS**

DOUTHAT PASSIVE TREATMENT SYSTEM
CONCEPTUAL DESIGNS

OTTAWA COUNTY, OKLAHOMA

NICHOLAS SHEPHERD DISSERTATION

CREW
Center for Restoration of Ecosystems and Watersheds
University of Oklahoma

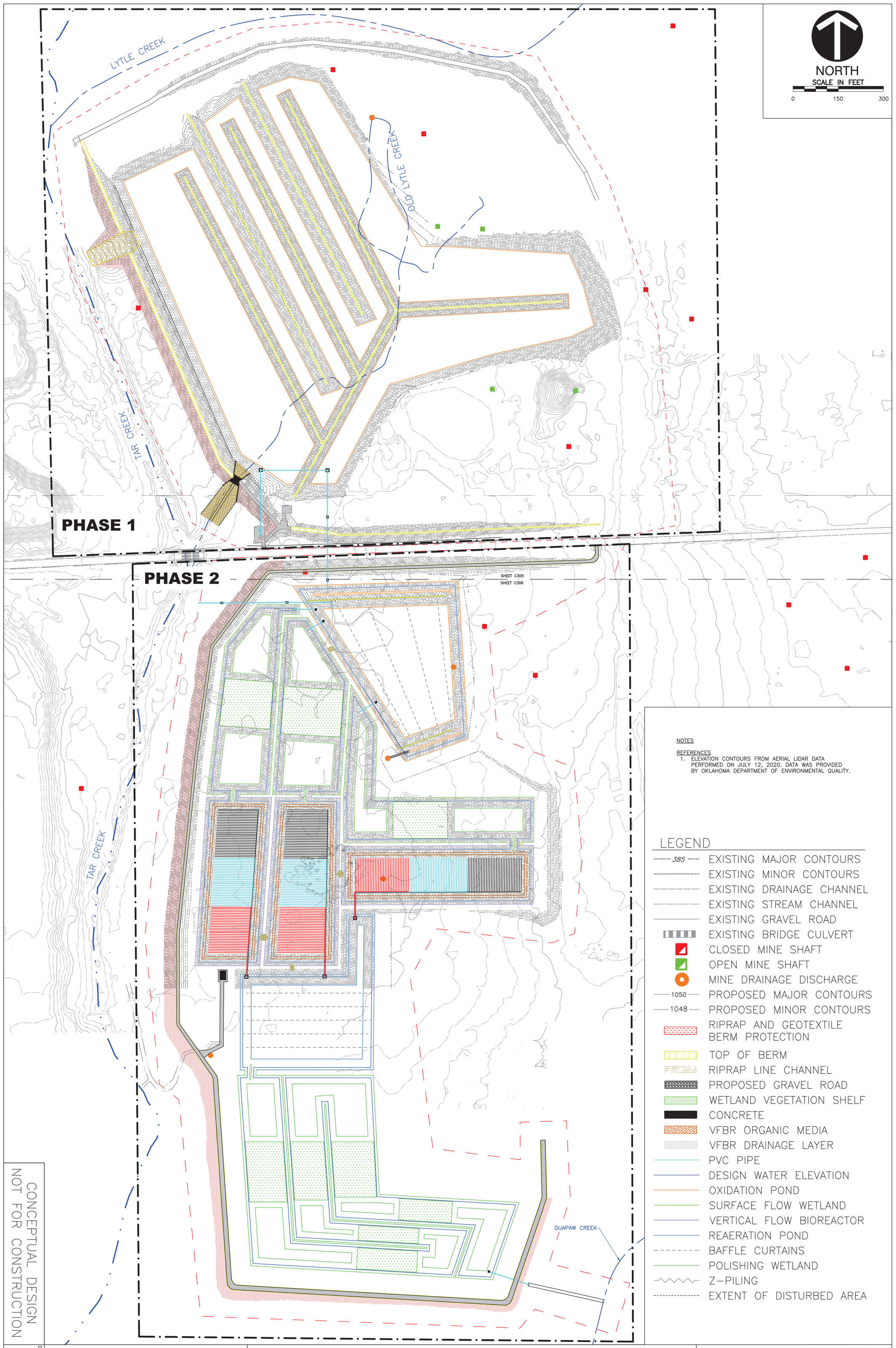

NOTES

REFERENCES
1. ELEVATION CONTOURS FROM AERIAL LIDAR DATA PERFORMED ON JULY 12, 2020. DATA WAS PROVIDED BY OKLAHOMA DEPARTMENT OF ENVIRONMENTAL QUALITY.

LEGEND

- EXISTING MAJOR CONTOURS (385)
- EXISTING MINOR CONTOURS
- EXISTING DRAINAGE CHANNEL
- EXISTING STREAM CHANNEL
- EXISTING GRAVEL ROAD
- EXISTING BRIDGE CULVERT
- CLOSED MINE SHAFT
- OPEN MINE SHAFT
- MINE DRAINAGE DISCHARGE
- PROPOSED MAJOR CONTOURS (1050)
- PROPOSED MINOR CONTOURS (1048)
- RIPRAP AND GEOTEXTILE BERM PROTECTION
- TOP OF BERM
- RIPRAP LINE CHANNEL
- PROPOSED GRAVEL ROAD
- WETLAND VEGETATION SHELF
- CONCRETE
- VFBR ORGANIC MEDIA
- VFBR DRAINAGE LAYER
- PVC PIPE
- DESIGN WATER ELEVATION
- OXIDATION POND
- SURFACE FLOW WETLAND
- VERTICAL FLOW BIOREACTOR
- REAERATION POND
- BAFFLE CURTAINS
- POLISHING WETLAND
- Z–PILING
- EXTENT OF DISTURBED AREA

CONCEPTUAL DESIGN
NOT FOR CONSTRUCTION

DRAWING NO.: C304

PTS-2 SITE LAYOUT

DATE:
DRAWING SCALE: **SEE DRAWING**
DRAWN BY: **NLS**

NICHOLAS SHEPHERD DISSERTATION

DOUTHAT PASSIVE TREATMENT SYSTEM CONCEPTUAL DESIGNS

OTTAWA COUNTY, OKLAHOMA

CREW
Center for Restoration of Ecosystems and Watersheds
University of Oklahoma

NICHOLAS SHEPHERD DISSERTATION

DOUTHAT PASSIVE TREATMENT SYSTEM CONCEPTUAL DESIGNS

OTTAWA COUNTY, OKLAHOMA

CREW
Center for Restoration of Ecosystems and Watersheds
University of Oklahoma

PTS-2 PHASE 1 INITIAL OXIDATION POND AND RETENTION BASIN

DATE:
DRAWING SCALE: SEE DRAWING
DRAWN BY: NLS

DRAWING NO.: **C305**

CONCEPTUAL DESIGN
NOT FOR CONSTRUCTION

LEGEND

- EXISTING MAJOR CONTOURS
- EXISTING MINOR CONTOURS
- EXISTING DRAINAGE CHANNEL
- EXISTING STREAM CHANNEL
- EXISTING GRAVEL ROAD
- EXISTING BRIDGE CULVERT
- CLOSED MINE SHAFT
- OPEN MINE SHAFT
- MINE DRAINAGE DISCHARGE
- PROPOSED MAJOR CONTOURS
- PROPOSED MINOR CONTOURS
- RIPRAP AND GEOTEXTILE BERM PROTECTION
- TOP OF BERM
- RIPRAP LINE CHANNEL
- PROPOSED GRAVEL ROAD
- WETLAND VEGETATION SHELF
- CONCRETE
- VFBR ORGANIC MEDIA
- VFBR DRAINAGE LAYER
- PVC PIPE
- DESIGN WATER ELEVATION
- OXIDATION POND
- SURFACE FLOW WETLAND
- VERTICAL FLOW BIOREACTOR
- REAERATION POND
- BAFFLE CURTAINS
- POLISHING WETLAND
- Z-PILING
- EXTENT OF DISTURBED AREA

NOTES

REFERENCES
1. ELEVATION CONTOURS FROM AERIAL LIDAR DATA PERFORMED ON JULY 12, 2020. DATA WAS PROVIDED BY OKLAHOMA DEPARTMENT OF ENVIRONMENTAL QUALITY.

NORTH
SCALE IN FEET
0 100 200

NORTH
SCALE IN FEET
0 80 160

18 IN. GATE VALVE
24 IN, 6 FT TALL AGRI DRAIN INLET STRUCTURE
24 IN. GATE VALVE
BOTTOM WALL ELEVATION: 796.0 FT.
17.5 FT WIDE COMPOUND WEIR
1.5 FT V-NOTCH WEIR IN CENTER
CONCRETE RETAINING WALL
RIPRAP ARMORED CHANNEL
2-WAY CLEANOUTS INSIDE CONCRETE BOX
15 IN. DIAMETER ADJUSTABLE RISER LOOP
18 IN. GATE VALVE
SEEP 40 ROAD DISCHARGE
20 FT. LONG, 18 IN. STAINLESS STEEL PIPE
INSTALLED AROUND EXISTING AIR VENT. TOP OF PIPE WILL BE 795 FT AMSL.
TEE ATTACHED TO TOP OF SS PIPE, VERTICAL WILL ACT AS RISER SET TO 805 FT AMSL.
HORIZONTAL PORTION OF TEE WILL DIRECT FLOW NORTH TO INITIAL OXIDATION POND.
CULVERTS
40 ROAD
10 FT. WIDE GRAVEL ROAD
TOP OF BERM: 807 FT.
8 OZ/SQ. YD. GEOTEXTILE
WITH CLASS B STONE OVERLAID
2-WAY CLEANOUTS INSIDE CONCRETE BOX
SHEET C305
SHEET C306
2-WAY CLEANOUTS
INSIDE CONCRETE BOX
24 IN. HEAVY DUTY FLAP GATE
OXIDATION POND BYPASS
INTERIOR BERM AND
Z-PILING
24 IN, 6 FT TALL AGRI DRAIN INLET STRUCTURE
ON CONCRETE PAD
OXIDATION POND
LIMITS OF DISTURBANCE
EMERGENCY OVERFLOW
801.5 FT.
SEEP LITTLE RED:
OVER EXCAVATE AND SEAL
SURFACE FLOW WETLANDS
INTERIOR BERM AND
Z-PILING
DIRECTIONAL BAFFLE CURTAINS
SEEP RAILROAD DISCHARGE
CAST-IN-PLACE CONCRETE CHANNEL, 4 FT. WIDE X 2 FT. DEEP
WITH 6 IN. THICK WALLS BOTTOM ELEVATION 799 FT.
1 FT. DIAMETER PVC. INVERT ELEVATION 797.0 FT., WITH A CAPPED TEE EXTENDING TO 794 FT.
OTHER END COMES TO 799.5' THROUGH CONCRETE CHANNEL.
10 IN. ADJUSTABLE RISER INSIDE 12 IN. TEE
SEEP RAILROAD DISCHARGE
4 FT. DIAMETER RCP. TOP ELEVATION: 805.0 FT.
BENTONITE PACKED AROUND RCP
10 FT. WIDE GRAVEL ROAD
TOP OF BERM: 807 FT.
OPEN CHANNEL
4:1 SLOPE
UNDERDRAIN CELL 1
UNDERDRAIN CELL 2
UNDERDRAIN CELL 3
VFBR OVERFLOW STRUCUTRES
801.0 FT.
VERTICAL FLOW BIOREACTORS
OPEN CHANNEL
4:1 SLOPE
SEAL SEEP CATTAILS
6" PERORATED PIPES
10" COLLECTION PIPES
EMERGENCY OVERFLOW
801.5 FT.
ADJUSTABLE RISERS
PREFABRICATED BUILDING
RE-AERATION POND
DIRECTIONAL BAFFLE CURTAINS
CAPTURE SEEP BLUE BARREL AND
ADD AN ADJUSTABLE RISER
OPEN CHANNEL
4:1 SLOPE
FINAL POLISHING SURFACE FLOW WETLAND
QUAPAW CREEK
24 IN, 6 FT TALL AGRI DRAIN INLET STRUCTURE
INSIDE CONCRETE BOX
24" HEAVY DUTY FLAP GATE

NOTES

REFERENCES
1. ELEVATION CONTOURS FROM AERIAL LIDAR DATA PERFORMED ON JULY 12, 2020. DATA WAS PROVIDED BY OKLAHOMA DEPARTMENT OF ENVIRONMENTAL QUALITY.

LEGEND
- 385 EXISTING MAJOR CONTOURS
- EXISTING MINOR CONTOURS
- EXISTING DRAINAGE CHANNEL
- EXISTING STREAM CHANNEL
- EXISTING GRAVEL ROAD
- EXISTING BRIDGE CULVERT
- CLOSED MINE SHAFT
- OPEN MINE SHAFT
- MINE DRAINAGE DISCHARGE
- 1050 PROPOSED MAJOR CONTOURS
- 1048 PROPOSED MINOR CONTOURS
- RIPRAP AND GEOTEXTILE BERM PROTECTION
- TOP OF BERM
- RIPRAP LINE CHANNEL
- PROPOSED GRAVEL ROAD
- WETLAND VEGETATION SHELF
- CONCRETE
- VFBR ORGANIC MEDIA
- VFBR DRAINAGE LAYER
- PVC PIPE
- DESIGN WATER ELEVATION
- OXIDATION POND
- SURFACE FLOW WETLAND
- VERTICAL FLOW BIOREACTOR
- REAERATION POND
- BAFFLE CURTAINS
- POLISHING WETLAND
- Z-PILING
- EXTENT OF DISTURBED AREA

CONCEPTUAL DESIGN
NOT FOR CONSTRUCTION

DRAWING NO.: C306

PTS-2 PASSIVE TREATMENT SYSTEM GRADING

DATE:
DRAWING SCALE: **SEE DRAWING**
DRAWN BY: **NLS**

NICHOLAS SHEPHERD DISSERTATION

DOUTHAT PASSIVE TREATMENT SYSTEM CONCEPTUAL DESIGNS

OTTAWA COUNTY, OKLAHOMA

CREW
Center for Restoration of Ecosystems and Watersheds
University of Oklahoma

Table 6E.1: Phase 1 present value construction cost estimate for the conceptual PTS-1 design (see Appendix 6G for cost explanations)

Cost Category	Item	Unit	Quantity	Unit Cost	Total Cost
1. Mobilization/Demobilization	Mobilization/Demobilization	LS	1	10% of Construction Cost	$295,000
2. Bonds and permits	Performance Bond	LS	1	2% of Construction Cost	$59,000
	Payment Bond	LS	1	2% of Construction Cost	$59,000
	Maintenance Bond	LS	1	5% of Construction Cost	$147,000
	Stormwater Pollution Prevention Plan	LS	1	$20,000	$20,000
3. Clearing and grubbing	Clearing and grubbing	Ac.	25	$2,500	$63,000
4. Erosion Control	Erosion control	LF	9,800	$7.00	$69,000
5. Earthwork	Berm Construction: Purchase, Excavate, Load and Haul	Cu. Yd.	17,800	$16.00	$285,000
	Berm Construction: Grade and Compact	Cu. Yd.	17,801	$8.00	$142,000
	Grading: Cut material for pond and berm	Cu. Yd.	48,813	$14.00	$683,000
	Road Construction	LF	4,968	$20.00	$99,000
	8 oz/sy Geotextile	Sq, Ft.	97,440	$1.00	$97,000
	Class B Stone for Creek side of Berm	Cu. Yd.	7,218	$35.00	$253,000
6. Flow Control Structures	8'x10' x 6' deep Concrete Box	Ea.	2	$20,484	$41,000
	8'x4'x8 feet deep Concrete Box	Ea.	1	$16,095	$16,000
	AgriDrains	Ea.	2	$4,134.81	$8,000
	Stainless Steel Valves	Ea.	2	$65,943	$132,000
	Sch. 40 24" PVC Pipe and Fittings	LF	590	$420.66	$248,000
	S40 Capture System	LS	1	$38,436	$38,000
	Weir Construction	LS	1	$360,000	$360,000
7. Drainage	Drainage Channel on 40 Rd	LF	900	$150.00	$135,000
8. Fencing and Vegetation	Fence Removal	LF	1,000	$5.00	$5,000
	Fence	LF	6,500	$13.75	$89,000
	Gate	Ea.	1	$1,000	$1,000
	Vegetation	Ac.	36	$4,500	$162,000
9. Surveying	Field Surveys	Ea.	3	$15,000	$45,000
10. Engineering Fees	Engineering Fees	LS	1	25% of Total Project	$888,000
	Total Cost				**$4,440,000**

Table 6E.2: Phase 1 five-year assessment period present value cost estimate for the conceptual PTS-1 design

Cost Category	Item	Y1	Y2[1]	Y3	Y4[1]	Y5	Cumulative
1. Sampling	Sampling Materials and Supplies	$25,000	$25,800	$26,500	$27,300	$28,100	$133,000
	Travel	$9,000	$9,300	$9,500	$9,800	$10,100	$48,000
	Salaries	$35,000	$36,100	$37,100	$38,200	$39,400	$186,000
2. Operations and Maintenance	Travel	$4,000	$4,100	$4,200	$4,400	$4,500	$21,000
	Salaries	$15,000	$15,500	$15,900	$16,400	$16,900	$80,000
	Materials and Supplies	$5,000	$20,600	$5,300	$21,900	$5,600	$58,000
3. Administration	Facilities and Administration (55%)	$51,200	$61,200	$54,300	$64,900	$57,600	$289,000
	Total Annual Cost	$144,000	$172,000	$153,000	$183,000	$162,000	
	Total Cost						**$815,000**

[1]Years 2 and 4 include an increased cost to allow for a subcontractor to be hired to adjust the weir elevation

Table 6E.3: Phase 2 present value construction cost estimate for the conceptual PTS-1 design (see Appendix 6G for cost explanations)

Cost Category	Item	Unit	Quantity	Unit Cost	Total Cost
1.Mobilization/Demobilization	Mobilization/Demobilization	LS	1	10% of Construction Cost	$526,000
2. Bonds and permits	Performance Bond	LS	1	2% of Construction Cost	$105,000
	Payment Bond	LS	1	2% of Construction Cost	$105,000
	Maintenance Bond	LS	1	5% of Construction Cost	$263,000
	Stormwater Pollution Prevention Plan	LS	1	$20,000	$20,000
3. Clearing and grubbing	Clearing and grubbing	Ac.	20	$2,500	$50,000
4. Erosion Control	Erosion control	LF	4,700	$7.00	$33,000
5. Earthwork	Grading: Cut and haul	Cu. Yd.	42,008	$14.00	$588,000
	Grading: Grade and Compact	Cu. Yd.	75,144	$12.00	$902,000
	Road Construction	LF	4,500	$20.00	$90,000
	8 oz/sy Geotextile	Sq, Ft.	75,420	$1.00	$75,000
	Class B Stone for Creek side of Berm	Cu. Yd.	5,587	$35.00	$196,000
6. Flow Conveyance and media	8'x10' x 6' deep Concrete Box	Ea.	4	$20,484	$82,000
	8'x4'x8 feet deep Concrete Box	Ea.	3	$16,095	$48,000
	AgriDrains	Ea.	4	$4,134.81	$17,000
	Stainless Steel Valves	Ea.	3	$65,943	$198,000
	Sch. 40 24" PVC Pipe	LF	819	$420.66	$345,000
	Sch. 40 4" PVC Pipe (VFBR)	LF	29,760	$20.37	$606,000
	Sch. 40 8" PVC Pipe (VFBR)	LF	2,568	$65.55	$168,000
	Mushroom Compost	Cu. Yd.	2,976	$67.50	$201,000
	Woodchips	Cu. Yd.	2,976	$40.50	$121,000
	River rock	Cu. Yd.	4,108	$81.25	$334,000
	Seep Railroad Capture system	LS	1	$51,600	$52,000
	Class B Stone for Emergency bypass channels	Cu. Yd.	150	$35.00	$5,000
7. Reaeration System	Reaeration System	LS	1	$500,000	$500,000
	Prefabricated building (20' x 30')	LS	1	$41,195	$41,000
8. Drainage	Drainage Channel	LF	2,212	$150.00	$332,000
9. Fencing and Vegetation	Fence Removal	LF	3,032	$5.00	$15,000
	Fence	LF	5,800	$13.75	$80,000
	Gate	Ea.	1	$1,000	$1,000
	Wetland vegetation	Ac.	2.21	$11,525.30	$25,000
	Vegetation	Ac.	19.80	$4,500	$89,000
10. Surveying	Field Surveys	Ea.	3	$15,000	$45,000
11. Engineering Fees	Engineering Fees	LS	1	25% of Total Project	$1,289,000
	Total Cost				$7,546,000

Table 6E.4: Phase 2 five-year assessment period present value cost estimate for the conceptual PTS-1 design

Cost Category	Item	Y1	Y2	Y3[1]	Y4	Y5[1]	Cumulative
1. Sampling	Sampling Materials and Supplies	$35,000	$36,100	$37,100	$38,200	$39,400	$186,000
	Travel	$10,000	$10,300	$10,600	$10,900	$11,300	$53,000
	Salaries	$45,000	$46,400	$47,700	$49,200	$50,600	$239,000
2. Operations and Maintenance	Travel	$5,000	$5,200	$5,300	$5,500	$5,600	$27,000
	Salaries	$10,000	$10,300	$10,600	$10,900	$11,300	$53,000
	Materials and Supplies	$20,000	$20,600	$53,000	$21,900	$112,600	$228,000
3. Administration	Facilities and Administration (55%)	$68,800	$70,800	$90,400	$75,100	$126,900	$432,000
	Total Annual Cost	$194,000	$200,000	$255,000	$212,000	$358,000	
	Total Cost						**$1,218,000**

[1]Year 3 includes an increase cost for major rehabilitative maintenance that may be required following construction. Year 5 includes rehabilitative and replacement costs to mix VFBRs and replace batteries in solar battery bank

Table 6E.5: Summary of PTS-1 cost estimate showing present and future values based on 3% inflation rate

Year	Phase	Present Value	Future Value
1	Phase 1 Construction	$4,440,000	$4,440,000
2	Phase 1 Assessment Period	$140,000	$150,000
3		$170,000	$180,000
4		$140,000	$160,000
5		$170,000	$190,000
6		$140,000	$170,000
7	Phase 2 Construction	$7,550,000	$9,280,000
8	Phase 2 Assessment Period	$190,000	$250,000
9		$190,000	$250,000
10		$240,000	$320,000
11		$190,000	$270,000
12		$320,000	$450,000
	Phase 1 Total		**$5,300,000**
	Phase 2 Total		**$10,820,000**
	Project Completion Total		**$16,130,000**

Table 6E.6: Phase 1 present value construction cost estimate for the conceptual PTS-2 design (see Appendix 6G for cost explanations)

Cost Category	Item	Unit	Quantity	Unit Cost	Total Cost
1. Mobilization/Demobilization	Mobilization/Demobilization	LS	1	10% of Construction Cost	$628,000
2. Bonds and permits	Performance Bond	LS	1	2% of Construction Cost	$126,000
	Payment Bond	LS	1	2% of Construction Cost	$126,000
	Maintenance Bond	LS	1	5% of Construction Cost	$314,000
	Stormwater Pollution Prevention Plan	LS	1	$20,000	$20,000
3. Clearing and grubbing	Clearing and grubbing	Ac.	25	$2,500	$63,000
4. Erosion Control	Erosion control	LF	9,800	$7.00	$69,000
5. Earthwork	Berm Construction: Purchase, Excavate, Load and Haul	Cu. Yd.	17,800	$16.00	$285,000
	Berm Construction: Grade and Compact	Cu. Yd.	17,800	$8.00	$142,000
	Grading: Cut material for pond and berm	Cu. Yd.	334,436	$12.00	$4,013,000
	Road Construction	LF	4,968	$20.00	$99,000
	8 oz/sy Geotextile	Sq. Ft.	97,440	$1.00	$97,000
	Class B Stone for Creek side of Berm	Cu. Yd.	7,218	$35.00	$253,000
6. Flow Control Structures	8'x10' x 6' deep Concrete Box	Ea.	2	$20,484	$41,000
	8'x4'x8 feet deep Concrete Box	Ea.	1	$16,095	$16,000
	AgriDrains	Ea.	2	$4,134.81	$8,000
	Stainless Steel Valves	Ea.	2	$65,943	$132,000
	Sch. 40 24" PVC Pipe and Fittings	LF	590	$420.66	$248,000
	S40 Capture System	LS	1	$38,436	$38,000
	Weir Construction	LS	1	$360,000	$360,000
7. Drainage	Drainage Channel on 40 Rd	LF	900	$150.00	$135,000
8. Fencing and Vegetation	Fence Removal	LF	1,000	$5.00	$5,000
	Fence	LF	6,500	$13.75	$89,000
	Gate	Ea.	1	$1,000	$1,000
	Vegetation	Ac.	36	$4,500	$162,000
9. Surveying	Field Surveys	Ea.	3	$15,000	$45,000
10. Engineering Fees	Engineering Fees	LS	1	25% of Total Project	$1,879,000
	Total Cost				$9,394,000

Table 6E.7: Phase 1 five-year assessment period present value cost estimate for the conceptual PTS-2 design

Cost Category	Item	Y1	Y2[1]	Y3	Y4[1]	Y5	Cumulative
1. Sampling	Sampling Materials and Supplies	$25,000	$25,800	$26,500	$27,300	$28,100	$133,000
	Travel	$9,000	$9,300	$9,500	$9,800	$10,100	$48,000
	Salaries	$35,000	$36,100	$37,100	$38,200	$39,400	$186,000
2. Operations and Maintenance	Travel	$4,000	$4,100	$4,200	$4,400	$4,500	$21,000
	Salaries	$15,000	$15,500	$15,900	$16,400	$16,900	$80,000
	Materials and Supplies	$5,000	$20,600	$5,300	$21,900	$5,600	$58,000
3. Administration	Facilities and Administration (55%)	$51,200	$61,200	$54,300	$64,900	$57,600	$289,000
	Total Annual Cost	$144,000	$172,000	$153,000	$183,000	$162,000	
	Total Cost						**$815,000**

[1]Years 2 and 4 include an increased cost to allow for a subcontractor to be hired to adjust the weir elevation

Table 6E.8: Phase 2 present value construction cost estimate for the conceptual PTS-2 design (see Appendix 6G for cost explanations)

Cost Category	Item	Unit	Quantity	Unit Cost	Total Cost
1.Mobilization/Demobilization	Mobilization/Demobilization	LS	1	10% of Construction Cost	$1,152,000
2. Bonds and permits	Performance Bond	LS	1	2% of Construction Cost	$230,000
	Payment Bond	LS	1	2% of Construction Cost	$230,000
	Maintenance Bond	LS	1	5% of Construction Cost	$576,000
	Stormwater Pollution Prevention Plan	LS	1	$20,000	$20,000
3. Clearing and grubbing	Clearing and grubbing	Ac.	30	$2,500	$75,000
4. Erosion Control	Erosion control	LF	7,918	$7.00	$55,000
5. Earthwork	Grading: Cut and haul	Cu. Yd.	294,433	$12.00	$3,533,000
	Grading: Grade and Compact	Cu. Yd.	92,124	$12.00	$1,105,000
	Road Construction	LF	5,060	$20.00	$101,000
	8 oz/sy Geotextile	Sq, Ft.	124,078	$1.00	$124,000
	Class B Stone for Creek side of Berm	Cu. Yd.	9,191	$35.00	$322,000
6. Flow Conveyance and media	8'x10' x 6' deep Concrete Box	Ea.	4	$20,484	$82,000
	8'x4'x8 feet deep Concrete Box	Ea.	3	$16,095	$48,000
	AgriDrains	Ea.	4	$4,134.81	$17,000
	Stainless Steel Valves	Ea.	3	$65,943	$198,000
	Sch. 40 24" PVC Pipe	LF	1,075	$420.66	$452,000
	Sch. 40 6" PVC Pipe (VFBR)	LF	36,025	$38.28	$1,379,000
	Sch. 40 10" PVC Pipe (VFBR)	LF	3,796	$83.97	$319,000
	Mushroom Compost	Cu. Yd.	9,443	$67.50	$637,000
	Woodchips	Cu. Yd.	9,443	$40.50	$382,000
	River rock	Cu. Yd.	16,479	$81.25	$1,339,000
	Seep Railroad Capture system	LS	1	$51,600	$52,000
	Class B Stone for Emergency bypass channels	Cu. Yd.	150	$35.00	$5,000
7. Reaeration System	Reaeration System	LS	1	$500,000	$500,000
	Prefabricated building (20' x 30')	LS	1	$41,195	$41,000
8. Drainage	Drainage Channel	LF	2,300	$150.00	$345,000
9. Fencing and Vegetation	Fence Removal	LF	3,032	$5.00	$15,000
	Fence	LF	10,550	$13.75	$145,000
	Gate	Ea.	3	$1,000	$3,000
	Wetland vegetation	Ac.	4.28	$11,525.30	$49,000
	Vegetation	Ac.	25	$4,500.00	$113,000
10. Surveying	Field Surveys	Ea.	3	$20,000	$60,000
11. Engineering Fees	Engineering Fees	LS	1	25% of Total Project	$2,842,000
	Total Cost				**$16,548,000**

Table 6E.9: Phase 2 five-year assessment period present value cost estimate for the conceptual PTS-2 design

Cost Category	Item	Y1	Y2	Y3[1]	Y4	Y5[1]	Cumulative
1. Sampling	Sampling Materials and Supplies	$35,000	$36,100	$37,100	$38,200	$39,400	$186,000
	Travel	$10,000	$10,300	$10,600	$10,900	$11,300	$53,000
	Salaries	$45,000	$46,400	$47,700	$49,200	$50,600	$239,000
2. Operations and Maintenance	Travel	$5,000	$5,200	$5,300	$5,500	$5,600	$27,000
	Salaries	$10,000	$10,300	$10,600	$10,900	$11,300	$53,000
	Materials and Supplies	$20,000	$20,600	$63,700	$21,900	$157,600	$284,000
3. Administration	Facilities and Administration (55%)	$68,800	$70,800	$96,300	$75,100	$151,700	$463,000
	Total Annual Cost	$194,000	$200,000	$271,000	$212,000	$427,000	
	Total Cost						**$1,304,000**

[1]Year 3 includes an increase cost for major rehabilitative maintenance that may be required following construction. Year 5 includes rehabilitative and replacement costs to mix VFBRs and replace batteries in solar battery bank

Table 6E.10: Summary of PTS-2 cost estimate showing present and future values based on 3% inflation rate

Year	Phase	Present Value	Future Value
1	Phase 1 Construction	$9,390,000	$9,390,000
2	Phase 1 Assessment Period	$140,000	$150,000
3		$170,000	$180,000
4		$140,000	$160,000
5		$170,000	$190,000
6		$140,000	$170,000
7	Phase 2 Construction	$16,550,000	$20,350,000
8	Phase 2 Assessment Period	$190,000	$250,000
9		$190,000	$250,000
10		$260,000	$340,000
11		$190,000	$270,000
12		$380,000	$540,000
	Phase 1 Total		**$10,260,000**
	Phase 2 Total		**$22,000,000**
	Project Completion Total		**$32,260,000**

APPENDIX 6F
Cost Estimate Explanations

Cost Category Explanations

Phase 1

Cost Category 1: Mobilization/Demobilization

The price includes all costs for project start-up, including costs of insurance, transportation of supplies and equipment to the job site, installation, and erection of equipment, creating Contractor staging area, and temporary facilities of every kind, as well as all costs for removing same and site cleanup. Given the remoteness of the site, the mobilization was estimated to be greater than usual, at 10% of the construction cost.

Cost Category 2: Bonds and Permits

The bonds and permits category include all performance, payment, and maintenance bonds required for the project. Additionally, the category will include the Storm Water Pollution Prevention Plan (SWPPP). The price includes all required labor, materials, equipment, and expenses (including permit fees) to develop and maintain a Storm Water Pollution Prevention Plan (SWPPP) in accordance with applicable State and Federal regulatory requirements.

Cost Category 3: Clearing and Grubbing

Clearing and grubbing include all materials, equipment, and labor required to complete the removal of all trees, stumps, and other woody vegetation to a minimum depth of 18 inches below the existing grade. The area used in the cost estimate is an approximation based on the vegetation coverage within the Phase 1 project area.

Cost Category 4: Erosion Control

Erosion control includes any materials, equipment, and labor required to install the necessary erosion control devices, including straw wattles, silt fencing, and rock check dams. The cost estimate would be more defined in a completed design as the location, type, and quantity of the erosion controls would be specified in the drawings.

Cost Category 5: Earthwork

The earthwork category includes multiple items that specify the type of earthwork. The berm construction excavation and haul cost assume that offsite clay will have to be purchased and hauled to the site because onsite clay will not be sufficient for berm material. If onsite material is an option, this cost will decrease substantially. The berm construction grading and compaction is the cost to move material around the site once it has been hauled to the site, and the berm will require compaction in incremental lifts as it is being constructed.

Grading: cut material includes material that will be excavated to create the bottom of the initial oxidation pond. It is assumed that this material will not meet the remedial action goals and all cut material will be hauled to the repository. If this can be completed by only using offroad haul trucks, the price would likely decrease.

Road construction includes a gravel road that would be constructed on the majority of the berm as shown in the drawings. Additionally, the road construction would include gravel parking pads at the seep 40 discharge and inside the berm, near the outflow structures as shown on the drawings.

The class B stone and geotextile material will cover the portion of the newly constructed berm that is on the creek side face. The stone layer is 2 ft thick, matching the stone thickness of the Operable Unit 1 berm design.

Cost Category 6: Flow Control Structures

The flow control structures include the 24-inch PVC pipe to route water into the berm from S40, and to create the stub for the future connection to the Phase 2 design. Two 8 ft x 10 ft concrete boxes will house the inflow/outflow stainless steel valves and Agri-Drain. The 8 ft x 4 ft concrete box will house a cleanout and protect the stub for the future connection to the Phase 2 system. The S40 capture system will include the stainless-steel pipe and fittings, and equipment to push the pipe into the ground around the discharge, seal and capture the discharge to divert the water into the height-adjustable PVC pipe structure as shown in the drawings. The weir construction includes cast-in-place concrete for the berm retaining walls, weir base, and weir support structure. It also includes the construction and installation of the height-adjustable stainless steel weir plate and the parts and pieces used to secure the weir. The cost of the weir construction is an approximation and will likely change if a full design is created.

Cost Category 7: Drainage Channel on 40 Rd

The drainage channel category consists of reconstructing the stormwater drainage channel along the northern side of 40 Road that will be altered during the construction of the southern berm and installing culverts for the gravel parking area at seep 40.

Cost Category 8: Fencing and Vegetation

Fencing includes the removal of the existing fence on the southern side of the Phase 1 project site and constructing a new fence around the perimeter of the site. Vegetation is a cost estimate for seedbed preparation, lime and fertilizer additions, and broadcast seeding of the disturbed terrestrial land on the project site.

Cost Category 9: Surveying

Surveying consists of establishing survey control points, performing as-built surveys, resetting survey control points, and providing construction quantities based on their survey. It is estimated that three surveys will be conducted, an initial survey, a grading confirmation survey, and a final as-built survey.

Cost Category 10: Engineering Fees

The engineering fees were estimated at 25% of the project and would include the engineering and design of Phase 1, acquiring the necessary project permits from the Army Corps of Engineers, and at 25%, the cost is expected to cover small redesigns that may be required due to unforeseen circumstances during construction.

Phase 2

Cost Category 1: Mobilization/Demobilization

The price includes all costs for project start-up, including costs of insurance, transportation of supplies and equipment to the job site, installation, and erection of equipment, creating Contractor staging area, and temporary facilities of every kind, as well as all costs for removing same and site cleanup. Given the remoteness of the site, the mobilization was estimated to be greater than usual, at 10% of the construction cost.

Cost Category 2: Bonds and Permits

The bonds and permits category include all performance, payment, and maintenance bonds required for the project. Additionally, the category will include the Storm Water Pollution Prevention Plan (SWPPP). The price includes all required labor, materials, equipment, and expenses (including permit fees) to develop and maintain a Storm Water Pollution Prevention Plan (SWPPP) in accordance with applicable State and Federal regulatory requirements.

Cost Category 3: Clearing and Grubbing

Clearing and grubbing include all materials, equipment, and labor required to complete the removal of all trees, stumps, and other woody vegetation to a minimum depth of 18 inches below the existing grade. The area used in the cost estimate is an approximation based on the vegetation coverage within the Phase 1 project area.

Cost Category 4: Erosion Control

Erosion control includes any materials, equipment, and labor required to install the necessary erosion control devices, including straw wattles, silt fencing, and rock check dams. The cost estimate would be more defined in a completed design as the location, type, and quantity of the erosion controls would be specified in the drawings.

Cost Category 5: Earthwork

The earthwork for Phase 2 assumes that excess cut material will not meet the remedial action goals and all cut material will be hauled to the repository. The decrease in cost compared to Phase 1 assumes a path will be created from the southern side to the repository so off-road trucks can haul directly to the repository.

The grade and compact earthwork item assume that there will be onsite clay material that meets the criteria for the berm material and has a low enough permeability for the lining of the ponds. The excess material from creating the ponds will be graded and compacted to create the berm.

Road construction includes a gravel road that would be constructed on top of the berm and includes the parking areas and base for the solar panel shed as shown on the drawings.

The class B stone and geotextile material will cover the outer face on the north and west side of the berm because these faces are the most likely to experience elevated flow velocities. The stone layer is 2 ft thick, matching the stone thickness of the Operable Unit 1 berm design.

Cost Category 6: Flow Conveyance

The 24-inch PVC pipe is used to connect the Phase 1 stub to the Phase 2 oxidation pond, as the bypass from the oxidation pond, and as the outflow pipe from the PTS.

Three 8 ft x 10 ft concrete boxes will collect water at the inflow of the reaeration pond from each of the three VFBRs, the fourth 8 ft x 10 ft concrete box will house the AgriDrain at the outflow of the system. The 8 ft x 4 ft concrete box will house cleanouts and stainless-steel values located on the inflow pipe from Phase 1 and two on the bypass pipe from the oxidation pond as shown in the drawings. Three AgriDrains are located in the oxidation pond to evenly split the flow into the three parallel wetlands. The fourth AgriDrain is at the system effluent. The 4” PVC perforated pipe is the collection pipes in the VFBR and the 8” PVC is the gathering line that conveys the water to the reaeration pond. The mushroom compost and river rock will be placed into the VFBR as the media and drainage layers. The Class B Stone is used for the emergency bypass channels between each of the VFBRs and from the center VFBR into the reparation pond.

The Seep Railroad capture system will include the stainless-steel pipe and fittings, and equipment to push the pipe into the ground around the discharge, seal and capture the discharge to divert the water into the height-adjustable PVC pipe structure that discharges water into a concrete channel, as shown in the drawings.

Cost Category 7: Reaeration System

The reaeration system item will include all parts and materials to construct the solar system, battery bank, blowers, and the PVC pipe, hoses, and float mix aerators. The prefabricated 20 ft by 30 ft building will house the battery bank and blowers, along with O&M equipment.

Cost Category 8: Drainage

The drainage channel category consists of constructing two stormwater drainage channels on the east side of the project site to divert the runoff water from the east around the system and to Tar Creek.

Cost Category 9: Fencing and Vegetation

Fencing includes the removal of the existing fence on the north and east sides of the Phase 2 project site and constructing a new fence around the perimeter of the site. Vegetation is a cost estimate for seedbed preparation, lime and fertilizer additions, and broadcast seeding of the disturbed terrestrial land on the project site. The wetland vegetation cost item is the estimate to seed the wetland shelves in the surface flow wetlands and polishing units. The cost of the wetland vegetation can likely be decreased if a portion of the existing cattail marsh is preserved as a source to plant the wetland shelves.

Cost Category 10: Surveying

Surveying consists of establishing survey control points, performing as-built surveys, resetting survey control points, and providing construction quantities based on their survey. It is estimated that three surveys will be conducted, an initial survey, a grading confirmation survey, and a final as-built survey.

Cost Category 11: Engineering Fees

The engineering fees were estimated at 25% of the project and would include the engineering and design of Phase 2, acquiring the necessary project permits from the Army Corps of Engineers, and at 25%, the cost is expected to cover small redesigns that may be required due to unforeseen circumstances during construction.

APPENDIX 7A
Mine Pool and Groundwater Raw Data

Table A7.1: Water chemistry of samples collected in the Picher field mine pool at the Douthat Wells

Site Name	Date Time	Surface Elevation	Underground Void Elevations		Sample Elevation	Temperature	Specific Conductivity	DO Sat	DO Conc	pH	Alkalinity	Total Hardness	Turbidity	Sulfate	Chloride	$\delta^{18}O$	$\delta^{2}H$
			Floor	Ceiling													
	M/D/Y HH:MM:SS	(m AMSL)	(m AMSL)	(m AMSL)	(m AMSL)	°C	µS/cm	%	mg/L		mg/L CaCO3 eq.	mg/L	NTU	mg/L	mg/L	VSMOW (‰)	VSMOW (‰)
Douthat Discharge Well	11/11/21 14:42	244.4	185.3	197.8	244.45	15.58	2,225	18.50	1.83	6.21	132.50	1,736.46	0.70	1,457.50	11.27		
Douthat Discharge Well	11/12/21 9:16	244.4	185.3	197.8	213.97	14.62	2,206	36.20	3.66	6.23							
Douthat Discharge Well	11/12/21 9:27	244.4	185.3	197.8	204.83	14.78	2,206	29.80	3.00	6.23							
Douthat Discharge Well	11/12/21 9:40	244.4	185.3	197.8	198.73	14.99	2,214	27.10	2.71	6.23							
Douthat Discharge Well	11/12/21 9:53	244.4	185.3	197.8	192.63	15.23	2,229	37.30	3.72	6.30							
Douthat Discharge Well	11/12/21 10:19	244.4	185.3	197.8	189.59	15.30	2,770	23.80	2.37	6.09		2,023.33					
Douthat Discharge Well	11/12/21 10:04	244.4	185.3	197.8	186.54	15.28	3,280	31.50	3.12	6.03	352.00	2,275.67	2.05	2,281.60	20.39		
Douthat Discharge Well	11/12/21 10:31	244.4	185.3	197.8	182.58	15.32	3,318	30.50	3.03	6.04		2,193.51		2,281.20	19.87		
Douthat Well	8/9/20 18:53	245.5	186.4	198.9	185.80	17.21	3,437	39.80	3.79	5.65	346.50	2,137.86	87.07			-5.75	-32.98
Douthat Well	12/22/20 11:25	245.5	186.4	198.9	186.11	16.48	3,422	30.00	2.90	5.82	358.50	2,340.28	86.95	2,241.30		-5.81	-31.76
Douthat Well	2/25/21 14:40	245.5	186.4	198.9	186.11	15.82	3,234	28.40	2.78	6.06	345.00	2,010.29	1.51	2,184.70		-5.71	-31.26
Douthat Well	11/12/21 11:30	245.5	186.4	198.9	199.82	15.64	2,241	16.90	1.67	6.25		1,759.74					
Douthat Well	11/12/21 11:22	245.5	186.4	198.9	190.68	15.61	2,309	18.70	1.85	6.16		1,829.40					
Douthat Well	11/12/21 11:06	245.5	186.4	198.9	185.80	15.66	3,291	28.10	2.76	6.02	349.50	2,278.44	1.39	2,242.10	21.05		

Table A7.1: Continued

Site Name	Date Time	Surface Elevation	Underground Void Elevations		Sample Elevation		Arsenic	Calcium	Cadmium	Copper	Iron	Potassium	Lithium	Magnesium	Manganese	Nickel	Lead	Sulfur	Silicon	Zinc
			Floor	Ceiling																
	M/D/Y HH:MM:SS	m AMSL	m AMSL	m AMSL	m AMSL		mg/L	mg/L	mg/L	mg/L	mg/L	mg/L	mg/L	mg/L	mg/L	mg/L	mg/L	mg/L	mg/L	mg/L
Douthat Discharge Well	11/11/21 14:42	244.4	185.3	197.8	244.45	Total		621.69	0.02	0.00	17.35	5.59	0.07	44.72	0.80	0.13	0.04	492.80	8.06	6.11
						Dissolved		621.26	0.02	0.00	17.37	5.61	0.07	44.85	0.80	0.13	0.03	496.50	8.08	6.15
Douthat Discharge Well	11/12/21 10:19	244.4	185.3	197.8	189.59		0.03	677.06	0.02	0.00	141.19	11.05	0.14	80.81	1.47	0.59	0.24	648.52	9.42	9.44
Douthat Discharge Well	11/12/21 10:04	244.4	185.3	197.8	186.54	Total	0.03	666.49	0.04	0.00	261.97	14.08	0.25	145.79	3.41	1.34	0.44	805.42	6.64	36.21
						Dissolved		669.38	0.04	0.00	262.70	13.98	0.25	146.76	3.39	1.33	0.43	817.98	6.60	36.46
Douthat Discharge Well	11/12/21 10:31	244.4	185.3	197.8	182.58	Total	0.02	640.42	0.04	0.00	264.87	13.20	0.25	144.37	3.25	1.33	0.42	878.87	5.93	34.70
Douthat Well	8/9/20 18:53	245.5	186.4	198.9	185.80	Total		609.76	0.04	0.00	269.30	13.73	0.25	147.40	3.56	1.45	0.52	782.10	6.68	38.49
						Dissolved		611.97	0.04	0.00	271.27	13.63	0.24	148.11	3.56	1.45	0.51	787.08	6.51	38.09
Douthat Well	12/22/20 11:25	245.5	186.4	198.9	186.11	Total		658.16	0.05	0.01	283.58	14.99	0.26	169.26	3.63	1.48	0.49	884.39	8.56	39.67
Douthat Well	2/25/21 14:40	245.5	186.4	198.9	186.11	Total		664.11	0.04	0.01	258.79	13.44	0.25	161.93	3.35	1.33	0.44	870.94	6.83	36.18
						Dissolved		584.39	0.04	0.01	230.43	13.57	0.26	133.85	3.39	1.37	0.47	733.95	7.02	36.05
Douthat Well	11/12/21 11:30	245.5	186.4	198.9	199.82	Total		630.08	0.02	0.00	18.05	5.67	0.07	45.28	0.81	0.13	0.04	501.20	8.12	6.20
Douthat Well	11/12/21 11:22	245.5	186.4	198.9	190.68	Total		661.07	0.01	0.00	25.65	6.15	0.07	43.41	0.78	0.13	0.05	528.86	10.88	4.22
Douthat Well	11/12/21 11:06	245.5	186.4	198.9	185.80	Total		662.75	0.04	0.00	260.77	14.14	0.25	145.02	3.41	1.34	0.44	806.51	6.65	35.97
						Dissolved		668.64	0.04	0.00	264.55	14.26	0.26	147.89	3.42	1.34	0.44	821.51	6.72	36.10

Table A7.2: Water chemistry of samples collected in the Picher field mine pool at locations inside of the 1.6 km radius of the Douthat mine drainage discharges

Site Name	Date Time	Surface Elevation	Underground Void Elevations		Sample Elevation	Temperature	Specific Conductivity	DO Sat	DO Conc	pH	Alkalinity	Total Hardness	Turbidity	Sulfate	Chloride	$\delta^{18}O$	$\delta^{2}H$
			Floor	Ceiling													
	M/D/Y HH:MM:SS	(m AMSL)	(m AMSL)	(m AMSL)	(m AMSL)	°C	µS/cm	%	mg/L		mg/L CaCO3 eq.	mg/L	NTU	mg/L	mg/L	VSMOW (‰)	VSMOW (‰)
Fyre Well	3/1/20 10:40	248.8	204.0	221.1	212.87	15.57	1,546	10.50	1.05	6.24	131.50	998.56	1.26	809.60		-5.40	-30.22
Fyre Well	2/25/21 15:49	248.8	204.0	221.1	213.78	15.19	799	13.90	1.39	6.50	93.00	446.01	3.93	331.20		-5.35	-28.28
Fyre Well	12/15/21 12:06	248.8	204.0	221.1	212.87	16.93	1,380	31.20	3.00	6.32	151.00	925.26	2.28	739.20	8.10	-5.38	-19.30
Baby Jim Shaft	2/15/20 16:53	246.9	185.0	195.4	216.41	15.77	668	16.80	1.67	6.63							
Baby Jim Shaft	2/15/20 16:37	246.9	185.0	195.4	204.22	15.09	667	9.40	0.94	6.64	161.00	360.44	3.50	189.10			
Baby Jim Shaft	2/15/20 16:16	246.9	185.0	195.4	199.64	15.40	1,801	11.90	1.19	6.42							
Baby Jim Shaft	2/15/20 15:51	246.9	185.0	195.4	195.07	15.46	1,870	10.90	1.08	6.45	157.00	1,266.50	2.92	969.70		-5.06	-29.61
Baby Jim Shaft	2/27/21 9:26	246.9	185.0	195.4	195.38	16.07	1,656	21.50	2.11	6.74	179.00	1,068.05	0.66	795.40		-5.27	-28.23
Baby Jim Shaft	11/13/21 10:15	246.9	185.0	195.4	210.92	15.60	809	26.70	2.66	6.90		494.84					
Baby Jim Shaft	11/13/21 10:06	246.9	185.0	195.4	202.69	15.63	1,543	23.70	2.34	6.74							
Baby Jim Shaft	11/13/21 9:56	246.9	185.0	195.4	197.51	15.71	1,599	21.00	2.08	6.81							
Baby Jim Shaft	11/13/21 9:44	246.9	185.0	195.4	194.16	15.36	1,632	22.20	2.21	6.76	190.50	1,170.20	1.20	756.70	11.20		
Admiralty #3 Shaft	2/15/20 11:32	249.6	181.4	189.9	238.81	12.34	708	53.50	5.70	7.13							
Admiralty #3 Shaft	2/15/20 11:49	249.6	181.4	189.9	231.19	14.15	741	71.40	7.32	6.94							
Admiralty #3 Shaft	2/15/20 12:25	249.6	181.4	189.9	223.72	11.49	740	44.40	4.83	7.24							
Admiralty #3 Shaft	2/15/20 13:20	249.6	181.4	189.9	197.82	14.43	742	68.60	6.99	6.98	190.00	445.85	0.10	208.90			
Admiralty #3 Shaft	2/15/20 14:07	249.6	181.4	189.9	188.67	15.00	2,136	17.40	1.75	6.07	91.50	1,608.80	26.47	1,269.50		-5.20	-33.19
Admiralty #3 Shaft	12/22/20 13:11	249.6	181.4	189.9	188.67	16.10	2,389	24.60	2.40	6.18	150.50	1,804.64	28.60	1,423.80		-5.36	-29.95
Admiralty #3 Shaft	2/25/21 13:37	249.6	181.4	189.9	188.67	15.44	2,328	19.40	1.92	6.39	150.00	1,645.62	2.16	1,483.50		-5.33	-30.12
Admiralty #3 Shaft	11/13/21 11:25	249.6	181.4	189.9	194.77	15.29	712	70.30	7.03	6.93		459.49					
Admiralty #3 Shaft	11/13/21 11:03	249.6	181.4	189.9	188.67	15.38	2,270	21.60	2.15	6.28	141.00	1,805.69	1.11	1,314.70	13.02		
Blue Goose Well	3/1/20 9:08	253.0	153.9	157.3	173.74	16.68	1,930	21.70	2.10	6.69						-4.91	-25.55
Blue Goose Well	3/1/20 9:23	253.0	153.9	157.3	164.59	16.46	1,939	23.60	2.29	6.77							
Blue Goose Well	3/1/20 8:20	253.0	153.9	157.3	156.06	15.99	3,441	22.30	2.18	6.12	347.00	941.81	29.00	805.90			
Blue Goose Well	12/21/20 17:43	253.0	153.9	157.3	161.54	16.57	2,660	23.30	2.25	5.70	118.00	1,913.89	312.67	1,745.00		-2.58	-14.17
Blue Goose Well	2/26/21 8:50	253.0	153.9	157.3	161.54	16.24	2,641	26.30	2.56	5.19	34.50	1,796.30	52.43	1,806.80		-2.11	-13.79
Blue Goose Well	2/26/21 17:26	253.0	153.9	157.3	161.54	16.58	2,648	32.80	3.17	5.54		1,835.04					
Blue Goose Well	11/12/21 16:51	253.0	153.9	157.3	169.16	16.32	2,427	27.70	2.70	5.39							
Blue Goose Well	11/12/21 16:33	253.0	153.9	157.3	161.54	16.43	2,496	26.40	2.57	5.02	31.50	1,884.67	77.77	1,780.60	4.83	-2.08	-3.25

Table A7.2: Continued

Site Name	Date Time M/D/Y HH:MM:SS	Surface Elevation (m AMSL)	Underground Void Elevations Floor (m AMSL)	Underground Void Elevations Ceiling (m AMSL)	Sample Elevation (m AMSL)		Arsenic mg/L	Calcium mg/L	Cadmium mg/L	Copper mg/L	Iron mg/L	Potassium mg/L	Lithium mg/L	Magnesium mg/L	Manganese mg/L	Sodium mg/L	Nickel mg/L	Lead mg/L	Sulfur mg/L	Silicon mg/L	Zinc mg/L
Fyre Well	3/1/20 10:40	248.8	204.0	221.1	212.87	Total	0.04	380.57	0.01	0.00	25.55	2.92	0.03	13.17	0.36	17.25	0.09	0.06	282.80	10.64	2.22
						Dissolved	0.05	378.50	0.01	0.00	25.41	2.89	0.03	12.98	0.36	17.19	0.09	0.06	280.91	10.58	2.20
Fyre Well	2/25/21 15:49	248.8	204.0	221.1	213.78	Total		177.45	0.00	0.01	9.33	2.99	0.01	8.60	0.27	10.63	0.05		128.83	7.64	2.02
						Dissolved		164.23	0.00	0.01	9.00	3.02	0.02	8.73	0.27	10.64	0.05		113.29	7.81	2.01
Fyre Well	12/15/21 12:06	248.8	204.0	221.1	212.87	Total	0.04	348.52	0.01	0.00	22.20	3.11	0.03	10.60	0.33	14.27	0.07	0.04	249.01	11.06	2.15
						Dissolved	0.04	353.09	0.00	0.00	22.09	3.12	0.03	10.59	0.33	14.27	0.08	0.04	253.86	11.06	2.04
Baby Jim Shaft	2/15/20 16:37	246.9	185.0	195.4	204.22	Total		124.59	0.00	0.00	0.55	4.10	0.03	11.98	0.90	10.71	0.03		62.64	7.35	2.26
						Dissolved		125.06	0.00	0.00	0.25	4.12	0.03	11.60	0.88	10.74	0.03		62.81	7.29	2.23
Baby Jim Shaft	2/15/20 15:51	246.9	185.0	195.4	195.07	Total		449.05	0.00	0.00	8.98	5.46	0.06	42.37	0.70	25.28	0.11	0.03	362.83	4.63	4.25
						Dissolved		437.42	0.00	0.00	8.85	5.48	0.06	42.33	0.70	25.35	0.11	0.03	353.92	4.62	4.27
Baby Jim Shaft	2/27/21 9:26	246.9	185.0	195.4	195.38	Total		406.86	0.00	0.01	2.36	5.38	0.05	30.56	0.61	22.25	0.08		314.76	4.15	3.08
						Dissolved		377.25	0.00	0.01	2.34	5.37	0.05	30.62	0.61	21.92	0.08		273.79	4.21	3.07
Baby Jim Shaft	11/13/21 10:15	246.9	185.0	195.4	210.92	Total		168.73	0.00	0.00	0.98	4.46	0.04	17.86	0.91	12.89	0.04		84.37	7.51	1.81
Baby Jim Shaft	11/13/21 9:44	246.9	185.0	195.4	194.16	Total		415.59	0.00	0.00	5.46	5.22	0.05	35.52	0.62	17.43	0.08		292.99	4.16	2.87
						Dissolved		409.94	0.00	0.00	5.52	5.28	0.05	35.60	0.62	17.58	0.08		291.80	4.18	2.84
Admiralty #3 Shaft	2/15/20 13:20	249.6	181.4	189.9	197.82	Total		158.05	0.01	0.00	0.03	1.22		12.44		2.80	0.03		69.48	5.20	4.14
						Dissolved		155.57	0.01	0.00	0.01	1.22		12.57		2.80	0.03		68.56	5.17	4.21
Admiralty #3 Shaft	2/15/20 14:07	249.6	181.4	189.9	188.67	Total		564.24	0.04	0.00	4.05	4.77	0.06	41.39	0.77	23.14	0.13		475.86	7.38	8.42
						Dissolved		575.48	0.04	0.00	2.72	4.77	0.06	41.74	0.76	23.10	0.13		483.37	7.41	8.47
Admiralty #3 Shaft	12/22/20 13:11	249.6	181.4	189.9	188.67	Total		644.93	0.01	0.01	28.26	6.77	0.08	47.18	0.90	33.82	0.18	0.05	574.09	8.07	5.04
Admiralty #3 Shaft	2/25/21 13:37	249.6	181.4	189.9	188.67	Total		639.27	0.01	0.01	24.59	6.82	0.09	48.31	0.95	34.93	0.16	0.02	571.75	7.26	4.98
						Dissolved		578.70	0.01	0.01	24.42	6.84	0.09	48.73	0.96	34.54	0.17		492.20	7.42	5.06
Admiralty #3 Shaft	11/13/21 11:25	249.6	181.4	189.9	194.77	Total		165.91	0.02	0.00	0.04	1.20		10.98	0.00	1.69	0.03		59.45	6.04	6.48
Admiralty #3 Shaft	11/13/21 11:03	249.6	181.4	189.9	188.67	Total		651.68	0.01	0.01	21.68	5.81	0.07	45.70	0.82	21.02	0.13	0.04	518.06	8.45	5.50
						Dissolved		648.00	0.01	0.00	21.44	5.82	0.07	45.58	0.82	20.99	0.13	0.04	528.09	8.44	5.45
Blue Goose Well	3/1/20 9:08	253.0	153.9	157.3	173.74	Dissolved		207.50	0.00	0.00	0.29	11.43	0.48	83.92	0.05	130.75	0.03		251.02	6.04	0.15
Blue Goose Well	3/1/20 8:20	253.0	153.9	157.3	156.06	Total		243.25	0.01	0.00	21.20	12.25	0.46	81.23	0.15	126.64	0.08	0.11	278.07	7.23	1.09
						Dissolved	0.06	570.16	0.02	0.00	197.23	32.31	0.29	174.25	1.09	102.09	1.50	0.43	773.54	8.80	18.49
Blue Goose Well	12/21/20 17:43	253.0	153.9	157.3	161.54	Total	0.06	680.16	0.03	0.01	189.35	20.97	0.15	52.35	0.64	50.15	0.12	0.45	697.54	21.70	2.03
						Dissolved	0.06	662.94	0.02	0.00	114.19	20.29	0.14	53.05	0.49	50.18	0.11	0.17	692.75	18.24	1.63
Blue Goose Well	2/26/21 8:50	253.0	153.9	157.3	161.54	Total	0.03	655.38	0.02	0.01	142.23	27.45	0.11	38.82	0.53	32.63	0.13	0.28	688.41	28.61	0.82
						Dissolved	0.04	601.28	0.02	0.01	127.29	27.52	0.11	39.14	0.53	32.33	0.15	0.23	602.74	29.10	0.64
Blue Goose Well	2/26/21 17:26	253.0	153.9	157.3	161.54	Total	0.06	663.41	0.02	0.01	126.82	23.41	0.11	43.36	0.53	36.95	0.12	0.31	689.63	24.68	1.49
Blue Goose Well	11/12/21 16:33	253.0	153.9	157.3	161.54	Total	0.03	685.70	0.02	0.01	145.79	29.25	0.10	41.89	0.59	20.53	0.14	0.40	650.66	29.41	0.84
						Dissolved	0.03	670.74	0.02	0.01	131.33	28.44	0.09	41.66	0.58	20.26	0.13	0.22	643.61	28.61	0.45

Table A7.3: Water chemistry of samples collected in the Picher field mine pool at locations outside of the 1.6 km radius of the Douthat mine drainage discharges

Site Name	Date Time	Surface Elevation	Underground Void Elevations		Sample Elevation	Temperature	Specific Conductivity	DO Sat	DO Conc	pH	Alkalinity	Total Hardness	Turbidity	Sulfate	Chloride	$\delta^{18}O$	$\delta^{2}H$
			Floor	Ceiling													
	M/D/Y HH:MM:SS	(m AMSL)	(m AMSL)	(m AMSL)	(m AMSL)	°C	µS/cm	%	mg/L		mg/L CaCO3 eq.	mg/L	NTU	mg/L	mg/L	VSMOW (‰)	VSMOW (‰)
John Hunt Shaft	2/15/20 8:25	248.4	189.3	193.2	239.42	8.88	164	44.30	5.13	7.05							
John Hunt Shaft	2/15/20 8:41	248.4	189.3	193.2	229.06	11.84	256	26.70	2.89	6.81							
John Hunt Shaft	2/15/20 9:33	248.4	189.3	193.2	210.62	10.99	257	27.10	2.99	6.89	81.00	126.26	3.29	39.69		-5.18	-27.74
John Hunt Shaft	2/28/20 18:09	248.4	189.3	193.2	211.84	14.51	288	34.50	3.51	6.45		132.44					
John Hunt Shaft	2/25/21 17:22	248.4	189.3	193.2	212.45	13.96	291	24.10	2.49	7.01	91.50	153.51	3.80	55.90		-6.15	-33.27
John Hunt Shaft	12/15/21 11:09	248.4	189.3	193.2	212.45	16.49	253	42.00	4.10	6.84	98.50	122.39	1.15	32.35	1.14	-4.17	-17.61
Mary Ann Shaft	2/29/20 16:08	252.6	204.8	209.6	225.19	17.12	571	15.30	1.47	6.77		285.32					
Mary Ann Shaft	2/29/20 16:01	252.6	204.8	209.6	216.04	17.26	574	18.30	1.75	6.79							
Mary Ann Shaft	2/29/20 15:52	252.6	204.8	209.6	209.95	17.79	570	54.50	5.18	6.78	83.00	287.72	17.00	172.70		-4.81	-24.55
Mary Ann Shaft	2/29/20 15:34	252.6	204.8	209.6	206.90	20.29	604	22.50	2.03	6.85							
Mary Ann Shaft	2/25/21 12:25	252.6	204.8	209.6	206.59	13.92	640	22.80	2.34	7.00	108.00	367.90	14.73	219.20		-5.85	-32.86
Mary Ann Shaft	11/13/21 12:52	252.6	204.8	209.6	213.30	15.63	544	16.30	1.62	7.00							
Mary Ann Shaft	11/13/21 12:42	252.6	204.8	209.6	207.51	15.40	570	18.90	1.89	7.02	98.00	307.45	12.30	180.40	4.64	-5.19	-23.40
Lucky Jenny Shaft	2/29/20 18:33	260.6	199.3	205.4	246.89	14.10	1,482	92.70	9.49	6.84							
Lucky Jenny Shaft	2/29/20 18:30	260.6	199.3	205.4	220.98	14.04	1,485	89.00	9.13	6.83							
Lucky Jenny Shaft	2/29/20 17:52	260.6	199.3	205.4	211.84	14.17	1,479	91.20	9.32	6.93							
Lucky Jenny Shaft	2/29/20 17:17	260.6	199.3	205.4	205.74	14.77	1,476	90.40	9.12	6.78	89.50	934.99	16.97	802.30		-4.94	-26.51
Lucky Jenny Shaft	2/26/21 15:08	260.6	199.3	205.4	205.74	14.26	1,753	104.80	10.68	6.75	63.00	1,130.35	1.53	1,006.50		-6.31	-33.51
Lucky Jenny Shaft	11/13/21 14:36	260.6	199.3	205.4	241.71	14.68	1,837	99.00	10.00	6.22							
Lucky Jenny Shaft	11/13/21 14:28	260.6	199.3	205.4	230.12	14.64	1,835	97.00	9.81	6.21		1,237.21					
Lucky Jenny Shaft	11/13/21 14:20	260.6	199.3	205.4	214.88	14.75	1,830	95.80	9.66	6.20							
Lucky Jenny Shaft	11/13/21 14:12	260.6	199.3	205.4	210.62	14.88	1,828	94.80	9.53	6.19							
Lucky Jenny Shaft	11/13/21 14:01	260.6	199.3	205.4	205.74	14.86	1,826	95.80	9.63	6.19	53.67	1,243.81	2.92	1,045.90	4.25	-5.35	-29.06
LaSalle Well	2/25/21 11:08	260.9	176.8	196.0	195.08	13.55	2,312	25.00	2.58	6.50	156.00	1,593.55	39.00	1,426.90		-5.40	-29.16
LaSalle Well	1/9/22 15:14	260.9	176.8	196.0	198.43	15.03	2,343	14.50	1.45	6.32	165.00	1,777.37	17.93	1,498.90	18.44	-4.93	-25.47
RHMW2 Well	3/5/20 12:17		202.7	212.4	244.54	16.63	3,255	43.70	4.21	5.85	305.00	2,159.25	2.21	1,994.30		-5.36	-32.26
RHMW2 Well	3/18/21 15:14		202.7	212.4	244.54	16.41	3,247	24.80	2.40	5.99	290.50	2,270.68			27.07	-5.67	-30.02
OCC #3 Well	2/28/20 21:04		191.4	200.9	195.93	14.81	2,785	13.40	1.34	6.12	240.50	1,887.41	0.75	1,642.00		-5.65	-32.60
OCC #3 Well	8/17/21 11:41		191.4	200.9		19.07	2,589	53.60	4.93	6.01	248.50	2,023.35	31.40	1,620.20	21.91	-5.71	-27.63

Table A7.3: Continued

Site Name	Date Time	Surface Elevation	Underground Void Elevations		Sample Elevation		Arsenic	Calcium	Cadmium	Copper	Iron	Potassium	Lithium	Magnesium	Manganese	Sodium	Nickel	Lead	Sulfur	Silicon	Zinc
			Floor	Ceiling																	
	M/D/Y HH:MM:SS	(m AMSL)	(m AMSL)	(m AMSL)	(m AMSL)		mg/L	mg/L	mg/L	mg/L	mg/L	mg/L	mg/L	mg/L	mg/L	mg/L	mg/L	mg/L	mg/L	mg/L	mg/L
John Hunt Shaft	2/15/20 9:33	248.4	189.3	193.2	210.62	Total		45.26	0.01	0.00	0.22	2.21		3.22	0.01	2.62	0.02		11.86	4.82	2.15
						Dissolved		45.85	0.01	0.00	0.04	2.19		3.21		2.61	0.02		12.08	4.51	2.12
John Hunt Shaft	2/28/20 18:09	248.4	189.3	193.2	211.84	Total		47.60	0.02	0.01	0.20	2.18		3.30		2.72	0.02		12.99	4.74	2.23
John Hunt Shaft	2/25/21 17:22	248.4	189.3	193.2	212.45	Total		55.25	0.01	0.01	0.28	2.59		3.78	0.01	3.14	0.02		17.34	5.06	2.32
						Dissolved		56.25	0.01	0.01	0.04	2.59		3.80	0.01	3.12	0.02		17.20	4.74	2.29
John Hunt Shaft	12/15/21 11:09	248.4	189.3	193.2	212.45	Total		43.91	0.02	0.01	0.10	2.49		3.10	0.07	2.22	0.02		9.18	4.79	1.91
						Dissolved		43.87	0.02	0.01	0.04	2.49		3.09	0.07	2.25	0.02		9.17	4.71	1.89
Mary Ann Shaft	2/29/20 16:08	252.6	204.8	209.6	225.19	Total		99.96	0.00		4.19	4.72	0.02	8.67	0.53	6.62	0.04		66.50	6.76	0.51
Mary Ann Shaft	2/29/20 15:52	252.6	204.8	209.6	209.95	Total		101.10	0.00	0.00	4.28	4.70	0.02	8.57	0.54	6.57	0.04		66.57	6.74	0.50
						Dissolved		99.90		0.00	3.24	4.72	0.02	8.68	0.51	6.61	0.04		66.85	6.68	0.42
Mary Ann Shaft	2/25/21 12:25	252.6	204.8	209.6	206.59	Total		130.33	0.00	0.00	4.84	5.94	0.03	10.31	3.09	8.64	0.04		86.88	8.23	0.22
						Dissolved		118.44			4.16	5.96	0.03	10.37	3.91	8.53	0.04		72.48	8.34	0.01
Mary Ann Shaft	11/13/21 12:42	252.6	204.8	209.6	207.51	Total		109.72	0.00	0.00	6.60	5.70	0.02	8.13	0.95	6.12	0.04		65.66	7.79	0.24
						Dissolved		110.35	0.00	0.00	5.33	5.73	0.02	8.19	0.85	6.19	0.04		66.39	7.59	0.03
Lucky Jenny Shaft	2/29/20 17:17	260.6	199.3	205.4	205.74	Total		298.65	0.03	0.01	0.71	4.89	0.22	45.97	0.31	30.25	0.15	0.12	285.46	6.36	5.73
						Dissolved		301.17	0.03	0.01	0.01	4.86	0.22	46.04	0.31	30.34	0.15		287.61	5.81	5.14
Lucky Jenny Shaft	2/26/21 15:08	260.6	199.3	205.4	205.74	Total		366.05	0.02	0.01	0.20	6.10	0.33	52.54	0.36	40.41	0.17		383.94	6.08	4.93
						Dissolved		341.36	0.02	0.01	0.01	6.13	0.34	53.03	0.36	40.09	0.17		336.30	6.12	4.95
Lucky Jenny Shaft	11/13/21 14:28	260.6	199.3	205.4	230.12	Total		368.84	0.03	0.01	0.30	8.61	0.52	76.80	0.68	47.53	0.29		402.34	8.34	9.52
Lucky Jenny Shaft	11/13/21 14:01	260.6	199.3	205.4	205.74	Total		371.85	0.03	0.01	0.31	8.57	0.52	76.59	0.67	47.31	0.29		404.42	8.33	9.75
						Dissolved		368.71	0.03	0.01	0.05	8.62	0.52	77.59	0.66	47.55	0.29		404.01	8.24	9.62
LaSalle Well	2/25/21 11:08	260.9	176.8	196.0	195.08	Total	0.05	624.22	0.11	0.04	46.24	6.08	0.09	46.42	1.04	43.19	0.20	2.37	566.46	7.16	17.11
						Dissolved	0.03	561.71	0.01	0.01	38.57	6.01	0.09	46.39	0.96	42.91	0.17	0.06	486.46	6.43	5.26
LaSalle Well	1/9/22 15:14	260.9	176.8	196.0	198.43	Total	0.04	632.75	0.02	0.01	47.16	5.69	0.09	55.20	1.00	33.79	0.17	0.35	577.04	6.50	5.75
						Dissolved	0.03	620.11	0.01	0.00	44.89	5.80	0.10	55.61	0.98	34.69	0.17	0.08	570.45	6.35	4.70
Mid-Continent Well	1/9/22 13:54	252.7	172.5	175.6	220.68	Total		321.55	0.01	0.01	23.20	5.79	0.05	25.78	0.61	23.69	0.03	0.08	224.35	6.35	0.53
						Dissolved		314.03	0.00	0.00	22.02	5.47	0.05	25.66	0.60	23.66	0.02	0.04	221.11	4.91	0.01
RHMW2 Well	3/5/20 12:17		202.7	212.4	244.54	Total	0.08	639.43	0.02	0.00	149.70	26.30	0.27	136.65	1.38	86.97	0.70	0.28	735.76	32.30	3.63
						Dissolved	0.08	647.40	0.02	0.00	150.81	26.63	0.28	137.22	1.38	97.74	0.71	0.28	744.64	32.48	3.70
RHMW2 Well	3/18/21 15:14		202.7	212.4	244.54	Total	0.10	674.91	0.02	0.00	149.51	24.11	0.28	142.20	1.33	94.66	0.66	0.26	641.24	30.99	3.64
						Dissolved	0.10	662.16	0.02	0.01	146.75	24.26	0.28	135.65	1.34	95.17	0.67	0.26	641.87	31.31	3.67
OCC #3 Well	2/28/20 21:04		191.4	200.9	195.93	Total		662.13	0.01		83.34	12.19	0.11	56.85	1.08	71.74	0.22	0.18	619.22	10.29	26.17
						Dissolved		663.02	0.01	0.00	83.92	12.13	0.11	56.52	1.08	71.61	0.22	0.18	616.84	10.24	25.90
OCC #3 Well	8/17/21 11:41		191.4	200.9	195.63	Total	0.03	708.70	0.02	0.01	91.33	13.06	0.15	61.63	1.22	64.73	0.24	0.17	594.04	10.59	26.12
						Dissolved		699.52	0.02	0.00	89.77	13.05	0.14	61.81	1.22	65.23	0.24	0.16	599.00	10.50	26.21

Table A7.4: Water chemistry of groundwater samples collected from wells in the Boone and Roubidoux aquifers in Ottawa County, OK, near the Picher field abandoned mining operations

Site Name	Date Time	Sample Elevation	Temperature	Specific Conductivity	DO Sat	DO Conc	pH	Alkalinity	Total Hardness	Turbidity	Sulfate	Chloride	$\delta^{18}O$	$\delta^{2}H$
	M/D/Y HH:MM:SS	m AMSL	C	µS/cm	%	mg/L		mg/L CaCO3 eq.	mg/L	NTU	mg/L	mg/L	VSMOW (‰)	VSMOW (‰)
Boone Well 1	6/10/21 12:48	207.26	17.60	298	71.10	6.78	6.56	105.00		1.69	9.06	13.33	-5.64	-26.72
Boone Well 1	11/11/21 12:00	207.26	17.03	317	92.20	8.89	6.83	72.67		36.20	14.64	13.17	-5.45	-27.90
Boone Well 2	6/10/21 13:11	198.12	17.02	219	51.40	4.96	6.71	87.50		1.70	8.94	4.22	-5.43	-30.70
Boone Well 2	11/11/21 11:45	198.12	15.89	453	46.00	4.55	6.81	175.50		1.60	9.92	7.94	-6.10	-37.24
Boone Well 3	12/15/21 18:19	187.45	16.95	1,202	18.70	1.80	8.46	555.67		18.67	51.82	71.40	-6.21	-32.26
Boone Well 4	1/9/22 18:22	177.39	13.25	760	13.40	1.40	7.45	328.00		21.00	59.98	38.45	-6.26	-35.36
Boone Well 5	12/16/21 16:44	229.51	15.03	536	69.60	7.00	7.20	236.00		7.92	15.40	17.61	-5.44	-26.04
Roubidoux Well 1	9/14/21 10:30		18.45	402	80.60	7.56	7.81	132.50		0.50	41.00		-6.53	-29.19
Roubidoux Well 2	9/14/21 11:18		20.00	560	91.00	8.26	7.93	140.50		0.39	99.40		-6.83	-33.09
Roubidoux Well 3	10/15/20 9:39		19.44	328	51.00	4.68	7.60						-7.18	-40.44
Roubidoux Well 3	9/14/21 9:30		19.91	324	56.60	5.15	7.86	124.50		1.15	14.77		-6.98	-33.15
Roubidoux Well 4	12/16/21 9:20		17.51	344	54.00	5.16	7.65	147.50		4.59	17.65	7.06	-6.58	-39.86

Table A7.4: Continued

Site Name	Date Time	Sample Elevation		Arsenic	Calcium	Cadmium	Copper	Iron	Potassium	Lithium	Magnesium	Manganese	Sodium	Nickel	Lead	Sulfur	Silicon	Zinc
	M/D/Y HH:MM:SS	(m AMSL)		mg/L	mg/L	mg/L	mg/L	mg/L	mg/L	mg/L	mg/L	mg/L	mg/L	mg/L	mg/L	mg/L	mg/L	mg/L
Boone Well 1	6/10/21 12:48	207.26	Total		55.84		0.00	0.09	5.51		2.65	0.01	3.70	0.02		2.64	4.59	0.02
			Dissolved		58.04		0.00	0.03	5.52		2.72	0.01	3.74	0.02		4.25	4.59	0.04
Boone Well 1	11/11/21 12:00	207.26	Total		76.34		0.00	2.11	3.88		2.48	0.17	3.68	0.02		3.70	5.29	0.02
			Dissolved		60.03		0.00	0.01	3.77		2.40	0.00	3.75	0.02		3.73	4.64	0.02
Boone Well 2	6/10/21 13:11	198.12	Total		41.10		0.00	0.11	3.36		2.52	0.00	2.30	0.02		1.97	4.17	0.04
			Dissolved		41.10		0.00	0.03	3.34		2.52	0.00	2.30	0.01		2.04	4.02	0.04
Boone Well 2	11/11/21 11:45	198.12	Total		97.10		0.01	0.15	5.06		3.74	0.00	2.83	0.02		2.97	4.62	0.07
			Dissolved		95.80		0.01	0.04	5.07		3.74	0.00	2.87	0.01		3.38	4.58	0.07
Boone Well 3	12/15/21 18:19	187.45	Total	0.02	5.79		0.00	0.86	56.56	0.59	3.79	0.03	214.93	0.05		11.49	12.42	0.10
			Dissolved	0.03	4.78		0.00	0.17	56.67	0.59	3.41	0.01	222.58	0.03		11.72	8.06	0.02
Boone Well 4	1/9/22 18:22	177.39	Total		61.05	0.0010	0.00	1.36	8.43	0.20	21.87	0.05	76.15	0.03		16.62	7.34	0.13
			Dissolved		58.41		0.00	0.63	8.45	0.20	21.89	0.04	76.82	0.02		16.79	6.90	0.01
Boone Well 5	12/16/21 16:44	229.51	Total		111.99	0.0022	0.03	1.00	2.36		1.49	0.02	14.24	0.02	0.17	5.26	4.84	0.25
			Dissolved		105.77	0.0018	0.00	0.03	2.47		1.37	0.00	13.58	0.02		4.87	4.65	0.21
Roubidoux Well 1	9/14/21 10:30		Total		47.35		0.00	0.17	3.31	0.05	19.83	0.01	8.37	0.02		19.15	4.55	0.01
			Dissolved		45.40			0.11	3.26	0.05	18.73	0.01	8.18	0.02		17.82	4.48	0.00
Roubidoux Well 2	9/14/21 11:18		Total		70.44		0.00	0.23	3.62	0.03	31.76	0.01	10.33	0.02		42.46	5.01	0.01
			Dissolved		70.23		0.00	0.14	3.64	0.03	32.10	0.01	10.43	0.02		42.78	4.96	0.01
Roubidoux Well 3	10/15/20 9:39		Total		32.02		0.01	0.15	2.50	0.02	15.38	0.00	8.88	0.02		4.88	4.57	0.01
Roubidoux Well 3	9/14/21 9:30		Total		32.60		0.01	0.27	2.88	0.02	14.30	0.01	10.43	0.02		4.75	4.69	0.00
			Dissolved		32.81			0.06	2.88	0.02	14.35	0.00	10.41	0.02		4.94	4.66	0.00
Roubidoux Well 4	12/16/21 9:20		Total		33.57		0.03	0.13	3.30	0.09	15.08	0.00	14.17	0.02		5.83	4.26	0.01
			Dissolved		33.82		0.01	0.06	3.34	0.09	15.14	0.00	14.41	0.02		6.00	4.29	0.01